

To Chiara.

*Senza di te un albero
non sarebbe più un albero.
Nulla senza di te
sarebbe quello che è. (G.C.)*

Image on the cover: *Piano Phase*, Steve Reich, 1967. A 12-note, even-semiquaver melody of five different modal pitches is set up in unison with itself on two pianos; the lead player gradually speeds up very slightly until he has moved one semiquaver ahead and continues this process of phasing until both instruments are back in unison.

Acknowledgment

This thesis was written during my last year while I was PhD student in mathematical-physics at SISSA-ISAS. The beginning of my experience in Trieste and my approach to the hard and rigorous teachings of the first year courses were at first glance full of difficulties; but now I am surely grateful for the beautiful mathematics I have learnt during this time.

The findings presented in these pages are the final results of a long standing collaboration with Francesco Calogero: as written by me and David Gomez-Ullate in a paper on the occasion of his 70th birthday, the work with him has been full of pleasant and rewarding moments that extend far beyond scientific matters.

I really want to thank also the constant supervision and the illuminating discussions during this last year with Boris Dubrovin, whose suggestions about the way of presenting mathematical results in a suitable form were very much appreciated.

Another very important acknowledgment goes to the other two collaborators who worked (and are still working) on the papers that report the main findings illustrated in the pages of this thesis: Paolo Maria Santini e David Gomez-Ullate. Their contributions in terms of science and friendship cannot be defined in other way than fundamental.

I should also acknowledge the discussions (in which I was not always directly involved, but that were useful to prove the results reported herein) with Jean-Pierre Francoise, Yuri Fedorov, François Leyvraz, Jaume Llibre, Alexander Mikhailov, Carles Simó, Robert Conte, Ovidiu Costin, Herman Flaschka, Giovanni Gallavotti, Nalini Joshi, Martin Kruskal, Orlando Ragnisco, Simonetta Abenda, Andrew Hone and Alexander Turbiner.

Last but not least, I want to thank my parents, my grandparents and my brother, for the love and the constant patience they had for me during these years.

CONTENTS

1	Introduction	9
1.1	Two important ingredients	11
1.1.1	Riemann surfaces and monodromy groups	12
1.1.2	The trick	14
1.2	Analysis of two many-body problems	17
1.2.1	The Calogero-Moser many-body problem	17
1.2.2	The Goldfish many-body problem	27
1.2.2.1	Unitary coupling constants	31
1.2.2.2	Generic coupling constants: the two-body case	35
1.2.2.3	Generic coupling constants: the N -body case	37
1.2.2.4	Generic coupling constants: dynamical behavior	41
1.3	Non-integrability and analyticity in complex time	43
1.3.1	Ziglin and Yoshida Theorems	46
1.4	The Aristotelian three-body problem	47
2	A Simple Three-Body Problem	59
2.1	Presentation of the model	60
2.2	Hamiltonian character of the model	63
2.3	Equilibrium configurations and similarity solutions	66
2.4	Properties of the solutions of the auxiliary model	70
2.4.1	Analysis <i>à la Painlevé</i>	72
2.4.2	Implications of the analysis <i>à la Painlevé</i>	75
2.5	General solution by quadratures	76
2.5.1	Movable singularities	80
2.5.2	Fixed singularities	82
2.5.3	Comparison with the findings of Section 2.4	83
2.6	Behavior of the physical model	83
2.6.1	Solution of the physical model	86
2.6.2	The polynomial equation 2.98	89
3	The Riemann Surface	95
3.1	The case $0 < \mu < 1$	96
3.1.1	The Riemann surface and its singularities	96
3.1.2	Defining a new congruence operation	97
3.1.3	Roots dynamics and topological properties	98

3.1.4	Branch points enumeration	100
3.1.5	Graph Theory and Monodromy Group	102
3.1.6	The bumping rule	105
3.1.7	Link with the Continued Fractions Theory	108
3.1.8	Following a single zero	111
3.1.9	The period formula for $0 < \mu < 1$ and $\mu \in \mathbb{Q}$	112
3.1.10	The irrational case: $\mu \notin \mathbb{Q}$	114
3.1.11	A remarkable example	116
3.2	The case $\mu > 1$	118
3.2.1	The Riemann surface and its singularities	119
3.2.2	Roots dynamics and topological properties	121
3.2.3	Branch points enumeration	124
3.2.4	Graph Theory and Monodromy Group	126
3.2.5	The bumping rules	130
3.2.6	The period formula for $\mu > 1$ and $\mu \in \mathbb{Q}$	132
3.2.7	The irrational case: $\mu \notin \mathbb{Q}$	135
3.3	The case $\mu < 0$	137
3.3.1	The period formula for $\mu < 0$	137
4	Complex Dynamics	139
4.1	Root behavior in terms of the initial conditions	139
4.1.1	The two circles B and Ξ	141
4.2	Dependence of the solution on initial conditions	147
4.2.1	Sections of phase space	151
4.2.1.1	Case $\mu > 1$	152
4.2.1.2	Case $0 < \mu < 1$	152
4.2.2	Sensitive dependence on initial conditions	154
4.2.3	Rational approximations to irrational values of μ	156
4.3	Outlook	159
A	The Algebraic Equations (2.39)	163
B	Solution of the ODE (2.86)	165
C	Explicitly Solvable Cases	167
D	Relation with More Standard 3-Body Problems	169
	Bibliography	175

CHAPTER 1

Introduction

The aim of this thesis is to present a *new* approach to explain the transitions from *regular* to *irregular* motions for dynamical systems as travels on Riemann surfaces. Particularly, we introduce a *new* and simple Hamiltonian dynamical system, interpretable as a many-body problem in the plane, providing an example of this mechanism [1] [2] [3]. We focus on the three body case, showing that it is solvable, in the sense that we can explicitly write the solutions in terms of the independent (*real*) time variable and we prove that there exist open domains of initial conditions, having *full dimensionality* in the phase space, such that *all* trajectories emerging from them are *completely periodic* of a basic period T ; studying the analytical structure of the solutions of an *auxiliary* problem which evolves with respect to a *complex* time variable, we prove that there are also other *completely periodic* solutions, but with periods which are *integer multiples* of T ; nevertheless we prove that there are *non-periodic* and *irregular* solutions and that this model exhibits *sensitive dependance on the initial conditions*.

The starting point of our discussion will be the theory of *integrable systems*, particularly the classical models that are amenable to exact treatments. We will mainly deal with the (usual) concept of *Liouville* integrability: a Hamiltonian system, characterized by the Hamiltonian function $H(\underline{q}, \underline{p})$ with $(\underline{q}, \underline{p}) \in \mathbb{R}^{2N}$, is defined as *completely integrable* if there exist N first integrals $I_1 = H, I_2, \dots, I_N$ which are functionally independent, which Poisson-commute and which generate complete flows. Indeed, in this case, the motion is confined to the submanifold M in phase space determined by the level sets of I_1, I_2, \dots, I_N :

$$M = \{(\underline{q}, \underline{p}) \in \mathbb{R}^{2N} \text{ s/t } I_j(\underline{q}, \underline{p}) = c_j \forall j\}.$$

Then a canonical transformation $(q_i, p_i) \mapsto (J_i, \phi_i)$ to *action-angle* variables exists such that

$$H(\underline{q}, \underline{p}) = \tilde{H}(\underline{J}),$$

where \tilde{H} is the new Hamiltonian function in terms of the action variables $\underline{J} = (J_1, \dots, J_N)$. If the manifold M is compact, then it is diffeomorphic to a torus,

$$M \simeq T^N = \{\phi_1, \dots, \phi_N \text{ MOD } 2\pi\}$$

and the evolution in the action-angle variables is trivial:

$$J_i = J_i^0, \phi_i = \phi_i^0 + \omega_i t, \forall i,$$

where J_i^0, ϕ_i^0 and ω_i are constants. If the frequencies $\omega_1, \dots, \omega_N$ are independent in the field of rationals \mathbb{Q} , then the trajectories fill densely the torus and the motion is called *quasi-periodic*.

In the context of the investigation of dynamical systems, recently a simple trick has been introduced [4]. In essence, it merely amounts to a change of independent variable, in particular from the *real* independent variable t (“time”) to an appropriate *complex* variable τ (and is generally associated with a corresponding, rather trivial, change of dependent variables, amounting essentially to multiplication by a common prefactor). It associates, to any dynamical system belonging to a quite large class (characterized by the *complex* independent variable τ), a related system characterized by a (*real*) “deformation parameter” ω having the dimension (and significance) of a (circular) frequency.

Our philosophy is to consider the ω -deformed system, whose evolution takes place in the *real* time t , as the “physical” model, and the undeformed system as an “auxiliary” model that, as we will see, plays an essential role to understand the time evolution of the *physical* system. When the deformation parameter vanishes, $\omega = 0$, the ω -deformed system coincides with the original system, but for $\omega > 0$ the two systems differ, and, most importantly, the *physical* system is *isochronous*.

We define *isochronous* a system that features an *open* set of initial data, having *full dimensionality* in its phase space, such that *all* the solutions emerging out of it remain in it and are *completely periodic* with the same period T . The boundary of this region is generally characterized by special initial data that yield motions leading in finite time to *singularities*: for instance if the *physical* system under consideration is interpretable as a many-body problem with interparticle forces singular at zero separation, typically these special motions feature *particle collisions*.

Remarkably this simple approach allows to identify many interesting models (a list of recent publications in which this phenomenology is explored and/or exploited can be read in [5] and at the beginning of Subsection 1.2 – note however that in several of the cited papers the *isochronicity* phenomenon constitutes only a minor aspect of the results being reported).

An interesting question is what happens for initial data located *outside* of the region yielding *isochronous* motions with the basic period. There may be other *open* phase space regions characterized by motions that are again *completely periodic*, but with periods that are *integer* multiples of the basic period. And also other *open* phase space regions where the generic motions are *aperiodic*, either *ordered* (for instance, characterized in configuration space by *limit cycles*) or *disordered*, this latter characterization being justified not only because these motions do not display any simple pattern, but because they feature a *sensitive dependence* on their initial data. This entire phenomenology is naturally interpretable in terms of travel on a certain (circular) path on the Riemann surfaces defined by the solutions of the *auxiliary* model, considered as functions of its independent (*complex*) variable τ . This mechanism, including the possible *onset* of some kind of *deterministic chaos*, has been discussed in [6] and [7], where we analyzed two many-body problems in the plane via numerical and analytical techniques (see Section 1.2), and the main purpose of the results reported in this thesis, and in other papers to follow, is to make further progress in the understanding of this phenomenology.

To this end we introduce and discuss a neat Hamiltonian system, somewhat analogous but simpler than the well-known many-body model considered in [6]. Remarkably, the *general* solution of this problem can be obtained via *quadratures* all of which can be performed in terms of *elementary functions*; yet this model is adequate to display and analyze in remarkable detail and rigorously the rich phenomenology outlined above (and this is the main difference with previous works, for example [6] or [7], in which this phenomenology was studied in a more qualitative way). In particular, as regards the regime characterized by motions that are *completely periodic*, but with periods which are *integer* multiples of the basic period T , exact formulas giving these periods – which depend *sensitively* on the initial data, and may be *arbitrarily large* – are obtained, even though they are far from

trivial (as demonstrated, for instance, by their dependence, for certain values of the coupling constants featured by the model, on the coefficients of *arbitrarily large order* of the *simple-continued-fraction* expansion of a certain ratio of the coupling constants). Likewise, in the *aperiodic* regime, it turns out to be possible to describe to a remarkable extent the motion and in particular to clarify how the trajectories are influenced by the initial data.

As we will show in Subsection 1.3, the investigation of the relation between the *integrability* of differential equations and the analyticity properties of their solutions goes back to such eminent mathematicians as Carl Jacobi, Sophia Kowalewskaya, Henri Poincaré, Paul Painlevé and his school: the main idea at the base of their results in this sense could be rephrased saying that, *to have integrability, the only movable singularities should be poles if we consider the evolution of the independent variable t in the complex t -plane*. In this context, Martin Kruskal proposed a new approach, a brief rendition of which might be the statement that, *to have integrability, movable branch points are also allowed, provided they are not dense in the complex t -plane*. The results presented in this thesis, constitute progress along this line of thinking.

In the next Section 1.1 we will describe some useful background notions to introduce the reader in the context of our line of research. In Section 1.2 we will present the main findings of the two already cited papers [6] and [7], where the Calogero-Moser respectively the Goldfish model are analyzed. In Section 1.3 we discuss some results concerning the relation between the *integrability* of a dynamical system and the analyticity properties of its solutions; we moreover report two beautiful rigorous theorems by Ziglin and Yoshida. Finally, in Section 1.4 we introduce the *new* many-body problem, that will be the object of this thesis in the remaining three chapters. This thesis is structured so that, to have a global idea of the main results, it is possible to read just Chapter 1 and Chapter 4. In Chapters 2 and 3 we reported all the proofs and the discussion (through a quite *new algebraic-geometric-combinatorial* approach) of the Riemann surface Γ associated to the *nondifferential* equation in terms of which we write the solution of the three-body problem introduced at the end of the present chapter.

The results presented in Subsections 1.2.1 and 1.2.2 are published in [6] respectively [7]. The results reported in Subsections 1.4 and 4.1 are published in [1]. The results reported in Chapter 2 and Chapter 3 constitute the main part of the paper in preparation [2]. The results reported in Section 4.2 are part of the paper in preparation [3].

1.1 Two important ingredients

In this section we present two ingredients that were of great importance in the research presented in this thesis.

The first one, the notion of monodromy group associated to a certain Riemann surface, will be fundamental in proving most of the results reported in Chapter 3 and, as we will see, is one of the main instruments we use to explain transitions from regular to irregular motions for dynamical systems.

The second one, the *so-called* trick, was one of the fundamental ideas used to construct (whenever they were new) and to study the many-body problems presented in this work and many others, particularly the Aristotelian model that we will introduce in Section 1.4 and that we will analyze in detail in the next three chapters. Via the trick, we arrive to prove many results, like the isochronicity (for certain initial conditions) of the models to which it is applicable.

1.1.1 Riemann surfaces and monodromy groups

In this section we briefly describe the idea of Riemann surface and of monodromy group. As it will be clear in the next sections, these concepts play a fundamental role in the work presented in this thesis. We begin with two examples to illustrate the concept of monodromy group. The first example is given by the following second order ODE

$$\tau^2 \zeta''(\tau) + \frac{1}{6} \tau \zeta'(\tau) + \frac{1}{6} \zeta = 0 \quad , \quad (1.1)$$

in which the apices indicate differentiation with respect to τ . For this equation, we write the following ordered basis of the solution space

$$B_1 = \left\{ \tau^{\frac{1}{2}}, \tau^{\frac{1}{3}} \right\} \quad . \quad (1.2)$$

Both elements of the basis B_1 have a branch point in the origin of the complex τ -plane, respectively a branch point of order 1 and a branch point of order 2. We can continue the two function $\tau^{1/2}$ and $\tau^{1/3}$ analytically in the complex τ -plane around 0. If we do this along any positively oriented (i.e. anticlockwise) single closed path γ that includes the origin, then, after a complete loop, B_1 becomes

$$\tilde{B}_1 = \left\{ -\tau^{\frac{1}{2}}, e^{\frac{2\pi i}{3}} \tau^{\frac{1}{3}} \right\} \quad . \quad (1.3)$$

The effects of the path γ on B_1 can be represented by left multiplication with the following (2×2) matrix

$$g_1 = \begin{pmatrix} -1 & 0 \\ 0 & e^{\frac{2\pi i}{3}} \end{pmatrix}, \quad \tilde{B}_1 = g_1 \cdot B_1 \quad . \quad (1.4)$$

Each closed path γ around the origin in the complex τ -plane gives rise to a matrix representing the change of basis from B_1 . Such a matrix equals g_1^n , where n is the winding number of the path γ around 0 (i.e. the number of times γ effectively loops around the origin, counting positively the complete anticlockwise loops and negatively the complete clockwise loops around the origin). All matrices that are obtained in this way form a group, which is generated by g_1 . This group is known as the *monodromy group* of equation (1.1). Notice that $g_1^6 = g$, so equation (1.1) has a finite monodromy group of order 6.

The second example is given by the following second order ODE, similar to the previous equation (1.1):

$$\tau^2 \zeta''(z) - \tau \zeta'(\tau) + \zeta = 0 \quad , \quad (1.5)$$

Also in this case we can write an ordered basis of the solution space

$$B_2 = \{z, z \log(\tau)\} \quad . \quad (1.6)$$

The solution $\tau \log(\tau)$ is not algebraic. As before, we can consider the analytical continuation of the basis B_2 along any positively oriented closed path γ in the complex τ -plane around the origin. Such a path transforms the basis B_2 into

$$\tilde{B}_2 = \{\tau, \tau \log(\tau) + 2\pi i k \tau\} \quad , \quad (1.7)$$

where $k \in \mathbb{Z}$ is the winding number of γ . Like before, the effects of the path γ on B_2 can be represented by left multiplication with the following (2×2) matrix

$$g_2 = \begin{pmatrix} 1 & 2\pi i k \\ 0 & 1 \end{pmatrix}, \quad \tilde{B}_2 = g_2 \cdot B_2, \quad k \in \mathbb{Z} \quad . \quad (1.8)$$

In this case, the monodromy group of equation (1.5) is infinite.

To be more rigorous, first of all we need to introduce the idea of *Riemann surface*. Following [8], we define a Riemann surface Γ as a one-complex-dimensional connected complex analytic manifold.

A *curve* on Γ means a continuous map c of the closed interval $I = [0, 1]$ into Γ . The point $c(0)$ will be called the *initial point* of the curve, and $c(1)$ will be called the *terminal point* of the curve.

Suppose that P and Q are two points of Γ and c_1 and c_2 are two curves on Γ with initial point P and terminal point Q . We say that c_1 is *homotopic* to c_2 ($c_1 \sim c_2$) provided there is a continuous map $h : I \times I \rightarrow \Gamma$ with the following properties: $h(t, 0) = c_1(t)$, $h(t, 1) = c_2(t)$, $h(0, u) = P$ and $h(1, u) = Q$ for all t and u in $I = [0, 1]$.

Let P be now any point on Γ . We consider all closed curves (loops) on Γ which pass through P , namely all curves on Γ with initial and terminal point P . We say that two such curves, c_1 and c_2 , are *equivalent* whenever they are homotopic.

The set of equivalence classes of closed curves through P forms a group in the following manner: the product of the equivalence class of the curve c_1 with the equivalence class of the curve c_2 is the equivalence class of the curve c_1 followed by c_2 ; the inverse of the equivalence class of the curve $t \mapsto c_t$ is the curve $t \mapsto c(1 - t)$. The group of equivalence classes so constructed is called the *fundamental group of Gamma based at P*.

Let P and Q be any two points on Γ . The isomorphism between the fundamental group of Γ based at P and the fundamental group of Γ based at Q depends only on the homotopy class of the path from P to Q . The *fundamental group of Gamma*, $\pi_1(\Gamma)$, is therefore defined to be the fundamental group of Γ based at P , for any $P \in \Gamma$. The fundamental group $\pi_1(\Gamma)$ is a topological invariant.

The notion of fundamental group is strictly related to the one of monodromy group. Generally speaking, we see that for differential equations a single solution may give further linearly independent solutions by analytic continuation. (Linear) differential equations defined in an open, connected set M in the complex plane (which is a Riemann surface) have a monodromy group, which is a (linear) representation of the fundamental group of M , summarising all the analytic continuations along loops within M (the inverse problem, of constructing the equation, given a representation, is called the Riemann-Hilbert problem).

To explain in more precise terms in which way a monodromy group is a representation of the fundamental group of M , we need to introduce the idea of covering manifold, [9]. The manifold \tilde{M} is said to be a (*ramified*) *covering manifold* of the manifold M provided there is a continuous surjective map $f : \tilde{M} \rightarrow M$, called *covering map*, with the following property: for each $\tilde{P} \in \tilde{M}$ there exist a local coordinate $\tilde{\tau}$ on \tilde{M} vanishing at \tilde{P} , a local coordinate τ on M vanishing at $f(\tilde{P})$ and an integer $n > 0$ such that f is given by $\tau = \tilde{\tau}^n$ in terms of these local coordinates. Here the integer n depends only on the point $\tilde{P} \in \tilde{M}$. If $n > 1$, \tilde{P} is called a *branch point of order $n - 1$* . If $n = 1$, for all points $\tilde{P} \in \tilde{M}$ the cover is called *smooth*.

We say that $f : \tilde{M} \rightarrow M$ is of finite degree n if all points in M have exactly n preimages in \tilde{M} . Be P a point in M and consider the fiber $f^{-1}(P)$ over P . Denote the n points in this fiber $\{\tilde{P}_1, \dots, \tilde{P}_n\}$. Every loop γ in M based at P can be lifted to n paths $\tilde{\gamma}_1, \dots, \tilde{\gamma}_n$, where $\tilde{\gamma}_j$ is the unique lift of γ which has initial point \tilde{P}_j . In other words, $\tilde{\gamma}_j(0) = \tilde{P}_j$ for every j . Next consider the terminal points $\tilde{\gamma}_j(1)$; these also lie over P and indeed form the entire preimage set $f^{-1}(P)$. Hence each is a \tilde{P}_j for some j . We denote the terminal points $\tilde{\gamma}_j(1)$ by $\tilde{P}_{\sigma(j)}$, where the function σ is a permutation of the integer indices $\{1, 2, \dots, n\}$ which depends only on the homotopy class of the loop γ . Therefore we have a group homomorphism $\rho : \pi_1(M, P) \rightarrow \mathcal{S}_n$, where \mathcal{S}_n is the symmetric group of all the permutations on n indices. The *monodromy group* of M is the subgroup of \mathcal{S}_n which is the image of $\pi_1(M)$ through the group homomorphism ρ defined above.

For a many-body model described by a system of differential equations defined in an

open, connected set M in the complex plane we will build the Riemann surface Γ which is the covering manifold of M and then we will study the monodromy group of M (sometimes, we improperly say *the monodromy group of Γ*). We will see how the understanding of such a monodromy group is deeply connected with the comprehension of the dynamical behavior of the model itself.

1.1.2 The trick

To illustrate what the *trick* actually is, we begin with an example. Suppose to have the following autonomous ordinary differential equation of the first order:

$$\zeta''(\tau) = -a (\zeta'(\tau))^2 / \zeta(\tau) , \quad (1.9)$$

with given initial conditions $\zeta(0)$, $\zeta'(0)$ and where a is an arbitrary complex constant. If the independent variable τ is complex, then $\zeta(\tau)$, solution of (1.9), is a complex function of complex variable. Appended primes indicate derivation with respect to the complex “time” variable τ .

Now we set:

$$z(t) = \zeta(\tau) , \quad (1.10a)$$

$$\tau \equiv \tau(t) = \frac{[\exp(i\omega t) - 1]}{i\omega} , \quad (1.10b)$$

where ω is a real constant, whose meaning will be immediately clear. Applying the change of variables (1.10) to equation (1.9) we get

$$\ddot{z}(t) - i\omega\dot{z}(t) = -a (\dot{z}(t))^2 / z(t) . \quad (1.11)$$

Here and in what follows, superimposed dots indicate derivation with respect to the real time variable t , namely the “physical time”. So, equation (1.11) represents the physical evolutionary problem, while (1.9) is an auxiliary problem that we will use to understand the behavior of the solutions of (1.11). Notice that equation (1.11) has the same shape of equation (1.9), except for the additive velocity-proportional term $-i\omega\dot{z}(t)$. The change of variables (1.10) imposes the following relation between the initial conditions $\zeta(0)$, $\zeta'(0)$ and $z(0)$, $\dot{z}(0)$:

$$z(0) = \zeta(0) , \quad \dot{z}(0) = \zeta'(0) . \quad (1.12)$$

When the real time variable t evolves for a period

$$T = \frac{2\pi}{\omega} , \quad (1.13)$$

namely from $t = 0$ to $t = T$, the complex time variable τ moves counterclockwise from $\tau = 0$ to $\tau = 0$ along the closed circular contour \tilde{C} of radius $1/\omega$ and centered in i/ω on the complex τ -plane, see (1.10b). If the functions $\zeta(\tau)$, solutions of (1.9), are *holomorphic* (or just *meromorphic*), as functions of the complex variable τ , inside the circular contour \tilde{C} – or, more precisely, in the circular (closed) disk C defined by the contour \tilde{C} – then the corresponding functions $z(t)$ – namely the corresponding solutions of (1.11) – are *nonsingular* and *periodic* (with period T) with respect to the real time variable t .

If $a \neq -1$, the solution of (1.9) is

$$\zeta(\tau) = [k(1+a)(\tau - \tau_b)]^\gamma , \quad (1.14a)$$

with

$$\gamma = \frac{1}{1+a} , \quad (1.14b)$$

while k and τ_b are constant which depend on the initial conditions $\zeta(0)$, $\zeta'(0)$:

$$k = \zeta'(0) (\zeta(0))^a, \quad \tau_b = -\frac{\zeta(0)}{[(1+a)\zeta'(0)]}. \quad (1.14c)$$

If τ_b falls outside the disk C – namely, if the distance between τ_b and the point i/ω is greater than $1/\omega$ – then, for any value of the arbitrary constant a ($\neq -1$), the function $z(t)$, solution of (1.11), obtained from (1.14) via (1.10),

$$z(t) = \left\{ k(1+a) \left[\frac{\exp(i\omega t) - 1}{i\omega} - \tau_b \right] \right\}^\gamma, \quad (1.15)$$

is *nonsingular* and *periodic* of period T with respect to the real time variable t .

When the only singularity of $\zeta(\tau)$, solution of (1.9), inside the disk C , is a *rational* branch point, then the corresponding solution $z(t)$ of (1.11) is still *periodic* in the real time variable t , but with a bigger period which is an integer multiple of T . So, when τ_b falls inside the disk C – namely, when the distance between τ_b and the point i/ω is less than $1/\omega$ – then we have only two possibilities:

1. if a is a *rational* real number ($\neq -1$), then τ_b is a branch point of exponent γ and the function $z(t)$ – corresponding solution of the equation (1.11) – is still periodic in the real time variable t , but with a period that is an integer multiple of T (for instance, if $a = 2$, then $\gamma = 1/3$ and the period will be $3T$);
2. if a is *not* a *rational* real number, then τ_b is *not* a rational branch point and, if $|1 + i\omega\tau_b| < 1$, then $z(t)$ – corresponding solution of the equation (1.11) – is *not* a periodic function of the real time variable t .

Just for the sake of completeness, we discuss what happens if $a = -1$: in this case the the solution of 1.9 reads as follow:

$$\zeta(\tau) = \zeta(0) \exp(k\tau), \quad (1.16)$$

where k is the same of (1.14c) with $a = -1$. From (1.16) it is easy to convince oneself that, in this case, for any value of the initial conditions, the function $z(t)$ – solution of (1.11) with $a = -1$ – is *nonsingular* and *periodic* of period T in the real time variable t .

We must stress that the analysis presented here and the applicability of the *trick* – namely of a particular change of variable that permits to infer the behavior of the evolution of the solution of a certain differential equation with respect to a real time variable t from the properties and the analytic structure of the solution of another differential equation as a function of a complex variable τ – are generalizable to various families of systems of Newtonian (and Aristotelian) differential equations [5].

For instance, let us consider the family of N -body models, characterized by the following (complex and coupled) equations of motion:

$$\zeta_n'' = F_n(\underline{\zeta}), \quad \zeta_n \equiv \zeta_n(\tau), \quad \underline{\zeta} \equiv (\zeta_1, \dots, \zeta_N), \quad (1.17a)$$

where the N functions $F_n(\underline{\zeta})$ of the N dependent variables ζ_n are *arbitrary* functions, except for the fact that they must satisfy the following scaling property

$$F_n(\lambda \underline{\zeta}) = \lambda^{p+1} F_n(\underline{\zeta}), \quad (1.17b)$$

where p is a non-vanishing integer constant. Analogously to what we have done in the example presented at the beginning of this section, we set:

$$z_n(t) = \exp(i\Omega t) \zeta_n(\tau), \quad (1.18a)$$

$$\tau \equiv \tau(t) = \frac{\exp(ip\Omega t/2) - 1}{ip\Omega/2}, \quad (1.18b)$$

where Ω is a real constant ($p\Omega$ plays the same role of ω in (1.10)). This change of (dependent and independent) variables, (1.18) transforms equation (1.17a) in

$$\ddot{z}_n(t) - i(2 + p/2)\Omega \dot{z}_n - (1 + p/2)\Omega^2 z_n = F_n(\underline{z}), \quad (1.19)$$

$$z_n \equiv z_n(t), \quad \underline{z} \equiv (z_1, \dots, z_N).$$

If the functions $F_n(\underline{z})$ are *analytic* in a neighborhood of $\underline{z} = \underline{0}$, then it is possible to prove [5] that there exists, in a neighborhood of the equilibrium configuration $\underline{z} = \underline{0}$, a sphere of initial data $\underline{z}(0)$, $\dot{\underline{z}}(0)$, of *non-vanishing* measure in the phase space (with $4N$ real dimensions), such that *all* the corresponding solutions of (1.19) are *completely periodic*, with period $T = 2\pi/|\Omega|$ if p is even, and with period $2T = 4\pi i/|\Omega|$ if p is odd (in this case, the solutions are *antiperiodic* with period T , $\underline{z}(t+T) = -\underline{z}(t)$, because of the presence of the prefactor $\exp(i\Omega t)$ in equation (1.18a)). Indeed, the analyticity of the functions $F_n(\underline{\zeta})$ in a neighborhood of $\underline{\zeta} = \underline{\zeta}(0)$ ensure, through the standard (Cauchy) theorem of existence/unicity/analyticity applied to the initial-values problem for the system (1.17), that the solution $\underline{\zeta}(\tau)$, corresponding to the initial data $\underline{\zeta}(0)$, $\underline{\zeta}'(0)$, is an *analytic* function of the complex variable τ inside a disk D centered at $\tau = 0$, whose (non-vanishing) radius ρ depends on the initial data and on the functions F_n . But, if $\rho > 4/|p\Omega|$, see [5], to any τ -*analytic* solution $\underline{\zeta}(\tau)$ of (1.17) inside the disk D there corresponds (via (1.18)) a solution $\underline{z}(t)$ of (1.19) periodic in t (with period T or $2T$). The Calogero-Moser model belongs to this family of many-body problems.

A second example of family of many-body problems to which the trick is applicable is given by the following (complex and coupled) Newtonian equations of motion [5]:

$$\zeta_n'' = \sum_{l,m=1}^N \zeta_l' \zeta_m' F_{nlm}(\underline{\zeta}), \quad \zeta_n \equiv \zeta_n(\tau), \quad \underline{\zeta} \equiv (\zeta_1, \dots, \zeta_N), \quad (1.20)$$

with $F_{nlm}(\underline{\zeta})$ N^3 *arbitrary* functions in the N dependent variables ζ_n . As we did for the example reported at the beginning of this section, we introduce the following change of variables:

$$\underline{z}(t) = \underline{\zeta}(\tau), \quad \tau = \frac{\exp(i\omega t) - 1}{i\omega}, \quad (1.21)$$

where ω is a real constant (which plays the role of ω in (1.10)). One can easily verify that, via (1.21), we can recast equations (1.20) as follows

$$\ddot{z}_n = i\omega \dot{z}_n + \sum_{l,m=1}^N \dot{z}_l \dot{z}_m F_{nlm}(\underline{z}), \quad z_n \equiv z_n(t), \quad \underline{z} \equiv (z_1, \dots, z_N). \quad (1.22)$$

Analogously to the previous case, if the functions $F_{nlm}(\underline{z})$ are *analytic* in a neighborhood of $\underline{z} = \underline{0}$, then it is possible to verify (see [5]) that there exists, in a neighborhood of the equilibrium configuration $\underline{z} = \dot{\underline{z}} = \underline{0}$, a sphere of initial data $\underline{z}(0)$, $\dot{\underline{z}}(0)$, of *non-vanishing* volume in the phase space (having $4N$ real dimensions), such that *all* the corresponding solutions of (1.22) are *completely periodic* with period $T = 2\pi/|\omega|$. Indeed, like in the previous case, the standard (Cauchy) theorem of existence/unicity/analyticity applied to the initial values problem for the system (1.20) ensure that, if the functions $F_{nlm}(\underline{\zeta})$ are *analytic* in a neighborhood of $\underline{\zeta} = \underline{\zeta}(0)$, then the solution $\underline{\zeta}(\tau)$, corresponding to the initial data $\underline{\zeta}(0)$, $\underline{\zeta}'(0)$, is an *analytic* function of the complex variable τ inside a disk D centered at $\tau = 0$, whose non-vanishing radius ρ depends on the initial data and on the functions F_{nlm} . But, if $\rho > 2/|\omega|$, see [5], to any solution $\underline{\zeta}(\tau)$ of (1.20) which is *analytic* in τ inside the disk D there corresponds (via (1.21)) a solution $\underline{z}(t)$ of (1.22) periodic in t , with period $T = 2\pi/|\omega|$. The so-called Goldfish model belongs to this last family of many-body problems.

1.2 Analysis of two many-body problems

In this section we will report the main findings concerning two many-body problems in the plane. In the first subsection we deal with a complex generalization of the well-known Calogero-Moser model, while in the second subsection, we treat the so-called Goldfish model. Most of the results discussed in both cases derive from the application of the trick presented in the previous subsection. It is worth noting that these two models are just two examples of the great number of models to which the trick was actually applied. A list of recent publications in which the phenomenology related to the use of the trick is explored and/or exploited reads as follows [5] [10] [11] [12] [13] [14] [15] [16] [17] [18] [19] [20] [21] [22] [23] [24] [25] [26] [27] [28] [29] [30] [31] [32] [33] [34] [35] [36] [37] [38] [39] [40] [41]. Both models were studied via numerical and analytical techniques and our presentation follows in detail the content of two articles, of which the author of this thesis is a coauthors (see respectively [6] and [7]).

Here the trick is mainly used to derive a result of isochronicity of the solutions of the models for certain (open) sets of initial conditions. But the numerical and theoretical study of the implications of such a simple change of variables opened the way to the discoveries of a rich dynamical behavior which could be qualitatively explained by describing the analytical structure of the solutions of the corresponding models.

As we already showed in Subsection 1.1.2, the trick permits to associate to a “physical” model, which evolves with respect to a real time variable t , an “auxiliary” model, which evolves with respect to a complex time variable τ . In both the examples presented in this section we stopped at the qualitative analysis of the Riemann surfaces associated to the solutions of the “auxiliary” problem, pointing out that a complete comprehension of the structure of such a Riemann surface would lead us to a complete comprehension of the dynamical behavior of the “physical” problem; we moreover stressed the general validity of this idea as a tool to explain the transition from regular to irregular motions for many dynamical systems that manifest sensitive dependence on the initial conditions. The findings presented in this section motivated us to construct the “simple” many-body problem presented in Section 1.4, whose dynamical behavior is clearly explainable in terms of the complete description of a multi-sheeted (possibly *infinitely*-sheeted) Riemann surface associated to the solutions.

1.2.1 The Calogero-Moser many-body problem

In this section we analyze, in the *complex* domain, the dynamical system characterized by the Newtonian equations of motion

$$\ddot{z}_n + z_n = \sum_{m=1, m \neq n}^N g_{nm} (z_n - z_m)^{-3},$$

$$z_n \equiv z_n(t), \quad \dot{z}_n \equiv \frac{dz_n(t)}{dt}, \quad n = 1, \dots, N \quad (1.23)$$

which obtain in the standard manner from the Hamiltonian

$$H(\underline{z}, \underline{p}) = \frac{1}{2} \sum_{n=1}^N (p_n^2 + z_n^2) + \frac{1}{4} \sum_{n,m=1, n \neq m}^N g_{nm} (z_n - z_m)^{-2}, \quad (1.24a)$$

provided (as we hereafter assume)

$$g_{nm} = g_{mn}. \quad (1.24b)$$

Here and below N is an arbitrary positive integer ($N \geq 2$), the indices n, m run from 1 to N unless otherwise indicated, underlined quantities are N -vectors, say $\underline{z} \equiv (z_1, \dots, z_N)$, and

all quantities (namely, the N “canonical coordinates” z_n , the N “canonical momenta” p_n , the $N(N-1)/2$ “coupling constants” g_{nm}) are *complex*, while the independent variable t (“time”) is instead *real*. Of course the N complex equations of motion (1.23) can be reformulated [1] as $2N$ real — and as well Hamiltonian [2] — equations of motion, by introducing the real and imaginary parts of the coordinates z_n , $z_n \equiv x_n + iy_n$, or their amplitudes and phases, $z_n \equiv \rho_n \exp(i\theta_n)$:

$$\begin{aligned} \ddot{x}_n + x_n &= \sum_{m=1, m \neq n}^N r_{nm}^{-6} [a_{nm} x_{nm} (x_{nm}^2 - 3y_{nm}^2) - b_{nm} y_{nm} (y_{nm}^2 - 3x_{nm}^2)] \\ &= \sum_{m=1, m \neq n}^N r_{nm}^{-3} |g_{nm}| \cos(\gamma_{nm} - 3\theta_{nm}), \end{aligned} \quad (1.25a)$$

$$\begin{aligned} \ddot{y}_n + y_n &= \sum_{m=1, m \neq n}^N r_{nm}^{-6} [a_{nm} y_{nm} (y_{nm}^2 - 3x_{nm}^2) - b_{nm} y_{nm} (x_{nm}^2 - 3y_{nm}^2)] \\ &= \sum_{m=1, m \neq n}^N r_{nm}^{-3} |g_{nm}| \sin(\gamma_{nm} - 3\theta_{nm}), \end{aligned} \quad (1.25b)$$

where of course

$$\begin{aligned} z_n &= x_n + iy_n, \\ z_{nm} \equiv z_n - z_m &= x_n - x_m + i(y_n - y_m) \equiv x_{nm} + iy_{nm} = r_{nm} \exp(i\theta_{nm}), \\ g_{nm} &= a_{nm} + ib_{nm} = |g_{nm}| \exp(i\gamma_{nm}). \end{aligned} \quad (1.25c)$$

We shall return to the motivations for this choice to investigate the system (1.23) in the complex domain at the end of this section.

If all the coupling constants coincide, $g_{nm} = g$, the Hamiltonian system (1.23) is a well-known *completely integrable* many-body model (see for instance [5] and the references quoted there), and *all* its nonsingular solutions are *completely periodic* with period 2π , or possibly an integer multiple of 2π . (Indeed, in this *integrable* case the N coordinates $z_n(t)$ can be identified with the N zeros of a polynomial of degree N the coefficients of which are periodic in t with period 2π , so that the set of these N zeros is also periodic with period 2π , and each individual zero is therefore also periodic, although possibly with a larger period which is an integer multiple of 2π due to a possible reshuffling of the zeros as the motion unfolds; in the *real* case with all coupling constants *equal* and *positive*, $g_{nm} = g > 0$, when the motions are confined to the real axis and no such reshuffling can occur due to the singular and repulsive character of the two-body forces, *all* real solutions are *nonsingular* and *completely periodic* with period 2π , $\underline{z}(t+2\pi) = \underline{z}(t)$; see for instance [5]). Here we focus instead on the more general case with *completely arbitrary* coupling constants g_{nm} , which is generally believed *not* to be integrable. But even in this case — as proven in [12] — there does exist a domain of initial data $\underline{z}(0)$, $\dot{\underline{z}}(0)$ having *infinite* measure in phase space such that *all* the trajectories originating from it are *completely periodic* with period 2π , $\underline{z}(t+2\pi) = \underline{z}(t)$. As pointed out in [12], this is a somewhat surprising finding, inasmuch as it negates the expectation that, for a generic nonlinear dynamical system with several degrees of freedom that possesses completely periodic trajectories emerging from some specific initial data, any generic variation of these initial data destroys the complete periodicity of the trajectories or at least changes their period.

But, as shown in [12], this fact is a rather elementary consequence of the approach based on the “trick” introduced in Subsection 1.1.2 and rather extensively used recently to evince analogous results (see [5], the references quoted there, as well as [30, 11, 7] and the next subsection). This same trick can as well be exploited to investigate the remaining solutions,

namely those not belonging to the class of *completely periodic* solutions with period 2π the existence of which was proven in [12]. This was done in [6], where we also confirmed the insight thereby gained by exhibiting numerical solutions of (1.23) performed via a computer code created by the author of this thesis [42]. In particular we demonstrated the existence of open domains of initial data, having *nonvanishing* measures in the phase space of such data, which also yield *completely periodic* solutions, but with periods which are *integer multiples* of 2π , and we also elucidated the mechanism that originates *non-periodic* and *irregular* dynamics.

Why investigate the motion determined by the Newtonian equations (1.23) in the *complex*, rather than the *real*, domain? A clear hint that, at least from a mathematical point of view, this is a more natural environment to work in, comes already from the treatment of (1.23) in the *integrable* case with *equal* coupling constants, $g_{nm} = g$, since, as mentioned above, it is then appropriate to identify the N particle positions $z_n \equiv z_n(t)$ with the N zeros of a time dependent (monic) polynomial of degree N in z , say $P_N(z, t)$ such that $P_N[t, z_n(t)] = 0$ (see for instance [5]); and clearly the natural environment to investigate the zeros of a polynomial is the *complex* plane rather than the *real* line. In this context, as we anticipated in the previous section, an essential motivation to work in the complex comes from the important role that analyticity properties play in our treatment. Moreover motions roaming over the complex plane display a much richer dynamics than those restricted to the real line, especially in the case with singular interparticle forces, because of the possibility in the former case, but not in the latter, that particles go around each other. And it is then natural to re-interpret the (*complex*) N -body problem (1.23) as describing the (*real*) motion of N particles (*in the plane*), by introducing a one-to-one correspondence among the complex coordinates $z_n \equiv x_n + iy_n$, see (1.25c), and the real two-vectors in the plane $\vec{r}_n \equiv (x_n, y_n)$. But this approach, that is quite convenient to identify interesting many-body problems in the plane (see Chapter 4 of [5]), suffers in the present case from a drawback: the resulting many-body problem in the plane is not rotation-invariant, see (1.25)¹.

Instead of applying directly the trick to the system of ODEs (1.23), we firstly rewrite, mainly for notational convenience, these equations of motion, (1.23), as follows:

$$\ddot{z}_n + \omega^2 z_n = \sum_{m=1, m \neq n}^N g_{nm} (z_n - z_m)^{-3}, \quad (1.26a)$$

and we note that the corresponding Hamiltonian reads

$$H(\underline{z}, \underline{p}) = \frac{1}{2} \sum_{n=1}^N (p_n^2 + \omega^2 z_n^2) + \frac{1}{4} \sum_{n,m=1, n \neq m}^N g_{nm} (z_n - z_m)^{-2}. \quad (1.26b)$$

Here we introduce the additional constant ω , which is hereafter assumed to be *positive*, $\omega > 0$, and to which we associate the basic period

$$T = 2\pi/\omega. \quad (1.27)$$

In the following it will sometimes be convenient to set $\omega = 1$ so that (1.26a) coincide with (1.23) and the basic period becomes $T = 2\pi$, or to set instead $\omega = 2\pi$ so that the basic period becomes unity, $T = 1$. Of course these cases are all related via a rescaling of the dependent and independent variables, since clearly by setting

$$\tilde{z}(\tilde{t}) = az(t), \quad \tilde{t} = bt, \quad \tilde{\omega} = \omega/b, \quad \tilde{g}_{nm} = (a^2/b)^2 g_{nm} \quad (1.28a)$$

¹Actually, there is a simple trick to skip this problem, see [5]

with a, b two *positive* rescaling constants which can be chosen at our convenience, the ODEs (1.26a) get reformulated in a completely analogous “tilded” version,

$$\tilde{z}_n'' + \tilde{\omega}^2 \tilde{z}_n = \sum_{m=1, m \neq n}^N \tilde{g}_{nm} (\tilde{z}_n - \tilde{z}_m)^{-3}, \quad (1.28b)$$

where of course here the primes indicate differentiations with respect to the argument of the function they are appended to, $\tilde{z}' \equiv d\tilde{z}(\tilde{t})/d\tilde{t}$. Note in particular that by setting $b = a^2 = \omega$ one gets $\tilde{\omega} = 1$, $\tilde{g}_{nm} = g_{nm}$, namely the tilded version (1.28b) reproduces essentially (1.23).

Now, the “trick”. Let us set

$$z_n(t) = \exp(-i\omega t) \zeta_n(\tau), \quad (1.29a)$$

$$\tau \equiv \tau(t) = [\exp(2i\omega t) - 1]/(2i\omega). \quad (1.29b)$$

As can be readily verified, this change of (dependent and independent) variables, (1.29), transforms (1.26a) into

$$\zeta_n'' = \sum_{m=1, m \neq n}^N g_{nm} (\zeta_n - \zeta_m)^{-3}. \quad (1.30)$$

Here and below appended primes denote derivatives with respect to the new independent variable τ , while of course the dots in (1.26a) and below denote as usual derivatives with respect to the *real* time t .

The change of variables (1.29) entails the following relations among the initial data, $\underline{z}(0)$, $\dot{\underline{z}}(0)$, respectively $\underline{\zeta}(0)$, $\underline{\zeta}'(0)$, for (1.26a) respectively (1.30):

$$z_n(0) = \zeta_n(0), \quad (1.31a)$$

$$\dot{z}_n(0) = \zeta_n'(0) - i\omega \zeta_n(0). \quad (1.31b)$$

We now observe that, as the (real, “physical time”) variable t varies from 0 to $T/2 = \pi/\omega$, the (complex) variable τ travels (counterclockwise) full circle over the circular contour \tilde{C} , the diameter of which, of length $1/\omega = T/(2\pi)$, lies on the upper-half of the complex τ -plane, with its lower end at the origin, $\tau = 0$, and its upper end at $\tau = i/\omega$. Hence if the solution $\underline{\zeta}(\tau)$ of (1.30) which emerges from some assigned initial data $\underline{\zeta}(0)$, $\underline{\zeta}'(0)$ is *holomorphic*, as a (N -vector-valued) function of the complex variable τ , in the closed circular disk \mathbb{C} encircled by the circle \tilde{C} in the complex τ -plane, then the corresponding solution $\underline{z}(t)$ of (1.26a), related to $\underline{\zeta}(\tau)$ by (1.29), is *completely periodic* in t with period T , $\underline{z}(t+T) = \underline{z}(t)$ (see (1.27); and note that $\underline{\zeta}(\tau)$, considered as function of the *real* variable t , is then *periodic* with period $T/2$, but $\underline{z}(t)$ is instead *antiperiodic* with period $T/2$, $\underline{z}(t+T/2) = -\underline{z}(t)$, due to the prefactor $\exp(-i\omega t)$, see (1.29a)).

In [12] it was proven that there indeed exists a domain, having *infinite* measure in phase space, of initial data $\underline{\zeta}(0)$, $\underline{\zeta}'(0)$ such that the corresponding solutions $\underline{\zeta}(\tau)$ of (1.30) are *holomorphic* in τ in the disk \mathbb{C} — and this fact implies the existence of an open domain, having as well *infinite* measure in phase space, of corresponding initial data $\underline{z}(0)$, $\dot{\underline{z}}(0)$ such that the corresponding solutions $\underline{z}(t)$ of (1.26a) are *completely periodic* with period T , $\underline{z}(t+T) = \underline{z}(t)$. In [6] it was proven that the singularities of the solutions $\underline{\zeta}(\tau)$ of (1.30) — considered as functions of the complex variable τ — are *branch points* of *square-root* type, and it was possible to infer from this that, whenever the solution $\underline{\zeta}(\tau)$ of (1.30) has a *finite* number of such branch points *inside* the circle \tilde{C} — generally nested inside each other, namely occurring on different Riemann sheets — then the corresponding solution $\underline{z}(t)$ of (1.26a), considered as a function of the *real* “time” variable t , is again *completely periodic*, albeit now with a period which is an *integer multiple* of T . We also infer that when instead the solution $\underline{\zeta}(\tau)$ of (1.30) has an *infinite* number of such *square-root* branch points *inside*

the circle \tilde{C} — again, generally nested inside each other, namely occurring on different Riemann sheets — then the corresponding solution $\underline{z}(t)$ of (1.26a), considered again as a function of the *real* “time” variable t , may be *not periodic* at all indeed its behavior is generally so *irregular* to make one thinking of a *chaotic* dynamics (we will be more rigorous and explicit about this important point for what concerns the new many-body model we introduce at the end of this chapter).

We know of course that, if a solution $\underline{\zeta}(\tau)$ of (1.30) is holomorphic as a function of the complex variable τ *inside* the circle \tilde{C} — and we know that such solutions do exist, in fact in the context of the initial-value problem they emerge out of a set of initial data which has *infinite* measure in the phase space of such data [12] — then the solution $\underline{z}(t)$ of (1.26a) that corresponds to it via (1.29) is *completely periodic* with period T , see (1.27),

$$z_n(t + T) = z_n(t). \quad (1.32a)$$

But the transformation (1.29) actually implies an additional information, namely that in this case $\underline{z}(t)$ is *completely antiperiodic* with period $T/2$,

$$z_n(t + T/2) = -z_n(t). \quad (1.32b)$$

Let us instead assume that a branch point of a solution $\underline{\zeta}(\tau)$ of (1.30), occurring, say, at $\tau = \tau_b$, does fall *inside* the circle \tilde{C} in the complex τ -plane. Then, as we proved in [6], due to the *square-root* nature of this branch point, the evolution of the solution $\underline{\zeta}(\tau)$ of (1.30) as the *real* time variable t unfolds is obtained by following the *complex* time-like variable τ as it travels (1.29) along the circular contour \tilde{C} on a *two-sheeted* Riemann surface. Clearly the change of variable (1.29a), (1.29b) entails then that the corresponding solution $\underline{z}(t)$ of (1.26a) is just as well *completely periodic* with period T , see (1.32a), although in this case (1.32b) does no more hold. And of course this conclusion holds provided *only one* branch point of the solution $\underline{\zeta}(\tau)$ of (1.30) falls inside the circle \tilde{C} in the main sheet of the Riemann surface associated with this solution, and *no other* branch point occurs inside the circle \tilde{C} in the second sheet of this Riemann surface, namely on the sheet entered through the cut associated with the branch point occurring inside \tilde{C} on the main sheet of the Riemann surface (of course this Riemann surface might feature many other sheets associated with other branch points occurring elsewhere hence not relevant to our present discussion).

Let us now continue this analysis by considering, more generally, a solution $\underline{\zeta}(\tau)$ of (1.30) that possibly contains more than one branch point inside the circle \tilde{C} in the main sheet of its Riemann surface (that do not cancel each other) so that by travelling along the circle \tilde{C} *several* additional Riemann sheets are accessed from the main sheet, and let us moreover assume that, on these additional sheets, *additional* branch points possibly occur inside the circle \tilde{C} which give access to other sheets, and that possibly on these other sheets there be *additional* branch points and so on. Let in conclusion B be the *total number* of *additional* sheets accessed by a point travelling around and around on the circle \tilde{C} on the Riemann surface associated with the solution $\underline{\zeta}(\tau)$ of (1.30). This number B might coincide with the total number of branch points occurring, inside the circle \tilde{C} , on this Riemann surface — on all its sheets — or it might be smaller. Indeed, since each of these branch points is of *square-root* type, each of the associated cuts — if entered into — gives access to *one additional* sheet. But not all these sheets need be accessed; the total number B that are actually accessed depends on the structure of the Riemann surface, for instance no *additional* sheet at all is accessed if there is no branch point on the *main* sheet of the Riemann surface — even though other branch points may be present inside the circle \tilde{C} on other sheets of the Riemann surface associated with the solution $\underline{\zeta}(\tau)$ of (1.30). (It might also be possible that different branch points cancel each other pairwise as is the case for two branch points that are on the same sheet inside the circle \tilde{C} and generate a cut that starts at one of them

and ends at the other). In any case the overall time requested for the point $\tau(t)$ travelling on the Riemann surface to return to its point of departure (say, $\tau(0) = 0$ on the *main* sheet) is $(B + 1)T/2$, since a half-period $T/2$, see (1.29b), is required to complete a tour around the circle \tilde{C} on each sheet, and the number of sheets to be travelled before getting back to the point of departure is overall $B + 1$ (including the *main* sheet). Hence in this case, as the real time t evolves, the solution $\zeta(\tau)$ of (1.30), considered as a function of t , shall be *completely periodic* with period $(B + 1)T/2$. Hence (see (1.29)) if B is *even* the corresponding solution $\underline{z}(t)$ of (1.26a) will be *completely antiperiodic* with the same period $(B + 1)T/2$, $\underline{z}[t + (B + 1)T/2] = -\underline{z}(t)$, and *completely periodic* with the “odd” period $(B + 1)T$, $\underline{z}[t + (B + 1)T] = \underline{z}(t)$. If instead B is *odd*, the solution $\zeta(\tau)$ of (1.30) as well as the corresponding solution $\underline{z}(t)$ of (1.26a) will both be *completely periodic* in t with the period $(B + 1)T/2$ (which might be “even” or “odd” — of course, as an integer multiple of the basic period T), $\underline{z}[t + (B + 1)T/2] = \underline{z}(t)$ (so, in this case, the trajectories of $\underline{z}(t)$ will display no symmetry, in contrast to the previous case).

In this analysis the assumption was implicitly understood that the total number B of *additional* sheets accessed by travelling round and round on the circle \tilde{C} on the Riemann surface associated with the solution $\zeta(\tau)$ of (1.30) be *finite* (a number B which, as we just explained, might coincide with, or be smaller than, the total number of branch points of that Riemann surface that are located *inside* the circle \tilde{C} in the complex τ -plane); and moreover we implicitly assumed that no branch point occur exactly on the circle \tilde{C} . Let us now elaborate on these two points.

If a branch point τ_b occurs exactly on the circle \tilde{C} so that the cut associated with it is actually traversed when travelling around on the circle \tilde{C} , opening the way to new sheets, then the “physical” equations of motion (1.26a) become singular, due to a particle collision occurring at the *real* time t_c defined mod $(T/2)$ (see (1.27)) by the formula

$$\tau_b = [\exp(2i\omega t_c) - 1]/(2i\omega). \quad (1.33)$$

Indeed it is easy to check via (1.29) that the condition that t_c be *real* coincides with the requirement that the corresponding value of τ_b , as given by (1.33), fall just on the circular contour \tilde{C} in the complex τ -plane. The singularity is of course due to the divergence, at the collision time $t = t_c$, of the right-hand side of the equations of motion (1.26a); in [6] we showed that there is however no corresponding divergence of the solution $\underline{z}(t)$, which rather has a branch point of *square root* type at $t = t_c$. But of course this entails that the speeds of the colliding particles diverge at the collision time $t = t_c$ proportionally to $|t - t_c|^{-1/2}$, and their accelerations diverge proportionally to $|t - t_c|^{-3/2}$.

There is no *a priori* guarantee that the number of branch points inside \tilde{C} of a solution $\zeta(\tau)$ of (1.30) be *finite*, nor that the number B of *additional* sheets accessed according to the mechanism described above by moving around the circle \tilde{C} on the Riemann surface associated with that solution $\zeta(\tau)$ of (1.30) be *finite* (of course B might be *infinite* only if the number of branch points inside \tilde{C} is itself *infinite*). Obviously in such a case ($B = \infty$), although the complex number $\tau \equiv \tau(t)$, see (1.29b), considered as a function of the *real* “time” variable t , is still periodic with period $T/2$, neither the solution $\zeta(\tau)$ of (1.30), nor the corresponding solution $\underline{z}(t)$ of (1.26a), will be periodic. The question that might then be raised is whether such a solution — in particular, such a solution $\underline{z}(t)$ of the “physical” Newtonian equations of motion (1.23) corresponding to the many-body problem characterized by the Hamiltonian (1.24a) — displays a “chaotic” behavior, namely, in the context of the initial-value problem, a “sensitive dependence” on the initial data. We shall return to this question below.

So far we have discussed the relation among the analytic structure of a solution $\zeta(\tau)$ of (1.30) and the corresponding solution $\underline{z}(t)$ of (1.26a). Let us now return to the simpler cases considered at the very beginning of this analysis and let us consider how the *transition*

from one of the two regimes described there to the other occurs in the context of the initial-value problem for (1.26a), and correspondingly for (1.30), see (1.31). Hence let us assume again that the initial data for (1.26a), and correspondingly for (1.30) (see (1.31)), entail that no branch point of the corresponding solution $\underline{\zeta}(\tau)$ of (1.30) occurs *inside* the circular contour \tilde{C} on the *main* sheet of the associated Riemann surface, so that the corresponding solution $\underline{z}(t)$ of (1.26a) satisfies both (1.32a) and (1.32b). Let us imagine then to modify with continuity the initial data, for instance by letting them depend on an appropriate scaling parameter. As a consequence the branch points of the solution $\underline{\zeta}(\tau)$ of (1.30) move, and the Riemann surface associated to this solution $\underline{\zeta}(\tau)$ of (1.30) gets accordingly modified. We are interested in a movement of the branch points which takes the closest one of them on the *main* sheet of the Riemann surface from outside to inside the circle \tilde{C} . In the process that branch point will cross the circle \tilde{C} , and the particular set of initial data that correspond to this happening is then just a set of initial data that entails the occurrence of a collision in the time evolution of the many-body problem (1.26a), occurring at a *real* time $t = t_c$ defined by (1.33), as discussed above. After the branch point has crossed the contour \tilde{C} and has thereby entered inside the circular disk \mathbb{C} , the corresponding solution $\underline{z}(t)$ of (1.26a) is again collision-free but its periodicity properties are changed. One might expect that the new solution continue then to satisfy (1.32a) but cease to satisfy (1.32b). This is indeed a possibility, but it is not the only one. Indeed, since the time evolution of the solution $\underline{z}(t)$ of (1.26a) obtains via (1.29) by following the time evolution of the corresponding solution $\underline{\zeta}(\tau)$ of (1.30) as the point $\tau \equiv \tau(t)$ goes round the circle \tilde{C} on the Riemann surface associated with that solution, the occurrence of a branch point *inside* the circle \tilde{C} on the *main* sheet of that Riemann surface entails that the access is now open to a second sheet, and then possibly to other sheets if, on that second sheet, there also are branch points inside the circle \tilde{C} . If this latter possibility does not occur, namely if on that second sheet there are no branch points inside the circle \tilde{C} , then indeed there occurs for the corresponding solution $\underline{z}(t)$ of (1.26a) a transition from a periodicity property characterized by the validity of both (1.32a) and (1.32b), to one characterized by the validity of (1.32a) but not of (1.32b). If instead there is at least one branch point in the second sheet inside the circle \tilde{C} , then the periodicity — if any — featured after the transition by the solution $\underline{z}(t)$ of (1.26a) depends, as discussed above, on the number B of sheets that are sequentially accessed before returning — if ever — to the *main* sheet.

To simplify our presentation we have discussed above the *transition* process by taking as point of departure for the analysis the *basic periodic solution* — that characterized by the validity of both (1.32a) and (1.32b), the existence of which has been demonstrated in [12]— and by discussing how a continuous modification of the initial data may cause a transition to a different regime of periodicity, with the transition occurring in correspondence to the special set of initial data that yields a solution characterized by a particle collision, namely a set of initial data for which the Newtonian equations of motion become singular at a finite *real* time t_c (defined mod($T/2$)). But it is clear that exactly the same mechanism accounts for every transition that occurs from a solution $\underline{z}(t)$ of (1.26a) characterized by a type of periodicity to a solution $\underline{z}(t)$ of (1.26a) characterized by a different periodicity regime — or by a lack of periodicity.

The final point to be discussed is the question we postponed above, namely the character of the *nonperiodic* solutions $\underline{z}(t)$ of (1.26a) (if any), which we now understand to be characterized, in the context of the mechanism described above, by access to an endless sequence of different sheets — all of them generated by branch points of *square-root* type — of the Riemann surface associated with the corresponding solution $\underline{\zeta}(\tau)$ of (1.30). The following two possibilities can be imagined in this connection — which of course does not entail they are indeed both realized.

The first possibility — which we surmise to be the most likely one to be actually realized

— is that an *infinity* of such relevant branch points occur quite closely to the circular contour \tilde{C} , hence that there be some of them that occur arbitrarily close to \tilde{C} . This then entails that the corresponding *nonperiodic* solutions $\underline{z}(t)$ of (1.26a) manifest a *sensitive dependence* on their initial data (which we consider to be the signature of a *chaotic* behavior). Indeed a modification, however small, of such initial data entails a modification of the pattern of such branch points, which shall cause some of them to cross over from one to the other side of the circular contour \tilde{C} . But then the two solutions $\underline{z}(t)$ of (1.26a) corresponding to these two assignments of initial data — before and after the modification, however close these data are to each other — will eventually evolve *quite differently*, since their time evolutions are determined by access to two *different* sequences of sheets of the Riemann surfaces associated with the two corresponding solutions $\underline{\zeta}(\tau)$ of (1.30) — two Riemann surfaces which themselves need not be very different (to the extent one can make such statements when comparing two objects having as complicated a structure as a Riemann surface with an *infinite* number of sheets produced by an *infinite* number of branch points of *square-root* type). So this is the mechanism whereby a *complicated* and *non-periodic* behavior may develop for the system (1.23) — but of course not in the *integrable* case with equal coupling constants (in that case, as mentioned above, the number of branch points of the solutions $\underline{\zeta}(\tau)$ of (1.30) is always *finite*, since the N coordinates $\zeta_n(\tau)$ are in this case the N zeros of a polynomial of degree N the coefficients of which are polynomials in the variable τ [5]). Note that the emergence of such a complex dynamics would not be associated with a local exponential divergence of trajectories in phase space — it would be rather analogous to the mechanism that causes a chaotic behavior in the case of, say, a triangular billiard with angles which are irrational fractions of π — a complex dynamics also not due to a local separation of trajectories in phase space, but rather to the eventual emergence of a different pattern of reflections (indeed of any two such billiard trajectories, however close their initial data, one shall eventually miss a reflection near a corner which the other one does take, and from that moment their time evolutions become quite different).

A different possibility, which we consider unlikely but we cannot *a priori* exclude at this stage of our analysis, is that *nonperiodic* solutions $\underline{z}(t)$ of (1.26a) exist which are associated with a Riemann surface of the corresponding solutions $\underline{\zeta}(\tau)$ of (1.30) that, even though it possesses an *infinite* number of relevant branch points inside the circular contour \tilde{C} , it features all of them — or at least most of them, except possibly for a *finite* number of them — located in a region well inside \tilde{C} , namely separated from it by an annulus of *finite* thickness. Clearly in such a case two *nonperiodic* solutions $\underline{z}(t)$ of (1.26a) which emerge from sufficiently close initial data separate slowly and gradually throughout their time evolution, hence they do *not* display a *sensitive dependence* on their initial data — hence, in such a case there would be solutions which are *nonperiodic* (nor, of course, multiply periodic) but which nevertheless do not display a *chaotic* behavior — or, to be more precise, there would be sets of initial data, having nonvanishing measure in the phase space of initial data, which yield such *nonperiodic* (yet *nonchaotic*) solutions.

As an example of the dynamics generated by the model (1.26a), we display in Figure 1.2 a numerical solution of the Newtonian equations of motion (1.26a), obtained with the numerical integration software MBS [42], with $\omega = 2\pi$ — hence $T = 1$ (see (1.27)) — characterized by the following parameters:

$$N = 3; \quad g_{12} = g_{21} = 10, \quad g_{23} = g_{32} = 3, \quad g_{31} = g_{13} = -10. \quad (1.34)$$

The sequence of motions which appears in Figure 1.2 is characterized by sets of initial data linked to each other by the formulas

$$x_n(0) = \lambda^{-1}x_n^{(0)}, \quad y_n(0) = \lambda^{-1}y_n^{(0)}, \quad (1.35a)$$

$$\dot{x}_n(0) = \lambda\dot{x}_n^{(0)} - 2\pi(\lambda - \lambda^{-1})y_n^{(0)}, \quad \dot{y}_n(0) = \lambda\dot{y}_n^{(0)} + 2\pi(\lambda - \lambda^{-1})x_n^{(0)}, \quad (1.35b)$$

λ	0.5	1	1.2	1.5	2	2.2	2.5	3	3.5	4
Period	1	1	HSL	HSL	14	14	17	17	17	17
Symmetry	Yes	No	—	—	No	Yes	Yes	Yes	Yes	Yes
Figure 1.2	a	b	—	c	d	—	—	—	e	—

λ	4.05	4.15	4.2	4.5	5	10	18	20	30	50
Period	17	10	9	7	7	7	7	7	7	7
Symmetry	Yes	No	No	No	No	Yes	Yes	Yes	Yes	Yes
Figure 1.2	—	f	g	—	h	—	i	—	—	—

Figure 1.1: Different values of the period in terms of λ

of course with $z_n \equiv x_n + iy_n$. Here λ is a *positive* rescaling parameter the different values of which identify different sets of initial data (while the data $x_n^{(0)}$, $y_n^{(0)}$, $\dot{x}_n^{(0)}$, $\dot{y}_n^{(0)}$ are kept fixed). For the example shown in Figure 1.2 we choose the following values of the parameters $x_n^{(0)}$, $y_n^{(0)}$, $\dot{x}_n^{(0)}$, $\dot{y}_n^{(0)}$ characterizing the initial data via (1.35):

$$\begin{aligned}
 x_1^{(0)} &= 1, & y_1^{(0)} &= 0, & \dot{x}_1^{(0)} &= 0, & \dot{y}_1^{(0)} &= 2, \\
 x_2^{(0)} &= 0, & y_2^{(0)} &= 1, & \dot{x}_2^{(0)} &= 4, & \dot{y}_2^{(0)} &= 0, \\
 x_3^{(0)} &= 0.5, & y_3^{(0)} &= 0.5, & \dot{x}_3^{(0)} &= -0.5, & \dot{y}_3^{(0)} &= 1.
 \end{aligned} \tag{1.36}$$

Notice that the trajectories of particle 1, 2 respectively 3 are shown in red, green, respectively blue. In the following table we indicate, for different values of λ , the corresponding observed periods of the numerical simulation and (in the last row) the corresponding images in Figure 1.2. When the numerical simulation seems to be *non-periodic* (suggesting an *irregular*, potentially *chaotic*, dynamics) we use the acronym HSL, which stands for “Hic Sunt Leones”.

The results reported in this subsection provide an additional explicit instance of a phenomenon whose rather general scope has been already advertized via a number of other examples, treated elsewhere in more or less complete detail [12, 5, 30, 11].

An analogous treatment to that given here will be presented in the next subsection, in the context of the “generalized goldfish model” [4, 43, 5], which is somewhat richer inasmuch as it features branch points the nature of which depends on the values of the coupling constants (in contrast to the case treated herein, where all relevant branch points are of square-root type), and has moreover the advantage that its treatment in the \mathbb{C}_N context is directly interpretable as a genuine (i.e., rotation-invariant) real many-body problem *in the plane*. On the other hand the class of many-body problems with inverse-cube interparticle potentials, as considered herein, have been (especially, of course, in the integrable version with equal coupling constants) much studied over the last quarter century, while the “goldfish” model has not yet quite acquired a comparable “classical” status.

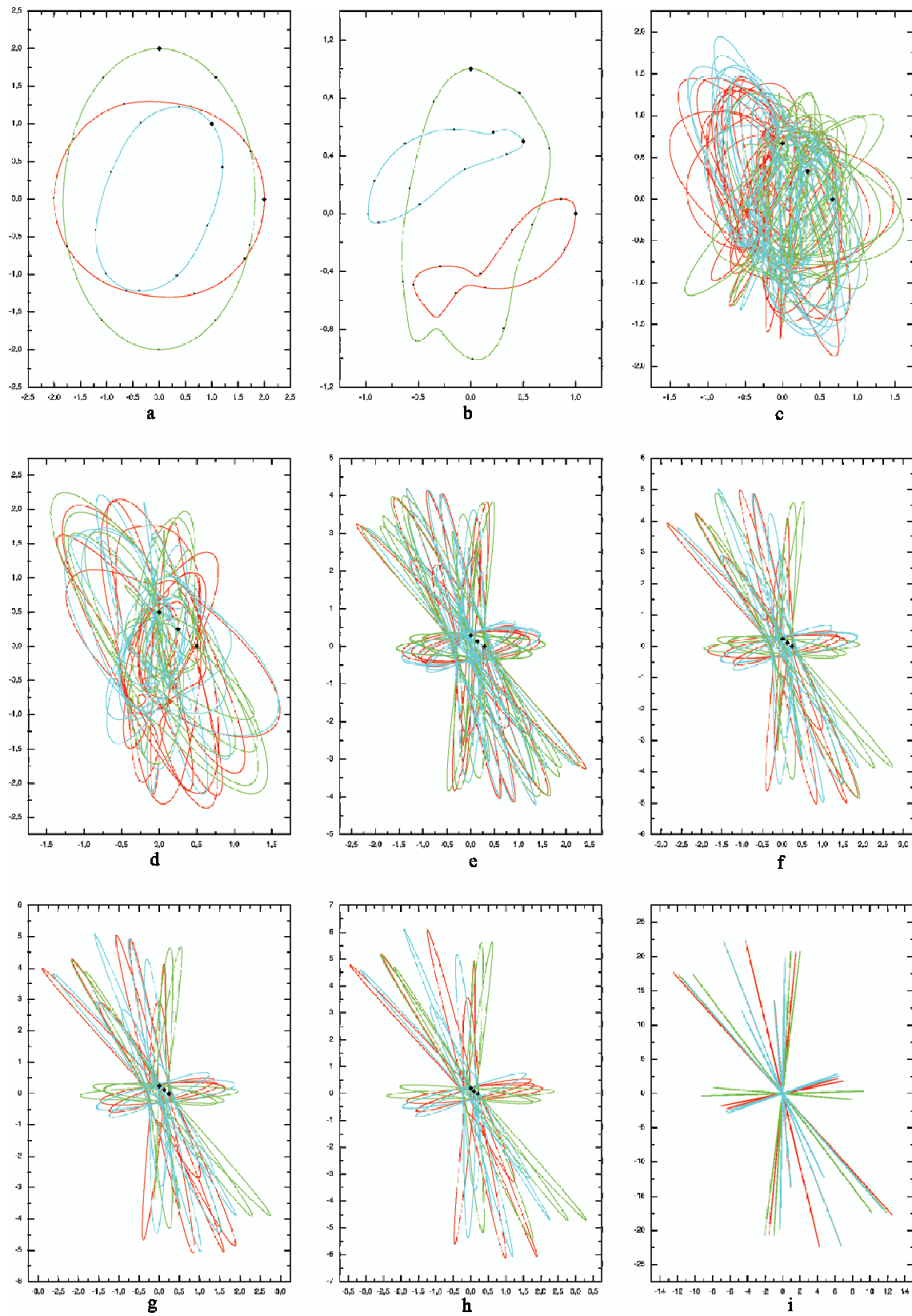


Figure 1.2: A numerical example of the dynamics of the Calogero-Moser model.

1.2.2 The Goldfish many-body problem

In this subsection, we describe the N -body problem in the plane characterized by the following Newtonian equations of motion²:

$$\begin{aligned} \ddot{\vec{r}}_n &= \omega \hat{k} \wedge \dot{\vec{r}}_n + 2 \sum_{m=1; m \neq n}^N (r_{nm})^{-2} (\alpha_{nm} + \alpha'_{nm} \hat{k} \wedge) \\ &\times \left[\dot{\vec{r}}_n (\dot{\vec{r}}_m \cdot \vec{r}_{nm}) + \dot{\vec{r}}_m (\dot{\vec{r}}_n \cdot \vec{r}_{nm}) - \vec{r}_{nm} (\dot{\vec{r}}_n \cdot \dot{\vec{r}}_m) \right]. \end{aligned} \quad (1.37a)$$

Here and below the subscripted indices run from 1 to N (unless otherwise indicated), the number of moving particles N is a positive integer, the N two-vectors $\vec{r}_n \equiv \vec{r}_n(t)$ identify the positions of the moving point-particles in a plane which for notational convenience we imagine immersed in ordinary three-dimensional space, so that $\vec{r}_n \equiv (x_n, y_n, 0)$; \hat{k} is the unit three-vector orthogonal to that plane, $\hat{k} \equiv (0, 0, 1)$, so that $\hat{k} \wedge \vec{r}_n \equiv (-y_n, x_n, 0)$;

$$\vec{r}_{nm} \equiv \vec{r}_n - \vec{r}_m, \quad r_{nm}^2 = r_n^2 + r_m^2 - 2\vec{r}_n \cdot \vec{r}_m; \quad (1.37b)$$

superimposed dots denote of course time derivatives; ω is a *real* – indeed, without loss of generality, *positive* – constant, $\omega > 0$, which sets the time scale, and to which we associate the period

$$T = 2\pi/\omega \quad (1.38)$$

and α_{nm} and α'_{nm} are *real* “coupling constants”. Note that this N -body model in the plane is invariant under both translations and rotations; it is Hamiltonian; it features one-body and two-body velocity-dependent forces; when the latter are missing – namely, when all the two-body coupling constants α_{nm} , α'_{nm} vanish,

$$\alpha_{nm} = \alpha'_{nm} = 0, \quad (1.39a)$$

it represents the physical situation of N electrically charged particles moving in a plane under the influence of a constant magnetic field orthogonal to that plane (“cyclotron”). In such a case of course every particle moves uniformly, with the same period T , see (1.38), on a circular trajectory the center \vec{c}_n and radius ρ_n of which are determined by the initial data (position and velocity) of each particle:

$$\vec{r}_n(t) = \vec{c}_n + \vec{\rho}_n \sin(\omega t) - \hat{k} \wedge \vec{\rho}_n \cos(\omega t), \quad (1.39b)$$

$$\vec{c}_n = \vec{r}_n(0) + \hat{k} \wedge \vec{\rho}_n, \quad \vec{\rho}_n = \dot{\vec{r}}_n(0)/\omega. \quad (1.39c)$$

Let us begin by tersely reviewing the findings reported in [29, 5]. First of all we note that it is convenient to identify the *physical* plane in which the motion takes place with the *complex* plane, via the relation

$$\vec{r}_n \equiv (x_n, y_n, 0) \Leftrightarrow z_n \equiv x_n + iy_n, \quad (1.40)$$

whereby the real Newtonian equations of motion in the plane (1.37) become the following equations determining the motion of the N points $z_n \equiv z_n(t)$ in the complex z -plane:

$$\ddot{z}_n = i\omega \dot{z}_n + 2 \sum_{m=1; m \neq n}^N a_{nm} \dot{z}_n \dot{z}_m / (z_n - z_m), \quad (1.41a)$$

²The rich phenomenology featured by the solutions of this many-body problem in the plane led us to refer to it, at least colloquially among us, as a “goldfish”, thereby extending to this model the terminology that was initially suggested for its integrable variant [43].

with

$$a_{nm} = \alpha_{nm} + i\alpha'_{nm}. \quad (1.41b)$$

Hereafter we always use this *avatar*, (1.41), of the equations of motion (1.37), and we moreover exploit the following key observation [29, 5, 4, 44, 7], the trick already introduced in the previous sections: via the change of (independent) variable

$$\underline{z}(t) = \underline{\zeta}(\tau), \quad \tau = [\exp(i\omega t) - 1] / (i\omega), \quad (1.42)$$

the system (1.41) becomes

$$\zeta_n'' = 2 \sum_{m=1; m \neq n}^N a_{nm} \zeta_n' \zeta_m' / (\zeta_n - \zeta_m). \quad (1.43)$$

Here and below the underlined notation indicates an N -vector, say $\underline{z} \equiv (z_1, \dots, z_N)$, $\underline{\zeta} \equiv (\zeta_1, \dots, \zeta_N)$ and so on, and the primes denote of course differentiations with respect to the independent variable τ . Note that the constant ω has completely disappeared from (1.43); nor does it feature in the relations among the initial data for (1.41) and (1.43), which read simply

$$\underline{z}(0) = \underline{\zeta}(0), \quad \dot{\underline{z}}(0) = \dot{\underline{\zeta}}(0). \quad (1.44)$$

This of course entails that, to obtain the solution $\underline{z}(t)$ of (1.41) corresponding to a given set of initial data $\underline{z}(0)$, $\dot{\underline{z}}(0)$, one can solve (1.43) with the *same* set of initial data, see (1.44), thereby determine $\underline{\zeta}(\tau)$, and then use (1.42) to obtain $\underline{z}(t)$ (hence as well, via (1.40), the solution of the initial-value problem for (1.37)). This possibility – to infer the behavior of the evolution in the *real* time variable t of the solutions $\underline{z}(t)$ of (1.41) (namely as well of the solutions of the physical many-body problem in the plane (1.37)) from the properties of the solutions $\underline{\zeta}(\tau)$ of (1.43) as functions of the *complex* variable τ – is one of the main tools of our investigation. Indeed, when the *real* time variable t evolves over one period T – say, from $t = 0$ to $t = T$ – the *complex* time-like variable τ goes from $\tau = 0$ back to $\tau = 0$ by traveling counter-clock-wise – see (1.42) – on the circular contour \tilde{C} centered in the complex τ -plane at i/ω and having radius $1/\omega$. Hence whenever all the functions $\zeta_n(\tau)$ – obtained as solutions of (1.43) – are *holomorphic*, as functions of the complex variable τ , inside that circular contour \tilde{C} – or, more precisely, in the (closed) circular disk C defined by that contour \tilde{C} – the corresponding functions $z_n(t)$ – namely the corresponding solutions of (1.41) – are *nonsingular* and *completely periodic* in the *real* time variable t , with period T , see (1.38). (This also entails that, if the only singularities of a solution $\underline{\zeta}(\tau)$ of (1.43) inside the disk C are a *finite* number of *rational* branch points, then the corresponding solution $\underline{z}(t)$ of (1.41) is again *completely periodic* in the *real* time t , albeit possibly with a larger period which is then an entire multiple of T).

Now we note that *all* solutions $\underline{\zeta}(\tau)$ of (1.43), corresponding to *arbitrary* initial data $\underline{\zeta}(0)$, $\dot{\underline{\zeta}}(0)$ (with the only restriction that these data be nonsingular, namely $|\zeta_n'(0)| < \infty$ and $\zeta_n(0) \neq \zeta_m(0)$, see the right-hand side of (1.43)), yield solutions $\underline{\zeta}(\tau)$ which are *holomorphic* in the neighborhood of $\tau = 0$, as implied by the standard theorem [45] which guarantees the existence, uniqueness and analyticity of the solutions of analytic ODEs, in a sufficiently small circular disk D centered in the complex τ -plane at the origin, $\tau = 0$, where the initial data defining the solution are given. The size of this disk D is determined by the location of the singularity of $\underline{\zeta}(\tau)$ closest to the origin, and the structure of the right-hand side of (1.43) clearly entails that a *lower* estimate of this distance – namely of the radius ρ of D – reads as follows:

$$\rho > R\tilde{\zeta}/\tilde{\zeta}' \quad (1.45a)$$

with R a positive constant (dependent on the values of the coupling constants a_{nm} but not on the initial data) and $\tilde{\zeta}$ respectively $\tilde{\zeta}'$ providing *lower* respectively *upper* estimates of the moduli of $\zeta_n(0) - \zeta_m(0)$ respectively $\zeta'_n(0)$, say

$$\tilde{\zeta} = \min_{n,m=1,\dots,N; n \neq m} |\zeta_n(0) - \zeta_m(0)|, \quad (1.45b)$$

$$\tilde{\zeta}' = \max_{n=1,\dots,N} |\zeta'_n(0)| \quad (1.45c)$$

(for a derivation of this formula, including an explicit expression for R , see Appendix A of [7]). Let us now assume the initial data, see (1.44), to entail (via (1.45)) that $\rho > 2/\omega$. Then the disk D includes the disk C , and this entails that the solutions $\zeta(\tau)$ of (1.43) are *holomorphic* functions of the *complex* variable τ in the (closed) disk C , hence (see (1.42)) the corresponding solutions $\underline{z}(t)$ of (1.41) are *completely periodic* functions of the *real* variable t , with period T , see (1.38).

This observation, together with the *lower* estimate (1.45) of ρ , imply the existence of a set, of *nonvanishing* (in fact, *infinite*) measure in phase space, of initial data $\underline{z}(0)$, $\dot{\underline{z}}(0)$ which yield *completely periodic* solutions of (1.41) (hence as well of (1.37)). But before formulating this in the guise of the following Proposition 2, let us interject the following obvious

Remark 1. If $\underline{z}(t)$ is the solution of (1.41) corresponding to initial data $\underline{z}(0)$, $\dot{\underline{z}}(0)$, then $\tilde{\underline{z}}(t) = c\underline{z}(bt)$ is the solution of the equations of motion that obtain from (1.41) by replacing in it ω with $\tilde{\omega} = b\omega$, and of course the corresponding initial data read $\tilde{\underline{z}}(0) = c\underline{z}(0)$, $\dot{\tilde{\underline{z}}}(0) = bc\dot{\underline{z}}(0)$. Here b, c are of course arbitrary (nonvanishing!) rescaling constants.

Let us now formulate Proposition 2

Proposition 2. *Let $\underline{z}(t)$ be the solution of (1.41) with*

$$\omega = b\bar{\omega}, \quad (1.46a)$$

corresponding to the assigned initial data

$$\underline{z}(0) = c\underline{u}, \quad \dot{\underline{z}}(0) = \mu\underline{v}, \quad [\text{with } u_n \neq u_m \text{ if } n \neq m], \quad (1.46b)$$

where the positive numbers b, c, μ play the role of scaling parameters (as we shall immediately see). Then the solution $\underline{z}(t)$ is completely periodic with period T , see (1.38),

$$\underline{z}(t+T) = \underline{z}(t), \quad (1.47)$$

provided one of the following conditions hold:

(i) *for given $a_{nm}, \omega, \underline{z}(0)$ and \underline{v} , the scaling number μ , hence as well the initial velocities $\dot{z}_n(0)$, are sufficiently small: $0 \leq \mu \leq \mu_c$, where μ_c is a positive number, $\mu_c > 0$, whose value depends on the given quantities;*

(ii) *for given $a_{nm}, \omega, \dot{\underline{z}}(0)$ and \underline{u} , the scaling number c is sufficiently large, $c > c_c$ (hence the initial positions of the N particles in the plane are sufficiently well separated), with c_c a positive number, $c_c > 0$, whose value depends on the given quantities;*

(iii) *for given $a_{nm}, \bar{\omega}, \underline{z}(0)$ and $\dot{\underline{z}}(0)$, the scaling number b , hence as well the circular frequency $\omega = b\bar{\omega}$, is sufficiently large, $b > b_c$, where b_c is a positive number, $b_c > 0$, whose value depends on the given quantities.*

Remark 3. The first two formulations (items (i) and (ii)) of Proposition 2 refer to the *same* equations of motion, with modified (rescaled) initial conditions; the third formulation (item (iii)) refers to *different* equations of motion (due to the change via rescaling of the constant ω) with the *same* initial conditions. But in fact these 3 formulations are *completely equivalent*, see Remark 1.

Before proceeding in reviewing this model, we report two additional remarks:

Remark 4. Suppose to be in the case – to which attention will be hereafter restricted – in which the (possibly complex) coupling constants a_{nm} depend *symmetrically* on their two indices:

$$a_{nm} = a_{mn}. \quad (1.48)$$

Then the equations of motion (1.41) are Hamiltonian, being derivable in the standard manner from the Hamiltonian

$$H(\underline{z}, \underline{p}) = \sum_{n=1}^N \left\{ i\omega z_n / c + \exp(cp_n) \prod_{m=1; m \neq n}^N [z_n - z_m]^{-a_{nm}} \right\} \quad (1.49)$$

(and let us recall that this entails that the “physical” equations of motion (1.37) are as well Hamiltonian [5]). Note the presence, in this expression of the Hamiltonian function $H(\underline{z}, \underline{p})$, of the arbitrary (nonvanishing) constant c , which does not feature in the equations of motion (1.41). Also note that $H(\underline{z}, \underline{p})$, in contrast to the equations of motion (1.41), is *not* quite invariant under translations ($z_n \rightarrow \tilde{z}_n = z_n + z_0$), although the only effect of such a translation on $H(\underline{z}, \underline{p})$ is addition of a constant.

Moreover, as clearly implied by the equations of motion (1.41) with (1.48), the center of mass,

$$Z(t) = N^{-1} \sum_{n=1}^N z_n(t), \quad (1.50)$$

moves *periodically* (with period T , see (1.38)) on a circular trajectory (in the complex z -plane):

$$Z(t) = Z(0) + \dot{Z}(0) [\exp(i\omega t) - 1] / (i\omega). \quad (1.51)$$

Remark 5. The third and last fact we like to recall is that, if all the coupling constants in (1.41) are unity,

$$a_{nm} = 1, \quad (1.52)$$

then the equations of motion (1.41) are *integrable* indeed *solvable* [5, 46], the solution of the corresponding initial-value problem being given by the following neat prescription: *the N coordinates $z_n(t)$ which constitute the solution $\underline{z}(t)$ of the equations of motion (1.41) corresponding to the initial data $\underline{z}(0)$, $\dot{\underline{z}}(0)$ are the N roots of the following algebraic equation in the variable z :*

$$\sum_{m=1}^N \dot{z}_m(0) / [z - z_m(0)] = i\omega / [\exp(i\omega t) - 1]. \quad (1.53)$$

Note that, after elimination of all denominators, this is a polynomial equation of degree N for the variable z , with all coefficients of the polynomial *periodic* in t with period T , see (1.38). Hence the set $\underline{z}(t)$ of its N zeros is as well *periodic* with period T . It is therefore clear that, in this special *solvable* case, see (1.52), *all* nonsingular solutions of (1.41) are *completely periodic*, with a period that is either T or an integer multiple of T (we will discuss in more detail this interesting case in Subsection 1.2.2.1).

As we just saw, Proposition 2 entails that the equations of motion (1.41) (as well as the equivalent “physical” equations of motion (1.37)) possess a lot of *nonsingular* and *completely periodic* solutions. This finding was validated [7] by simulations performed via the computer program created by the author of this thesis to solve numerically the equations of motion (1.41). The comprehension of many results discussed in this thesis began with the effort to understand certain remarkable features of these numerical simulations – in particular the

existence, in the cases characterized by *real* and *rational* values of the coupling constants a_{nm} in (1.41), of *additional* sets of initial data, also of *nonvanishing* measure in phase space, yielding *nonsingular* and *completely periodic* solutions with periods which are *integer multiples* of T , see (1.38) – via a mechanism, at which we already hinted in the previous sections, associated with *rational* branch points of the solutions $\zeta(\tau)$, which is indeed also responsible in the *solvable* case (with $a_{nm} = 1$) to yield *completely periodic* solutions with such larger periods (integer multiples of T). The findings reported here also suggest the existence of other *integrable* – but presumably not *solvable* – cases of the many-body problem (1.37), as well as of *nonintegrable* cases for which however *integrable behaviors*, such as those associated with *completely periodic* motions, emerge from sectors of initial data having nonvanishing measure in phase space; and they display as well a mechanism for the transition from *regular* to *irregular* motions (for other regions of phase space, of course only in the *nonintegrable* cases) characterized by a sensitive dependence on the initial data which seems to be *not* associated with any local exponential divergence of trajectories over time – in analogy to the type of *chaotic behavior* that ensues when a particle moves *freely* (except for the reflections on the borders) inside, say, a triangular plane billiard whose angles are *irrational* fractions of π .

1.2.2.1 Unitary coupling constants

In this subsection we analyze the periodicity of the solutions of (1.41) in the case of unitary coupling constants, namely when all $a_{ij} = 1$. The results reported herein essentially refer to [47].

As it is carefully described by F. Calogero in his book [5], one technique to construct solvable many-body problems is to look at the evolution of the zeros of a polynomial whose coefficients evolve in a known manner. A very simple (linear) evolution rule for the coefficients generally produces a complicated (nonlinear) evolution for the zeros by virtue of the highly nonlinear relation between the zeros and the coefficients of a polynomial. More precisely consider the following monic polynomial of degree N with τ -dependent coefficients

$$P(\zeta, \tau) = \zeta^N + \sum_{j=1}^N c_j(\tau) \zeta^{N-j} = \prod_{i=1}^N [\zeta - \zeta_i(\tau)]. \quad (1.54)$$

For instance, if $P(\zeta, \tau)$ is made to satisfy $P_{\tau\tau} = 0$, the zeros and coefficients evolve according to

$$c_i'' = 0, \quad (1.55)$$

$$\zeta_i'' = 2 \sum_{\substack{j=1 \\ j \neq i}}^N \frac{\zeta_i' \zeta_j'}{\zeta_i - \zeta_j}. \quad (1.56)$$

We can thus see that the evolution in τ of the coefficients is trivial, while the evolution of the zeros is governed precisely by the equations (1.43) with all coupling constants a_{ij} equal to one. It is worth to note that the equations (1.56) have also been analyzed independently by Prosen in the context of quantum chaos and random gaussian polynomials [48] and are a particular case of a larger class of integrable systems derived by Ruisjenaars and Schneider [49].

As we observed in Remark 5 in this case the explicit solution $\{z_1(t), \dots, z_N(t)\}$ of (1.41) corresponding to the initial data $\{z_i(0), \dot{z}_i(0)\}$ can be obtained by solving the following polynomial equation in z

$$\sum_{i=1}^N \frac{\dot{z}_i(0)}{z - z_i(0)} = \frac{i\omega}{\exp(i\omega t) - 1}. \quad (1.57)$$

Yet the best way to understand the periodicity is to realize that $z_i(t) = \zeta_i(\tau)$ are the zeros of a polynomial whose coefficients $c_j(\tau)$ are periodic functions of t (since they are linear functions of τ , and τ is a periodic function of t). After one period, the coefficients of the polynomial go back to their previous values, the set of zeros is periodic with period T , but the zeros might have exchanged their position. More specifically,

$$\{z_1(t+T), z_2(t+T), \dots, z_N(t+T)\} = \{z_{\pi(1)}(t), z_{\pi(2)}(t), \dots, z_{\pi(N)}(t)\}, \quad (1.58)$$

where $\pi \in \mathcal{S}_N$ is an element of the symmetric group of N elements. Every permutation $\pi \in \mathcal{S}_N$ can be decomposed as a product of disjoint cycles, each cycle containing the particles that are exchanging their positions. The period of the solution corresponds to the *order* of the permutation, i.e. the least integer q such that $\pi^q = \text{id}$. For fixed N the period of the solution of (1.56) is therefore given by

$$\{\text{lcm}(\lambda_1, \dots, \lambda_s) : \lambda_1 + \dots + \lambda_s = N\} \quad (1.59)$$

for some partition $\lambda \equiv \{\lambda_1, \dots, \lambda_s\}$ of N . The maximum of this quantity,

$$G(N) = \max_{\lambda \vdash N} \{\text{lcm}(\lambda)\}, \quad (1.60)$$

over all partitions of N is sometimes called the Landau function [50] in the literature. As an example all partitions of $N = 7$ can be found in Table 1.3 below, where it is clear that $G(7) = 12$. For a certain particle number N , we denote by $T(N)$ the set of all possible

Figure 1.3: Orders of a permutation of 7 elements

Partition	lcm	Partition	lcm
{7}	7	{1, 1, 1, 4}	4
{1, 6}	6	{1, 1, 2, 3}	6
{2, 5}	10	{1, 2, 2, 2}	2
{3, 4}	12	{1, 1, 1, 1, 3}	3
{1, 1, 5}	5	{1, 1, 1, 2, 2}	2
{1, 2, 4}	4	{1, 1, 1, 1, 1, 2}	2
{1, 3, 3}	3	{1, 1, 1, 1, 1, 1, 1}	1
{2, 2, 3}	6		

periods³, which clearly includes all numbers from 1 to N . The first few values of $T(N)$ have been collected in Table 1.4. These are all the possible periods for a fixed N , but which

Figure 1.4: Possible periods for the first few N

N	$T(N)$	N	$T(N)$
1	1	7	1-7, 10, 12
2	1-2	8	1-8, 10, 12, 15
3	1-3	9	1-9, 10, 12, 14, 15, 20
4	1-4	10	1-10, 12, 14, 15, 20, 21, 30
5	1-5, 6	11	1-11, 12, 14, 15, 18, 20, 21, 24, 28, 30
6	1-6	12	1-12, 14, 15, 18, 20, 21, 24, 28, 30, 35, 42, 60

of these periods is actually exhibited by the system depends on the choice of initial data

³Of course we are assuming here that $\omega = 2\pi$ so that the fundamental period T is unity.

$\{z_i(0), \dot{z}_i(0)\}$ and in general it is not easy to predict *a priori*. We turn then to the following

Question: Do initial data $\{z_i(0), \dot{z}_i(0)\}$ exist such that the solution $\{z_1(t), \dots, z_N(t)\}$ of the system (1.41) with $a_{ij} = 1$ has every possible period in $T(N)$?

In [47] we argue that this is indeed the case. To this purpose we first show that (1.56) admits a period N solution. Indeed, by inserting the following ansatz into (1.56)

$$\zeta_j(\tau) = A + B_j(\tau - \tau_b)^\Gamma, \quad j = 1, \dots, N, \quad (1.61)$$

it can be seen [44, 5] that the system admits the similarity solution (1.61) provided that

$$\Gamma = 1/N, \quad B_j = B e^{2\pi i \frac{j}{N}}, \quad j = 1, \dots, N. \quad (1.62)$$

This special similarity solution corresponds to placing all particles on the vertices of a regular N -gon and the only singularity occurs at $\tau = \tau_b$ where all particles collide simultaneously. If the branch point τ_b sits outside the circle C in the complex τ -plane with centre at i/ω and radius $1/\omega$ then the period of this solution is one (see Figure 1.2.2.1a) as we showed in the previous section. On the contrary, if the initial conditions are such that τ_b sits inside C , then the solution has period N (see Figure 1.2.2.1b) as it will visit the N -sheeted Riemann surface associated to the N -th root. In this motion the j -th particle takes the position of the $(j+1)$ -th particle after every fundamental period. Note from (1.61), (1.62) and (1.44) that, given initial data $\{z_i(0), \dot{z}_i(0)\}$, the branch point occurs at

$$\tau_b = -\frac{z_i(0)}{Nz'_i(0)} \quad (1.63)$$

so that it is always possible to choose initial data such that τ_b falls inside the circle C and the corresponding solution has period N .

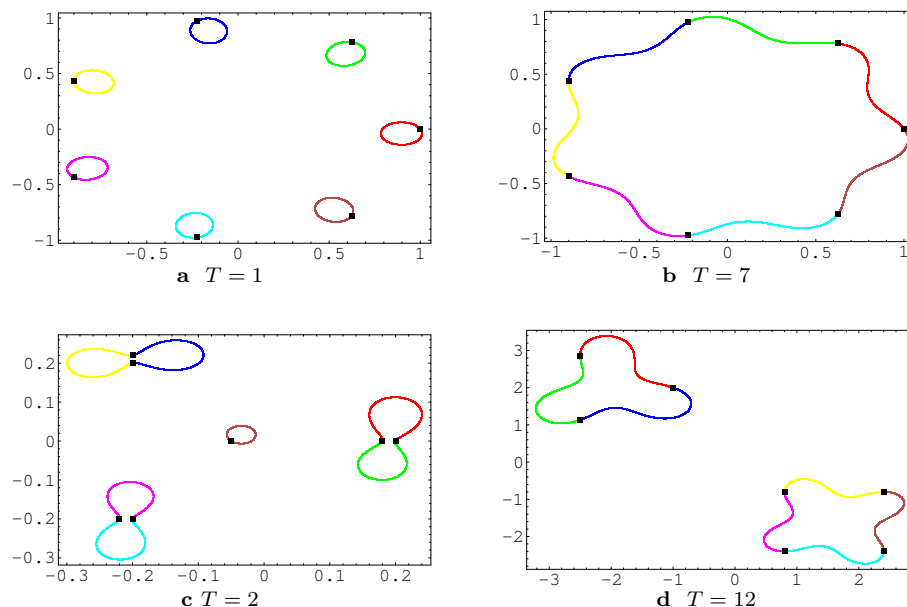


Figure 1.5: A few different periodic motions for $N = 7$

The next step comes by noting that, when two groups of particles are very far apart, their motions can be analyzed independently of each other. Without loss of generality, we assume that the first $i = 1, \dots, M$ particles belong to the first group while the rest belong

to the second group. The equations of motions are

$$\zeta_i'' = 2 \sum_{\substack{j=1 \\ j \neq i}}^M \frac{\zeta_i' \zeta_j'}{\zeta_i - \zeta_j} + 2 \sum_{\substack{j=M+1 \\ j \neq i}}^N \frac{\zeta_i' \zeta_j'}{\zeta_i - \zeta_j}, \quad i = 1, \dots, M, \quad (1.64)$$

$$\zeta_i'' = 2 \sum_{\substack{j=M+1 \\ j \neq i}}^N \frac{\zeta_i' \zeta_j'}{\zeta_i - \zeta_j} + 2 \sum_{\substack{j=1 \\ j \neq i}}^M \frac{\zeta_i' \zeta_j'}{\zeta_i - \zeta_j}, \quad i = M + 1, \dots, N. \quad (1.65)$$

If generic initial conditions are chosen (i.e. such that no collisions occur at finite time), the velocities are bounded for all time from 0 to $G(N)T$, say $\max |\zeta_i'(\tau)| < K$. Now we choose the initial position of the particles such that the two groups are a distance D apart :

$$\zeta_i(0) = w_i, \quad i = 1, \dots, M, \quad (1.66)$$

$$\zeta_i(0) = D + w_i, \quad i = M + 1, \dots, N, \quad (1.67)$$

with $|D| \gg |w_i|$. It is clear that in the limit of D going to infinity the second terms in (1.64) and (1.65) become negligible with respect to the first terms, and the system effectively decouples. The period of the system for these initial conditions is clearly the least common multiple of the periods of the two subgroups. If we keep in mind that a system of N particles has a period N solution, the above argument can be applied iteratively to show that initial conditions exist such that every single period in $T(N)$ is realized.

So the maximal period of the periodic solutions of (1.41) when all the coupling constants are equal to 1 is given by the Landau function $G(N)$ defined in (1.60). We conclude this section discussing some properties of $G(N)$ and we give its asymptotic behavior for large N . The first few values of $G(N)$ together with the corresponding prime factors are shown in Table 1.6 (Grantham [51] has computed $G(N)$ up to $N = 500\,000$). From the first few values it is already possible to observe the unruly behavior of $G(N)$.

Figure 1.6: First few values of $G(N)$

N	$G(N)$	Prime factors of $G(N)$	N	$G(N)$	Prime factors of $G(N)$	N	$G(N)$	Prime factors of $G(N)$
1	1	1	11	30	$2 \cdot 3 \cdot 5$	21	420	$2^2 \cdot 3 \cdot 5 \cdot 7$
2	2	2	12	60	$2^2 \cdot 3 \cdot 5$	22	420	$2^2 \cdot 3 \cdot 5 \cdot 7$
3	3	3	13	60	$2^2 \cdot 3 \cdot 5$	23	840	$2^3 \cdot 3 \cdot 5 \cdot 7$
4	4	2^2	14	84	$2^2 \cdot 3 \cdot 7$	24	840	$2^3 \cdot 3 \cdot 5 \cdot 7$
5	6	$2 \cdot 3$	15	105	$3 \cdot 5 \cdot 7$	25	1260	$2^2 \cdot 3^2 \cdot 5 \cdot 7$
6	6	$2 \cdot 3$	16	140	$2^2 \cdot 5 \cdot 7$	26	1260	$2^2 \cdot 3^2 \cdot 5 \cdot 7$
7	12	$2^2 \cdot 3$	17	210	$2 \cdot 3 \cdot 5 \cdot 7$	27	1540	$2^2 \cdot 5 \cdot 7 \cdot 11$
8	15	$3 \cdot 5$	18	210	$2 \cdot 3 \cdot 5 \cdot 7$	28	2310	$2 \cdot 3 \cdot 5 \cdot 7 \cdot 11$
9	20	$2^2 \cdot 5$	19	420	$2^2 \cdot 3 \cdot 5 \cdot 7$	29	2520	$2^3 \cdot 3^2 \cdot 5 \cdot 7$
10	30	$2 \cdot 3 \cdot 5$	20	420	$2^2 \cdot 3 \cdot 5 \cdot 7$	30	4620	$2^2 \cdot 3 \cdot 5 \cdot 7 \cdot 11$

No explicit expression of $G(N)$ as a function of N is known, yet results on the asymptotic behaviour of $G(N)$ for large N are known as far back as the early 1900s. This asymptotic behaviour (see Figure 1.7) is given by

$$\log G(N) = (N \log N)^{1/2} + \frac{N^{1/2} \log \log N}{2 (\log N)^{1/2}} + O\left(\sqrt{\frac{N}{\log N}}\right). \quad (1.68)$$

The first term of this formula was proved by Landau in his *Handbuch* [50], while the subsequent terms of the asymptotic behaviour were proved later by Shah [52]. Since then there has been a number of papers devoted to the study of this function (see, for instance, [53]).

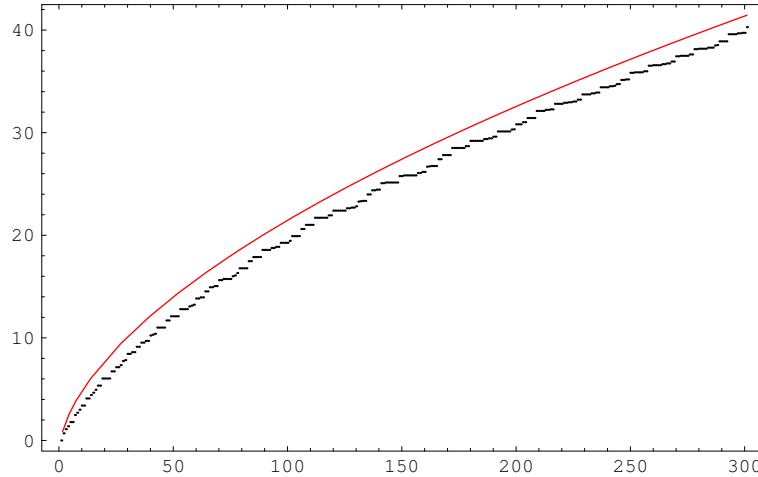


Figure 1.7: The functions $\log G(N)$ and $\sqrt{N \log N}$ for N up to 301

1.2.2.2 Generic coupling constants: the two-body case

In the following subsections, we will shortly analyze the case with *arbitrary* coupling constants.

We will start treating the two-body problem. This is of interest in itself, but even more so for the insight it provides, not only for the two-body case but as well for the N -body case, on the nature of the singularities of the solutions $\zeta(t)$ of (1.43) as functions of the complex variable τ , hence on the periodicity of the corresponding solutions $\underline{z}(t)$ of the “physical” equations of motion (1.41).

For $N = 2$ the equations of motion (1.43) are consistent with the assignment (corresponding to the standard separation of the center of mass and relative motions)

$$\zeta_1(\tau) + \zeta_2(\tau) = \zeta_1(0) + \zeta_2(0) + V\tau, \quad (1.69a)$$

$$\zeta_1(\tau) - \zeta_2(\tau) = \zeta(\tau), \quad (1.69b)$$

namely

$$\zeta_1(\tau) = [\zeta_1(0) + \zeta_2(0) + V\tau + \zeta(\tau)]/2, \quad (1.69c)$$

$$\zeta_2(\tau) = [\zeta_1(0) + \zeta_2(0) + V\tau - \zeta(\tau)]/2, \quad (1.69d)$$

where (see (1.50), (1.44) and (1.69a))

$$V = \zeta_1'(0) + \zeta_2'(0) = \zeta_1'(\tau) + \zeta_2'(\tau) = 2\dot{Z}(0) \quad (1.70)$$

is a (generally complex) constant and the difference $\zeta(\tau)$ satisfies the second-order ODE

$$\zeta'' = a \left[V^2 - (\zeta')^2 \right] / \zeta. \quad (1.71)$$

Here and throughout this section $a = a_{12} = a_{21}$ is the relevant “coupling constant”, and primes denote of course differentiations with respect to τ .

This ODE is easily integrated once (after multiplying it by the factor $2\zeta'/[V^2 - (\zeta')^2]$), and one gets thereby

$$(\zeta')^2 = V^2 + B\zeta^{-2a}, \quad (1.72a)$$

$$(\zeta')^2 = V^2 \left[1 + (\zeta/L)^{-2a} \right], \quad (1.72b)$$

with $B = -4\zeta'_1(0)\zeta'_2(0)[\zeta(0)]^{2a}$ – or, when $V \neq 0$, equivalently but notationally more conveniently, $L = (B/V^2)^{1/(2a)} = \zeta(0) \left\{ [\zeta'(0)/V]^2 - 1 \right\}^{1/(2a)}$ – a (generally complex) integration constant.

In the special case $V = 0$ the first-order ODE (1.72a) can be easily integrated once more, and one obtains thereby [7] the solution of (1.71) in closed form: for $a \neq -1$,

$$\zeta(\tau) = c(\tau - \tau_b)^\gamma \quad (1.73)$$

with

$$\gamma = 1/(1+a); \quad (1.74)$$

for $a = -1$,

$$\zeta(\tau) = c \exp(\beta\tau). \quad (1.75)$$

Here c , τ_b and β are arbitrary (complex) constants, and it is easily seen that τ_b respectively β are related to the initial data by the relations

$$\tau_b = -(1+a)^{-a} \zeta(0)/\zeta'(0) \quad (1.76)$$

respectively

$$\beta = \zeta'(0)/\zeta(0). \quad (1.77)$$

For $V \neq 0$ the ODE (1.72) can of course be generally integrated by a further quadrature, but the corresponding formula in terms of the hypergeometric function $F(A, B; C; Z)$ [54],

$$\zeta F\left(1/2, -1/(2a); 1 - 1/(2a); [\zeta/L]^{-2a}\right) = V(\tau - \tau_b), \quad (1.78)$$

is not particularly enlightening, except in the few special cases in which the hypergeometric function reduces to elementary functions.

For $a = -1$, one easily finds

$$\zeta(\tau) = L \sinh[(V/L)(\tau - \tau_0)], \quad (1.79)$$

with τ_0 a (complex) constant (related of course to the initial data: $\zeta(0) = -L \sinh[(V/L)\tau_0]$). Hence in this case $\zeta(\tau)$ is an entire function of τ , and via (1.42) this entails that *all* solutions of the Newtonian equations of motion (1.41) (with $N = 2$) are in this case *nonsingular* and *completely periodic* with period T , see (1.38) (as entailed by (1.69) with (1.75,1.77) or (1.79)).

In [7], we presented an analysis of the emergence of periodic motions in the two-body problem (1.41) for an *arbitrary* value of the coupling constant a . The conclusions of such an analysis depend essentially on the nature, and location, of the branch points featured by the solutions of the first-order ODE (1.72) (with $V \neq 0$; the $V = 0$ case is completely illuminated by the explicit solution (1.73,1.76) with (1.74), hence our treatment below refers exclusively to the $V \neq 0$ case).

Three cases must be distinguished, depending on the value of the real part of the coupling constant a .

Case (i):

$$\operatorname{Re}(a) > 0. \quad (1.80a)$$

In this case the branch point at, say, $\tau = \tau_b$, is characterized by the exponents γ and $1 - \gamma$, see (1.74), with the behavior of $\zeta(\tau)$ for $\tau \approx \tau_b$ given by the formula

$$\zeta(\tau) = L\gamma^{-\gamma}[(V/L)(\tau - \tau_b)]^\gamma \times \left\{ 1 + \sum_{l=1}^{\infty} \sum_{k=0}^l g_{kl} [(V/L)(\tau - \tau_b)]^{k\gamma} [(V/L)(\tau - \tau_b)]^{2l(1-\gamma)} \right\} \quad (1.80b)$$

(for a justification of this formula, including the significance of the coefficients g_{kl} , see formulas (B.20) with (B.2) in Appendix B of [7]). Note that this formula entails $\zeta(\tau_b) = 0$ (as well as $|\zeta'(\tau_b)| = \infty$, since (1.74) and (1.80a) entail $0 < \text{Re}(\gamma) < 1$), namely this singularity is associated with a “collision” of the two particles (see (1.69b)), which both move with infinite speed when they collide. This singularity is analogous to that which obtains in the $V = 0$ case, see (1.73).

Case (ii):

$$-1 < \text{Re}(a) < 0. \quad (1.81a)$$

In this case the branch point at, say, $\tau = \tau_b$, is characterized by the exponent

$$\beta = -2a, \quad (1.81b)$$

with the behavior of $\zeta(\tau)$ for $\tau \approx \tau_b$ given by the formula

$$\zeta(\tau) = \pm V (\tau - \tau_b) \left\{ 1 + \sum_{l=1}^{\infty} g_l [\pm (V/L) (\tau - \tau_b)]^{l\beta} \right\}. \quad (1.81c)$$

This singularity, however, is generally *not* of the same type as that which obtains in the $V = 0$ case, see (1.73) (except for those values of a such that $\gamma = (1+a)^{-1}$ and $\beta = -2a$ differ by an integer). In both cases ($V = 0$, see (1.73) with (1.74) and (1.81a); $V \neq 0$, see (1.81)) $\zeta(\tau_b) = 0$, namely this singularity is again associated with a “collision” of the two particles (see (1.69b)); however, in the $V = 0$ case $|\zeta'(\tau_b)| = \infty$, while in the $V \neq 0$ case $\zeta'(\tau_b) = \pm V$ and this entails (see (1.69)) that either $\zeta'_1(\tau)$ or $\zeta'_2(\tau)$ vanishes at $\tau = \tau_b$ so that

$$\zeta'_1(\tau_b) \zeta'_2(\tau_b) = 0. \quad (1.81d)$$

Case (iii):

$$\text{Re}(a) < -1. \quad (1.82)$$

In this case both behaviors, (1.80b) respectively (1.81c), are possible, so both type of branch points, characterized by the exponents $\gamma = (1+a)^{-1}$ respectively $\beta = -2a$, may be present: but the first type of branch point, characterized by the exponent γ (which obtains now for all values of V) corresponds now to the phenomenon of “escape to infinity” ($|\zeta(\tau_b)| = |\zeta'(\tau_b)| = \infty$), while the second type of branch point, characterized by the exponent β (which obtains only if V does *not* vanish, $V \neq 0$) corresponds to the phenomenon of “two-body collision” ($\zeta(\tau_b) = 0$, with $\zeta'(\tau_b) = \pm V$ entailing (1.81d)).

1.2.2.3 Generic coupling constants: the N -body case

In this subsection we investigate the branch point structure in the complex τ -plane of the solutions $\zeta(\tau)$ of the equations of motion (1.43), since the nature and location of these branch points determine the behavior of the solutions $\underline{z}(t)$ of the equations of motion (1.41), namely of the Newtonian equations of motion (1.37), as functions of the *real* time variable t . Let us re-emphasize that it is indeed the structure of the Riemann surface associated with the solution $\zeta(\tau)$ of the equations of motion (1.43) that determines whether the corresponding solution $\underline{z}(t)$ of the “physical” equations of motion (1.41) namely (1.37) does or does not become *singular* as function of the *real* time variable t , and if it is not singular throughout time whether or not it is *completely periodic*, and if it is periodic then with what period (whether T , see (1.38), or an integer multiple of T). The rule to evince these conclusions is quite simple, see (1.42): to obtain $\underline{z}(t)$ as function of the *real* variable

t one must follow the corresponding solution $\underline{\zeta}(\tau)$ (namely, that characterized by the *same* initial data, see (1.44)) as the *complex* “time-like” variable τ travels, *on the Riemann surface associated with that solution* $\underline{\zeta}(\tau)$, round and round counterclockwise along the circular contour \tilde{C} centered at i/ω and of radius $1/\omega$.

The implications of this analysis have already been discussed in the preceding subsection in the context of the two-body problem. The situation in the N -body case is somewhat analogous. Indeed the structure of the evolution equations (1.43) entails that the same two mechanisms discussed in the two-body case are *generically* responsible for the emergence of singularities, at some complex values τ_b , of the solutions of these equations of motion, (1.43), for an arbitrary number N of particles: namely, singularities arise either from the “collision” of two particles, characterized by the relation $\zeta_1(\tau_b) = \zeta_2(\tau_b)$ (with $|\zeta_1(\tau_b)| = |\zeta_2(\tau_b)| < \infty$, where we assign, without loss of generality, the labels 1 and 2 to the two “colliding” particles), or from the simultaneous “escape to infinity” of two or more (say, M) particles, characterized by the relation $|\zeta_1(\tau_b)| = |\zeta_2(\tau_b)| = \dots = |\zeta_M(\tau_b)| = \infty$ (where, without loss of generality, we assumed the M “particles” $\zeta_n(\tau)$ that escape to infinity as $\tau \rightarrow \tau_b$ to be labelled by the first M indices, $n = 1, \dots, M$). Note that here we use again inverted commas around the word “collision” and “escape to infinity” to underline that only in the special cases in which, via the transformation (1.42), to the value τ_b there corresponds a *real* value t_c (namely, $\tau_b = [\exp(i\omega t_c) - 1] / (i\omega)$ with t_c *real*; see (1.42)), the “collision”, or the “escape to infinity”, corresponds indeed to a real event for the physical problem (1.41) namely (1.37).

The statement we just made is not meant to exclude the possibility that “collisions” involving simultaneously more than two particles occur and cause correspondingly a singularity: indeed the exact solutions (with $M > 2$) presented in Subsection 1.2.2.1 provide examples of solutions characterized by such phenomena. But it stands to reason – and it is confirmed by our analysis, see [7] – that M -particle “collisions” with $M > 2$ are *not generic*, namely they are *not* associated to solutions emerging from the assignment of *generic* initial data: indeed for a *generic* solution of the equations of motion (1.43) the *complex* equation $\zeta_1(\tau_b) = \zeta_2(\tau_b)$ generally has at least one *complex* solution τ_b (and more likely many such solutions, indeed quite possibly an infinity of them), while one should not expect the $M - 1$ complex equations $\zeta_1(\tau_b) = \zeta_2(\tau_b) = \dots = \zeta_M(\tau_b)$, with $M > 2$, to possess any solution at all (although, as we showed in [7], there are of course *special* solutions $\underline{\zeta}(\tau)$ of (1.43) for which such multiple equations do possess solutions). Let us then understand the type of singularity associated to these two types of “events”. To this end the discussion of the preceding section is helpful (especially to guess at the nature of the singularity associated with such “events”), but a new treatment in the N -body context is nevertheless necessary.

“Two-body collisions”. We analyze firstly the singularities associated with “two-body collisions”. For notational convenience let us assume, without loss of generality, that the two particles involved in the two-body event – which happens at $\tau = \tau_b$ – carry the labels 1 and 2, and let us call a the coupling constant associated with this particle pair,

$$a = a_{12} = a_{21}. \quad (1.83)$$

Let us firstly assume that

$$\operatorname{Re}(a) > 0, \quad (1.84a)$$

so that the real part of the branch-point exponent $\gamma = 1/(1+a)$, (see (1.74), satisfies the restriction

$$0 < \operatorname{Re}(\gamma) < 1. \quad (1.84b)$$

It can then be shown (see Appendix C of [7]) that in the neighborhood of a “two-body

collision” occurring at $\tau = \tau_b$ the solution $\underline{\zeta}(\tau)$ of (1.43) features the following behavior:

$$\begin{aligned} \zeta_s(\tau) &= b + (-1)^{s-1} c(\tau - \tau_b)^\gamma + v(\tau - \tau_b) \\ &+ \sum_{k=1}^{\infty} \sum_{l,m=0; l+m \geq 1}^{\infty} g_{klm}^{(s)} (\tau - \tau_b)^{k+l\gamma+m(1-\gamma)}, \quad s = 1, 2, \end{aligned} \quad (1.85a)$$

$$\begin{aligned} \zeta_n(\tau) &= b_n + v_n(\tau - \tau_b) \\ &+ \sum_{k=1}^{\infty} \sum_{l=\delta_{k1}}^{\infty} \sum_{m=0}^{\infty} g_{klm}^{(n)} (\tau - \tau_b)^{k+l\gamma+m(1-\gamma)}, \quad n = 3, \dots, N. \end{aligned} \quad (1.85b)$$

In these formulas the $2N$ (complex) constants b, c, v, τ_b and b_n, v_n (with $n = 3, \dots, N$) are arbitrary, except for the inequalities

$$b \neq b_n, \quad b_n \neq b_m, \quad n, m = 3, \dots, N, \quad (1.85c)$$

while the coefficients of the sums are determined in terms of these constants (see Appendix C of [7]). Clearly these formulas, (1.85), entail $\zeta_1(\tau_b) = \zeta_2(\tau_b) = b \neq \zeta_n(\tau_b) = b_n \neq \zeta_m(\tau_b) = b_m$ for $n \neq m, 3 \leq n, m \leq N$ with $|\zeta_1(\tau_b)| = |\zeta_2(\tau_b)| = |b| < \infty$ but (see (1.85a) and (1.84b)) $|\zeta_1'(\tau_b)| = |\zeta_2'(\tau_b)| = \infty$, while $|\zeta_n(\tau_b)| = |b_n| < \infty$ and (see (1.85b) and (1.84b)) $|\zeta_n'(\tau_b)| = |v_n| < \infty, n = 3, \dots, N$. This confirms that the corresponding event is to be interpreted as a “collision” of the two particles 1 and 2, with both colliding particles moving infinitely fast at the collision time $\tau = \tau_b$. What interests us most is the nature of the corresponding singularity: a *branch point* characterized by the exponents γ and $1 - \gamma$, see (1.74). And the fact that such a singularity is associated with an expression of the solution $\underline{\zeta}(\tau)$ of (1.43) that features, see (1.85), the *maximal* number, $2N$, of arbitrary constants, demonstrates the *generic* character of such singularities, which are therefore likely to be featured by the solutions $\underline{\zeta}(\tau)$ corresponding to a *generic* set of initial data.

Likewise, if the inequality (1.84a) is reversed,

$$\operatorname{Re}(a) < 0, \quad (1.86a)$$

let us introduce the number β

$$\beta = -2a \quad (1.86b)$$

so that (see (1.86a))

$$\operatorname{Re}(\beta) > 0. \quad (1.86c)$$

It can be shown that in the neighborhood of a “two-body collision” the behavior of the solutions $\underline{\zeta}(\tau)$ is characterized, rather than by (1.85), by the following expressions:

$$\zeta_1(\tau) = b + c(\tau - \tau_b)^{1+\beta} + \sum_{k,l=1; k+l \geq 3}^{\infty} g_{kl}^{(1)} (\tau - \tau_b)^{k+l\beta}, \quad (1.87a)$$

$$\zeta_2(\tau) = b + v_2(\tau - \tau_b) - c(\tau - \tau_b)^{1+\beta} + \sum_{k=1}^{\infty} \sum_{l=2\delta_{k1}}^{\infty} g_{kl}^{(2)} (\tau - \tau_b)^{k+l\beta}, \quad (1.87b)$$

$$\zeta_n(\tau) = b_n + v_n(\tau - \tau_b) + \sum_{k=2}^{\infty} \sum_{l=0}^{\infty} g_{kl}^{(n)} (\tau - \tau_b)^{k+l\beta}, \quad n = 3, \dots, N, \quad (1.87c)$$

In these formulas the $2N$ (complex) constants b, c, v_2, τ_b and b_n, v_n (with $n = 3, \dots, N$) are *arbitrary* (except, again, for the inequalities (1.85c)), while the coefficients of the sums are determined in terms of these constants (see Appendix C of [7]). Clearly these formulas

(see (1.87) and (1.85c)) entail again $\zeta_1(\tau_b) = \zeta_2(\tau_b) = b \neq \zeta_n(\tau_b) = b_n \neq \zeta_m(\tau_b) = b_m$ for $n \neq m$, $3 \leq n, m \leq N$ with $|\zeta_1(\tau_b)| = |\zeta_2(\tau_b)| < \infty$, but now (see (1.87a) with (1.86c) and (1.87b)) $\zeta'_1(\tau_b) = 0$, $\zeta'_2(\tau_b) = v_2$ (so that $\zeta'_1(\tau_b)\zeta'_1(\tau_b) = 0$; see the right-hand side of (1.43)), while of course again $|\zeta_n(\tau_b)| = |b_n| < \infty$ and (see (1.84b)) $|\zeta'_n(\tau_b)| = |v_n| < \infty$ for $n = 3, \dots, N$. Hence the corresponding event is again to be interpreted as a “collision” of the two particles 1 and 2, but now with particle 1 having *zero* velocity at the time of the collision, in contrast to particle 2 which moves with velocity v_2 (note the notational distinction thereby introduced among the two colliding particles); while for our purposes the interpretation of these formulas, (1.87a,b,c), is that the nature of the corresponding singularity is a *branch point* characterized by the exponent β , see (1.86b). And again the fact that such a singularity is associated with an expression of the solution $\zeta_n(\tau)$ of (1.43) that features, see (1.87a,b,c), the *maximal* number, $2N$, of *arbitrary* constants, demonstrates the *generic* character of such singularities, which are therefore likely to be featured by the solutions $\zeta(\tau)$ corresponding to a *generic* set of initial data.

“**Many-body collisions**”. The singularities associated with “collisions” involving more than two particles can be discussed in an analogous manner (also taking advantage of the results of Subsection 1.2.2.2), but in view of their lack of genericity we forsake their treatment here, and we rather proceed to discuss the singularities associated with “escapes to infinity”.

This phenomenon can only occur if, for some group of the interacting particles, which without loss of generality is hereafter assumed to be formed by the M particles with labels from 1 to M (where $2 \leq M \leq N$), the quantity A ,

$$A = (2/M) \sum_{n,m=1; n>m}^M a_{nm}, \quad (1.8a)$$

has real part *less than negative unity*,

$$\operatorname{Re}(A) < -1, \quad (1.8b)$$

so that the corresponding quantity Γ ,

$$\Gamma = (1 + A)^{-1}, \quad (1.9a)$$

has *negative* real part,

$$\operatorname{Re}(\Gamma) < 0. \quad (1.9b)$$

The quantities a_{nm} appearing in the right-hand side of (1.8a) are of course the coupling constants that characterize the two-body interactions acting among the particles belonging to this group of M particles, see (1.43) or (1.41); and there may of course be, for a given N -body problem, several subgroups of particles such that the corresponding quantity Γ , defined according to the above prescription, has *negative* real part, see (1.9b). Let us assume for simplicity that there is just one such group. It is then easily seen that the dominant term at $\tau \approx \tau_b$ of the solution $\zeta(\tau)$ representing the “escape to infinity” of the M coordinates $\zeta_n(\tau)$, $n = 1, \dots, M$, reads

$$\zeta_n(\tau) \approx c_n (\tau - \tau_b)^\Gamma, \quad n = 1, \dots, M, \quad (1.10a)$$

$$\zeta_n(\tau) = b_n, \quad n = M + 1, \dots, N. \quad (1.10b)$$

In these formulas the N (complex) constants b_n are *arbitrary*, while the coefficients c_n , $n = 1, \dots, M$ are determined (up to a common rescaling factor) in terms of the coupling constants a_{nm} with $n, m = 1, \dots, M$ by the following relation

$$A = -2 \sum_{m=1; m \neq n}^M \frac{a_{nm} c_m}{(c_n - c_m)}, \quad n = 1, 2, \dots, M.$$

with (1.8a). Clearly these formulas (see (1.10) and (1.8b)) entail $|\zeta_n(\tau_b)| = |\zeta'_n(\tau_b)| = \infty$ for $n = 1, \dots, M$ and $\zeta_n(\tau_b) = b_n$ for $n = M + 1, \dots, N$. Hence the corresponding “event” at $\tau = \tau_b$ is indeed to be interpreted as the “escape to infinity” of the M particles with (conveniently chosen) labels from 1 to M .

1.2.2.4 Generic coupling constants: dynamical behavior

The behaviors of the corresponding solutions, $z(t)$, of the “physical” equations of motion (1.41) depends on the locations of the branch points τ_b in the complex τ -plane, which of course depend themselves on the initial data (and on the coupling constants a_{ij}). (Note that the analysis reported in the last two subsections is local, namely it applies in the neighborhood of each branch point; nothing excludes that there be several, or possibly an infinity, of them). If none of these branch points is located inside the disk C (centered in the complex τ -plane at $\tau = i/\omega$ and of radius $1/\omega$) nor on its boundary \tilde{C} , then the solutions $z_n(t)$ are *nonsingular* and *completely periodic* with period T , see (1.38). If instead one branch point, say at $\tau = \tau_b$, falls inside the disk C , then the motion is again *nonsingular* but generally *not* periodic, unless the branch point exponent is (*real* and) *rational*, in which case the motion *may* again be *nonsingular* and *completely periodic* (see below for a justification of the conditional), but with a larger period $\tilde{T} = qT$, where q is the (positive) integer in the denominator of the rational exponent characterizing the branch point, γ respectively Γ , see (1.74) respectively (1.9a), which depends of course on the two-body, respectively on the many-body, “coupling constant” a , respectively A , of the corresponding colliding particles, (indeed a necessary and sufficient condition for the branch point exponent to be *rational* is that a – or A – be themselves *rational*). And if τ_b falls just on the boundary of C , namely on the circular contour \tilde{C} , then at a finite *real* time t_c defined *mod*(T) by the formula $\tau_b = [\exp(i\omega t_c) - 1] / (i\omega)$ the “physical” equations of motion (1.41) become generally *singular*, either because the two particles collide, or because they escape to infinity.

If more than one branch point occurs inside the disk C the analysis must be adjusted accordingly; of course the outcome is critically affected not only by the presence of such branch points, but as well by which sheets they are located on, namely it depends on the overall structure of the Riemann surface associated with $\zeta(\tau)$, the key element being always the path travelled on that surface by the complex point $\tau = [\exp(i\omega t) - 1] / (i\omega)$ as the *real* variable t (“time”) evolves onward from the initial moment $t = 0$.

The general idea is to fix attention on the solution of (1.43) (rather than (1.41)) corresponding to the same initial data (see (1.44)). This defines the solution $\zeta_n(\tau)$ (with $n = 1, 2$, since we are now restricting attention to the two-body case; *but we will see in the next section that essentially the same reasoning applies in the N -body case*), to which is generally associated a multi-sheeted Riemann surface in the complex τ -plane. The behavior of the solution of the “physical” equations of motion (1.41) as a function of the, of course *real*, time t is then obtained by traveling on that Riemann surface following the circular contour \tilde{C} defined by (1.42). Depending on the structure of the Riemann surface, this may entail a motion that is *nonsingular and completely periodic* (with period T , see (1.38), or with a period which is an *integer multiple* of T), that is *singular* (if a branch point happens to sit just on the contour \tilde{C}), or that is *nonsingular but not periodic*. Two mechanisms may give rise to the latter outcome (no periodicity): (i) the nature of the branch points, if they are characterized by an exponent that is not a *real rational number* (whether this is going or not to happen is immediately predictable, since it depends on whether the coupling constant a is or is not itself a *real rational number*, see (1.74) and (1.81b)); (ii) even if the coupling constant is a *real rational number*, so that each branch point yields only a *finite* number of sheets, there still may be an *infinite* number of sheets due to an *infinity* of branch points (of course not all of them occurring necessarily on the same sheet, but possibly in a nested fashion), and it may then happen that by travelling along the contour

\tilde{C} an *endless* sequence of *new* sheets is accessed (a necessary condition for this to happen is that the Riemann surface feature an *infinity* of branch points *inside* the contour \tilde{C} – of course, on different sheets). Of course both mechanisms could be at work simultaneously.

Clearly the *completely periodic* motions correspond to an *integrable behavior* of the system; and *whatever* the value of the coupling constant a , there *always* exist at least a set (having *nonvanishing*, indeed *infinite*, measure in phase space) of initial data which yield such a behavior (*nonsingular* and *completely periodic* motions with period T , see (1.38)). As for the motions which are instead *not periodic*, one may well ask which kind of *complex* (or even *chaotic*) *dynamics* they display. The *irregular* behavior mainly manifests itself as “sensitive dependence on initial conditions”, a phenomenon due to whether it is *infinite* respectively *finite* the number of branch points which, by falling just inside or just outside the circular contour \tilde{C} , determine the (*infinite*) number of sheets that are accessed by a path following that contour \tilde{C} on the Riemann surface associated with the solution $\underline{\zeta}(\tau)$ of (1.43). Indeed, if that number of branch point is *finite*, two sets of initial data that are sufficiently close to each other (in phase space) yield two Riemann surfaces which are sufficiently similar to each other so that, throughout the two motions corresponding to the two sets of initial data, the *same sequence* of sheets is travelled. But if that number of branch points is *infinite*, then even two solutions $\underline{\zeta}(\tau)$ of (1.43) that are initially very close will be associated with two Riemann surfaces in which one relevant branch points falls in one case *inside*, and in the other *outside*, the circular contour \tilde{C} , hence, by travelling on \tilde{C} , after that point has been passed the corresponding trajectories of the physical problem (1.41) (or, equivalently, (1.37)) become different, because from that moment a *different sequence* of sheets is accessed of the two Riemann surfaces associated with the corresponding solutions $\underline{\zeta}(\tau)$ of the evolution equations (1.43). This is then to be interpreted as the cause of the numerically observed *complex dynamics*. We suppose that, for the kind of *chaotic* motions we are dealing with, there is no local exponential divergence of trajectories; the mechanism that causes the onset of *complex dynamics* in this case is rather analogous to that which characterizes the *nonperiodic* free motion of a point in, say, a triangular plane billiard with angles which are *irrational* fractions of π (then any two trajectories, however close they initially are – and for however long they remain close – eventually become topologically different because one of the two misses a reflection that the other one takes, and from that moment onwards their evolutions become quite different).

As an example of the dynamics generated by the model (1.41), we display in Figure 1.10 a numerical solution of the Newtonian equations of motion (1.41), obtained with the numerical integration software MBS [42], with $\omega = 2\pi$ – hence $T = 1$, see (1.38) – characterized by the following parameters:

$$\begin{aligned} N = 3; \quad a_{12} = a_{21} = a_{RG} = 1, \quad a_{13} = a_{31} = a_{RB} = 2, \\ a_{23} = a_{32} = a_{GB} = 3, \end{aligned} \tag{1.11}$$

where R , G and B refers to the color code used to label the three particles in the numerical simulations. The sequence of motions which appears in Figure 1.10 is characterized by sets of initial data linked to each other by the formulas

$$z_n(0) = z_n^{(0)}, \quad \dot{z}_n(0) = \mu \dot{z}_n^{(0)}. \tag{1.12}$$

of course with $z_n \equiv x_n + iy_n$. Here λ is a *positive* rescaling parameter the different values of which identify different sets of initial data (while the data $x_n^{(0)}$, $y_n^{(0)}$, $\dot{x}_n^{(0)}$, $\dot{y}_n^{(0)}$ are kept fixed). For the example shown in Figure 1.10 we choose the following values of the parameters $x_n^{(0)}$,

μ	0.5	0.780	0.781	1	1.213	1.214	1.219	1.220	1.241
Period	1	1	6	6	6	49	49	50	50
Figure 1.10	a	b	c	-	d	e	-	-	-

μ	1.242	1.25	1.293	1.294	1.295	1.400	1.401	1.41	1.442
Period	51	51	51	57	58	58	59	59	59
Figure 1.10	-	f	-	g	-	-	-	h	-

μ	1.443	1.721	1.722	1.8	1.944	1.945	2.053	2.054	2.1
Period	65	65	66	66	66	68	68	71	71
Figure 1.10	-	-	-	i	-	-	-	-	j

λ	2.108	2.109	2.164	2.165	2.17	2.171	2.172	2.2	2.5
Period	71	72	72	74	74	74	HSL	HSL	HSL
Figure 1.10	-	-	-	-	k	-	-	m	-

Figure 1.8: Different values of the period in terms of λ

Period Change	1 \rightarrow 6	6 \rightarrow 49	49 \rightarrow 50	50 \rightarrow 51	51 \rightarrow 57
Colliding Particles	R-B	R-G	R-G	R-G	R-G
Collision Time	0.48	3.54	24.72	20.59	43.75

Period Change	57 \rightarrow 58	58 \rightarrow 59	59 \rightarrow 65	65 \rightarrow 66	66 \rightarrow 68
Colliding Particles	R-G	R-G	R-G	R-G	R-B
Collision Time	31.49	27.37	8.35	44.25	54.41

Period Change	68 \rightarrow 71	71 \rightarrow 72	72 \rightarrow 74	74 \rightarrow HSL
Colliding Particles	G-B	R-G	R-B	R-G
Collision Time	56.26	5.63	13.75	24.905

Figure 1.9: Observed period jumps

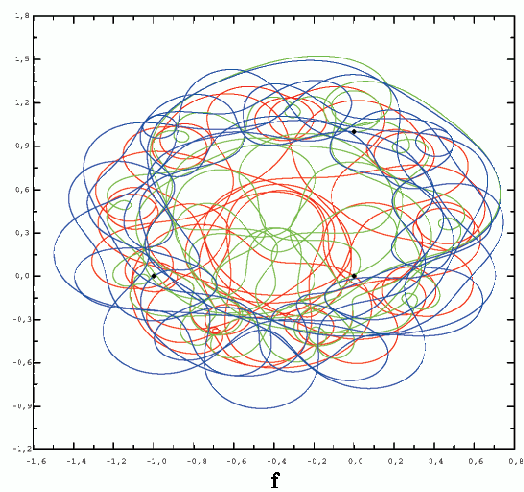
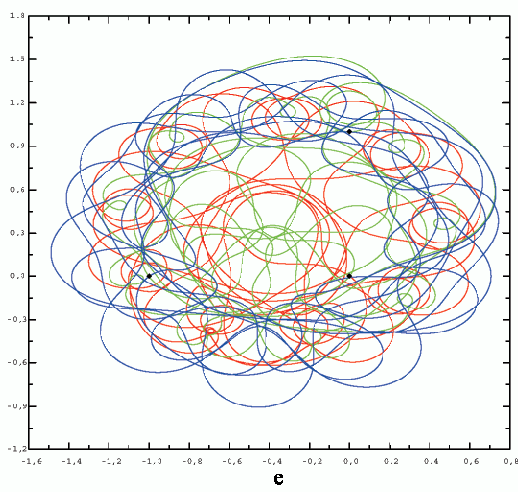
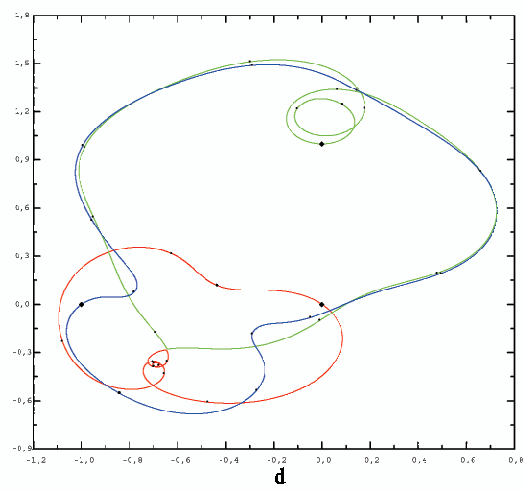
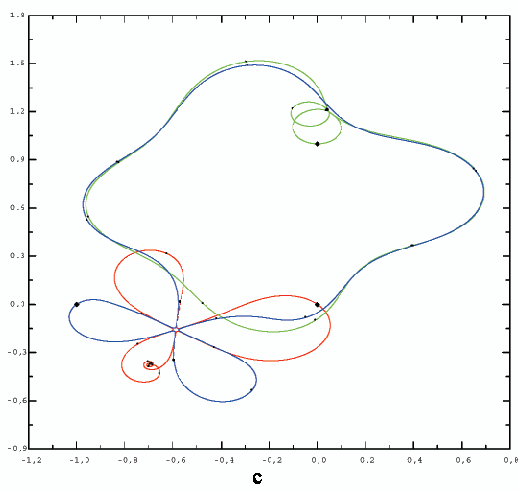
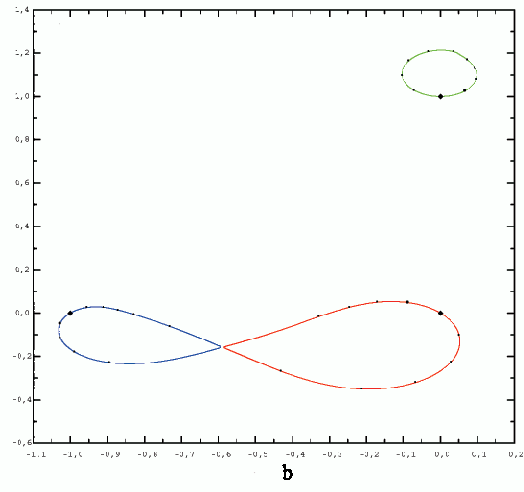
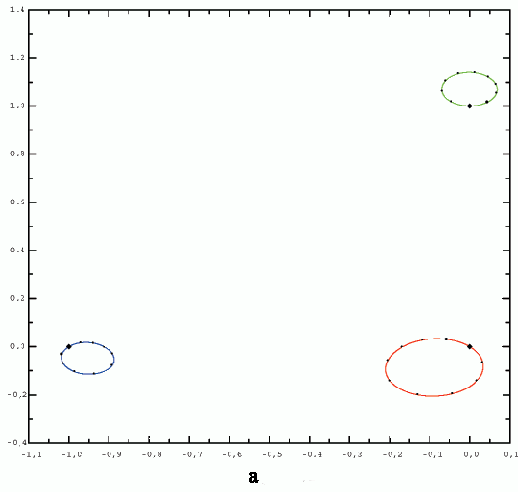
$y_n^{(0)}$, $\dot{x}_n^{(0)}$, $\dot{y}_n^{(0)}$ characterizing the initial data via (1.12):

$$\begin{aligned}
 x_1^{(0)} &= 0, & y_1^{(0)} &= 0, & \dot{x}_1^{(0)} &= -1, & \dot{y}_1^{(0)} &= 1; \\
 x_2^{(0)} &= 0, & y_2^{(0)} &= 1, & \dot{x}_2^{(0)} &= 1, & \dot{y}_2^{(0)} &= 0; \\
 x_3^{(0)} &= -1, & y_3^{(0)} &= 0, & \dot{x}_3^{(0)} &= -0.5, & \dot{y}_3^{(0)} &= -0.5.
 \end{aligned} \tag{1.13}$$

Notice that the trajectories of particle 1, 2 respectively 3 are shown in red, green, respectively blue. In the following tables we summarize, for different values of λ , the corresponding observed periods of the numerical simulation and the corresponding images in Figure 1.10; each period change and which of the three particles are involved in the corresponding collision (in this case we have the following values for the exponent γ : $\gamma_{RG} = 1/2$, $\gamma_{BR} = 1/3$ and $\gamma_{GB} = 1/4$). When the numerical simulation seems to be *non-periodic* (suggesting an *irregular*, potentially *chaotic*, dynamics) we use the acronym HSL, which stands for ‘‘Hic Sunt Leones’’.

1.3 Non-integrability and analyticity in complex time

The two models presented in the previous section emphasize the idea that there exists a link between the integrability properties of a dynamical system and the analytic structure of its solutions as functions of the independent variable (‘‘time’’, but considered as a *complex* variable).



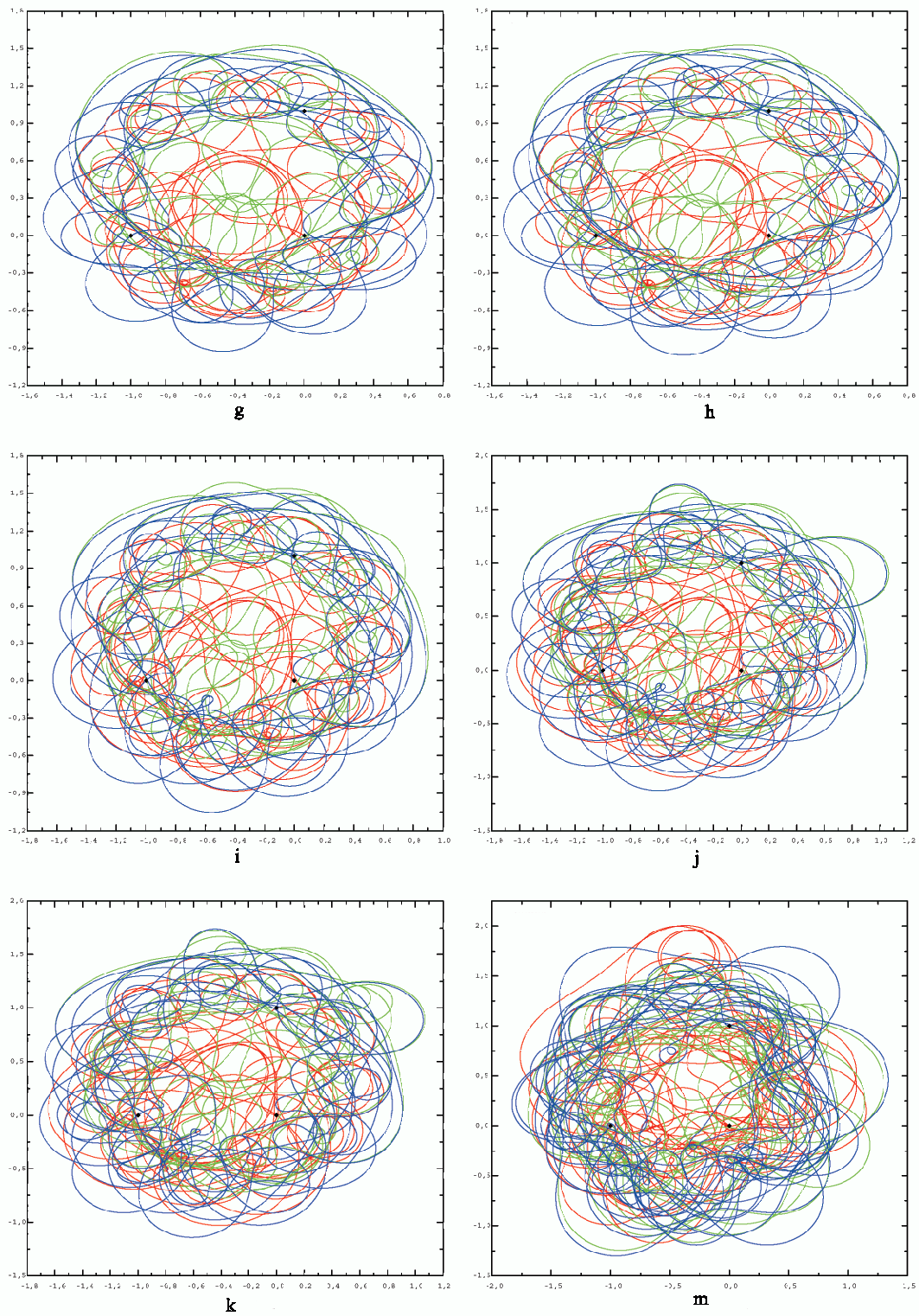


Figure 1.10: A numerical example of the dynamics of the Goldfish model.

This concept goes back to such eminent mathematicians as Carl Jacobi, Sophia Kowalewskaya, Henri Poincaré, Paul Painlevé and his school. This notion was also discussed several times by Martin Kruskal, whose main ideas – a synthetic if overly terse rendition of which might be the statement that *integrability is compatible with the presence of multivaluedness but only provided this is not excessive* – can be gleaned from some papers written by himself and some of his collaborators [55], or by others who performed theoretical and numerical investigations motivated by his ideas [56].

It is worth noting that most of the results reported in many of these works [56] have the disadvantage that they study such physical dynamical systems directly substituting the evolutionary real time variable with a complex time variable which must evolve on a closed contour on the complex plane, so that one can point out the presence of branch points and singularities. At the contrary, the advantage given by the trick is to offer the possibility of describe the real time physical behavior of a certain model studying an *auxiliary* model with respect to a complex time which evolves periodically along a closed path.

In Section 1.4 we will introduce a new (Aristotelian) model, that will be the main object of the remaining chapters of this thesis. The main interest of this many-body problem remains in the fact that it is possible to develop in full detail the line of investigation traced so far: namely, we will be able to completely describe the analytic structure of the solutions of the *auxiliary* model, obtained from the physical one via the trick, and to stress the physical implications of such findings, providing a prototype of a mechanism explaining the transition from *regular* to *irregular* motions as travel on Riemann surfaces.

1.3.1 Ziglin and Yoshida Theorems

In this subsection we present two rigorous results which emphasize the connection between non-integrability of dynamical systems and analytic structure of their solutions (in complex time).

The fundamental papers of Ziglin [57] gave the formulation of a very basic theorem about nonintegrability of analytic Hamiltonian systems. The idea of Ziglin's approach lies in a deep connection between properties of solutions of such systems on a complex time plane and the existence of first integral. This idea takes its origins in works of S. W. Kovalevskaya and A. M. Lyapunov. Ziglin works found a lot of continuations and many important applications [58], [59] and [60]. The main results concerns the existence on an N -th single-valued integral, for analytic Hamiltonian systems of N degrees of freedom which already possess $N - 1$ single-valued integrals. For the sake of semplicity, we will state Ziglin's theorem in the case $N = 2$.

Theorem 6. *Suppose to have an Hamiltonian dynamical system, characterized by the analytic Hamiltonian with two degrees of freedom of the following form*

$$H = \frac{1}{2} (p_1^2 + p_2^2) + V(q_1, q_2) , \quad (1.14)$$

and suppose it possesses the a solution $\{q_1(t), q_2(t)\}$ which satisfies the (straight line) relation

$$c_1 q_1(t) + c_2 q_2(t) = 0 \quad (1.15)$$

and which is a meromorphic function of t . Now consider the normal variational equation of that solution and assume that we know one non-resonant, diagonalizable matrix g_1 of the monodromy group of this normal variational equation. We recall that a matrix is said to be resonant if all its eigenvalues are roots of unity.

Then, if the system possesses a second single-valued first integral other than (1.14), any other matrix g_2 of the monodromy group of the normal variational equation either commute with g_1 or permute the eigenvectors of g_1 .

The details of this theorem are sufficiently complicated and to avoid to be too dispersive in the presentation we prefer to suggest to the interested reader to look at the cited bibliography, see [57] and [58]. We limit ourselves to stress some fundamental implications of Ziglin's theorem. One may use this theorem to derive, in specific examples, that the two matrixes g_1 and g_2 do not satisfy the *necessary conditions* of either commutation or mutual permutation of the eigenvectors, proving in this way the *non-integrability* of the corresponding Hamiltonian system.

We can write the singular expansion of the solutions q_1, q_2 in a neighborhood of the straight line (1.15) and near a singularity at $t = t_b$ in the following way:

$$q_j(t) = a_0^{(j)} (t - t_b)^{q_0^{(j)}} + a_1^{(j)} (t - t_b)^{q_1^{(j)}} + \dots + a_k^{(j)} (t - t_b)^{q_k^{(j)}} + \dots, \quad (1.16)$$

with $j = 1, 2$ and where $a_k^{(j)}$ and $q_k^{(j)}$ are constants. The $q_k^{(j)}$'s are the so-called Kowalveskaya exponents. Yoshida realized that the non-resonance condition on the matrices g_1 and g_2 mentioned in the theorem essentially implies that, while some of the exponents q_k^j are *rational* numbers, some others are *irrational* numbers. Particularly, Yoshida established, in the case of *homogeneous* potentials $V(q_1, q_2)$, a direct connection between the non-resonance condition of g_1, g_2 and the non-rationality of the Kowalveskaya exponents.

The central result proved by Yoshida concerns autonomous systems of ODEs of the form

$$\frac{dz_j}{dt} = F_j(\underline{z}), \quad \underline{z} \equiv (z_1, z_2, \dots, z_N), \quad j = 1, \dots, N. \quad (1.17a)$$

where the F_j 's are rational, homogeneous functions of the z_i 's, namely:

$$F_j(\lambda^{\kappa_1} z_1, \lambda^{\kappa_2} z_2, \dots, \lambda^{\kappa_N} z_N) = \lambda^{\kappa_j + 1} F_j(z_1, z_2, \dots, z_N), \quad (1.17b)$$

and it can be stated as follows

Theorem 7. *If any Kowalveskaya exponent of the system of ODEs (1.17) is irrational or complex, then this system cannot have $N - 1$ rational, homogeneous first integrals.*

1.4 The Aristotelian three-body problem

Purpose and scope of this section is to introduce and discuss a simple Hamiltonian dynamical system describing the motion of 3 particles in the (*complex*) plane. This 3-body problem is the prototype of a class of models (see [6, 7, 5] and the references cited in Subsection 1.2) that feature a transition from *very simple* (even *isochronous*) to *quite complicated* motions characterized by a *sensitive dependence* both on the initial data and the parameters (“coupling constants”) of the model. This transition can be explained as travel on Riemann surfaces. The interest of this phenomenology – illustrating the *onset* in a *deterministic* context of *irregular* motions – is underlined by its generality [5], suggesting its eventual relevance to understand natural phenomena and experimental investigations. The novelty of the model treated herein is that it allows a quite explicit mathematical treatment. In this section only some of our main findings are reported. The most interesting results, all the proofs and the conclusions are described in the following three chapters.

The model is characterized by the following equations of motion:

$$\dot{z}_n = -i\omega z_n + \frac{g_{n+2}}{z_n - z_{n+1}} + \frac{g_{n+1}}{z_n - z_{n+2}}. \quad (1.18)$$

Notation: here and hereafter indices such as n, m range from 1 to 3 and are defined MOD (3); superimposed dots indicate differentiations with respect to the *real* independent time variable t ; the dependent variables $z_n \equiv z_n(t)$ are *complex*, and indicate the positions

of 3 point “particles” moving in the *complex* z -plane; $i \equiv \sqrt{-1}$ is the *imaginary* unit; the parameter ω is *positive*, and it sets the time scale via the basic period

$$T = \frac{\pi}{\omega} ; \quad (1.19)$$

the 3 quantities g_n are arbitrary coupling constants, but in this thesis we essentially restrict consideration to the case in which they are all *real* and moreover satisfy the “semisymmetrical” restriction

$$g_1 = g_2 = g , \quad g_3 = f , \quad (1.20)$$

entailing that the two particles with labels 1 and 2 are *equal*, while particle 3 is *different*. More special cases are the “fully symmetrical”, or “integrable”, one characterized by the equality of *all* 3 coupling constants,

$$f = g , \quad g_1 = g_2 = g_3 = g , \quad (1.21)$$

and the “two-body” one, with only one nonvanishing coupling constant,

$$g_1 = g_2 = g = 0 , \quad g_3 = f \neq 0 . \quad (1.22a)$$

In this latter case clearly

$$z_3(t) = z_3(0) \exp(-i \omega t) \quad (1.22b)$$

and the remaining *two-body* problem is easily solvable,

$$z_s(t) = \exp(-i \omega t) \left[\frac{1}{2} [z_1(0) + z_2(0)] - (-)^s \left\{ \frac{1}{4} [z_1(0) - z_2(0)]^2 + f \frac{\exp(2i \omega t) - 1}{2i \omega} \right\}^{1/2} \right] , \quad s = 1, 2 . \quad (1.22c)$$

The justification for labelling the fully symmetrical case (1.21) as “integrable” will be clear from the following (or see Section 2.3.4.1 of [5]). The treatment of the more general case with 3 different coupling constants g_n is outlined in Appendix B.

Note that the equations of motion (1.18) are of “Aristotelian”, rather than “Newtonian”, type, inasmuch as they imply that the “velocities”, rather than the “accelerations”, are determined by the “forces”. These equations of motion are Hamiltonian, indeed they follow in the standard manner from the Hamiltonian function

$$H(\underline{z}, \underline{p}) = \sum_{n=1}^3 \left[-i \omega z_n p_n + g_n \frac{p_{n+1} - p_{n+2}}{z_{n+1} - z_{n+2}} \right] . \quad (1.23)$$

And they can be reformulated (see Chapter 2) as, still Hamiltonian, *real* (and *covariant*, even *rotation-invariant*) equations describing the motion of three point particles in the (*real*) horizontal plane.

The following *qualitative* analysis (confirmed by our *quantitative* findings, see below) is useful to get a first idea of the nature of the motions entailed by our model. For *large* values of (the modulus of) z_n the “two-body forces” represented by the last two terms in the right-hand side of (1.18) become *negligible* with respect to the “one-body (linear) force” represented by the first term, hence in this regime $\dot{z}_n \approx -i \omega z_n$ entailing $z_n(t) \approx \text{const} \exp(-i \omega t)$. One thereby infers that, when a particle strays far away from the origin in the complex z -plane, it tends to rotate (clockwise, with period $2T$) on a circle: hence the first *qualitative* conclusion that *all motions are confined*. Secondly, the *two-body* forces cause a *singularity* whenever there is a *collision* of *two* (or all *three*) of the particles, and

become dominant whenever *two* particles get very close to each other, namely in the case of *near misses*. But if the three particles move *aperiodically* in a *confined* region (near the origin) of the *complex* z -plane, an *infinity* of *near misses* shall indeed occur. And since the outcome of a *near miss* is generally quite *different* (whenever the two particles involved in it are *different*) depending on which side the particles slide past each other – and this, especially in the case of *very close* near misses, depends *sensitively* on the initial data of the trajectories under consideration – we see here a mechanism causing a *sensitive dependence* of the time evolution on its initial data. This suggests that our model (1.18), in spite of its simplicity, might also support quite complicated motions, possibly even displaying an “unpredictable” evolution in spite of its *deterministic* character. This hunch is confirmed by the results reported in this section and in the following chapters.

To investigate the dynamics of our “physical” model (1.18) it is convenient to introduce an “auxiliary” model, obtained from it via the following change of dependent and independent variables:

$$z_n(t) = \exp(-i\omega t) \zeta_n(\tau) \quad , \quad \tau(t) = \frac{\exp(2i\omega t) - 1}{2i\omega} \quad . \quad (1.24)$$

Note that initially the coordinates z_n and ζ_n coincide:

$$z_n(0) = \zeta_n(0) \quad . \quad (1.25)$$

The equations of motion of the auxiliary model follow immediately from (1.18) via (1.24) (or, even more directly, by noting that, for $\omega = 0$, $\tau = t$ and $z_n(t) = \zeta_n(\tau)$):

$$\zeta_n' = \frac{g_{n+2}}{\zeta_n - \zeta_{n+1}} + \frac{g_{n+1}}{\zeta_n - \zeta_{n+2}} \quad . \quad (1.26)$$

Here of course the appended prime denotes differentiation with respect to the (*complex*) variable τ .

The definition of $\tau(t)$ implies that as the (*real*) time variable t evolves onwards from $t = 0$, the *complex* variable τ travels round and round, making a full tour (counterclockwise) in every time interval T , on the circle \mathbb{C} the diameter of which, of length $d = 1/\omega$, lies on the imaginary axis in the *complex* τ -plane, with one end at the origin, $\tau = 0$, and the other at $\tau = i/\omega$. Hence these relations, (1.24), entail that if $\zeta_n(\tau)$ is *holomorphic* as a function of the *complex* variable τ in the closed disk D encircled by the circle \mathbb{C} , the corresponding function $z_n(t)$ is *periodic* in the *real* variable t with period $2T$ (indeed *antiperiodic* with period T):

$$z_n(t+T) = -z_n(t) \quad , \quad z_n(t+2T) = z_n(t) \quad . \quad (1.27)$$

But it is easy to prove (see Section 2.4) that the solution $\zeta_n(\tau)$ of (1.26) is *holomorphic* (at least) in the circular disk D_0 centered at the origin of the *complex* τ -plane and having the radius

$$r = \frac{\left(\min_{n,m=1,2,3; m \neq n} |\zeta_n(0) - \zeta_m(0)| \right)^2}{128 \max_{n=1,2,3} |g_n|} \quad . \quad (1.28)$$

One may therefore conclude that our physical system (1.18) is *isochronous with period* $2T$, see (1.19). Indeed an *isochronous* system is characterized by the property to possess one or more *open* sectors of its phase space, each having of course *full dimensionality*, such that *all* motions in each of them are *completely periodic* with the same *fixed period* (the periods may be different in these different sectors of phase space, but must be fixed, i e. independent of the initial data, within each of these sectors): and in our case clearly (at least) *all* the motions characterized by initial data $z_n(0)$ such that

$$\min_{n,m=1,2,3; m \neq n} |z_n(0) - z_m(0)| > 16 \sqrt{\frac{\max_{n=1,2,3} |g_n|}{2\omega}} \quad (1.29)$$

are *completely periodic* with period $2T$, see (1.27), since this inequality, implying (via (1.25) and (1.28)) $r > d$, entails that $\zeta_n(\tau)$ is *holomorphic* (at least) in a disk D_0 that includes, in the *complex* τ -plane, the disk D .

This argument is a first demonstration of the usefulness of the “trick” (1.24), associating the auxiliary system (1.26) to our physical system (1.18). More generally, this relationship (1.24) allows to infer the main characteristics of the *time evolution* of the solutions $z_n(t)$ of our physical system (1.18) from the *analyticity properties* of the corresponding solutions $\zeta_n(\tau)$ of the auxiliary system (1.26): indeed the evolution of $z_n(t)$ as the time t increases from the initial value $t = 0$ is generally related via (1.24) to the values taken by $\zeta_n(\tau)$ when τ rotates (counterclockwise, with period T) on the circle \mathbb{C} in the *complex* τ -plane and correspondingly $\zeta_n(\tau)$ travels on the Riemann surface associated to its *analytic* structure as a function of the *complex* variable τ . Suppose for instance that the *only* singularities of $\zeta_n(\tau)$ in the *finite* part of the *complex* τ -plane are *square-root branch points*, as it is indeed the case for our model (1.18) at least for a range of values of the ratio of the coupling constants f and g , see (1.20) and below.⁴ Then the *isochronous* regime corresponds to initial data such that the corresponding solution $\zeta_n(\tau)$ has *no branch points* inside the circle \mathbb{C} on the main sheet of its Riemann surface (i. e. that characterized by the initial data). Moreover, if there is a *finite (nonvanishing)* number of branch points inside the circle \mathbb{C} on the main sheet of the Riemann surface of $\zeta_n(\tau)$, and a *finite* number of branch points inside the circle \mathbb{C} on all the sheets that are accessed by traveling on the Riemann surface round and round on the circle \mathbb{C} , then clearly the corresponding solution $z_n(t)$ is still a *completely periodic* function of the time t , but now its period is a *finite integer multiple* jT of the basic period T , the value of j depending of course on the number of sheets that get visited along this travel before returning to the main sheet. Hence, in particular, whenever the *total* number q of (*square-root*) branch points of the solution $\zeta_n(\tau)$ of the auxiliary problem (1.26) is *finite*, the corresponding solution $z_n(t)$ of our physical model (1.18) is *completely periodic*, although possibly with a *very large* period (if q is *very large*) the value of which may depend, possibly quite sensitively, on the initial data. On the other hand if the number of (*square-root*) branch points possessed by the generic solution $\zeta_n(\tau)$ is *infinite*, and the Riemann surface associated with the function $\zeta_n(\tau)$ has an *infinite* number of sheets (as it can happen in our case, see below), then it is possible that, as τ goes round and round on the circle \mathbb{C} , the corresponding value of $\zeta_n(\tau)$ travels on this Riemann surface without ever returning to its main sheet, entailing that the time evolution of the corresponding function $z_n(t)$ is *aperiodic*, and that it depends *sensitively* on the initial data inasmuch as these data characterize the positions of the branch points hence the structure of the Riemann surface.

This terse analysis entails an important distinction among all these (*square-root*) branch points: the “active” branch-points are those located *inside* the circle \mathbb{C} on sheets of the Riemann surface accessed – when starting from the main sheet – by travelling round and round on that circle, so that they do affect the subsequent sequence of sheets that get visited; while the “inactive” branch points are, of course, those that fall *outside* the circle \mathbb{C} , as well as those that are located *inside* the circle \mathbb{C} but on sheets of the Riemann surface that do not get visited while travelling round and round on that circle (starting from the main sheet) and that therefore do *not* influence the time-evolution of the corresponding solution of our physical system (1.18). This distinction is of course influenced by the initial data of the problem, that characterize the initial pattern of branch points; clearly it is

⁴The nature of these singularities is generally independent from the particular solution under consideration and can be easily ascertained (see Chapter 2) via local analyses *à la Painlevé* of the generic solution of the equations of motion (1.26), while the number and especially the locations of these singularities – which generally affect all the 3 components $\zeta_n(\tau)$, up to some exceptions – depend on the specific solution under consideration and their identification requires a more detailed knowledge than can be obtained by a local analysis *à la Painlevé*.

not just a “local” characteristic of each branch point depending only on its position (for instance, *inside* or *outside* the circle \mathbb{C}): it depends on the overall structure of the Riemann surface, for instance if there is no branch point on its main sheet – that containing the point of departure of the travel round and round on the circle \mathbb{C} – then clearly *all* the other branch points are *inactive*, irrespective of their location.

Let us also emphasize that, whenever an *active* branch point is *quite close* to the circle \mathbb{C} it corresponds to a *near miss* involving *two* particles of our physical model (1.18), at which these two particles scatter against each other almost at right angles (corresponding to the *square-root* nature of the branch point). The difference between the cases in which such a branch point falls *just inside* respectively *just outside* the circle \mathbb{C} corresponds to a *near miss* in which the two particles slide past each other on one side respectively on the other (see figure 1.11), and this makes a substantial difference as regards the subsequent evolution of our 3-body system (unless the two particles are equal). The closer the *near*

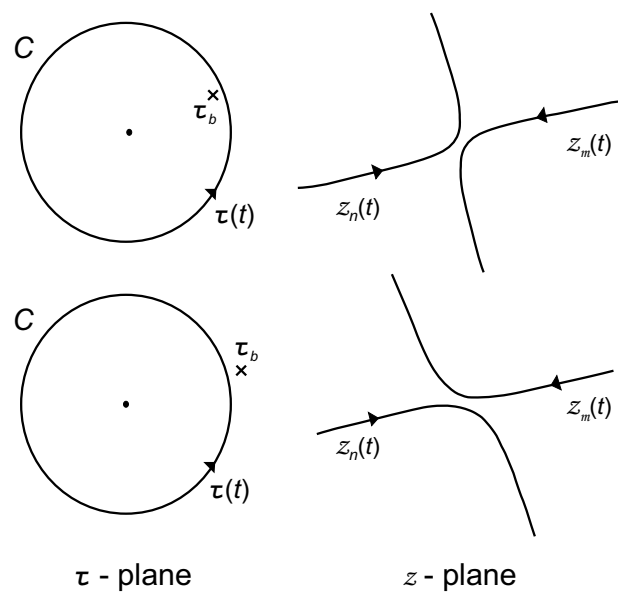


Figure 1.11: Scattering of two bodies in the three-body problem 1.18 corresponding to a *near miss*. The two outcomes originate from two sets of initial data close to each other such that a square-root branch point τ_b falls on different sides of the circle \mathbb{C} .

miss, the more significant this effect is, and the more *sensitive* it is on the *initial data*, a tiny change of which can move the relevant branch point from one side to the other of the circumference of the circle \mathbb{C} and correspondingly drastically affect the outcome of the *near miss*. This is the mechanism that accounts for the fact that, when the initial data are in certain sectors of their phase space (of course quite different from that characterized by the inequalities (1.29)), the resulting motion of the physical 3-body problem (1.18) is *aperiodic*, indeed nontrivially so: in such cases (as we show below) the *aperiodicity* is indeed associated with the coming into play of an *infinite* number of (*square-root*) branch points of the corresponding solution of the auxiliary problem (1.26) and correspondingly with an *infinite* number of *near misses* experienced by the particles throughout their time evolution, this phenomenology being clearly characterized by a *sensitive dependence* on the initial data.

This mechanism to explain the transition from *regular* to *irregular* motions – and in particular from an *isochronous* regime to one featuring *unpredictable* aspects – was already discussed [6, 7] in the context of certain many-body models somewhat analogous to that studied herein, for instance see Section 1.2. But those treatments were limited to providing

a *qualitative* analysis such as that presented above and to ascertaining its congruence with *numerical solutions* of these models. The interest of the simpler model introduced and discussed herein is to allow a detailed, *quantitative* understanding of this phenomenology. This is based on the following explicit solution of our model (1.18), obtained via the auxiliary problem (1.26):

$$z_s(t) = Z \exp(-i\omega t) - \frac{1}{2} \left(\frac{f+8g}{6i\omega} \right)^{1/2} [1 + \eta \exp(-2i\omega t)]^{1/2} \cdot \left\{ [\tilde{w}(t)]^{1/2} - (-)^s [12\mu - 3\tilde{w}(t)]^{1/2} \right\}, \quad s = 1, 2, \quad (1.30a)$$

$$z_3(t) = Z \exp(-i\omega t) + \left(\frac{f+8g}{6i\omega} \right)^{1/2} [1 + \eta \exp(-2i\omega t)]^{1/2} [\tilde{w}(t)]^{1/2}. \quad (1.30b)$$

Here the function $\tilde{w}(t)$ is defined via the relation

$$\tilde{w}(t) = w[\xi(t)], \quad (1.31)$$

with

$$\xi(t) = R [\eta + \exp(2i\omega t)] = \bar{\xi} + R \exp(2i\omega t), \quad (1.32)$$

and $w(\xi)$ implicitly defined by the *nondifferential* equation

$$(w-1)^{\mu-1} w^{-\mu} = \xi. \quad (1.33)$$

The parameter μ is defined in terms of the coupling constants g and f , see (1.20), as follows:

$$\mu = \frac{f+2g}{f+8g}, \quad (1.34)$$

and in (1.30)-(1.32) the *three* constants Z , R , and η (or $\bar{\xi}$) are defined in terms of the 3 initial data $z_n(0)$ as follows:

$$Z = \frac{z_1(0) + z_2(0) + z_3(0)}{3}, \quad (1.35a)$$

$$R = \frac{3(f+8g)}{2i\omega [2z_3(0) - z_1(0) - z_2(0)]^2} \left[1 - \frac{1}{\tilde{w}(0)} \right]^{\mu-1}, \quad (1.35b)$$

$$\bar{\xi} = R\eta, \quad (1.35c)$$

$$\eta = \frac{i\omega \left\{ [z_1(0) - z_2(0)]^2 + [z_2(0) - z_3(0)]^2 + [z_3(0) - z_1(0)]^2 \right\}}{3(f+2g)} - 1, \quad (1.35d)$$

$$\tilde{w}(0) = \frac{2\mu [2z_3(0) - z_1(0) - z_2(0)]^2}{[z_1(0) - z_2(0)]^2 + [z_2(0) - z_3(0)]^2 + [z_3(0) - z_1(0)]^2}. \quad (1.35e)$$

Note that the constant Z is the initial value of the center of mass of the system, and indeed the first term in the right-hand side of the solution (1.30) represents the motion of the center of mass of the system: just a circular motion around the origin, with a constant velocity entailing a period $2T$. Since the rest of the motion is independent of the behavior of the center of mass, in the study of this model attention can be restricted without significant loss of generality to the case when the center of mass does not move, $Z = 0$.

The nontrivial aspects of the motion are encoded in the time evolution of the function $\tilde{w}(t)$, see (1.30) and (1.31): let us emphasize in this connection that the dependent variable $w(\xi)$ is that solution of the *nondifferential* equation (1.33) uniquely identified by continuity, as the time t unfolds, hence as the variable $\xi \equiv \xi(t)$ goes round and round, in the *complex*

ξ -plane, on the circle Ξ with center $\bar{\xi}$ and radius $|R|$ (see (1.32)), from the initial datum assigned at $t = 0$,

$$w[\xi(0)] = w(\bar{\xi} + R) = \check{w}(0) \quad , \quad (1.36)$$

see (1.35e). This specification of the initial value $\check{w}(0)$ is relevant, because generally the *nondifferential* equation (1.33) has more than a single solution, in fact possibly an *infinity* of solutions, see below.

It is clear from (1.30) that the time evolution of the solution $z_n(t)$ of our model (1.18) is *mainly* determined by the time evolution of the function $\check{w}(t)$. Indeed,

1. The factor $[\eta \exp(-2i\omega t) - 1]^{1/2}$ displays a quite simple time evolution, *periodic* with period T if $|\eta| < 1$ and *antiperiodic* with period T hence *periodic* with period $2T$ if $|\eta| > 1$.
2. If $\check{w}(t)$ is *periodic* with period \check{T} , its square root $[\check{w}(t)]^{1/2}$, appearing in the right-hand side of the solution formulas (1.30), is clearly as well *periodic* with period \check{T} or *antiperiodic* with period \check{T} hence *periodic* with period $2\check{T}$ depending whether the closed trajectory of $\check{w}(t)$ in the complex \check{w} -plane does not or does enclose the (branch) point $\check{w} = 0$.
3. Likewise the square root $[12\mu - 3\check{w}(t)]^{1/2}$ (see (1.30)) is also *periodic* with period \check{T} or *antiperiodic* with period \check{T} hence *periodic* with period $2\check{T}$ depending whether the closed trajectory of $\check{w}(t)$ in the complex \check{w} -plane does not or does enclose the (branch) point $\check{w} = 4\mu$ (but note that a change of sign of this square root only entails an exchange between the two equal particles 1 and 2).
4. In conclusion one sees that – provided one considers particles 1 and 2 as *indistinguishable* – then, if the time evolution of $\check{w}(t)$ is *periodic* with period \check{T} , $\check{w}(t + \check{T}) = \check{w}(t)$, the physical motion of the 3 particles $z_n(t)$ is also *completely periodic* either with the same period \check{T} or with period $2\check{T}$, provided \check{T} is an *integer multiple* of T ;
5. Finally, if the motion of $\check{w}(t)$ is not periodic then clearly the functions $z_n(t)$ are also not periodic.

Hereafter we only discuss the time evolution of the function $\check{w}(t)$; actually, as explained below, in this thesis we limit our consideration to discussing the motion of a *generic* solution $\check{w}(t) = w[\xi(t)]$ of the *nondifferential* equation (1.33). Moreover, we consider only *generic* solutions of (1.18), namely those characterized by initial data that exclude one of the following special outcomes:

- (a) $\check{w}(t)$ takes, at some (*real*) time t_a , the value $\check{w}(t_a) = 4\mu$ entailing a *pair collision* of the 2 equal particles occurring at this time, $z_1(t_a) = z_2(t_a)$.
- (b) $\check{w}(t)$ takes, at some (*real*) time t_b , the value $\check{w}(t_b) = \mu$ entailing a *pair collision* of the different particle with one of the 2 equal particles occurring at this time, $z_1(t_b) = z_3(t_b)$ or $z_2(t_b) = z_3(t_b)$.
- (c) The constant η has unit modulus, $|\eta| = 1$, i. e. $\eta = \exp(2i\omega t_c)$ with t_c *real* (and of course defined MOD T) which entails a *triple collision* of the 3 particles occurring at the time t_c , $z_1(t_c) = z_2(t_c) = z_3(t_c)$.
- (c') $\check{w}(t)$ vanishes at some (*real*) time t_c , $\check{w}(t_c) = 0$ (but, as our notation suggests, this case (c') is just a subcase of (c), although this is not immediately obvious from (1.30) but requires using also (1.32) and (1.33)).

The initial data that give rise to solutions having one of these singularities form a set of null measure. It can be easily seen that these singular solutions $z_n(t)$ of our physical problem (1.18) correspond via (1.24) to special solutions $\zeta_n(\tau)$ of our auxiliary problem (1.26) possessing a *branch point* that sits *exactly* on the circle \mathbb{C} in the complex τ -plane: more precisely,

- (a) a *square-root* branch point featured by $\zeta_1(\tau)$ and $\zeta_2(\tau)$ but not by $\zeta_3(\tau)$,
- (b) a *square-root* branch point featured by all 3 functions $\zeta_n(\tau)$,
- (c) a branch point featured by all 3 functions $\zeta_n(\tau)$ the nature of which depends on the parameter μ .

As mentioned above, in this work we essentially confine our treatment to discussing the time evolution of a *generic* root $\tilde{w}(t)$ of the *nondifferential* equation (1.33) with (1.32), and in particular to identifying for which initial data its time evolution is *periodic*, and in such a case what the period is. Remarkably we find out that, for (*arbitrarily*) given initial data, *all* these roots have at most three different periods (one of which might be *infinite*, signifying an *aperiodic* motion), see Chapter 3; periods which we are able to determine explicitly (although the relevant formulas have some nontrivial, even “chaotic”, aspects, in a sense that will be more clear and explicit in the final Chapter 4). The question of identifying, among *all* the roots $\tilde{w}_j(t)$ of this *nondifferential* equation (1.33), the “physical” one $\tilde{w}(t)$ i. e. the one that evolves from the initial datum (1.35e), and in particular of specifying the character of its time evolution among the (at most 3) alternatives, see Chapter 3, was still an open problem at the time this thesis was written and it will be reported in [2]. Let us re-emphasize that the time evolution of $\tilde{w}(t) \equiv w[\xi(t)]$ coincides with the evolution of a *generic* root $w(\xi)$ of (1.33) as the independent variable ξ travels (making a complete counterclockwise tour in the *complex* ξ -plane in every time interval T) on the circle Ξ with center $\bar{\xi}$ and radius $|R|$, see (1.32), and correspondingly the dependent variable $w(\xi)$ travels on its Riemann surface. Note that this Riemann surface is completely defined by the single parameter μ , see (1.34) and (1.33), while the circle Ξ is defined by the initial data of the problem, see (1.32) with (1.35).

What therefore remains to be discussed is the *analytic* structure of the multivalued function $w(\xi)$ defined implicitly by the *nondifferential* equation (1.33) or, equivalently but more directly, the time dependence of the corresponding function $\tilde{w}(t) \equiv \tilde{w}[\xi(t)]$. To begin with, we consider the case in which the parameter μ is *rational*,

$$\mu = \frac{p}{q}, \quad (1.37)$$

with p and q coprime integers and q *positive*, $q > 0$. The extension of the results to the case of *irrational* μ is made subsequently; although, to avoid repetitions, we present below some results in a manner already appropriate to include also the more general case with μ *real*.

In the *rational* case (1.37) the *nondifferential* equation that determines the “dependent variable” $\tilde{w}(t)$ in terms of the “independent variable” t becomes *polynomial*, and takes one of the following 3 forms depending on the value of the parameter μ , see (1.37):

$$(\tilde{w} - 1)^{p-q} = [\bar{\xi} + R \exp(2i\omega t)]^q \tilde{w}^p, \quad \text{if } \mu > 1, \quad (1.38a)$$

$$[\bar{\xi} + R \exp(2i\omega t)]^q (\tilde{w} - 1)^{q-p} \tilde{w}^p = 1, \quad \text{if } 0 < \mu < 1, \quad (1.38b)$$

$$[\bar{\xi} + R \exp(2i\omega t)]^q (\tilde{w} - 1)^{q+|p|} = \tilde{w}^{|p|}, \quad \text{if } \mu < 0. \quad (1.38c)$$

The above expressions are polynomials (in the dependent variable \tilde{w}) of degree J :

$$J = \begin{cases} p, & \text{if } \mu > 1; \\ q, & \text{if } 0 < \mu < 1; \\ q + |p|, & \text{if } \mu < 0. \end{cases} \quad (1.39)$$

As for the boundaries of these 3 cases, let us recall that $\mu = 1$ corresponds, via (1.34), to $g = 0$, namely, see (1.20), to the trivially solvable *two-body* case, see (1.22), while $\mu = 0$ respectively $\mu = \infty$ correspond, via (1.34), to $f + 2g = 0$ respectively to $f + 8g = 0$ and require a separate treatment (see 2). Clearly the third case ($\mu < 0$) becomes identical to the first ($\mu > 1$) via the replacement

$$\tilde{w} \mapsto 1 - \tilde{w}, \quad \bar{\xi} \mapsto -\bar{\xi}, \quad R \mapsto -R, \quad -p \mapsto p - q, \quad q - p \mapsto p \quad (1.40)$$

without modifying q ; therefore in the following, without loss of generality, we often forsake a separate discussion of this third case.

Clearly the factor $[\bar{\xi} + R \exp(2i\omega t)]^q$, which carries all the time dependence in these polynomial equations, is *periodic* in t with period T , see (1.19) (except for the *special* initial conditions entailing $\bar{\xi} = 0$ in which case this factor is instead periodic with the shorter period T/q , see Chapter 2).

At issue is the behavior of the J roots $\tilde{w}_j(t)$ of our polynomial equation (1.38) whose coefficients evolve in time periodically with period T . Let us indicate with $\tilde{W}(t) \equiv \{\tilde{w}_j(t); j = 1, \dots, J\}$ the (*unordered*) set of these J roots. Obviously $\tilde{W}(t)$ is *periodic* with period T , $\tilde{W}(t + T) = \tilde{W}(t)$: after one period T the polynomial equation is unchanged, hence the set of its J roots is as well unchanged. But that does *not* imply that if one follows the time evolution of these J roots, each of them will return to its own initial value after one period, $\tilde{w}_j(T) = \tilde{w}_j(0)$, $j = 1, \dots, J$. This outcome will indeed obtain for the *open* domain of initial data of our problem that corresponds to the basic *isochronous* regime, see (1.27); but it does not happen for other initial data, in which cases for instance a *generic* root, say $\tilde{w}_{j_1}(t) \equiv \tilde{w}(t)$, may after one period land in the initial position of a different root, say $\tilde{w}(T) = \tilde{w}_{j_2}(0)$, and then after one more period end up in the initial position of yet another root, $\tilde{w}(2T) = \tilde{w}_{j_3}(0)$, and so on. Eventually, of course, after a time $\tilde{T} = \tilde{j}T$ which is a *finite integer* multiple \tilde{j} of the basic period T , with $1 \leq \tilde{j} \leq J$, the *generic* root $\tilde{w}(t)$ shall necessarily return to its initial position, $\tilde{w}(\tilde{T}) = \tilde{w}(0)$, entailing that its evolution as a function of the time t is *periodic* with this period \tilde{T} ,

$$\tilde{w}(t + \tilde{T}) \equiv \tilde{w}(t + \tilde{j}T) = \tilde{w}(t) . \quad (1.41)$$

This discussion clearly implies (via (1.30)) that, in the case now under consideration (with a *rational* value of the parameter μ , see (1.37)), *all* solutions of our physical problem (1.18) with (1.20) are *completely periodic* with a period which is either

$$\tilde{T} = \tilde{j}T \quad \text{with } 1 \leq \tilde{j} \leq J \quad (1.42)$$

and J defined by (1.39), or it is $2\tilde{T}$ (see the discussion above following (1.36)). The remaining, crucial question is: how does the value of the integer \tilde{j} (which might be *quite large* if J is *quite large*) depend on the initial data of our problem? In Chapter 3 we outline how to calculate, for given initial data, *all* the possible periods of the J roots $\tilde{w}_j(t)$ of (1.38), and in Chapter 4 we display formulas providing (at most) 3 alternative values for these periods; as already mentioned above, the explanation of how to identify which one of these 3 periods corresponds to that of the “physical” root $\tilde{w}(t)$ entails a more detailed treatment which is one of the open goal of research and it will be reported in [2].

But before doing so let us emphasize that via this discussion the time evolution of our original 3-body problem – describing the time evolution of the three points $z_n(t)$ in the *complex* z -plane – has been related to the time evolution of the J roots $\tilde{w}_j(t)$ of (1.38) in the *complex* w -plane, and in particular to the way they get permuted among themselves over the time evolution after each period T . As we will explain below, the possible complications of the motions of our physical model (1.18) are thereby related to the mechanisms at play to

permute these roots among themselves when one watches their time evolution at subsequent intervals T , $2T$, $3T$ and so on. And, in this context, it is significant to note that, whenever μ is *irrational*, one is in fact dealing with the dynamics of an *infinite* number of roots. This suggests that whenever the number J of roots is large, and even more so when μ is irrational (entailing $J = \infty$), the time evolution of our physical model (1.18) might be quite complicated, perhaps calling into play the theoretical tools of statistical mechanics rather than those of few-body dynamics (but we postpone such excursions to future publications).

As entailed by our discussion above, the issue of determining the value of the integer \tilde{j} is tantamount to understanding the structure of the Riemann surface associated with the function $w(\xi)$ of the *complex* variable ξ defined by the *nondifferential* equation (1.33), whose different sheets correspond of course to the different roots of this *nondifferential* equation. In the *rational* case (1.37) this equation is in fact *polynomial* of degree J in the dependent variable w . Specifically, what must be ascertained is the number of sheets of this Riemann surface that are accessed by $w(\xi)$ when the independent variable ξ travels in the *complex* ξ -plane round and round on the circle Ξ , whose center $\bar{\xi}$ and radius $|R|$ depend on the initial data of our physical problem, see (1.32) and (1.35). To this end one must gain and use a detailed understanding of the structure of this Riemann surface. In Chapter 3 we will see how this analysis is possible. Here we report the following basic information on the *analytic* structure of the function $w(\xi)$, referring to the general case with *real* μ (*rational* or *irrational*).

The nondifferential equation (1.33) defines a J -sheeted covering of the *complex* ξ -plane of genus *zero* (of course $J = \infty$ if μ is irrational). The function $w(\xi)$ defined implicitly by this equation features *square-root* branch points ξ_b located on a circle B centered at the origin of the *complex* ξ -plane:

$$\xi_b = \xi_b^{(k)} = r_b \exp(2\pi i \mu k) , \quad k = 1, 2, 3, \dots , \quad (1.43a)$$

$$\xi_b = \xi_b^{(k)} = r_b \exp\left[i \frac{2\pi p k}{q}\right] , \quad k = 1, 2, \dots, q , \quad (1.43b)$$

$$r_b = (\mu - 1)^{-1} \left(\frac{\mu - 1}{\mu}\right)^\mu . \quad (1.43c)$$

In the last, (1.43c), of these formulas it is understood for definiteness that the *principal* determination is taken of the μ -th power appearing in the right-hand side. The first of these formulas, (1.43a), shows clearly that the number of these branch points is *infinite* if the parameter μ is *irrational*, and that they then sit densely on the circle B in the complex ξ -plane centered at the origin and having radius $|r_b|$, see (1.43c). Note that this entails that the *generic* point on the circle B is *not* a branch point (just as a *generic real* number is *not rational*); but every generic point on the circle B has, if μ is *irrational*, some branch point (in fact, an *infinity* of branch points!) *arbitrarily* close to it (just as every generic *real* number has an *infinity* of *rational* numbers *arbitrarily* close to it). It is also important to realize that these branch points are generally on *different* sheets of the Riemann surface associated with the function $w(\xi)$: hence, they are dense if one considers the circle B in the *complex* ξ -plane, but they are not dense if one considers these branch points on the Riemann surface itself. As for the second of these formulas, (1.43b), it is instead appropriate to the case in which the parameter μ is *rational*, see (1.37), in which case the branch points sit again on the circle B in the complex ξ -plane, but there are only a *finite* number, q , of them (and note that the factor p appearing in the argument of the exponential in the right-hand side of this formula, (1.43b), is only relevant to characterize how the branch points $\xi_b^{(k)}$ are labelled via the index k). Both in the *irrational* and in the *rational* case at *all* these branch points the *nondifferential* equation (1.33) has a *double* root which takes the *same* value

$w(\xi_b) = \mu$. Note that this entails that circling around such a branch point in the complex ξ -plane corresponds to permuting 2 of the J roots $w_j(\xi)$ among themselves.

In addition, the function $w(\xi)$ possesses branch points at $\xi = 0$ and at $\xi = \infty$, the order of which depends on the value of μ , and is *rational* if the number μ is *rational*.

The branch point at $\xi = \infty$ has, if $\mu > 1$, exponent $-\frac{1}{\mu}$ ($= -\frac{q}{p}$ in the *rational* case),

$$\xi \approx \infty, \quad w(\xi) \approx a \xi^{-1/\mu} \approx 0, \quad a^\mu = -\exp(-i\pi\mu), \quad \mu > 0, \quad (1.44)$$

while it has instead two different exponents if $0 < \mu < 1$:

1. the exponent $-\frac{1}{\mu}$ ($= -\frac{q}{p}$ in the *rational* case) as given by the preceding formula (entailing $w \approx 0$)
2. the exponent $-\frac{1}{1-\mu}$ ($= \frac{q}{q-p}$ in the *rational* case) as given by the following formula (entailing $w \approx 1$),

$$\xi \approx \infty, \quad w(\xi) \approx 1 + a \xi^{-1/(1-\mu)} \approx 1, \quad a^{\mu-1} = 1, \quad 0 < \mu < 1. \quad (1.45)$$

The branch point at $\xi = 0$ is, if $\mu > 1$, of exponent $\frac{1}{\mu-1}$ ($= \frac{q}{p-q}$ in the *rational* case),

$$\xi \approx 0, \quad w(\xi) \approx 1 + a \xi^{1/(\mu-1)} \approx 1, \quad a^{\mu-1} = 1, \quad \mu > 1, \quad (1.46)$$

(note the formal analogy of this formula with the previous one, (1.45)), and it is instead *absent* if $0 < \mu < 1$, so that in this second case the *only* branch points in the finite part of the *complex* ξ -plane are those of *square-root* type, see (1.43a). This is the main cause of the difference between the results, see below, for this case ($0 < \mu < 1$) from those for the other two cases ($\mu > 1$ and $\mu < 0$), which are on the other hand essentially equivalent among each other being related by the transformation $\mu \mapsto 1 - \mu$, $w(\xi) \mapsto 1 - w(-\xi)$, see (1.33) (so that without loss of generality we often forsake an explicit discussion of the case with $\mu < 0$).

Note that these results entail that, in the *rational* case, see (1.37), making a circle around the branch point at $\xi = 0$, in the $p > q$ (i. e. $\mu > 1$) case when this branch point is present, causes a cyclic permutation of $p - q$ of the p roots w_j : this is particularly evident if one imagines to travel full circle around the branch point at $\xi = 0$ in its immediate vicinity, since for $\xi \approx 0$ the p roots w_j of (1.33) are clearly divided into *two* sets, a first set of $p - q$ roots, disposed equispaced on a circle of small radius ($\approx |\xi|^{q/(p-q)}$) centered at $w = 1$ in the *complex* w -plane, which then undergo a cyclic permutation among themselves, and a second set of q roots, disposed equispaced on a circle in the *complex* w -plane centered at the origin and having a large radius ($\approx |\xi|^{-1}$), each of which after the operation returns instead to its original position.

The permutation experienced by the J roots $\tilde{w}_j(t)$ due to a sequence of pairwise exchanges of roots – which take place whenever *square-root* branch points are included *inside* the circle Ξ traveled by the point $\xi(t)$ – causes a reshuffling of the roots which is nontrivial inasmuch as it depends on how many and on which pairs of roots get sequentially exchanged over each period, as determined by the number and identity of *square-root* branch points enclosed inside the circle Ξ traveled by $\xi(t)$ and by the detailed structure of the Riemann surface associated with these branch points, in particular on which sheets of this Riemann surface the relevant branch points are located. The reshuffling encompasses more roots when a second mechanism is simultaneously at play, i. e. that producing a cyclic permutation of $p - q$ roots (especially, of course, when $p - q$ is large) over each period, as caused by the presence of the branch point at $\xi = 0$: this second mechanism exists only if $\mu > 1$ (or $\mu < 0$, entailing the exchange $-p \mapsto p - q$), and provided the circle Ξ travelled by $\xi(t)$ *does include* the point $\xi = 0$. How we will see in the following chapters, this phenomenology

causes the possible periods $\tilde{T} = \tilde{j}T$ of the time evolution of the *generic* root $\tilde{w}(t)$ to depend on the initial data, but remarkably we will see that, for given initial data, there are (at most) only 3 possible values of these periods, and that they can be given explicitly in terms of the initial data and of the two numbers p and q see (1.37). Indeed we show below that analogous results can as well be given in the case when μ is *irrational*, in spite of the fact that the dependence on the initial data may then be quite *sensitive*.

CHAPTER 2

A Simple Three-Body Problem

In this and in the following chapter we will present a detailed analysis of the simple Hamiltonian three-body problem introduced in Section 1.4, discussing and proving all the results reported therein.

In Subsection 1.1.2 we introduced a simple trick, which associates, to any dynamical system belonging to a quite large class (characterized by the *complex* independent variable τ), a related system characterized by a (*real*) “deformation parameter” $\omega > 0$ having the dimension (and significance) of a (circular) frequency. Our philosophy is to consider the ω -deformed system, whose evolution takes place in the *real* time t , as the “physical” model, and the undeformed system as an “auxiliary” model that, as we will see, plays an essential role to understand the time evolution of the *physical* system.

In the following Section 2.1 we introduce again the Aristotelian model, already presented in Section 1.4. In Section 2.2 we describe the Hamiltonian character of our model, we exhibit the constants of motion it possesses, and we also indicate some possible reformulations of it which might appear more “physical” inasmuch as they describe motions taking place in the *real* plane rather than in the *complex* plane: namely, the *dependent* variables of our *physical* model can be reinterpreted to be (rather than *complex* numbers) *real* two-vectors, the time evolution of which takes place in the horizontal plane and is determined by *real* and *covariant* equations of motion. In Section 2.3 we discuss the equilibrium configurations of our *physical* model, and the behavior of this system in the neighborhood of these solutions, and we also obtain certain *exact* “similarity solutions” of our model and discuss their stability. In Section 2.4 we discuss the analytic structure of the solutions of the *auxiliary* model via local analysis *à la Painlevé*, since the analytic structure of these solutions plays a crucial role in determining the time evolution of our *physical* model. Already in parts of Sections 2.3 and 2.4, and in most of the subsequent developments, we find it convenient to restrict attention to the “semisymmetrical” subcase of our model, characterized by the equality of *two* of the *three* coupling constants g_n (see (2.2) in the following Section 2.1). In Section 2.5 we show how the *general solution* of our model can be achieved by *quadratures*, and in Section 2.6 we discuss the behavior of our model based on these results, reducing the problem of explaining the physical dynamics to understanding the structure of the Riemann surface associated to a certain *nondifferential* equation (which becomes an *algebraic* equation in case of *rational* coupling constants); this surface will be the main subject of the next Chapter 3. We confined in the Appendices certain calculations (to avoid interrupting inconveniently the flow of the presentation) as well as certain additional findings, including a list (in Appendix C) of several special cases in which the model discussed in this thesis can be solved in completely explicit form, and a discussion (in Appendix D) of the relation

of the model discussed in this thesis with more classical models.

The results reported herein mainly refers to a paper in preparation [2], co-authored by the author of this thesis in collaboration with F. Calogero, D. Gomez-Ullate and P. M. Santini.

2.1 Presentation of the model

In this section we reintroduce the new model treated in this thesis, already presented in 1.4, and we outline some of its analyticity and periodicity properties in connection with the theory presented in Chapter 1.

The undeformed *auxiliary* model on which we focus in this thesis is characterized by the following system of *three* coupled nonlinear ODEs:

$$\zeta'_n = \frac{g_{n+2}}{\zeta_n - \zeta_{n+1}} + \frac{g_{n+1}}{\zeta_n - \zeta_{n+2}} . \quad (2.1)$$

Notation: here and hereafter indices such as n , m range from 1 to 3 and are defined MOD 3; τ is the (*complex*) independent variable of this *auxiliary* model; the *three* functions $\zeta_n \equiv \zeta_n(\tau)$ are the dependent variables of this *auxiliary* model, and we shall assume them to be as well *complex*; an appended prime always denotes differentiation with respect to the argument of the functions they are appended to (here, of course, with respect to the *complex* variable τ); and the *three* quantities g_n are arbitrary “coupling constants” (possibly also *complex*; but in this work we restrict consideration mainly to the case with *real* coupling constants; this is in particular hereafter assumed in this section). In the following we will often focus on the “semisymmetrical case” characterized by the equality of *two* of the *three* coupling constants, say

$$g_1 = g_2 = g , \quad g_3 = f , \quad \varphi \equiv \frac{f}{g} , \quad (2.2)$$

since in this case the treatment is simpler yet still adequate to exhibit most aspects of the phenomenology we are interested in. More special cases are the “fully symmetrical”, or “integrable”, one characterized by the equality of *all three* coupling constants,

$$g = f , \quad g_1 = g_2 = g_3 = g , \quad \varphi = 1 , \quad (2.3)$$

and the “two-body” one, with only one nonvanishing coupling constant, say

$$g_1 = g_2 = g = 0 , \quad g_3 = f \neq 0 , \quad \varphi = \infty . \quad (2.4a)$$

In this latter case clearly

$$\zeta'_3 = 0 , \quad \zeta_3(\tau) = \zeta_3(0) \quad (2.4b)$$

(see (2.1)) and the remaining *two-body* problem is trivially solvable,

$$\zeta_s(\tau) = \frac{1}{2} [\zeta_1(0) + \zeta_2(0)] - (-)^s \left\{ \frac{1}{4} [\zeta_1(0) - \zeta_2(0)]^2 + f \tau \right\}^{1/2} , \quad s = 1, 2 ; \quad (2.4c)$$

while the justification for labelling the fully symmetrical case (2.3) as “integrable” will be clear from the following (or see Section 1.3.4.1 of [5]).

Before proceeding to introduce our *physical* model, let us note that the *auxiliary* system (2.1) is *invariant* under translations of both the independent variable τ (indeed, it is *autonomous*) and the dependent variables $\zeta_n(\tau)$ ($\zeta_n(\tau) \Rightarrow \zeta_n(\tau) + \zeta_0$, $\zeta'_0 = 0$), and it is moreover *invariant* under an appropriate simultaneous rescaling of the independent and

the dependent variables. Indeed clearly, if a triple of functions $\zeta_n(\tau)$ satisfies the system (2.1), the triple

$$\tilde{\zeta}_n(\tau) = A + C \zeta_n \left(\frac{\tau - \tau_0}{C^2} \right) , \quad (2.5)$$

satisfies the *same* system, for any *arbitrary* assignment of the *three* (possibly *complex*) constants A , C and τ_0 . Hence it is generally possible to obtain, via this property, the *general* solution of the system (2.1) (which must indeed feature *three* arbitrary constants) from a particular solution (provided this particular solution is not too special: see below). And let us also point out that, as immediately implied by (2.1), the center of mass of the *three* coordinates ζ_n ,

$$Z = \frac{\zeta_1(\tau) + \zeta_2(\tau) + \zeta_3(\tau)}{3} , \quad (2.6a)$$

is *constant* (it does not depend on the independent variable τ),

$$Z' = 0 , \quad Z(\tau) = Z(0) . \quad (2.6b)$$

The trick mentioned above, relating the *auxiliary* model to the *physical* model, amounts in our present case to the introduction of the (*real*) independent variable t ("physical time"), as well as the *three* (*complex*) dependent variables $z_n \equiv z_n(t)$, via the following positions:

$$\tau = \frac{\exp(2i\omega t) - 1}{2i\omega} , \quad (2.7a)$$

$$z_n(t) = \exp(-i\omega t) \zeta_n(\tau) . \quad (2.7b)$$

We hereafter assume the constant ω to be *real* (for definiteness, *positive*, $\omega > 0$; note that for $\omega = 0$ the change of variables disappears), and we associate to it the basic period T ,

$$T = \frac{\pi}{\omega} . \quad (2.8)$$

Note that this change of variables entails that the initial values $z_n(0)$ of the "particle coordinates" $z_n(t)$ coincide with the initial values $\zeta_n(0)$ of the dependent variables of the *auxiliary* model (2.1):

$$z_n(0) = \zeta_n(0) . \quad (2.9)$$

It is easily seen that, via this change of variables, (2.7), the equations of motion (2.1) satisfied by the quantities $\zeta_n(\tau)$ entail the following (*autonomous*) equations of motion (in the *real* time t) for the particle coordinates $z_n(t)$:

$$\dot{z}_n + i\omega z_n = \frac{g_{n+2}}{z_n - z_{n+1}} + \frac{g_{n+1}}{z_n - z_{n+2}} ; \quad (2.10)$$

here and hereafter superimposed dots indicate differentiations with respect to the time t .

So, this model (2.10) describes the "physical evolution" which we study. Note that its equations of motion, (2.10), are of *Aristotelian*, rather than *Newtonian*, type: the "velocities" \dot{z}_n , rather than the "accelerations" \ddot{z}_n , of the moving particles are determined by the "forces". In Appendix D we discuss the connection of this model with more classical many-body problems, characterized by *Newtonian* equations of motion.

As seen in Section 1.2, a fundamental aspect of our approach concerns the implications of the formula (2.7a) relating the old and new independent variables τ and t . It clearly entails that, as the (*real*, "physical") time variable t evolves onwards, the *complex* variable τ travels counterclockwise, performing a full round in every time interval T , on the circle C , whose diameter

$$d = \frac{1}{\omega} \quad (2.11)$$

lies on the imaginary axis in the complex τ -plane, with its lower end at the origin and its upper end at the point $\frac{i}{\omega}$. Therefore the time evolution of the (*complex*) particle coordinate $z_n(t)$ corresponds, via (2.7), to the evolution of the corresponding function $\zeta_n(\tau)$ of the variable τ as this *complex* variable travels round and round on the circle C and correspondingly $\zeta_n(\tau)$ travels on its Riemann surface (associated with this function $\zeta_n(\tau)$). In particular if the function $\zeta_n(\tau)$ is *holomorphic* in the (closed) disk D enclosed, in the *complex* τ -plane, by the circle C , the corresponding function $z_n(t)$ is clearly *antiperiodic* with period T hence *periodic* with period $2T$, see (2.7) and (2.8):

$$z_n(t + T) = -z_n(t) , \quad z_n(t + 2T) = z_n(t) . \quad (2.12)$$

In Section 2.4 we show that, for the model (2.1), there *always* exists an *open* region of initial data $\zeta_n(0)$ characterized by sufficiently *large* values of the moduli of all three *interparticle distances* $|\zeta_n(0) - \zeta_m(0)|$, that guarantees such a property of *holomorphy*. This implies the *isochronous* character of our model (2.10), a sufficient condition to guarantee the complete periodicity of its solution (we recall that a system is *isochronous* if it features an *open* set of initial data, having *full dimensionality* in its phase space, such that *all* the solutions emerging out of it remain in it and are *completely periodic* with the same period, see Subsection 1.1.2 and Section 1.2).

In the following Section 2.2 we show that the equations of motion (2.10), determining the motions of the *three* points $z_n(t)$ in the *complex* z -plane, are *Hamiltonian* and can moreover be reinterpreted as the *real* equations characterizing the (again *Hamiltonian*) motion of *three* point-like particles in the horizontal plane; this justifies our considering the z_n 's as "particle coordinates", and considering the model (2.1) as an "auxiliary" version of the "physical" model (2.10). It is however generally more convenient to work with the *complex* numbers $z_n(t)$ and $\zeta_n(\tau)$ rather than with the corresponding *real* two-vectors, and we shall generally do so hereafter.

Let us immediately emphasize two important *qualitative* aspects of the dynamics of our *physical* model (2.10). The "one-body force" represented by the second term, $i\omega z_n$, in the left-hand side of the equations of motion (2.10) becomes dominant with respect to the "two-body forces" appearing in the right-hand side in determining the dynamics whenever the (*complex*) coordinate z_n of the n -th particle becomes large (in modulus). Hence when $|z_n(t)|$ tends to diverge, the solution $z_n(t)$ is characterized by the behavior $z_n(t) \approx c \exp(-i\omega t)$, therefore the trajectory of the n -th particle tends to rotate (clockwise, with period $2T$) on a (large) circle. This effect causes the motions of this model to be *all confined*. Secondly, it is clear that the *two-body* forces (see the right-hand side of (2.10)) cause a *singularity* whenever there is a *collision* of *two* (or all *three*) of the particles as they move in the *complex* z -plane, and become dominant whenever *two* or *three* particles get very close to each other, namely in the case of *near misses*. But if the *three* particles move *aperiodically* in a *confined* region (near the origin) of the complex z -plane, a lot of *near misses* shall indeed occur. And since the outcome of a *near miss* is likely to be quite different depending on which side two particles scatter past each other – and this, especially in the case of very close *near misses*, depends *sensitively* on the initial data of the trajectory under consideration – we see here a mechanism complicating the motion associated with a some kind of *sensitive dependence* of the motion on its initial data. This suggests that our model (2.10), in spite of its simplicity, is likely to be rich enough to cause an interesting dynamical evolution. We will see that this is indeed the case.

Let us conclude this section with two remarks (somewhat related to each other).

Remark 1. This system (2.10) is still invariant under translations of the independent variable t (indeed, it is again *autonomous*) but, in contrast to (2.1), it is no more invariant under translations of the dependent variables $z_n(t)$ nor under a simple rescaling of the

independent variable t and of the dependent variables $z_n(t)$. Again, however, correspondingly to (2.5), if the triple $z_n(t)$ satisfies this system (2.10), the following *three-parameter* extension of it still satisfies the same system:

$$\tilde{z}_n(t) = A \exp(-i\omega t) + C \Phi(t) z_n \left(t - t_0 + \frac{\log[\Phi(t)]}{i\omega} \right) , \quad (2.13a)$$

$$\Phi(t) = C^{-1} \{1 + (C^2 - 1) \exp[-2i\omega(t - t_0)]\}^{1/2} , \quad (2.13b)$$

where A , C and t_0 are *three arbitrary* (possibly *complex*) constants. Hence one can again obtain, via this formula (which might however entail an analytic continuation to complex values of the independent variable t), the *general* solution of our system (2.10) from a particular solution of it (again, provided this particular solution is not too special, see below).

Remark 2. The *general solution* of the equations of motion (2.10) has the structure

$$z_n(t) = z_{CM}(t) + \check{z}_n(t) , \quad (2.14a)$$

where the *three* functions $\check{z}_n(t)$ satisfy themselves the same equations of motion (2.10) as well as the additional restriction

$$\check{z}_1(t) + \check{z}_2(t) + \check{z}_3(t) = 0 , \quad (2.14b)$$

which is clearly compatible with these equations of motion, and correspondingly $z_{CM}(t)$ is the center of mass of the system (2.10),

$$z_{CM}(t) = \frac{z_1(t) + z_2(t) + z_3(t)}{3} , \quad (2.15a)$$

and it evolves according to the simple formula (see also (2.6b) and (2.7))

$$z_{CM}(t) = z_{CM}(0) \exp(-i\omega t) = Z \exp(-i\omega t) . \quad (2.15b)$$

2.2 Hamiltonian character of the model

The equations of motion (2.10) are *Hamiltonian*. Consider indeed the Hamiltonian function

$$H(\underline{q}, \underline{p}; \underline{\tilde{q}}, \underline{\tilde{p}}) = \sum_{n=1}^3 \left[-i\omega q_n p_n + \tilde{q}_n \frac{p_{n+1} - p_{n+2}}{q_{n+1} - q_{n+2}} \right] . \quad (2.16)$$

Here, and below as well, the underlined symbol denotes a three-vector, for instance $\underline{q} \equiv (q_1, q_2, q_3)$. Note that this Hamiltonian only features the *positive* constant ω , in addition to the canonical variables q_n and \tilde{q}_n , and the corresponding canonical momenta p_n and \tilde{p}_n ; but in fact it does not depend on the canonical momenta \tilde{p}_n .

The standard Hamiltonian equations for the canonical coordinates yielded by this Hamiltonian read as follows:

$$\dot{q}_n + i\omega q_n = \frac{\tilde{q}_{n+2}}{q_n - q_{n+1}} + \frac{\tilde{q}_{n+1}}{q_n - q_{n+2}} , \quad (2.17a)$$

$$\dot{\tilde{q}}_n = 0 . \quad (2.17b)$$

The second set of these Hamiltonian equations, (2.17b), merely tell us that the three quantities \tilde{q}_n are time independent, and we identify them with the three coupling constants g_n introduced above:

$$\tilde{q}_n = g_n . \quad (2.18a)$$

The Hamiltonian equations (2.17a) are those of interest to us, and via the identifications (2.18a) and

$$q_n(t) = z_n(t) \quad (2.18b)$$

they clearly reproduce the equations of motion (2.10). And of course a way to obtain directly these equations of motion is to start from the Hamiltonian function

$$H(\underline{z}, \underline{p}) = \sum_{n=1}^3 \left[-i\omega z_n p_n + g_n \frac{p_{n+1} - p_{n+2}}{z_{n+1} - z_{n+2}} \right], \quad (2.19)$$

where the parameters g_n are the “coupling constants” and the only canonical variables are the three “particle coordinates” $z_n \equiv z_n(t)$ and the three canonical momenta $p_n \equiv p_n(t)$. Then the Hamiltonian equations of motion satisfied by the canonical variables z_n coincide directly with the equations (2.10) of our model, and they are supplemented by the following equations for the canonical momenta p_n ,

$$\dot{p}_n - i\omega z_n = \frac{g_{n+2} (p_n - p_{n+1})}{(z_n - z_{n+1})^2} + \frac{g_{n+1} (p_n - p_{n+2})}{(z_n - z_{n+2})^2}, \quad (2.20)$$

which however do not affect the time evolution of the particle coordinates z_n , because the canonical momenta p_n do not appear in the equations of motion (2.10) that determine their dynamics.

An analogous Hamiltonian structure can of course be formulated for the *auxiliary* problem characterized by the “equations of motion” (2.1). The Hamiltonian (in self-evident notation) reads

$$h(\underline{\zeta}, \underline{\pi}) = \sum_{n=1}^3 \left[g_n \frac{\pi_{n+1} - \pi_{n+2}}{\zeta_{n+1} - \zeta_{n+2}} \right], \quad (2.21)$$

and indeed it entails the equations of motion (2.1) for the canonical coordinates $\zeta_n \equiv \zeta_n(\tau)$, as well as the following equations for the corresponding canonical momenta $\pi_n \equiv \pi_n(\tau)$:

$$\pi'_n = \frac{g_{n+2} (\pi_n - \pi_{n+1})}{(\zeta_n - \zeta_{n+1})^2} + \frac{g_{n+1} (\pi_n - \pi_{n+2})}{(\zeta_n - \zeta_{n+2})^2}. \quad (2.22)$$

We have written out this Hamiltonian structure that subtends the *auxiliary* problem to emphasize the high symmetry of this Hamiltonian, (2.21), which is clearly invariant under translations of the canonical coordinates ζ_n , under translations of the canonical momenta π_n , and under the simultaneous rescaling of the canonical coordinates and of the canonical momenta, $\zeta_n \rightarrow c\zeta_n$, $\pi_n \rightarrow c\pi_n$. These properties entail the existence of the following three constants of motion (in addition of course to the Hamiltonian (2.21) itself):

$$Z = \frac{1}{3} \sum_{n=1}^3 \zeta_n, \quad \Pi = \sum_{n=1}^3 \pi_n, \quad S = \sum_{n=1}^3 \frac{\pi_n}{\zeta_n}. \quad (2.23)$$

The τ -independence of the center of mass coordinate Z was already noted in the preceding Section 2.1, see (2.6). We anticipate here also that, in the semisymmetrical case, the treatment of Section 2.5 entails the existence of a *fifth* constant of motion, which reads as follows (note that, as Z , it does not depend on the canonical momenta π_n):

$$\tilde{K} = (2\zeta_3 - \zeta_1 - \zeta_2)^{-2} \left[1 - \frac{(\zeta_1 - \zeta_2)^2 + (\zeta_2 - \zeta_3)^2 + (\zeta_3 - \zeta_1)^2}{2\mu (2\zeta_3 - \zeta_1 - \zeta_2)^2} \right]^{\mu-1}. \quad (2.24)$$

The constant μ that features in this formula is defined in terms of the coupling constants g and f , see (2.2):

$$\mu = \frac{f + 2g}{f + 8g} = \frac{\varphi + 2}{\varphi + 8}, \quad (2.25)$$

whose value, as we shall see, plays an important role in determining the dynamical evolution of our model: in particular, this evolution does largely depend on whether or not μ is a *real rational* number, and if it is *rational*,

$$\mu = \frac{p}{q} , \quad (2.26)$$

with p and q integers (and q *positive*, $q > 0$), on whether the two natural numbers $|p|$ and q are large or small. A hint of the importance of the role played by μ is now provided by the appearance of this number as an exponent in the right-hand side of (2.24), since this exponent characterizes the *multivaluedness* of the dependence of the constant \tilde{K} on the canonical coordinates ζ_n .

Of course the (τ -independent) “constants of motion” we just identified for the *auxiliary* problem (2.1) provide as well (t -independent) *constants of motion* for the *physical* problem (2.10), but, when written in terms of the particles coordinates $z_n \equiv z_n(t)$ and of the corresponding canonical momenta $p_n \equiv p_n(t)$ for this problem, the expressions of these quantities (in contrast to the expression of the Hamiltonian, see (2.19)), are no more *autonomous*, since via the relations (2.7), and the corresponding relations

$$p_n(t) = \exp(i\omega t) \pi_n(\tau) , \quad (2.27)$$

that relate (2.20) to (2.22), they read

$$Z = \frac{1}{3} \exp(i\omega t) \sum_{n=1}^3 z_n , \quad \Pi = \exp(-i\omega t) \sum_{n=1}^3 p_n , \quad S = \exp(-2i\omega t) \sum_{n=1}^3 \frac{p_n}{z_n} , \quad (2.28)$$

$$\tilde{K} = \exp(2i\omega t) (2z_3 - z_1 - z_2)^{-2} \left[1 - \frac{(z_1 - z_2)^2 + (z_2 - z_3)^2 + (z_3 - z_1)^2}{2\mu (2z_3 - z_1 - z_2)^2} \right]^{\mu-1} . \quad (2.29)$$

Let us now note the possibility to reformulate our problem, so that rather than describing the motions of points $z_n \equiv z_n(t)$ in the *complex* z -plane as determined by the *complex* equations of motion (2.10) (recall that $\omega > 0$), it refers to the motion of point particles in the horizontal plane, the position of which is identified by *real* (Cartesian) coordinates $x_n \equiv x_n(t)$, $y_n \equiv y_n(t)$. There is a standard trick to achieve this goal (see for instance [5]), namely by setting

$$z_n(t) = x_n(t) + i y_n(t) , \quad \vec{r}_n(t) = (x_n(t), y_n(t), 0) . \quad (2.30)$$

Note that the vectors \vec{r}_n identifying points in the horizontal plane are effectively two-vectors, but for notational convenience we prefer to consider this plane immersed in three-dimensional space and therefore to consider the vectors \vec{r}_n as three-vectors with vanishing third (vertical) component. It is then convenient to also set formally

$$\begin{aligned} g_n &= [\mathcal{R}e(s_n) + i\mathcal{I}m(s_n)]^2 = [\mathcal{R}e(s_n)]^2 - [\mathcal{I}m(s_n)]^2 + 2i\mathcal{R}e(s_n)\mathcal{I}m(s_n) , \\ \vec{s}_n &= (\mathcal{R}e(s_n), \mathcal{I}m(s_n), 0) , \quad \vec{s}_n \cdot \vec{s}_n = [\mathcal{R}e(s_n)]^2 + [\mathcal{I}m(s_n)]^2 , \quad \hat{k} = (0, 0, 1) , \end{aligned} \quad (2.31)$$

whereby the equations of motion (2.10) (or rather (2.17a) with (2.18b)) read as follows:

$$\begin{aligned} \dot{\vec{r}}_n + \omega \hat{k} \wedge \vec{r}_n &= \\ r_{n,n+1}^{-2} [-\vec{r}_{n,n+1} (\vec{s}_{n+2} \cdot \vec{s}_{n+2}) + 2 \vec{s}_{n+2} (\vec{s}_{n+2} \cdot \vec{r}_{n,n+1})] &+ \\ r_{n,n+2}^{-2} [-\vec{r}_{n,n+2} (\vec{s}_{n+1} \cdot \vec{s}_{n+1}) + 2 \vec{s}_{n+1} (\vec{s}_{n+1} \cdot \vec{r}_{n,n+2})] , & \end{aligned} \quad (2.32a)$$

where we introduced the short-hand notation

$$\vec{r}_{n,m} \equiv \vec{r}_n - \vec{r}_m \quad (2.32b)$$

entailing

$$r_{n,m}^2 = r_n^2 + r_m^2 - 2 \vec{r}_n \cdot \vec{r}_m . \quad (2.32c)$$

The symbol \wedge denotes of course the (three-dimensional) vector product, so that, for instance,

$$\hat{k} \wedge \vec{r}_n = (-y_n, x_n, 0) . \quad (2.32d)$$

These *real* equations of motions, (2.32a), for the three vectors \vec{r}_n in the horizontal plane are *covariant*, hence *rotation-invariant*, if they are supplemented with the following (trivial) equations for the three vectors \vec{s}_n :

$$\dot{\vec{s}}_n = 0 , \quad (2.32e)$$

and the identification (2.31) is guaranteed by prescribing it as initial condition. If instead the vectors \vec{s}_n in (2.32a) are considered as *given* constant vectors to begin with, see (2.31), then the equations of motion (2.32a) still have a *covariant* appearance, but the model is *no more rotation-invariant* because the *given* vectors \vec{s}_n identify certain preferred directions in the horizontal plane.

Note that these equations of motion, (2.32), are also Hamiltonian; the *real* Hamiltonian that produces them is the real part of the Hamiltonian (2.16) with (2.30), (2.18), (2.31) and with (in self-evident notation; but note the minus signs!)

$$\vec{p}_n = (\mathcal{R}e(p_n), -\mathcal{I}m(p_n), 0) , \quad \vec{\tilde{p}}_n = (\mathcal{R}e(\tilde{p}_n), -\mathcal{I}m(\tilde{p}_n), 0) , \quad (2.33)$$

namely

$$H_R(\vec{r}, \vec{p}; \vec{s}, \vec{\sigma}) = \sum_{n=1}^3 \left\{ -\omega (\hat{k} \cdot \vec{r}_n \wedge \vec{p}_n) + r_{n+1,n+2}^{-2} [2 (\vec{s}_n \cdot \vec{r}_{n+1,n+2}) (\vec{s}_n \cdot \vec{p}_{n+1,n+2}) - (\vec{s}_n \cdot \vec{s}_n) (\vec{r}_{n+1,n+2} \cdot \vec{p}_{n+1,n+2})] \right\} \quad (2.34)$$

where we denote by $\vec{\sigma}_n$ the canonical momenta (which however do not appear in the right-hand side) conjugated to the canonical variables \vec{s}_n , and we use of course the short-hand notation (2.32b) and a self-evident analogous notation for the vectors $\vec{p}_{n,m} \equiv \vec{p}_n - \vec{p}_m$. And as well Hamiltonian are the equations of motion (2.32a) with the vectors \vec{s}_n assigned as given constants, see (2.31), in which case of course only the vectors \vec{r}_n should be treated as canonical coordinates, and the vectors \vec{p}_n as the corresponding canonical momenta, in the expression (2.34) of the Hamiltonian.

This *real* Hamiltonian formulation opens the way to the study of quantal versions of our model, but this exercise is postponed to a separate work.

2.3 Equilibrium configurations and similarity solutions

In this section we discuss, firstly, the equilibrium configurations of our model, (2.10), and its behavior near equilibrium, and secondly, a special, explicit “similarity” solution of our model and its stability.

The *equilibrium configurations* of our model (2.10),

$$z_n(t) = \bar{z}_n , \quad \dot{z}_n(t) = 0 , \quad (2.35)$$

are clearly characterized by the algebraic equations

$$i \omega \bar{z}_n = \frac{g_{n+1}}{\bar{z}_n - \bar{z}_{n+2}} + \frac{g_{n+2}}{\bar{z}_n - \bar{z}_{n+1}} . \quad (2.36)$$

These algebraic equations entail

$$\bar{z}_1 + \bar{z}_2 + \bar{z}_3 = 0 \quad . \quad (2.37)$$

It is now convenient to set

$$\bar{z}_n = (2 i \omega)^{-1/2} \alpha_n \quad , \quad (2.38)$$

so that the equilibrium equations (2.36) read as follows:

$$\frac{\alpha_n}{2} = \frac{g_{n+1}}{\alpha_n - \alpha_{n+2}} + \frac{g_{n+2}}{\alpha_n - \alpha_{n+1}} \quad . \quad (2.39)$$

These algebraic equations can be conveniently (see below) rewritten as follows:

$$\alpha_n = \beta_{n+1} (\alpha_n - \alpha_{n+2}) + \beta_{n+2} (\alpha_n - \alpha_{n+1}) \quad , \quad (2.40a)$$

via the position

$$\beta_n = \frac{2 g_n}{(\alpha_{n-1} - \alpha_{n+1})^2} \quad . \quad (2.40b)$$

We now note that, in order that the three equations (2.40a) (which are linear in the three unknowns α_n , although only apparently so, see (2.40b)) have a nonvanishing solution, the quantities β_n must cause the following determinant to vanish:

$$\begin{vmatrix} \beta_2 + \beta_3 - 1 & -\beta_3 & -\beta_2 \\ -\beta_3 & \beta_3 + \beta_1 - 1 & -\beta_1 \\ -\beta_2 & -\beta_1 & \beta_1 + \beta_2 - 1 \end{vmatrix} = 0 \quad . \quad (2.41)$$

To analyze the *small oscillations* of our system (2.10) around its equilibrium configurations we set

$$z_n(t) = \bar{z}_n + \varepsilon w_n(t) \quad , \quad (2.42a)$$

and we then get (linearizing by treating ε as a small parameter)

$$\dot{w}_n + i \omega w_n + i \omega \beta_{n+1} (w_n - w_{n+2}) + \beta_{n+2} (w_n - w_{n+1}) = 0 \quad . \quad (2.42b)$$

Therefore the three exponents $\gamma^{(m)}$ characterizing the small oscillations around equilibrium via the formula

$$w_n^{(m)}(t) = \exp(-i \gamma^{(m)} \omega t) v_n^{(m)} \quad , \quad (2.42c)$$

that provides *three* independent solutions of the system of *linear* ODEs (2.42b), are the *three* eigenvalues of the symmetrical matrix

$$\mathbf{B} = \begin{pmatrix} \beta_2 + \beta_3 + 1 & -\beta_3 & -\beta_2 \\ -\beta_3 & \beta_3 + \beta_1 + 1 & -\beta_1 \\ -\beta_2 & -\beta_1 & \beta_1 + \beta_2 + 1 \end{pmatrix} \quad , \quad (2.43)$$

and the *three* 3-vectors $\vec{v}^{(m)} \equiv (v_1^{(m)}, v_2^{(m)}, v_3^{(m)})$ are the corresponding eigenvectors,

$$\sum_{\ell=1}^3 B_{n\ell} v_\ell^{(m)} = \gamma^{(m)} v_n^{(m)} \quad . \quad (2.44)$$

Hence the *three* exponents $\gamma^{(m)}$ are the *three* roots of the “secular equation” (a cubic polynomial in γ)

$$\begin{vmatrix} \beta_2 + \beta_3 + 1 - \gamma & -\beta_3 & -\beta_2 \\ -\beta_3 & \beta_3 + \beta_1 + 1 - \gamma & -\beta_1 \\ -\beta_2 & -\beta_1 & \beta_1 + \beta_2 + 1 - \gamma \end{vmatrix} = 0 \quad . \quad (2.45)$$

Clearly these *three* roots are given by the following formulas:

$$\gamma^{(1)} = 1, \quad \gamma^{(2)} = 2, \quad \gamma^{(3)} = 2 (\beta_1 + \beta_2 + \beta_3) . \quad (2.46)$$

Indeed the determinant (2.45) vanishes for $\gamma = \gamma^{(1)} = 1$ (when each line sums to zero) and for $\gamma = \gamma^{(2)} = 2$ (see (2.41)), and the third solution,

$$\gamma^{(3)} = 2 (\beta_1 + \beta_2 + \beta_3) , \quad (2.47)$$

is then implied by the trace condition

$$\text{tr} [\mathbf{B}] = 3 + 2 (\beta_1 + \beta_2 + \beta_3) = \gamma^{(1)} + \gamma^{(2)} + \gamma^{(3)} . \quad (2.48)$$

The first of these 3 solutions, $\gamma^{(1)} = 1$, corresponds to the center of mass motion (it clearly entails $v_n^{(1)} = v^{(1)}$, see (2.42c) and (2.43)).

In the semisymmetrical case (2.2) the equations (2.39) (or equivalently (2.40)) characterizing, via (2.38), the equilibrium configurations can be solved explicitly (see Appendix A). One finds that there are *two* distinct equilibrium configurations (in fact four, if one takes account of the trivial possibility to exchange the roles of the two “equal” particles with labels 1 and 2), the first of which reads simply

$$\bar{z}_3 = 0, \quad \bar{z}_1 = -\bar{z}_2 = \bar{z}, \quad (\bar{z})^2 = \frac{f + 2g}{2i\omega}, \quad (2.49)$$

while the second has a slightly more complicated expression (see Appendix A). Note however that, *in both cases*, there holds the relation

$$(\bar{z}_1 - \bar{z}_2)^2 + (\bar{z}_2 - \bar{z}_3)^2 + (\bar{z}_3 - \bar{z}_1)^2 = \frac{3(f + 2g)}{i\omega} . \quad (2.50)$$

Moreover, in both cases the corresponding values for the eigenvalue $\gamma^{(3)}$, see (2.47), are easily evaluated. The first solution yields

$$\gamma^{(3)} = \frac{f + 8g}{f + 2g} = \frac{\varphi + 8}{\varphi + 2} = \frac{1}{\mu} = \frac{q}{p} , \quad (2.51a)$$

where, for future reference, we expressed $\gamma^{(3)}$ not only in terms of the parameter μ , see (2.25), but as well in terms of its rational expression (2.26) (whenever applicable), while the second solution likewise yields

$$\gamma^{(3)} = \frac{f + 8g}{3g} = \frac{\varphi + 8}{3} = \frac{2}{1 - \mu} = \frac{2q}{q - p} . \quad (2.51b)$$

Note that this implies that in the “integrable” case (2.3) (namely, for $\varphi = 1$), both these formulas, (2.51a) and (2.51b), yield $\gamma^{(3)} = 3$; but it is easily seen that in this case only the first equilibrium configuration (2.49) actually exists. So in the “integrable” case the oscillations around the (only) equilibrium configuration (2.49) are the linear superposition of three periodic motions (see (2.42c)) with respective periods $2T$, T and $\frac{2T}{3}$ (see (2.8)). Also in the “two-body” case (2.4) the second equilibrium configuration does not exist, while the first formula, (2.51a), yields $\gamma^{(3)} = 1$, so in this case the small oscillations around the (only) equilibrium configuration (2.49) are the linear superposition of two periodic motions, with periods $2T$ and T (see (2.8); consistently with the explicit solution, easily obtainable from (2.4c) via (2.7)). But let us emphasize that in the general semisymmetrical case (with $g \neq 0$, $f \neq g$) both formulas, (2.51a) and (2.51b), yield (*real* but) *irrational* values for $\gamma^{(3)}$ if the ratio φ (see (2.2)) of the coupling constants or the number μ are themselves (*real*

and) *irrational*, and *complex* values for $\gamma^{(3)}$ if the ratio φ or the number μ are themselves *complex*.

As can be easily verified, the equilibrium configurations (2.35) with (2.36) are merely the special case corresponding to $z_{CM}(0) = 0$, $c = 0$ of the following two-parameter family of (*exact*) “similarity” solutions of our equations of motion (2.10):

$$z_n(t) = z_{CM}(t) + \tilde{z}_n(t; c) , \quad (2.52a)$$

$$\tilde{z}_n(t; c) \equiv \bar{z}_n [1 + c \exp(-2i\omega t)]^{1/2} , \quad (2.52b)$$

with the center of mass coordinate $z_{CM}(t)$ evolving according to (2.15b). The two *arbitrary* (*complex*) constants featured by this solution are of course $z_{CM}(0) = Z$ (see (2.15b)) and c , while the constants \bar{z}_n 's are defined as in the preceding section, see (2.36).

Clearly these (*exact*) solutions correspond, via the trick (2.7), the relation (2.38) (which is clearly consistent with (2.39) and (2.36)) and the simple relation

$$\tau_b = \frac{c - 1}{2i\omega} , \quad (2.53)$$

to the two-parameter family

$$\zeta_n(\tau) = Z + \alpha_n (\tau - \tau_b)^{1/2} , \quad (2.54)$$

of (*exact*) solutions of (2.1).

These solutions, (2.52), of our *physical* equations of motion (2.10) are a linear combination of two components (see the Remark 2 in Section 2.1, and note the consistency of (2.14b) with (2.37)). The first component, $z_{CM}(t)$, represents the motion of the center of mass of the system and is clearly *periodic* with period $2T$, see (2.15b) and (2.8). The second component, see (2.52b), which is itself a solution of the equations of motion (2.10), is *periodic* with period T , see (2.8), if $|c| < 1$, is *antiperiodic* with period T (hence *periodic* with period $2T$) if $|c| > 1$, and becomes *singular* in a finite time if $|c| = 1$ so that, say, $c = \exp(i\phi)$ with $0 < \phi < 2\pi$, the singularity corresponding in this case to a *triple* collision of all *three* particles occurring at the time $t = \frac{\phi}{2\omega}$.

Let us now discuss the stability of this solution, (2.52b) (note that an analogous discussion of the more general solution (2.52a) would entail no significant changes). To this end we set

$$z_n(t) = \tilde{z}_n(t; c) + \varepsilon \tilde{w}_n(t) , \quad (2.55a)$$

and we insert this *ansatz* in our equations of motion (2.10), linearizing them by treating ε as a small parameter. We thus get

$$\dot{\tilde{w}}_n + i\omega \tilde{w}_n + \frac{i\omega [\beta_{n+1} (\tilde{w}_n - \tilde{w}_{n+2}) + \beta_{n+2} (\tilde{w}_n - \tilde{w}_{n+1})]}{1 + c \exp(-2i\omega t)} = 0 , \quad (2.55b)$$

having used the definition (2.40b).

Clearly the solution of this system of ODEs reads

$$\tilde{w}_n(t) = \exp(-i\omega t) \chi_n(\vartheta) , \quad (2.56a)$$

with

$$\vartheta \equiv \vartheta(t) = t - (2i\omega)^{-1} \log \left[\frac{1 + c \exp(-2i\omega t)}{1 + c} \right] \quad (2.56b)$$

and the functions $\chi_n(\vartheta)$ solutions of the linear system of first order ODEs

$$\chi_n' + i\omega [\beta_{n+1} (\tilde{w}_n - \tilde{w}_{n+2}) + \beta_{n+2} (\tilde{w}_n - \tilde{w}_{n+1})] = 0 , \quad (2.56c)$$

where the primes denote of course differentiation with respect to ϑ . Hence (see (2.42b)) the *three* independent solutions of this linear system are

$$\chi_n^{(m)}(\vartheta) = \exp(i\omega\vartheta) w_n^{(m)}(\vartheta) \quad , \quad (2.56d)$$

with the functions $w_n^{(m)}$ defined by (2.42c) (of course with t replaced by ϑ), yielding via (2.42c) and (2.56a) with (2.56b) the following two equivalent expressions for the *three* independent solutions of the linear system (2.55b):

$$\tilde{w}_n^{(m)}(t) = \left[\frac{1 + c \exp(-2i\omega t)}{1 + c} \right]^{(\gamma^{(m)}-1)/2} \exp(i\gamma^{(m)}\omega t) \tilde{v}_n^{(m)} \quad , \quad (2.57a)$$

$$\tilde{w}_n^{(m)}(t) = \left[\frac{\exp(2i\omega t) + c}{1 + c} \right]^{(\gamma^{(m)}-1)/2} \exp(i\omega t) \tilde{v}_n^{(m)} \quad . \quad (2.57b)$$

Here the *three* exponents $\gamma^{(m)}$ are defined as above, see (2.46), and likewise the "eigenvectors" $\tilde{v}_n^{(m)}$ coincide with those defined above up to (*arbitrary*) normalization constants $c^{(m)}$,

$$\tilde{v}_n^{(m)} = c^{(m)} v_n^{(m)} \quad . \quad (2.57c)$$

Note the equivalence of the two expressions (2.57a) and (2.57b) (the motivation for writing these two versions of the same formula will be immediately clear).

For $m = 1, 2, 3$ these solutions, see (2.57b), are periodic functions of the (*real*) time t with period $2T$ if $|c| > 1$. If instead $|c| < 1$, the solutions (see (2.57a)) with $m = 1$ respectively $m = 2$ are periodic with periods $2T$ respectively T , while the solution with $m = 3$ is *periodic* if $\gamma^{(3)}$ (and consequently μ) is *real*, but with the period $\frac{2T}{|\gamma^{(3)}|}$ which is not congruent to T if $\gamma^{(3)}$ (and consequently μ) is *irrational*, while it grows exponentially with increasing time if $\mathcal{I}m[\gamma^{(3)}] < 0$ (implying instability of the solution (2.52) in this case), and it instead decays exponentially if $\mathcal{I}m[\gamma^{(3)}] > 0$ (implying a limit cycle behavior in configuration space, namely asymptotic approach to a solution *completely periodic* with period T or $2T$ depending whether the center of mass of the system is fixed at the origin or itself moving with period $2T$). The analysis of the behavior of our model, (2.10), when the coupling constants are *complex* is however postponed to a subsequent work; in this thesis we restrict attention to the case with *real* coupling constants.

2.4 Properties of the solutions of the auxiliary model

In this section we justify the assertions made in Section 2.1 about the properties of analyticity as functions of the complex variable τ of the solutions $\zeta_n(\tau)$ of the *auxiliary* model (2.1) (with arbitrary values of the 3 coupling constants g_n , i. e. *not* restricted by the semisymmetrical condition (2.2): except when this is explicitly specified, see below). In particular we show first of all that, for appropriate initial data characterized by *sufficiently large* values of the moduli of *all three* interparticle distances, namely by the condition (see (2.9)) that the quantity

$$\zeta_{\min} = \min_{n,m=1,2,3; n \neq m} |\zeta_n(0) - \zeta_m(0)| \quad (2.58)$$

be *adequately large*, the solutions $\zeta_n(\tau)$ are *holomorphic* in a disk D_0 of (*arbitrarily large*) radius d_0 centered at the origin, $\tau = 0$, of the complex τ -plane (of course the "adequately large" value of the quantity ζ_{\min} depends on d_0 and on the magnitude of the *three* coupling constants g_n ; see (2.66) below). We moreover discuss via a local analysis *à la Painlevé* the

nature of the singularities of the solutions $\zeta_n(\tau)$ of the *auxiliary* model (2.1) as functions of the *complex* variable τ .

To prove the first point, set

$$\varsigma_n(\tau) = \zeta_n(\tau) - \zeta_n(0) \ , \quad (2.59a)$$

so that these quantities $\varsigma_n(\tau)$ vanish initially,

$$\varsigma_n(0) = 0 \ , \quad (2.59b)$$

and, as a consequence of (2.1), satisfy the equations of motion

$$\begin{aligned} \zeta'_n(\tau) &= \frac{g_{n+1}}{\zeta_n(0) - \zeta_{n+2}(0) + \varsigma_n(\tau) - \varsigma_{n+2}(\tau)} \\ &+ \frac{g_{n+2}}{\zeta_n(0) - \zeta_{n+1}(0) + \varsigma_n(\tau) - \varsigma_{n+1}(\tau)} \ . \end{aligned} \quad (2.59c)$$

A standard theorem (see, for instance, [45]) guarantees then that these quantities $\varsigma_n(\tau)$ – hence as well the functions $\zeta_n(\tau)$, see (2.59a) – are *holomorphic* in τ (at least) in a disk D_0 centered at the origin $\tau = 0$ in the *complex* τ -plane, the radius d_0 of which is bounded *below* by the inequality

$$d_0 > \frac{b}{4M} \quad (2.60)$$

(this formula coincides with the last equation of Section 13.21 of [45], with the assignments $m = 3$ and $a = \infty$, the first of which is justified by the fact that the system (2.59c) features 3 coupled equations, the second of which is justified by the *autonomous* character of the equations of motion (2.59c)). The two *positive* quantities b and M in the right-hand side of this inequality are defined as follows. The quantity b is required to guarantee that the right-hand sides of the equations of motion (2.59c) be *holomorphic* (as functions of the dependent variables ς_n) provided these quantities satisfy the three inequalities

$$|\varsigma_n| \leq b \ ; \quad (2.61)$$

clearly in our case a sufficient condition to guarantee this is provided by the single restriction

$$b < \frac{\zeta_{\min}}{2} \ , \quad (2.62)$$

with ζ_{\min} defined by (2.58). The second quantity in the right-hand side of (2.60), $M \equiv M(b)$, is the *upper* bound of the right-hand sides of (2.59c) when the quantities ς_n satisfy the inequality (2.61); but of course the inequality (2.60) holds *a fortiori* if we overestimate M , as we shall presently do. Indeed clearly the equations of motion (2.59c) with (2.61) and (2.62) entail

$$M < \frac{4G}{\zeta_{\min} - 2b} \ , \quad (2.63)$$

with

$$G = \max_{n=1,2,3} |g_n| \ . \quad (2.64)$$

Insertion of (2.63) in (2.60) yields

$$d_0 > \frac{b(\zeta_{\min} - 2b)}{16G} \ , \quad (2.65)$$

hence, setting $b = \frac{\zeta_{\min}}{4}$ (to maximize the right-hand side; note the consistency of this assignment with (2.62)),

$$d_0 > \frac{\zeta_{\min}^2}{128G} \ , \quad (2.66)$$

confirming the assertion made above (that d_0 can be made *arbitrarily large* by choosing ζ_{\min} *adequately large*). Via (2.9), we can reformulate the inequality $d_0 > d$ into the inequality:

$$\min_{m,n=1,2,3; m \neq n} |z_n(0) - z_m(0)| > 16 \sqrt{\frac{\max_{n=1,2,3} |g_n|}{2\omega}} . \quad (2.67)$$

2.4.1 Analysis à la Painlevé

Next, let us show, via a local analysis *à la Painlevé*, that the singularities as functions of the complex variable τ of the *general* solutions $\zeta_n(\tau)$ of our *auxiliary* model (2.1) associated with a coincidence of *two* of the *three* components ζ_n are *square-root branch points* (recall that a singularity at finite τ of a solution $\zeta_n(\tau)$ of the evolution equations (2.1) may only occur when the right-hand side of these equations diverges). Such a singularity occurs for those values τ_b of the independent variable τ such that *two* of the *three* functions ζ_n coincide, for instance

$$\zeta_1(\tau_b) = \zeta_2(\tau_b) \neq \zeta_3(\tau_b) . \quad (2.68)$$

The *square-root* character of these branch points is evident from the following *ansatz* characterizing the behavior of the solutions of (2.1) in the neighborhood of these singularities:

$$\zeta_s(\tau) = \zeta_b - (-1)^s \alpha (\tau - \tau_b)^{1/2} + v_s (\tau - \tau_b) + \sum_{k=3}^{\infty} \alpha_s^{(k)} (\tau - \tau_b)^{k/2} , \quad s = 1, 2 \quad (2.69a)$$

$$\zeta_3(\tau) = \zeta_{3b} + v_3 (\tau - \tau_b) + \sum_{k=3}^{\infty} \alpha_3^{(k)} (\tau - \tau_b)^{k/2} , \quad (2.69b)$$

with

$$\alpha^2 = g_3 , \quad v_3 = -\frac{g_1 + g_2}{\zeta_b - \zeta_{3b}} , \quad v_s = \frac{g_s + 5g_{s+1}}{6(\zeta_b - \zeta_{3b})} , \quad s = 1, 2 , \quad (2.69c)$$

and the constants $\alpha_n^{(k)}$ determinable (in principle) recursively by inserting this *ansatz* in (2.1), so that, to begin with

$$\alpha_3^{(3)} = \frac{2\alpha(g_2 - g_1)}{3(\zeta_b - \zeta_3)^2} , \quad (2.69d)$$

$$\alpha_s^{(3)} = -(-)^s \frac{\alpha}{36(\zeta_b - \zeta_3)^2} \left[3(g_s - 7g_{s+1}) + \frac{(g_1 - g_2)^2}{g_3} \right] , \quad s = 1, 2 , \quad (2.69e)$$

and so on. It can be easily verified that this procedure is consistent for any assignment of the *three* constants τ_b , ζ_b , and ζ_{3b} , which remain undetermined except for the obvious restrictions $\tau_b \neq 0$, $\zeta_b \neq 0$, $\zeta_{3b} \neq \zeta_b$. The fact that (2.69) contains *three* arbitrary (*complex*) constants – the maximal number of integration constants compatible with the system of *three* first-order ODEs (2.1) – shows that this *ansatz* is indeed adequate to represent locally, in the neighborhood of its singularities occurring at $\tau = \tau_b$, the *general* solution of (2.1).

Let us emphasize that in this analysis we considered so far the general model with *three* arbitrary coupling constants g_n , and we discussed the case in which the singularity is associated with the coincidence of the two coordinates with labels 1 and 2, see (2.68). But note that, if attention is restricted to the semisymmetrical case in which these same two coordinates are singled out, see (2.2), then the vanishing of $\alpha_3^{(3)}$, see (2.69d), suggests that the square root branch point affect the two functions $\zeta_s(\tau)$, $s = 1, 2$, see (2.69a), but *not* the third function $\zeta_3(\tau)$, see (2.69b). This hunch is confirmed by the exact solution, see Section 2.5.

An analogous analysis of the behavior of the solutions of the system (2.1) near the values of the independent variable τ where a *triple* coincidence of all *three* functions ζ_n occurs (corresponding to the excluded assignment $\zeta_{3b} = \zeta_b$ in the above *ansatz* (2.69)), indicates, somewhat surprisingly, that such a *triple* coincidence,

$$\zeta_1(\tau_b) = \zeta_2(\tau_b) = \zeta_3(\tau_b) = Z \quad (2.70)$$

(see (2.6a)), does also occur for the *general* solution of the system (2.1). This conclusion is reached via a local analysis analogous to that performed above, and is then confirmed (for the semisymmetrical case, see (2.2)) by the *exact* treatment of Section 2.5. Indeed the natural extension of the above *ansatz* (2.69) characterizing the behavior of the solutions of (2.1) in the neighborhood of such singularities, corresponding to a *triple* coincidence, see (2.70), of the *three* functions $\zeta_n(\tau)$, reads as follows:

$$\zeta_n(\tau) = Z + \eta_n (\tau - \tau_b)^{(1-\gamma)/2} + \alpha_n (\tau - \tau_b)^{1/2} + o\left(|\tau - \tau_b|^{1/2}\right) , \quad (2.71a)$$

provide

$$\operatorname{Re}(\gamma) < 0 . \quad (2.71b)$$

Here the *three* constants α_n are determined, as can be easily verified, just by the *three* nonlinear algebraic equations (2.39) that were found in the preceding section while investigating the equilibrium configurations of our *physical* system (2.10), while the *three* constants η_n , as well as the exponent γ , are required to satisfy the algebraic equations

$$\frac{(\gamma - 1) \eta_n}{2} = \frac{g_{n+1} (\eta_n - \eta_{n+2})}{(\alpha_n - \alpha_{n+2})^2} + \frac{g_{n+2} (\eta_n - \eta_{n+1})}{(\alpha_n - \alpha_{n+1})^2} . \quad (2.71c)$$

These algebraic equations, (2.39) and (2.71c), can be conveniently rewritten as follows:

$$\alpha_n = \beta_{n+1} (\alpha_n - \alpha_{n+2}) + \beta_{n+2} (\alpha_n - \alpha_{n+1}) , \quad (2.72a)$$

$$(\gamma - 1) \eta_n = \beta_{n+1} (\eta_n - \eta_{n+2}) + \beta_{n+2} (\eta_n - \eta_{n+1}) , \quad (2.72b)$$

via the introduction of the quantities β_n , see (2.40b). Note that in this manner these two sets of equations, (2.72a) and (2.72b), have a quite similar look, which should however not mislead the reader to underestimate their basic difference: the *three* equations (2.72a) are merely a convenient way to rewrite, via the definition (2.40b), the *three nonlinear* equations (2.39), which determine (albeit not uniquely, see Appendix A) the *three* constants α_n ; while the equations (2.72b) are *three linear* equations for the *three* quantities η_n , hence they can determine these *three* unknowns only up to a common multiplicative constant (provided they admit a *nontrivial* solution: see below).

Of course these linear equations (2.72b) admit the *trivial* solution $\eta_n = 0$, and it is easily seen that there indeed is a special (*exact*) solution of the equations of motion (2.1) having this property, see (2.54) with the constants α_n determined by (2.39) and computed, for the semisymmetrical model, in Appendix A. This “similarity solution” (2.54) of the system (2.1) has been discussed in Section 2.3; but let us emphasize here that it only provides a *two*-parameter (Z and τ_b) class of solutions of the equations of motion (2.1), while the *general* solution of this system of *three* first-order ODEs must of course feature *three* arbitrary parameters.

A *general* solution of the evolution equations (2.1) corresponds instead to the *ansatz* (2.71a) if the linear equations (2.72b) for the *three* coefficients η_n admit a *nonvanishing* solution, because in such a case, as mentioned above, a common scaling parameter for these *three* coefficients remains as an additional (*third*) free parameter (besides Z and τ_b). The condition for this to happen is the vanishing of the determinant of the coefficients

of these *three* linear equations, (2.72b), namely again the validity of the determinantal condition (2.45), a *cubic* equation for the unknown γ , which determines, as discussed in the preceding section, the *three* values (2.46) of this quantity. But the first two of these values, $\gamma = \gamma^{(1)} = 1$ and $\gamma = \gamma^{(2)} = 2$ (see (2.46)), are *not* consistent with the requirement (2.71b). The third solution, $\gamma = \gamma^{(3)} = 2(\beta_1 + \beta_2 + \beta_3)$ (see (2.46)) might instead be consistent with the requirement (2.71b), and whenever this happens the *ansatz* (2.71) indicates that the *general* solution of the system of ODEs (2.1) does feature a “triple coincidence”, see (2.70), and identifies the character of the corresponding *branch point*.

In the semisymmetrical case (2.2) the equations characterizing the equilibrium configuration, (2.39) or equivalently (2.72), can be solved (see Appendix A). One finds that there are *two* distinct solutions of these nonlinear equations (2.39) (in fact *four*, since each solution has a trivial counterpart obtained by exchanging the role of the two “equal” particles with labels 1 and 2). The *first* solution yields for $\gamma = \gamma^{(3)}$ the value (2.51a), which is consistent with the condition (2.71b) iff

$$-8 < \operatorname{Re}(\varphi) < -2 \quad (2.73a)$$

entailing

$$\operatorname{Re}(\mu) < 0 \quad , \quad (2.73b)$$

and it yields for the branch point exponent, see (2.71a), the value

$$\frac{1-\gamma}{2} = -\frac{3}{\varphi+2} = \frac{\mu-1}{2\mu} = \frac{p-q}{2p} \quad ; \quad (2.74)$$

while the *second* solution yields for $\gamma^{(3)}$ the value (2.51b), which is consistent with the condition (2.71b) iff

$$\operatorname{Re}(\varphi) < -8 \quad (2.75a)$$

entailing

$$\operatorname{Re}(\mu) > 1, \quad (2.75b)$$

and it yields for the branch point exponent, see (2.71a), the value

$$\frac{1-\gamma}{2} = -\frac{\varphi+5}{6} = \frac{\mu+1}{2(\mu-1)} = \frac{p+q}{2(p-q)} \quad . \quad (2.76)$$

Note that these findings imply that the branch point associated with “triple coincidences” is not (only) of *square-root* type, being also characterized, see (2.71a), by the exponent $\frac{1-\gamma}{2}$, the value of which depends on the ratio φ of the coupling constants, or equivalently on the value of the parameter μ , see (2.74) and (2.76); however this kind of branch point is *not* present if

$$\operatorname{Re}(\varphi) > -2, \quad 0 < \operatorname{Re}(\mu) < 1, \quad (2.77)$$

since in this case neither (2.73) nor (2.75) are satisfied.

The results presented in this section are not quite rigorous, since the local analysis of the singularities we performed above on the basis of appropriate *ansätze* should be complemented by proofs that the relevant expansions converge. Moreover this analysis provide information on the nature of the branch points, but neither on their number nor their location. These results will be confirmed and complemented in Section 2.5, by the analysis of the *exact* general solution of the equations of motion (2.1). Our motivation for having nevertheless presented here a discussion of the character of the singularities of the solutions of (2.1) via a local analysis *à la Painlevé* is because an analogous treatment may be applicable to models which are not as explicitly solvable as that treated in this thesis (see for instance [6] and [7]).

2.4.2 Implications of the analysis *à la Painlevé*

The local analysis *à la Painlevé* performed in the previous subsection establishes – perhaps not quite rigorously (but these findings are then confirmed in Section 2.6 by an investigation of the *exact* solution obtained by quadratures in Section 2.5) – the nature of the branch points of the solutions $\zeta_n(\tau)$ of (2.1), but it does not tell us anything about their number and their locations. We now indicate how one may conclude, on the basis of the results mentioned above about the behavior of the solutions $z_n(t)$ of the *physical* problem (2.10) in the neighborhood of its equilibrium configurations, that, at least in the case with $\varphi > -2$ hence $0 < \mu < 1$, the number of branch points is certainly *infinite* if the numbers φ and μ are *irrational*. This finding is then confirmed by the exact treatment of Section 2.5 (and it holds even if the restriction $\varphi > -2$ hence $0 < \mu < 1$ does not apply), but the line of reasoning presented here deserves to be emphasized in view of its possible use in the context of other problems (such as, for instance, those treated in [6] and [7]) which do not allow making as much progress towards the solution of the corresponding equations of motion as can be achieved (see Section 2.5) for the problem discussed in this thesis.

Let us therefore focus on the subcase with $\varphi > -2$ hence $0 < \mu < 1$, when the solutions $\zeta_n(\tau)$ of the *auxiliary* equations (2.1) *only* feature *square-root* branch points in the *finite* part of the complex τ -plane (a result, let us emphasize, that, as mentioned above, can be obtained via a local analysis *à la Painlevé*). This fact characterizes the structure of the Riemann surfaces associated with these functions $\zeta_n(\tau)$, since every *square-root* branch point connects only *two* sheets of these Riemann surfaces, and thereby, via (2.7), it influences the time evolution of the particle coordinates $z_n(t)$. Indeed if the structure of the Riemann surface associated with the function $\zeta_n(\tau)$ entails that by traveling on it along the circle C one returns to the main sheet after a *finite* number M of turns – as it is certainly the case if the number of *square-root* branch points of the function $\zeta_n(\tau)$ which fall *inside* the circle C , in all the sheets of this Riemann surface, is *finite*, hence the number of sheets accessed via this travel is as well *finite* – then the corresponding component $z_n(t)$ of the solution of our model (2.10) is necessarily *periodic* with a period which is a *finite integer* multiple of the basic period T (specifically, with period MT if M is *even*, $2MT$ if M is *odd*, in which latter case the function $z_n(t)$ is *antiperiodic* with period MT hence the corresponding trajectory of the n -th particle is symmetrical around the origin in the complex z -plane: see (2.7)). A nontrivial result (implied by our treatment, see Sections 2.5 and 2.6; this result could however *not* be obtained via a local analysis *à la Painlevé*) is that, in the semisymmetrical case, see (2.2), the number of branch points, hence the number of sheets of the Riemann surface, is indeed *finite*, if the ratio φ of the coupling constants, hence as well the parameter μ , see (2.25) and (2.26), are *real* and *rational*. Hence in this *rational* case *all* the nonsingular solutions of our model (2.10) are *completely periodic* with a period that is a (possibly quite large) integer multiple of T . But the point we wish to emphasize at the moment is that, independently of this more specific finding, once via a local analysis *à la Painlevé* it has been shown that *all* the branch points in the finite part of the *complex* τ -plane are of *square-root* type, then a necessary condition in order that $z_n(t)$ might *not* be periodic with a period which is a *finite integer* multiple of T is that the number of sheets that get accessed by travelling along the circle C on the Riemann surface associated to the function $\zeta_n(\tau)$ is *infinite*, so that by travelling on it one never returns to the main sheet – and clearly a necessary (but not sufficient, see below) condition for this to happen is that the overall *number of square-root branch points* of the function $\zeta_n(\tau)$ which fall *inside* the circle C , in all the sheets of this Riemann surface, be itself *infinite*. The following argument, based on the results of Section 2.3 reported above, implies that this is certainly the case if the ratio φ of the coupling constants, hence as well the parameter μ , see (2.25), is *not* a *real* and *rational* number.

This conclusion is reached via the following “*reductio ad absurdum*” argument. Suppose

that the number of branch points were *finite*, hence that the number of sheets of the Riemann surface associated with $\zeta_n(\tau)$ were *finite*; then the corresponding solution $z_n(t)$ would *necessarily* be *periodic* with a period that is a (possibly quite large) *integer* multiple of T . But then the behavior of $z_n(t)$ in the neighborhood of its equilibrium configurations would as well *necessarily* be *periodic* with a period that is a *finite integer* multiple of T . However the findings of Section 2.3, as reported above, show that this is *not* necessarily the case if the ratio φ of the coupling constants, hence as well the parameter μ , see (2.25), is *not* a *real* and *rational* number. Hence in this case the number of branch points *cannot* be *finite*. And let us re-emphasize that this argument requires no additional information besides that provided on the solutions $\zeta_n(\tau)$ of the *auxiliary* problem (2.1) by the local analysis *à la Painlevé* as performed in Section 2.4 below and reported above, and the information provided by the standard investigation of the behavior of the solution $z_n(t)$ of the *physical* problem (2.10) in the neighborhood of its equilibrium configurations, as performed in Section 2.3 (and Appendix A) and also reported above.

Actually the same conclusion that the number of square-root branch points of the *general* solution $\zeta_n(\tau)$ of the *auxiliary* model (2.1) is *infinite* if the ratio of the coupling constants is *irrational* could be arrived at more directly (i.e., without the need to investigate the behavior of the *physical* system (2.10) in the vicinity of its equilibrium configurations) via a standard analysis *à la Painlevé* by including in it the treatment of the behavior of the solution $\zeta_n(\tau)$ around the point at infinity in the *complex* τ plane and by thereby noting that this behavior corresponds to a branch point with an *irrational* exponent, which is of course incompatible with the presence of *only* square-root branch points in the *finite* part of the complex τ plane if this number were *finite*.

2.5 General solution by quadratures

In this section we obtain and discuss the *general solutions* of our models, (2.1) and (2.10). But since the *general solution* of the *physical* model (2.10) is easily obtained via the trick (2.7) from the *general solution* of the *auxiliary* problem (2.1), we focus to begin with on this model.

A first constant of the motion is provided by the center-of-mass coordinate

$$Z = \frac{\zeta_1 + \zeta_2 + \zeta_3}{3} , \quad (2.78a)$$

since the equations of motion (2.1) clearly entail

$$Z' = 0 \quad (2.78b)$$

hence

$$Z(\tau) = Z(0) . \quad (2.78c)$$

And clearly the *general solution* of (2.1) reads

$$\zeta_n(\tau) = Z + \check{\zeta}_n(\tau) , \quad (2.79a)$$

with the set of 3 functions $\check{\zeta}_n(\tau)$ providing themselves a solution of (2.1), independent of the value of Z and satisfying the (compatible) constraint

$$\check{\zeta}_1(\tau) + \check{\zeta}_2(\tau) + \check{\zeta}_3(\tau) = 0 . \quad (2.79b)$$

(Note the consistency, via (2.7), of this observation with the 2 in Section 2.1).

It is moreover clear that the equations of motion (2.1) entail

$$\zeta'_1 \zeta_1 + \zeta'_2 \zeta_2 + \zeta'_3 \zeta_3 = g_1 + g_2 + g_3 , \quad (2.80a)$$

hence there also holds the relation

$$\zeta_1^2 + \zeta_2^2 + \zeta_3^2 = 2 (g_1 + g_2 + g_3) (\tau - \tau_0) . \quad (2.80b)$$

It is now convenient to set, as in the Appendix B of [6],

$$\zeta_s = Z - \left(\frac{2}{3}\right)^{1/2} \rho \cos \left[\theta - (-1)^s \frac{2\pi}{3} \right] , \quad s = 1, 2, \quad (2.81a)$$

$$\zeta_3 = Z - \left(\frac{2}{3}\right)^{1/2} \rho \cos(\theta) . \quad (2.81b)$$

Then, summing the squares of these three formulas and using the *identities*

$$\cos(\theta) + \cos\left(\theta + \frac{2\pi}{3}\right) + \cos\left(\theta - \frac{2\pi}{3}\right) = 0 , \quad (2.82)$$

$$\cos^2(\theta) + \cos^2\left(\theta + \frac{2\pi}{3}\right) + \cos^2\left(\theta - \frac{2\pi}{3}\right) = \frac{3}{2} , \quad (2.83)$$

one easily gets

$$\zeta_1^2 + \zeta_2^2 + \zeta_3^2 = 3 Z^2 + \rho^2 \quad (2.84a)$$

or equivalently

$$\rho^2 = \frac{1}{3} \left[(\zeta_1 - \zeta_2)^2 + (\zeta_2 - \zeta_3)^2 + (\zeta_3 - \zeta_1)^2 \right] , \quad (2.84b)$$

hence, from (2.80b),

$$\rho^2 = 2 (g_1 + g_2 + g_3) (\tau - \tau_0) - 3 Z^2 = 2 (g_1 + g_2 + g_3) (\tau - \tau_1) , \quad (2.84c)$$

$$\tau_1 = \tau_0 + \frac{3 Z^2}{2 (g_1 + g_2 + g_3)} \quad (2.84d)$$

which also entails

$$\rho' \rho = g_1 + g_2 + g_3 . \quad (2.84e)$$

Here we assume that the sum of the *three* coupling constants g_n does not vanish, $g_1 + g_2 + g_3 \neq 0$. The special case in which this sum does instead vanish is treated in Appendix B. The expression of the constant τ_1 in terms of the initial data is of course (see (2.84c))

$$\tau_1 = - \frac{\rho^2(0)}{2 (g_1 + g_2 + g_3)} , \quad (2.85a)$$

namely (see (2.84c))

$$\tau_1 = - \frac{\zeta_1^2(0) + \zeta_2^2(0) + \zeta_3^2(0) - 3 Z^2}{2 (g_1 + g_2 + g_3)} , \quad (2.85b)$$

or equivalently

$$\tau_1 = - \frac{(\zeta_1 - \zeta_2)^2 + (\zeta_2 - \zeta_3)^2 + (\zeta_3 - \zeta_1)^2}{6 (g_1 + g_2 + g_3)} . \quad (2.85c)$$

There remains to compute $\theta(\tau)$, or rather

$$u(\tau) = \cos \theta(\tau) . \quad (2.86)$$

Inserting the *ansatz* (2.81) in the equation of motion (2.1) with $n = 3$, one easily gets

$$\begin{aligned} & \rho^2 (\cos \theta)' (4 \cos^2 \theta - 1) \\ = & (4 g_1 + 4 g_2 + g_3) \cos \theta - 4 (g_1 + g_2 + g_3) \cos^3 \theta \\ & + \sqrt{3} (g_1 - g_2) \sin \theta . \end{aligned} \quad (2.87)$$

From now on in this section – for simplicity, and because it is sufficient for our purposes – we restrict attention to the semisymmetrical case (2.2), so that the last equation becomes simply, via (2.86),

$$\begin{aligned} & \rho^2 u' (4u^2 - 1) \\ = & (f + 8g) u - 4(f + 2g) u^3. \end{aligned} \quad (2.88)$$

The general case *without* the restriction (2.2) is treated in Appendix B.

This ODE can be easily integrated via a quadrature (using (2.84c)), and this leads to the following formula:

$$[u(\tau)]^{-2\mu} \left[u^2(\tau) - \frac{1}{4\mu} \right]^{\mu-1} = K (\tau - \tau_1), \quad (2.89)$$

where the parameter μ is defined by (2.25) and K is an integration constant. Here we are of course assuming that $f + 8g \neq 0$ (see (2.25)); the case when this does *not* happen is treated in Appendix B. (Also recall that, as promised above, we shall treat in Appendix B the case in which the sum of the three coupling constants g_n vanishes, namely when $f + 2g = 0$, which entails $\mu = 0$, see (2.25)). As for the quantity K in (2.89), it is an (*a priori arbitrary*) integration constant. It is a matter of elementary algebra to express this constant in terms of the original dependent variables ζ_n (via (2.89), (2.84c), (2.86) and (2.81)), and one thereby obtains the relation

$$K = 12(f + 2g) \tilde{K} \quad (2.90)$$

with \tilde{K} defined by (2.24). This finding justifies the assertion that \tilde{K} is a constant of motion, see Section 2.2; and of course it determines the value to be assigned to the constant K in the context of the *initial-value* problem. Likewise the value to be assigned, in the context of the *initial-value* problem, to the constant τ_1 appearing in the right-hand side of (2.89) is given by the formula

$$K \tau_1 = -[u(0)]^{-2\mu} \left[u^2(0) - \frac{1}{4\mu} \right]^{\mu-1}, \quad (2.91)$$

where (see (2.86) and (2.81b))

$$u(0) = - \left(\frac{3}{2} \right)^{1/2} \frac{\zeta_3(0) - Z}{\rho(0)} \quad (2.92a)$$

namely (see (2.84c) and (2.6))

$$u(0) = - \frac{2\zeta_3(0) - \zeta_1(0) - \zeta_2(0)}{\left[2 \left\{ [\zeta_1(0) - \zeta_2(0)]^2 + [\zeta_2(0) - \zeta_3(0)]^2 + [\zeta_3(0) - \zeta_1(0)]^2 \right\} \right]^{1/2}}. \quad (2.92b)$$

(Of course in these formulas the initial values $\zeta_n(0)$ of the coordinates $\zeta_n(\tau)$ of the *auxiliary* problem (2.1) can be replaced by the initial values $z_n(0)$ of the *physical* problem (2.10), see (2.9)).

Let us emphasize that we have now reduced, via (2.81) with (2.84c) and (2.86), the solution of our problem (2.1) to the investigation of the function $u(\tau)$ of the *complex* variable τ , defined for $\tau \neq 0$ as the solution of the (*nondifferential*) equation (2.89) that evolves by continuity from $u(0)$ at $\tau = 0$.

Before proceeding with our discussion let us pause and see how the findings obtained so far look in the two (“integrable” and “two-body”) special cases. In the “integrable” case (2.3)

$$\mu = \frac{1}{3}, \quad (2.93a)$$

(see (2.25)), so (2.89) becomes the *cubic* equation

$$u(\tau) [u^2(\tau) - 3] = \tilde{K} (\tau - \tau_1)^{3/2} \quad ; \quad (2.93b)$$

and in the “two-body” case (2.4)

$$\mu = 1 \quad , \quad (2.94a)$$

(see (2.25)), so (2.89) yields

$$u(\tau) = [K (\tau - \tau_1)]^{-1/2} \quad (2.94b)$$

entailing (see (2.4), (2.81b), (2.84c) and (2.86))

$$\zeta_3(\tau) = \zeta_3(0) = Z - 2 \left(\frac{f}{3K} \right)^{1/2} \quad , \quad (2.94c)$$

consistently, of course, with (2.4b).

To proceed with our analysis an additional change of variables is now convenient. We introduce the new (*complex*) independent variable ξ by setting

$$\xi = \frac{K (\tau - \tau_1)}{4\mu} \quad , \quad (2.95)$$

and the new (*complex*) dependent variable $w \equiv w(\xi)$ by setting

$$w(\xi) = 4\mu [u(\tau)]^2 \quad . \quad (2.96)$$

Thereby the expression of the solution (2.81) of our original problem (2.1) reads

$$\begin{aligned} \zeta_s(\tau) &= Z - \left(\frac{f+2g}{3K} \right)^{1/2} \xi^{1/2} \left\{ -[w(\xi)]^{1/2} + (-)^s [12\mu - 3w(\xi)]^{1/2} \right\} \quad , \\ s &= 1, 2 \quad , \end{aligned} \quad (2.97a)$$

$$\zeta_3(\tau) = Z - 2 \left(\frac{f+2g}{3K} \right)^{1/2} [\xi w(\xi)]^{1/2} \quad , \quad (2.97b)$$

while the (*nondifferential*) equation that determines the dependence of $w(\xi)$ on the (*complex*) variable ξ reads

$$[w(\xi) - 1]^{\mu-1} [w(\xi)]^{-\mu} = \xi \quad . \quad (2.98)$$

Note that this equation is *independent* of the *initial data* ; it only features the constant μ , which *only* depends on the coupling constants, see (2.25).

We conclude that the solution of our *physical* problem (2.10) as the *real* time variable t evolves onwards from $t = 0$ is essentially given, via (2.97) and (2.7), by the evolution of the solution $w(\xi)$ of this (*nondifferential*) equation, (2.98), as the *complex* variable ξ travels round and round on the circle Ξ in the *complex* ξ -plane defined by the equation (see (2.95))

$$\xi = \bar{\xi} + R \exp(2i\omega t) = R [\exp(2i\omega t) + \eta] \quad , \quad (2.99a)$$

namely on the circle with center $\bar{\xi}$ and radius $|R|$. The parameters R and $\bar{\xi}$ (or η) depend on the initial data according to the formulas (implied by (2.95), (2.7), (2.90), (2.24), (2.85c))

$$R = \frac{3(f+8g)}{2i\omega [2\zeta_3(0) - \zeta_1(0) - \zeta_2(0)]^2} \left[1 - \frac{1}{w_0} \right]^{\mu-1} \quad , \quad (2.99b)$$

$$\bar{\xi} = R\eta \quad , \quad (2.99c)$$

$$\eta = \frac{i\omega \left\{ [\zeta_1(0) - \zeta_2(0)]^2 + [\zeta_2(0) - \zeta_3(0)]^2 + [\zeta_3(0) - \zeta_1(0)]^2 \right\}}{3(f + 2g)} - 1, \quad (2.99d)$$

$$w_0 = \frac{2\mu [2\zeta_3(0) - \zeta_1(0) - \zeta_2(0)]^2}{[\zeta_1(0) - \zeta_2(0)]^2 + [\zeta_2(0) - \zeta_3(0)]^2 + [\zeta_3(0) - \zeta_1(0)]^2}. \quad (2.99e)$$

Of course in these formulas the initial values $\zeta_n(0)$ of the coordinates $\zeta_n(\tau)$ of the *auxiliary* problem (2.1) can be replaced by the initial values $z_n(0)$ of the coordinates $z_n(t)$ of the *physical* problem (2.10), see (2.9).

Remark 3. These formulas are of course applicable without further ado only in the generic case when they yield nonvanishing and nondivergent values for the quantities R , η and $\bar{\xi}$, as we hereafter assume. This is not always the case, for instance for the initial data that correspond to the (first) equilibrium configuration $z_1(0) = -z_2(0) = \left(\frac{f+2g}{2i\omega}\right)^{1/2}$, $z_3(0) = 0$ (see Section 2.3), clearly the parameter w_0 vanishes, see (2.99e), hence R *vanishes* or *diverges* depending whether the parameter μ is *positive* or *negative*, see (2.99b), and η *vanishes*, see (2.99d).

Let us emphasize that, as the complex variable ξ travels on the circle Ξ – taking the time T to make each round, see (2.99a) and (2.8) – the dependent variable $w(\xi)$ travels on the Riemann surface determined by its dependence on the *complex* variable ξ , as entailed by the equation (2.98) that relates $w(\xi)$ to its argument ξ – starting at $t = 0$ from $\xi = \xi_0$,

$$\xi_0 = \bar{\xi} + R = (\eta + 1) R, \quad (2.100a)$$

$$\xi_0 = \frac{i\omega R \left\{ [\zeta_1(0) - \zeta_2(0)]^2 + [\zeta_2(0) - \zeta_3(0)]^2 + [\zeta_3(0) - \zeta_1(0)]^2 \right\}}{3(f + 2g)} \quad (2.100b)$$

(see (2.99)) and correspondingly from $w(\xi_0) = w_0$, (see (2.99e)).

Let us therefore now discuss the structure of this Riemann surface, namely the analytic properties of the function $w(\xi)$ defined by (2.98). There are two types of singularities, the "fixed" ones occurring at values of the independent variable ξ , and correspondingly of the dependent variable w , that can be read directly from the structure of the equation (2.98) under investigation, and the "movable" ones (this name being given to underline their difference from the *fixed* ones) occurring at values of the independent and dependent variables, ξ and w , that cannot be directly read from the structure of the equation (2.98) under investigation.

2.5.1 Movable singularities

To investigate their nature it is convenient to differentiate (2.98), obtaining thereby (using again (2.98))

$$\xi w' = -\frac{w(w-1)}{w-\mu}, \quad (2.101)$$

where the prime indicates of course differentiation with respect to ξ . (Note that this ODE is implied by the nondifferential equation (2.98), while its solution reproduces the nondifferential equation (2.98) up to multiplication of its right-hand side by an arbitrary constant). The position of the singularities, ξ_b , and the corresponding values of the dependent variable, $w_b \equiv w(\xi_b)$, are then characterized by the vanishing of the denominator in the right-hand side of this formula, yielding the relation

$$w_b = \mu, \quad (2.102)$$

which, combined with (2.98) (at $\xi = \xi_b$) is easily seen to yield

$$\xi_b = \xi_b^{(k)} = r \exp(2\pi i \mu k), \quad k = 1, 2, 3, \dots, \quad (2.103a)$$

$$\xi_b = \xi_b^{(k)} = r \exp\left[i \frac{2\pi p k}{q}\right], \quad k = 1, 2, \dots, q, \quad (2.103b)$$

$$r = (\mu - 1)^{-1} \left(\frac{\mu - 1}{\mu}\right)^\mu. \quad (2.103c)$$

In the last, (2.103c), of these formulas it is understood that the principal determination is to be taken of the μ -th power appearing in the right-hand side. The first of these formulas, (2.103a), shows clearly that the number of these branch points is *infinite* if the parameter μ is *irrational*, and that they then sit densely on the circle B in the complex ξ -plane centered at the origin and having radius r , see (2.103c). Note that this entails that the *generic* point on the circle B is *not* a branch point (just as a *generic real* number is *not rational*); but every generic point on the circle B has some branch point (in fact, an *infinity* of branch points!) *arbitrarily* close to it (just as every *generic real* number has an *infinity* of *rational* numbers *arbitrarily* close to it). As for the second of these formulas, (2.103b), it is instead appropriate to the case in which the parameter μ is *rational*, see (2.26), in which case the branch points sit again on the circle B in the complex ξ -plane, but there are only a *finite* number, q , of them.

Proposition 4. *The singularities ξ_b are all square root branch points.*

Proof. Set, for $\xi \approx \xi_b$,

$$w(\xi) = \mu + a (\xi - \xi_b)^\beta + o\left(|\xi - \xi_b|^{\mathcal{R}e(\beta)}\right), \quad (2.104a)$$

with the assumption (immediately verified, see below) that

$$0 < \mathcal{R}e(\beta) < 1. \quad (2.104b)$$

It is then immediately seen that the insertion of this *ansatz* in (2.101) (is consistent and) yields

$$\beta = \frac{1}{2}, \quad a^2 = \frac{2(1-\mu)}{\xi_b} = -2 \left(\frac{\mu}{\mu-1}\right)^\mu. \quad (2.104c)$$

□

Note that these results confirm the treatment of Section 2.4: the *square root* branch points of $w(\xi)$ identified here, see (2.102), are easily seen to correspond, via (2.97), to the pair coincidence $\zeta_1(\tau_b) = \zeta_3(\tau_b)$ or $\zeta_2(\tau_b) = \zeta_3(\tau_b)$; while there is an additional class of *square-root* branch points which only affect $\zeta_1(\tau)$ and $\zeta_2(\tau)$, but neither $\zeta_3(\tau)$ nor $w(\xi)$, and occur at

$$w = 4\mu \quad (2.105a)$$

due to the vanishing of the second *square-root* term inside the curly bracket in the right-hand side of (2.97a), and correspond therefore to the coincidence $\zeta_1(\tau_b) = \zeta_2(\tau_b)$. The corresponding values of ξ (as implied by (2.105a) with (2.98)) are

$$\xi = \frac{(4\mu - 1)^{\mu-1}}{(4\mu)^\mu} = \frac{1}{4\mu} \left(1 - \frac{1}{4\mu}\right)^{\mu-1} \quad (2.105b)$$

(we use the plural to refer to these values because of the multivaluedness of the function in the right-hand side of this formula).

2.5.2 Fixed singularities

Next, let us consider the “fixed” singularities, which clearly can only occur at $\xi = \infty$ and at $\xi = 0$, with corresponding values for w .

Let us investigate firstly the nature of the singularities at $\xi = \infty$. Two behaviors of $w(\xi)$ are then possible for $\xi \approx \infty$, depending on the value of (the real part of) μ . The first is characterized by the *ansatz*

$$w(\xi) = a \xi^\beta + o\left(|\xi|^{\mathcal{R}e(\beta)}\right), \quad \mathcal{R}e(\beta) < 0, \quad (2.106a)$$

and its insertion in (2.98) yields

$$\beta = -\frac{1}{\mu}, \quad a^\mu = -\exp(i\pi\mu), \quad (2.106b)$$

which is consistent with (2.106a) iff

$$\mathcal{R}e(\mu) > 0. \quad (2.106c)$$

The second is characterized by the *ansatz*

$$w(\xi) = 1 + a \xi^\beta + o\left(|\xi|^{\mathcal{R}e(\beta)}\right), \quad \mathcal{R}e(\beta) < 0, \quad (2.107a)$$

and its insertion in (2.98) yields

$$\beta = \frac{1}{\mu - 1}, \quad a^{\mu-1} = 1, \quad (2.107b)$$

which is consistent with (2.107a) iff

$$\mathcal{R}e(\mu) < 1. \quad (2.107c)$$

Then we can formulate the following

Proposition 5. *There are three possibilities: if $\mathcal{R}e(\mu) > 1$, only the first ansatz, (2.106), is applicable, and it characterizes the nature of the branch point of $w(\xi)$ at $\xi = \infty$; if $\mathcal{R}e(\mu) < 0$, only the second ansatz, (2.107), is applicable, and it characterizes the nature of the branch point of $w(\xi)$ at $\xi = \infty$; while if $0 < \mathcal{R}e(\mu) < 1$, both ansätze, (2.106) and (2.107), are applicable, so both types of branch points occur at $\xi = \infty$.*

Next, let us investigate the nature of the singularity at $\xi = 0$. It is then easily seen, by an analogous treatment, that two behaviors are possible, as displayed by the following *ansätze*: either

$$w(\xi) = a \xi^\beta + o\left(|\xi|^{\mathcal{R}e(\beta)}\right), \quad \mathcal{R}e(\beta) > 0, \quad (2.108a)$$

$$\beta = -\frac{1}{\mu}, \quad a^\mu = -\exp(i\pi\mu), \quad (2.108b)$$

which is applicable iff

$$\mathcal{R}e(\mu) < 0; \quad (2.108c)$$

or

$$w(\xi) = 1 + a \xi^\beta + o\left(|\xi|^{\mathcal{R}e(\beta)}\right), \quad \mathcal{R}e(\beta) > 0, \quad (2.109a)$$

$$\beta = \frac{1}{\mu - 1}, \quad a^{\mu-1} = 1, \quad (2.109b)$$

which is applicable iff

$$\mathcal{R}e(\mu) > 0. \quad (2.109c)$$

This analysis entails the following

Proposition 6. *The function $w(\xi)$ features a branch point at $\xi = 0$ the nature of which is characterized by the relevant exponent β , see (2.108) or (2.109b), whichever is applicable (see (2.108c) and (2.109c)). There is no branch point at all at $\xi = 0$ if neither one of the two inequalities (2.108c) and (2.109c) holds, namely if $0 < \mathcal{R}e(\mu) < 1$.*

2.5.3 Comparison with the findings of Section 2.4

These results confirm those reported in Section 2.4, since clearly the branch point at $\xi = 0$ corresponds via (2.97) to the *triple* coincidence (2.70). Indeed if $\mathcal{R}e(\mu) < 0$ the insertion of (2.108a) in (2.97) yields (via (2.95))

$$\zeta_s(\tau) = Z + \left(-1 + (-)^s i \sqrt{3}\right) C (\tau - \tau_1)^{\frac{(\beta+1)}{2}} + o\left(|\tau - \tau_1|^{\mathcal{R}e\left[\frac{(\beta+1)}{2}\right]}\right) \quad s = 1, 2, \quad (2.110a)$$

$$\zeta_3(\tau) = Z + 2C (\tau - \tau_1)^{\frac{(\beta+1)}{2}} + o\left(|\tau - \tau_1|^{\mathcal{R}e\left[\frac{(\beta+1)}{2}\right]}\right), \quad (2.110b)$$

where C is a constant. And it is then clear that the exponent $\frac{\beta+1}{2}$, with $\beta = -\frac{1}{\mu}$ (see (2.108)), appearing in this formula, coincides with the exponent $\frac{1-\gamma}{2} = \frac{\mu-1}{2\mu}$ (see (2.74)) appearing in the *ansatz* (2.71a). Likewise, if $\mathcal{R}e(\mu) > 1$ the insertion of (2.109a) in (2.97) yields (via (2.95))

$$\begin{aligned} \zeta_s(\tau) = Z &+ C \left[-(b + (-)^s c) (\tau - \tau_1)^{1/2} - (\tilde{b} + (-)^s \tilde{c}) (\tau - \tau_1)^{\beta+1/2} \right] \\ &+ o\left[|\tau - \tau_1|^{\mathcal{R}e(\beta+1/2)}\right], \quad s = 1, 2, \end{aligned} \quad (2.111a)$$

$$\zeta_3(\tau) = Z + 2C \left[b (\tau - \tau_1)^{1/2} - \tilde{b} (\tau - \tau_1)^{\beta+1/2} \right] + o\left[|\tau - \tau_1|^{\mathcal{R}e(\beta+1/2)}\right], \quad (2.111b)$$

It is then again clear that the exponent $\beta + \frac{1}{2}$, with $\beta = \frac{1}{\mu-1}$ (see (2.109b)), appearing in this formula, coincides with the exponent $\frac{1-\gamma}{2} = \frac{\mu+1}{2(\mu-1)}$ (see (2.76)) appearing in the *ansatz* (2.71a). And the lack, predicted in Section 2.4 for the case $0 < \mathcal{R}e(\mu) < 1$, of any *non-square-root* branch point in the finite part of the complex τ -plane is now as well confirmed.

2.6 Behavior of the physical model

In this section we discuss the implications of the findings obtained so far, as regards the actual behavior of the solutions of our *physical* model (2.10).

We explained in the previous sections the mechanism that guarantees the *isochronous* character of our *physical* model (2.10): there is an *open* domain of initial data $z_n(0)$ such that the corresponding solutions of the *auxiliary* problem (2.1) are *holomorphic* in the open disk D encircled by the circle C in the *complex* τ -plane, and via (2.7) this guarantees the *isochronous* character, see (2.12), of the solutions $z_n(t)$ of our *physical* model (2.10) that evolve from these initial data. We also outlined above how the presence of branch points of $\zeta_n(\tau)$ *inside* the disk D may affect the time-periodicity of the corresponding *physical* coordinate $z_n(t)$. Let us now pursue a bit more this analysis here, to better explain – albeit still *qualitatively* – the mechanism whereby *nonisochronous* solutions $z_n(t)$ of our physical model (2.10) may emerge, either *completely periodic* ones but with a larger period than that characterizing the *isochronous* regime, or even *aperiodic* ones which display some kind of *complicated* behavior (possibly characterized by a *sensitive dependence* on the initial data, see Chapter 4. A more detailed – as it were, *quantitative* – dissection of the phenomenology of the motions of our *physical* model is then reported below (in this section),

on the basis of the exact *general solution* of its equations of motions (2.10), as obtained (for the semisymmetrical case) in Section 2.5 and discussed in Section 2.6 (and in [2]).

An important aspect to understand the relation – already outlined above – among the time evolution of a solution $z_n(t)$ of the physical model (2.10) and the analytic structure of the solution $\zeta_n(\tau)$ that corresponds to it via (2.7), is the distinction among *active* and *inactive* branch points of the function $\zeta_n(\tau)$, a distinction we now illustrate by again referring, to simplify the presentation here, to the case in which the branch points possessed by the generic solution $\zeta_n(\tau)$ in the finite part of the *complex* τ -plane are *all* of *square-root* type (namely, the semisymmetrical case with $0 < \mu < 1$). Recall that, as implied by the relation (2.7), the behavior of the solution $z_n(t)$ of our equations of motion (2.10) as function of the (*real*) time variable t is obtained by travelling round and round along the circle C on the Riemann surface associated with the solution $\zeta_n(\tau)$ of the evolution equation (2.1). This outcome is therefore influenced by the branch points of $\zeta_n(\tau)$ that characterize this Riemann surface. However, not all these branch points do influence the behavior of the solution $z_n(t)$ of our model.

Definition: Let us qualify as *active* those branch points that do influence the time evolution of the solution $z_n(t)$, because the cuts associated with them are actually traversed when travelling around on the circle C and therefore do open the way to new sheets, and instead as *inactive* those branch points that do not cause this effect – either because they are *outside* the circle C , or because they belong to a pair of (*square-root*) branch points connected by a cut that falls *inside* C on the *same* sheet of the Riemann surface (which is therefore not traversed when travelling on the circle C ; however, this phenomenon does not happen in our case), or because they are inside C but sit on a sheet that does *not* get accessed *at all* during the travel on the circle C (this is indeed a crucial mechanism to account for the complications in the behavior of our model, as it will be eventually clear, see below).

Due to the *square-root* character of these branch points, each of the cuts associated with them opens the way to just *one* new sheet, hence the number of new sheets (besides the basic one) visited along the entire travel equals the number A of *active* branch points; therefore overall the number M of sheets visited (including the *main* one) along this travel on the Riemann surface, before returning to the point of departure on the *main* sheet, exceeds by one the number of *active* branch points, $M = 1 + A$, and this – since clearly a complete round must be made on each of the sheets visited – entails that the time taken for the entire tour before returning to the initial value on the *main* sheet is $M T = (1 + A) T$ (see (2.8)), hence this is also the *periodicity* (or *antiperiodicity*, see (2.7)) of $z_n(t)$ (as discussed above). Note that this implies that, even in the case in which the *total* number of branch points of the solution $\zeta_n(\tau)$ is *finite* (as it is indeed the case, see below, when the ratio φ of the coupling constants, see (2.2), hence the parameter μ , see (2.25) and (2.26), is *real* and *rational*), hence *all* the (nonsingular) solutions $z_n(t)$ of our model (2.10) are *completely periodic*, nevertheless if the number of branch points that fall *inside* the circle C is *quite large*, the period of the motion can also be *quite large*, and moreover it may depend in a *sensitive* manner on the detailed structure of the Riemann structure associated with the corresponding solution $\zeta_n(\tau)$, since it is this structure – as it is clear from this discussion, and as we shall further discuss below – that determines the number A of *active* branch points.

The number of branch points included inside C depends of course, via the solution $\zeta_n(\tau)$, on the initial data (see (2.9)) that determine this solution; hence a change in these initial data causes a rearrangement of the branch points pattern. Since the period of the motion generally changes whenever, as an effect of the change of the *initial* data, one *active* branch point is added or subtracted (for instance, by entering in, or exiting from, the circle C in the complex τ -plane), there shall be circumstances when even a *minute* change in the

initial data has this effect, and might thereby entail a *major* change in the period of the motion. So, even in the *rational* case when *all* nonsingular solutions $z_n(t)$ of our physical model (2.10) are *completely periodic* with a period which is a *finite integer* multiple of T , it may happen that there is a *sensitive* dependence on the initial data, inasmuch as a *minute* change in such data might cause a *major* change in the period of the motion. This mechanism might of course manifest itself in an even more dramatic manner if the number of branch points, hence the number of sheets of the relevant Riemann surface, is *infinite*, as it is certainly the case if the ratio φ of the coupling constants, see (2.2), hence the parameter μ , see (2.25), are *not* rational: then a minute change in the initial data may even cause the transition from a *periodic* to an *aperiodic* motion, or from an *aperiodic* motion to another *aperiodic* motion which is quite different (see Chapter 4).

A natural question at this point is: what if an *active* branch point falls *exactly* on the circle C ? Then the corresponding solution of the *physical* problem runs into a singularity, which, as implied by its equations of motion (2.10), corresponds necessarily to the *collision* of a *pair*, or a *triple*, of particles. Is this “likely” to happen? Of course not, since the set of *initial* data that yield a *collision* has clearly *lower* dimensionality than the set of *all* initial data. Actually, this statement might not be quite evident, since the motions of the *three* particles with coordinates $z_n(t)$ in the *complex* z -plane entailed by our model (2.10) are *confined* for all time, hence one might well wonder whether, in the *aperiodic* case, the *generic* solution shall eventually run – possibly after a very long time – into a particle *collision*; that this is *not* the case is completely clear from the exact solution obtained in Section 2.5. This is consistent with the fact that the chance to hit a point particle with a point particle in the plane is *nil*. However, in the case of *confined aperiodic* motions there shall occur lots of *near misses*, and they constitute the “physical cause” of the fact that any two motions, however close they initially are, become eventually quite different. In terms of the solutions $\zeta_n(\tau)$ of the *auxiliary* problem (2.1), the corresponding analysis is even more cogent: generally the functions $\zeta_n(\tau)$ corresponding to a generic solution of the evolution equations (2.1) feature an *infinity* of *square-root* branch points in the τ -plane (nested on the infinite sheets of the corresponding Riemann surfaces), and clearly the probability that any one of them (and in particular one sitting on a sheet that gets actually accessed by travelling on the Riemann surface of $\zeta_n(\tau)$ as τ rotates on the circle C in the *complex* τ -plane) does fall *exactly* on the circle C is *nil*; while, at least for the solutions $\zeta_n(\tau)$ of the *auxiliary* model (2.1) that correspond to initial data yielding *disordered motions* of our *physical* model (2.10), there clearly occur – as we show below – *active* branch points *arbitrarily close* to the circle C (corresponding via the trick (2.7) to *arbitrarily close near misses* of a collision for the particles evolving according to our *physical* model (2.10)).

In conclusion – as suggested by the above analysis, and substantiated by the results reported below – the *qualitative* picture of the solutions of our model (2.10), in the semisymmetrical case with coupling constants f and g that are *not* congruent (so that neither their ratio φ , see (2.2), nor the parameter μ , see (2.25), are *rational* numbers) features an *open* region of initial data yielding *isochronous* motions with period $2T$, see (2.8), other *open* regions of initial data yielding *completely periodic* solutions with periods that are *integer multiples* of T , *open* regions that yield *multiply periodic* motions, and possibly *open* regions yielding *aperiodic* motions which might be *very complicated* (as we shall see below, the latter regime only occurs for values of the parameter μ which are *irrational* and are *outside* of the interval $0 \leq \mu \leq 1$). These regions of *initial* data are separated by (*lower dimensional*) boundaries, corresponding to *initial* data out of which emerge motions that eventually run into a *singularity*, namely a particle *collision*.

The physical origin of the *irregular* aspect of the *aperiodic* motions is due to the fact that, as the *three* particles move in a confined region of the plane, there are eventually *near misses* of collisions in which particles pass *arbitrarily close* to each other; the *sensitive*

dependence on the initial data is due to the fact that, however close two slightly different sets of initial data causing two *disordered* motions are, eventually the two corresponding motions shall feature a *near miss* (in fact, eventually, an infinity of such *near misses*) in which two particles scatter past each other *differently* (namely, on different sides), and as a consequence the two motions, while being analogous to each other until that moment, become quite different thereafter (their subsequent motion being eventually characterized by an *infinity* of such *near misses*).

The *qualitative* understanding provided by the above discussion of the time evolution of our *physical* model (2.10) (and indeed of many other models, see for instance [6] and [7]) entails that a more detailed, *quantitative*, understanding of the solutions $z_n(t)$ of this model (in the regime we are mainly interested in, when the motions are *not* isochronous) requires an understanding of the structure of the Riemann surface associated with the corresponding solutions $\zeta_n(\tau)$ of the *auxiliary* model (2.1) sufficiently detailed to allow us to predict the sequence of different sheets of this Riemann surface that are visited when the *complex* variable τ rotates on the circle C in the complex τ -plane. Such more detailed understanding is remarkably possible – even when the corresponding motions are very complicated – on the basis of the exact *general* solution of our *physical* model (2.10) as obtained in Section 2.5, and it will be reported in the next chapter.

2.6.1 Solution of the physical model

The *general* solution of the equations of motions (2.10) reads as follows:

$$z_s(t) = Z \exp(-i\omega t) - \frac{1}{2} \left(\frac{f+8g}{6i\omega} \right)^{1/2} [1 + \eta \exp(-2i\omega t)]^{1/2} \cdot \left\{ [\check{w}(t)]^{1/2} - (-)^s [12\mu - 3\check{w}(t)]^{1/2} \right\}, \quad s = 1, 2, \quad (2.112a)$$

$$z_3(t) = Z \exp(-i\omega t) + \left(\frac{f+8g}{6i\omega} \right)^{1/2} [1 + \eta \exp(-2i\omega t)]^{1/2} [\check{w}(t)]^{1/2}, \quad (2.112b)$$

where the function $\check{w}(t)$ is defined via the relation

$$\check{w}(t) = w[\xi(t)] \quad (2.113)$$

with $\xi(t)$ given by formula (2.99a) and the function $w(\xi)$ satisfies the *nondifferential* equation (2.98). The *three* constants Z , R , and η (or $\bar{\xi}$) are defined in terms of the *three* initial data $z_n(0)$, see below.

Note that the formula (2.99a) implies that, as the time t evolves, the point $\xi(t)$ travels uniformly (counterclockwise, performing a full round in the time T , see (2.8)) on the circle Ξ in the complex ξ -plane, the center $\bar{\xi}$ and radius $|R|$ of which are defined in terms of the initial data by the formulas (see (2.99) with (2.9))

$$\bar{\xi} = R\eta, \quad (2.114a)$$

$$\eta = \frac{i\omega \left\{ [z_1(0) - z_2(0)]^2 + [z_2(0) - z_3(0)]^2 + [z_3(0) - z_1(0)]^2 \right\}}{3(f+2g)} - 1, \quad (2.114b)$$

$$R = \frac{3(f+8g)}{2i\omega [2z_3(0) - z_1(0) - z_2(0)]^2} \left[1 - \frac{1}{\check{w}(0)} \right], \quad (2.114c)$$

$$Z = \frac{z_1(0) + z_2(0) + z_3(0)}{3}. \quad (2.114d)$$

The dependent variable $\check{w}(t)$ is correspondingly defined via (2.113) from the solution of the *nondifferential* equation (2.98), and it is identified, as the time t unfolds from $t = 0$, hence

as the variable $\xi \equiv \xi(t)$ goes round and round, in the *complex* ξ -plane, on the circle Ξ , by continuity from the initial datum (see (2.99e) with (2.9))

$$\check{w}(0) = w[\xi(0)] = \frac{2\mu [2z_3(0) - z_1(0) - z_2(0)]^2}{[z_1(0) - z_2(0)]^2 + [z_2(0) - z_3(0)]^2 + [z_3(0) - z_1(0)]^2}. \quad (2.115)$$

This specification is necessary, since generally the *nondifferential* equation (2.98) has more than a single solution, in fact possibly an *infinity* of solutions, see below.

Let us note first of all that these formulas, (2.112), entail that a pair collision occurs at the time $t = t_c$, if at that time $\check{w}(t_c) = 4\mu$ (entailing $z_1(t_c) = z_2(t_c)$) or $\check{w}(t_c) = \mu$ (in which case the pair collision involves the *different*, third particle); and likewise a *triple* collision occurs at the time t_c if $\eta = \exp(2i\omega t_c)$ (note that this formula defines t_c – of course $\text{MOD } T$ – but it yields a *real* value for this quantity only if $|\eta| = 1$). Clearly these collisions only occur for special (*nongeneric*) initial data (see also below). And it is as well clear from these formulas, (2.112), what the effect on the overall motion is of a (small) change of initial data – say, as some parameter δ characterizing the initial data is changed with continuity from a *small negative* value to a *small positive* value, with the vanishing value $\delta = 0$ corresponding to the initial data causing the collision, and the *negative* and *positive* (but *very small*) values of δ corresponding of course to *near misses*. Then, if the collision is a *pair* collision among the two *equal* particles (hence it corresponds to the branch point at $\check{w} = 4\mu$, see the last square-root in the right-hand side of (2.112)), the trajectory of the *different*, third particle is essentially unaffected by the sign of δ , while those of the two *equal* particles get exchanged among each other after the *near miss* for *positive* δ with respect to those corresponding to the *near miss* for *negative* δ . If the collision is instead a *triple* collision, then the trajectories (in the center of mass system) of *all three* particles are equally affected by the change of initial data from those corresponding to a *near miss* with *negative* δ to those corresponding to a *near miss* with *positive* δ , since the *difference* among these trajectories is caused – see (2.112) – by the *different* time evolution of the factor

$$[\eta \exp(-2i\omega t) - 1]^{1/2} = \exp(-i\omega t) [\eta - \exp(2i\omega t)]^{1/2} \quad (2.116)$$

depending on the value relative to *unity* of the absolute value of the parameter η (this parameter depends of course on the initial data, and for $\delta = 0$ its absolute value is just unity, $|\eta| = 1$, corresponding to the occurrence of the *triple* collision; while the two equivalent ways (2.116) to write this factor are indicative of its different time evolution, as function of the real time t , depending whether $|\eta|$ is *larger* or *smaller* than *unity*). Finally, in the vicinity of a *pair* collision involving the third, *different* particle (which corresponds to $\check{w} = \mu$, see (2.112)) the *different* behaviors of the trajectories of the third particle and that of that one of the two equal particles which is involved in the collision (and indeed, as a consequence, also of the remaining particle), among the cases with initial data characterized by a *positive*, or instead a *negative*, value of δ , is due to the *different* evolution in these two cases of the function $\check{w}(t)$ due to the *square-root* branch points characterizing the function $w(\xi)$ where $w = \mu$.

As entailed by this analysis based on the explicit expression, (2.112), of the solution of our *physical* problem (2.10), the more complicated aspect of its time evolution is determined by the function $\check{w}(t)$; hence, for the sake of simplicity, hereafter (in this section) we focus mainly on the time evolution of this function. In fact let us focus to begin with on the less specifically identified function $\tilde{w}(t)$ related by the formula $\tilde{w}(t) = w[\xi(t)]$ with (2.99a) to some solution of the equation (2.98), reserving the notation $\check{w}(t)$ (see (2.113)) for the “physical” one among the functions $\tilde{w}(t)$ that enters in the right-hand side of the solution formula (2.112) and is uniquely identified by the initial datum (2.115).

Let us consider to begin with the *rational* case $\mu = p/q$, see (2.26). Then the equation (2.98) that determines via (2.113) and (2.99a) the time evolution of $\tilde{w}(t)$ is *polynomial* in

w , and it reads

$$[w(\xi) - 1]^{p-q} = \xi^q [w(\xi)]^p$$

if $0 < q < p$, namely if $p > p - q > 0$, $\mu > 1$, (2.117a)

$$\xi^q [w(\xi) - 1]^{q-p} [w(\xi)]^p = 1$$

if $0 < p < q$, namely if $p > 0$, $q - p > 0$, $0 < \mu < 1$, (2.117b)

$$\xi^q [w(\xi) - 1]^{|p-q|} = [w(\xi)]^{|p|}$$

if $p < 0 < q$, namely if $p - q < p < 0$, $\mu < 0$. (2.117c)

As indicated, which one of these *three* polynomial equations (in the dependent variable $w \equiv w(\xi)$) is relevant depends on the values of the *two* integers p and $q > 0$ (see (2.26)). These *two* integers also determine the degree J of each of these *three* polynomial equations: $J = p > 0$ for the first (case $p > p - q > 0$, $\mu > 1$), $J = q$ for the second (case $p > 0$, $q - p > 0$, $0 < \mu < 1$) and $J = |p - q| = q - p = q + |p|$ for the third (case $p - q < p < 0$, $\mu < 0$). Of course the degree J of the polynomial equation (2.117) coincides with the number of its roots $w_j(\xi)$, $j = 1, 2, \dots, J$. We are eventually interested in the time-evolution of just one of these J roots, say $\tilde{w}(t) = w_1[\xi(t)]$ with (2.99a), but as indicated above it will be useful in the following to also consider the evolution of a generic one of the J roots, say $\tilde{w}_j(t) = w_j[\xi(t)]$ (again with (2.99a); occasionally we will indicate such a root just as $\tilde{w}(t)$).

The function $[\xi(t)]^q$, see (2.99a), which characterizes the time dependence of the polynomial equation under consideration, see (2.117), is clearly *periodic* with period T , see (2.8) (except in *three* special cases: if the initial data imply $\bar{\xi} = 0$, $R \neq 0$, when it is *periodic* with period $\frac{T}{q}$; if the initial data imply $R = 0$, $\bar{\xi} \neq 0$, when it becomes a (time-independent) nonvanishing *constant*; and if the initial data imply $\bar{\xi} = R = 0$, when it *vanishes identically*; for simplicity we do not consider any one of these three special cases in this section). Therefore the set of its J roots is as well *periodic* with the same period:

$$\{\tilde{w}_j(t + T); j = 1, \dots, J\} = \{\tilde{w}_j(t); j = 1, \dots, J\} . \quad (2.118)$$

But this does *not necessarily* imply that, if one follows with continuity the time evolution of a specific root – and in particular that of the root $\tilde{w}_1(t) = \tilde{w}(t)$ – its evolution shall be periodic with period $\frac{T}{2}$: after one period the root $\tilde{w}(t)$ can take the place of another root, indeed its time evolution, if considered at times t_k which are *integer* multiples of the basic period T , $t_k = kT$, $k = 0, 1, 2, 3, \dots$, generally amounts to hopping from one to the other of the “initial” J roots $\tilde{w}_j(0) = w_j(\xi_0)$ of the polynomial equation (2.117) evaluated at the initial time $t = 0$, namely for $\xi = \xi(0) = \xi_0 = \bar{\xi} + R$ (see (2.99a) and (2.114)). Hence this motion – and in particular the motion of $\tilde{w}(t)$ as a function of the time t as it unfolds continuously from $t = 0$ – is generally *periodic* with a period \check{T} that is a *finite integer* multiple of the basic period T , see (2.8), $\check{T} = \check{j}T$ with the integer \check{j} not larger than J , $1 \leq \check{j} \leq J$. Several remarks are now appropriate.

Remark 7. This finding establishes that *all* the nonsingular solutions of our *physical* model (2.10) are *completely periodic* with a period that is a *finite integer* multiple of the basic period, see (2.8), whenever the ratio φ of the coupling constants f and g featured by this model (in the semisymmetrical case, to which, let us recall, our consideration is now restricted), hence as well the parameter μ , see (2.2) and (2.25), is a *rational* number, see (2.26) (which is the case under present discussion).

Remark 8. The *isochronous* character of our model entails that there is an *open* domain of initial data $z_n(0)$ (characterized by adequately large values of all *three* interparticle distances $|z_n(0) - z_m(0)|$, as explained above: see the *sufficient* condition (2.67)) such that the corresponding evolution of the particle coordinates $z_n(t)$ is *completely periodic*, see (2.12). To such data there corresponds a very simple periodicity of *all* the J roots $\tilde{w}_j(t)$, namely $\tilde{w}_j(t+T) = \tilde{w}_j(t)$, $j = 1, 2, \dots, J$. The periodic evolution of $\tilde{w}(t)$ shall be moreover characterized by the property of the *closed* contour which this quantity travels on, in the complex w -plane, over each period T , to include neither the point $\tilde{w} = 0$ nor the point $\tilde{w} = 4\mu$, see (2.112) and (2.12).

Remark 9. The analysis we just made entails that, if the initial data are *outside* of the region yielding *isochronous* motions, see (2.12), the time evolution of $\tilde{w}(t)$, while certainly *periodic* with a period which is a *finite integer* multiple of the basic period T , see (2.8), could however feature a period $\check{T} = \check{j}T$ which is a *quite large* multiple, \check{j} , of the basic period T , if the number J (determined, as explained above, by p and q : see (2.117) and the paragraph following this equation) is itself *quite large*. And if J is *very large*, the actual value of the period of the time evolution of $\tilde{w}(t)$ – which, in units of the basic period T , is just the number \check{j} of other initial roots $\tilde{w}_j(0)$ of the relevant polynomial of degree J that $\tilde{w}(t)$ visits, over its time evolution, at the times $t_k = kT$, $k = 1, 2, 3, \dots$, before returning to its own initial value $\tilde{w}(0)$ at $t = t_{\check{j}} = \check{T} = \check{j}T$ – depends in a rather *sensitive* manner on the *initial* data. Note that, under these circumstances, the time evolution of our *physical* system (2.10) is largely characterized by this sequence of initial roots $\tilde{w}_j(0)$ that $\tilde{w}(t)$ visits over each period of its time evolution: indeed the task to solve the initial-value problem of our *physical* model (2.10) corresponds then essentially to computing, for every given initial data $z_n(0)$, the period of the corresponding time evolution of $\tilde{w}(t)$ (hence, up to rather simple additional adjustments, see (2.112), the period of the motion of the *three* particles $z_n(t)$) and, more specifically, to ascertaining the detailed sequence of initial roots $\tilde{w}_j(0)$ actually visited, at the times $t = t_k$, by $\tilde{w}(t)$ as it moves around from one of them to another one of them, starting from $\tilde{w}(0)$ at $t = 0$ and returning to $\tilde{w}(0)$ at $t = \check{T} = \check{j}T$, an evolution which largely characterizes, see (2.112), the trajectories traced by the coordinates $z_n(t)$ of the *three* particles over each period of their motion.

2.6.2 The polynomial equation 2.98

The results we reported so far entail a close relationship among the motion, in the *complex* z -plane, of the 3 particles that are the protagonists of our *physical* model (2.10), and the time evolution, in the complex w -plane, of the J roots of the polynomial equation (2.117) as $\xi \equiv \xi(t)$ travels round and round on the circle Ξ , see (2.99a). As already indicated above, this implies the possibility that the motion described by the coordinates $z_n(t)$ of our *three* particles in the *complex* z -plane be *quite complicated* if the natural number J is *very large*; it also implies that our 3-body problem (2.10) is now seen to be somehow equivalent to a J -body problem – the time evolution in the *complex* w -plane of the J roots of the polynomial equation (2.117) as $\xi \equiv \xi(t)$ travels round and round on the circle Ξ , see (2.99a) – naturally suggesting that for its understanding the tools of statistical mechanics might play a role. This is particularly significant in the case, discussed below, when the ratio φ of the coupling constants of our model, see (2.2), hence as well the parameter μ , see (2.25), are *irrational* numbers, which corresponds (see below) to the case in which the number J diverges – so that, in such (*generic!*) case the dynamics of our *three*-body problem (2.10) becomes naturally connected with the dynamics of an assembly of an *infinite* number of points on the complex plane.

The next discussion is aimed at providing a *qualitative* understanding of the motion in the *complex* w -plane of the J roots $\tilde{w}_j(t)$ of the polynomial equation (2.117) with (2.99a).

This treatment pushes the analysis a bit further than that given above; and we now return, to simplify the presentation, to considering the case when J is *finite* (although this analysis is largely applicable as well without this restriction). Let us note to begin with that clearly, for a *generic* value of the independent *complex* variable ξ , the J roots $w_j \equiv w_j(\xi)$ of the polynomial equation (2.117) are *all distinct*; but there are *special* values of ξ at which *two* roots of the polynomial equation (2.117) coincide. These *special* values are of course precisely those at which the solution $w(\xi)$ of the polynomial equation (2.117) has a *square-root* branch point: at these branch points the value of w is $w = \mu$ (as indicated by the above discussion and proven below), and the *square-root* character of these branch points reflects the fact that just *two* roots of the polynomial equation (2.117) coincide there – indeed the fact (easily proven, see Section 2.6) that *all* the branch points of the polynomial equation (2.117) occurring at *finite* values of ξ (namely, $\xi \neq 0$ and $\xi \neq \infty$) are of *square-root* type (and entail $w = \mu$) implies that for *no finite* values of ξ the polynomial equation (2.117) possesses roots of *higher multiplicity* than *two*; while for $\xi = 0$ clearly (2.117a) has the root $w = 1$ with multiplicity $p - q$, (2.117c) has the root $w = 0$ with multiplicity $|p|$, and (2.117b) has *no root at all*; and for $\xi = \infty$ clearly (2.117a) has the root $w = 0$ with multiplicity p , (2.117c) has the root $w = 1$ with multiplicity $|p - q|$, and (2.117b) has the root $w = 0$ with multiplicity p and the root $w = 1$ with multiplicity $q - p$.

Again, for the sake of simplicity, let us restrict the following discussion to the case when $0 < \mu < 1$, see (2.117b), when the branch points in the *finite* part of the complex ξ -plane (*including* the origin, $\xi = 0$) are *all* of *square-root* type. Let us then start our analysis of the time evolution of the J roots of the polynomial equation (2.117b) from the consideration of a set of initial data *inside* the *isochronous* region (recall that the initial data affect the time evolution of the roots $\tilde{w}_j(t)$ inasmuch as they determine the center $\bar{\xi}$ and the radius $|R|$ of the circle Ξ in the complex ξ -plane on which $\xi(t)$ rotates as the *real* time t evolves: see (2.99a) and (2.114)). To these initial data there corresponds, for each of the J roots $\tilde{w}_j(t)$ of the polynomial equation (2.117b), a closed trajectory that is traveled in a time T and that starts at the value $\tilde{w}_j(0)$ and ends – for each of the roots – back at its initial value $\tilde{w}_j(0)$. Let us now change gradually, *with continuity*, the initial data, so as to eventually exit from the *isochronous* regime. At some point along this process there is a specific set of initial data that causes *two* roots – say, the roots $\tilde{w}_k(t)$ and $\tilde{w}_\ell(t)$ – of the polynomial equation (2.117b) to coincide at some value t_b (so that $\tilde{w}_k(t_b) = \tilde{w}_\ell(t_b) = \mu$); and, along this process of gradual modification of the initial data, what happens is that, *just before* and *just after* the set of initial data that causes the *two* trajectories of the two roots $\tilde{w}_k(t)$ and $\tilde{w}_\ell(t)$ to *coincide*, the initial data yield trajectories $\tilde{w}_k(t)$ and $\tilde{w}_\ell(t)$ that experience a *near miss* at $t = t_b$ and that cause the *two* roots, for the data *just after* those causing the collision of these *two* roots at $t = t_b$, to *exchange* their time evolution (with respect to that prevailing for the initial data just before those causing the collision), so that at the time $t = T$ the outcome entails $\tilde{w}_k(T) = \tilde{w}_\ell(0)$ and $\tilde{w}_\ell(T) = \tilde{w}_k(0)$. A further continuation of the process of gradual change of the initial data shall eventually cause another collision of *two other* roots, and a further minute additional change of the initial data transforms that collision into a *near miss*, with subsequent exchange of the time evolution of the *two* roots involved in that event. And this mechanism will be repeated as the process of gradual change of the *initial* data is continued. It is via this mechanism that the trajectories of the J roots yielded by a *generic* set of initial data yield a permutation of the roots after one basic period T , that gets then iterated, at the times $t_k = kT$, $k = 1, 2, 3, \dots$ – as explained above. Note that, in the context of our *physical three-body* problem (2.10), the phenomenology we just described corresponds to a *collision*, or to a *near miss*, involving a pair of physical particles described by the *complex* coordinates $z_n(t)$ (and including the *different*, third particle $z_3(t)$), *only* when the pair *collision*, or *near miss*, among the roots $\tilde{w}_j(t)$ involves, as one of the *two* protagonist roots, the fundamental root $\tilde{w}_1(t) \equiv \tilde{w}(t)$ that

enters in the solution formula (2.112).

The discussion we just gave entails that, to get a complete understanding of the time evolution of our main root $\check{w}(t)$ one must understand the structure of the Riemann surface associated to the solution $w(\xi)$ of the polynomial equation (2.117) – and, more generally, of the nondifferential equation (2.98) when μ is not a *rational* number – in sufficient detail to be able to describe the sequence over time of its sheets that get visited when the independent variable ξ rotates on the circle Ξ in the complex ξ -plane as entailed by (2.99a), and correspondingly the dependent variable $\check{w}(t) = w_1[\xi(t)]$ travels on its Riemann surface, starting from its initial value $\check{w}(0) = \check{w}_0$ (see (2.115)), taken on the main sheet of this Riemann surface, and returning there at the time $\check{T} = jT$ after having visited $j - 1$ additional sheets (this necessarily happens if μ is a *rational* number, see (2.26); it might, but need not, happen if μ is *irrational* see below). We will see how this understanding is possible in the next chapter.

The distinguished points characterizing the structure of this Riemann surface are of course the branch points of the solution $w(\xi)$ of the polynomial equation (2.117) – and, more generally, of the nondifferential equation (2.98) when μ is *not a rational* number. The positions of those of *square-root* type are given by the following formula (established in Section 2.6, see (2.102) and (2.103)):

$$\xi_b = \xi_b^{(k)} = r \exp(2\pi i \mu k), \quad k = 1, 2, 3, \dots,$$

$$r = (\mu - 1)^{-1} \left(\frac{\mu - 1}{\mu} \right)^\mu,$$

and, as already mentioned above, at all these branch points the function $w(\xi)$ takes the same value,

$$w(\xi_b) = \mu.$$

These results are a direct consequence of the (*nondifferential*) equation (2.98). Note that the formula (2.103) implies that these *square-root* branch points *all* reside on the circle B centered at the origin of the *complex* ξ -plane and having radius $|r|$ (incidentally, one may assume without loss of generality that the principal determination is taken in the evaluation of the μ -th root appearing in the right-hand side of (2.103c)). Note that, as written here, this formula (2.103) applies generally, including the case in which the parameter μ is *irrational*; of course in the *rational* case, see (2.26), the number of *different* branch points yielded by this formula is just q , and they are equally spaced on the circle B ; while if μ is instead *irrational*, there is an *infinity* of such *square-root* branch points, *all* of them located on the circle B (hence in this case they are *densely* located on this circular contour, so that each point on it has an *infinity* of branch points *arbitrarily close* to it; yet the *generic* point on this contour is *not* a branch point – the situation is exactly analogous to that of the set of *rational numbers* who sit *densely* on the *real* line, since every *real* number has an *infinity* of *rational numbers* *arbitrarily close* to it; yet the *generic real* number is *not* rational).

Let us emphasize that the structure of this Riemann surface does *not* depend *at all* on the initial data of our problem, which indeed do *not* feature *at all* in the *nondifferential* equation (2.98) nor, of course, in (2.117). It is completely determined by the single parameter μ , which determines the number and distribution of the *square-root* branch points, see (2.103), and the value of $w(\xi)$ at the branch points, see (2.102), and in addition it fixes the character of the additional branch points occurring at $\xi = 0$ and at $\xi = \infty$: at $\xi = 0$ there is *no* branch point *at all* if $0 < \mu < 1$, there is a branch point of order $\frac{1}{\mu-1}$ if $\mu > 1$ (and the corresponding value of w is $w = 1$) and there is a branch point of order $-\frac{1}{\mu}$ if $\mu < 0$ (and the corresponding value of w is $w = 0$); while at $\xi = \infty$ there is a branch point of order $\frac{1}{\mu-1}$ if $\mu < 0$ (and the corresponding value of w is $w = 1$), there is a branch point of order $-\frac{1}{\mu}$ if $\mu > 1$ (and the corresponding value of w is $w = 0$), and there are *two* branch

points if $0 < \mu < 1$, one of order $\frac{1}{\mu-1}$ (and the corresponding value of w is $w = 1$) and the other of order $-\frac{1}{\mu}$ (and the corresponding value of w is $w = 0$). Note that the character of these branch points at $\xi = 0$ and at $\xi = \infty$ – in contrast to those occurring on the circle B , see (2.103), which are *all of square-root type* – depends on the value of the parameter μ : in particular, these branch points are of *rational type* if and only if μ is itself a *rational number*.

The time evolution of the roots $\tilde{w}_j(t) = w_j[\xi(t)]$ – the number J of which is *finite* if μ is *rational* (in which case the nondifferential equation (2.98) becomes *polynomial*, see (2.117), as discussed in detail above), and is instead *infinite* if μ is *irrational* – depends of course on the *initial data* of our problem, inasmuch as these data determine the center and the radius of the circle Ξ in the complex ξ -plane on which the point $\xi(t)$ rotates as the *real time* t evolves, see (2.99a) and (2.114). It is thus clear that the time evolution of these roots depends crucially on the relative positions of the circles Ξ and B in the *complex* ξ -plane, as well as on the property of the circle Ξ to include, or instead not to include, the central point $\xi = 0$ of the *complex* ξ -plane.

Let us merely sketch the main points here:

1. in this framework a gradual change in the initial data corresponds to a gradual modification (of the center and the radius) of the circle Ξ ;
2. the *isochronous* sector of initial data yields values of the center $\bar{\xi}$ and of the radius R of the circle Ξ small enough to guarantee that this circle be *completely enclosed* by the circle B on which the branch points are located and that moreover the center $\xi = 0$ of the *complex* ξ -plane be *outside* of the circle Ξ ;
3. the more interesting changes in the dynamical behavior of the time evolution of the roots $\tilde{w}_j(t)$ obtain when the circle Ξ crosses the circle B , and moreover (except if $0 < \mu < 1$) when it crosses the center point $\xi = 0$;
4. a *collision* of two roots $\tilde{w}_j(t)$ occurs whenever the circles Ξ crosses the circle B just at the location of a branch point, and the corresponding branch point is categorized as *active* if and only if one of the two roots involved in this collision is the *physical* one, $\tilde{w}_1(t) = \tilde{w}(t)$, otherwise it must be categorized as *inactive*: in the *active* case hitting the branch point corresponds to the occurrence of a singularity of the solution of the equations of motion of our *physical* model (2.10) due a collision of the *different*, third particle $z_3(t)$ with one of the two equal particles, $z_1(t)$ or $z_2(t)$, while in the *inactive* case there is no corresponding singularity of the solution of the equations of motion of our *physical* model (2.10);
5. likewise, if and when the value of $\xi(t)$, while traveling on the circle Ξ and crossing the circle B , happens to be *very close* to a branch point (of those sitting on the circle B);
6. and note that this certainly happens whenever μ is *irrational* and therefore these branch points sit *densely* on B), a *near miss* occurs among the time evolution of two roots $\tilde{w}_j(t)$, which, as regards the corresponding solution $z_n(t)$ of our *physical* model (2.10), entails a *near miss* in the time evolution of $z_3(t)$ and one of the other two particles, $z_1(t)$ or $z_2(t)$, if and only if the fundamental root $\tilde{w}_1(t) = \tilde{w}(t)$ is one of the two roots involved in the corresponding *near miss*;
7. if the initial data are such that the circle Ξ goes through the point $\xi = 0$, this corresponds to a multiple collision of several (indeed, if μ is not *rational*, an *infinity* of) roots $\tilde{w}_j(t)$ (but only if μ is *outside* of the *closed* interval $0 \leq \mu \leq 1$), and correspondingly there occurs a *three-body* collision in the time evolution of our *physical* model (2.10) if one of these roots is the *physical* root $\tilde{w}(t)$;

8. and likewise if the initial data are such that $\xi(t)$, while traveling on the circle Ξ , happens to be *very close* to the point $\xi = 0$, then the corresponding solution of our *physical* model (2.10) experiences a *triple near miss* (but, of course, again only if μ is *outside* of the *closed* interval $0 \leq \mu \leq 1$, and only if the fundamental root $\tilde{w}_1(t) = \check{w}(t)$ is one of those involved in the multiple root collision).

Clearly, to achieve a full, *quantitative* understanding of the time evolution of our *physical* problem (2.10) – namely, a solution of its initial-value problem – the following questions should be answered, for any given set of initial data: is the motion going to be *singular*, *completely periodic*, *multiply periodic* or *aperiodic*; if *singular*, what kind of *particle collision* is responsible for the *singularity*, and *when* does it happen; if it is *periodic*, then what is its *period* \check{T} ; and, if this period is very large, for instance $\check{T} = \check{j}T$ with \check{j} a *very large* integer, can one also provide some information on the behavior of the system at intermediate times, say at the times $t_k = kT$, $k = 1, 2, \dots, \check{j} - 1$; and likewise, when the motion is *aperiodic*, can one provide a specific prescription to compute the particle positions, if perhaps not at every future time (which clearly would be a somewhat extreme request, especially when the motion provides an instance of some kind of *chaotic* behavior: see Chapters 3 and 4), at least at a discrete set of future times, for instance at the times $t_k = kT$, $k = 1, 2, 3, \dots$. The answer to some of these questions has already been given by the various explanations provided above; answered and still-unanswered questions are all addressed in the next two chapters.

CHAPTER 3

The Riemann Surface

In this chapter we focus our attention on the *nondifferential* equation (2.98)

$$(w - 1)^{\mu-1} w^{-\mu} = \xi$$

which defines the (multi-valued) function $w \equiv w(\xi)$. In the previous chapter we showed that the solutions of the three-body problem (2.10), in the semisymmetrical case (2.2), can be written in terms of the function $\check{w}(t) = w(\xi(t))$, where the variable ξ evolves in time following (2.99a).

In this chapter we start the analysis of the structure of the Riemann surface Γ associated to (2.98) for a *generic* variable ξ , evolving on a *generic* (usually *closed*) path on the complex ξ -plane and only after that we come back in our presentation to the geometrical consequences of the *physical* evolution (2.99a). We will finally choose the physical path defined by (2.99a) at the beginning of the next Chapter 4, where we study the main implications of the findings reported in this chapter.

It turns out that the equation (2.98) describes an *algebraic* curve in the case of a *rational* value of $\mu = p/q$ (namely, it is sufficient that both the coupling constants f and g are *rational* numbers, see (2.25) and (2.26)). We will describe the case with *irrational* μ (given by *irrational* values of f and g) taking an appropriate limit of the case with *rational* μ . Moreover in the analysis we distinguish between the three basic cases $\mu < 0$, $0 < \mu < 1$ and $\mu > 1$, as implied by (2.73), (2.75), (2.77) and the analysis reported in the following Subsection 2.4.2.

To study the structure of the Riemann surface Γ , we make use of various techniques, from *topology*, to *algebraic geometry*, from *number-theory* to *graph theory* and *combinatorics*, achieving, at least in the case with *rational* μ , to reconstruct and to describe a subset of the monodromy group associated to (2.98). We also describe a remarkable example for the (*quadratic*) *irrational* value $\mu = \frac{2}{3+\sqrt{5}}$, in which a machinery of *simple continued fraction theory* and *Fibonacci's numbers* is involved and makes possible to give an explicit asymptotic result about the periodicity of the roots of (2.98) for a certain (physical) choice of closed ξ -paths.

In the final chapter we will see how the knowledge gained in this Chapter 3 on the Riemann surface Γ will open the way to a more complete understanding of the physical complex dynamics generated by the simple three-body problem described in this work.

3.1 The case $0 < \mu < 1$

Here we study the Riemann surface Γ consisting of points $(\xi, w) \in \Gamma$ such that:

$$w^{-\mu}(w-1)^{\mu-1} = \xi, \quad (3.1)$$

where

$$\mu \in \mathbb{Q} \quad \text{and} \quad 0 < \mu = \frac{p}{q} < 1$$

and $p \in \mathbb{N}$ and $q \in \mathbb{N}^+$ are coprime natural numbers. Therefore Γ is an *algebraic* Riemann surface characterized by the polynomial (of degree q) equation

$$(w-1)^{q-p}w^p\xi^q = 1, \quad 0 < p < q \quad (3.2)$$

which defines the q -valued function $w = w(\xi)$. Since, $\forall \xi \in \mathbb{C}$, the polynomial (3.2) admits q complex roots and each root corresponds to a sheet of the Riemann surface Γ , it follows that Γ is a q -sheeted covering of the complex ξ plane.

3.1.1 The Riemann surface and its singularities

The Riemann surface Γ possesses the following distinguished points.

1) $\xi \sim \infty$. If $|\xi| \gg 1$, there are two different asymptotics:

$$\begin{aligned} w(\xi) &\sim -(-\xi)^{-\frac{q}{p}}, \quad \xi \sim \infty, \\ w(\xi) &\sim 1 + \xi^{-\frac{q}{q-p}}, \quad \xi \sim \infty. \end{aligned} \quad (3.3)$$

Therefore the ∞ -*configuration* consists of p roots lying on a small circle of radius $O(|\xi|^{-\frac{q}{p}})$ around the origin, and of $(q-p)$ roots lying on a small circle of radius $O(|\xi|^{-\frac{q}{q-p}})$ around 1 (see Figure 3.1). From the point of view of the Riemann surface, we see that, at $\xi = \infty$, the branch point $(\infty, 0)$, of order $(p-1)$, attaches p sheets and the branch point $(\infty, 1)$, of order $(q-p-1)$, attaches $(q-p)$ sheets.

2) In the finite part of Γ there are only q square root branch points (SRBPs):

$$(\xi_b^{(j)}, \mu) \in \Gamma, \quad j = 1, \dots, q, \quad (3.4)$$

defined by the equation:

$$\xi^q = \frac{(-)^{q-p}q^q}{p^p(q-p)^{q-p}}. \quad (3.5)$$

Therefore the *SRBP configuration* consists of q SRBPs lying on the circle centered at the origin and of radius

$$r_b = \frac{q}{q-p} \left(\frac{q-p}{p} \right)^{\frac{q}{q-p}} > 0; \quad (3.6)$$

here we use the positive principal determination. We find it convenient to order them in a sequential and counterclockwise way (see Figure 3.2); a convenient choice of the first SRBP $\xi_b^{(1)}$, clearly arbitrary at this stage, is suggested by the direct problem and will be discussed in the following sections. Each SRBPs corresponds to the collision of a pair of roots.

The genus of Γ is 0; this is an immediate consequence of the Hurwitz formula (see [61])

$$V = 2(J + G - 1), \quad (3.7)$$

where V is the ramification index of the surface, J is the number of sheets and G is its genus. In our case: $J = q$ and $V = q + (q-p-1) + (p-1)$, entailing $G = 0$.

Equation (3.2) exhibits several symmetries. The ones used here are:

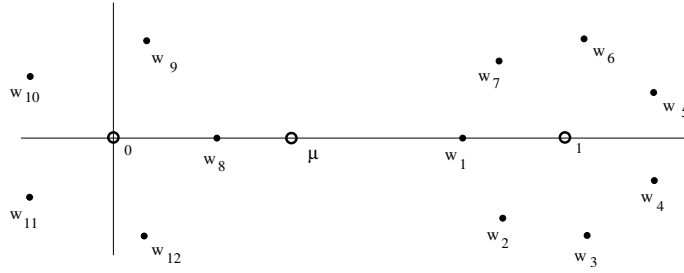


Figure 3.1: The basic configuration of roots, for $\xi \in \gamma_1$, $|\xi| \gg 1$, for the Riemann surface $q = 12$, $p = 5$.

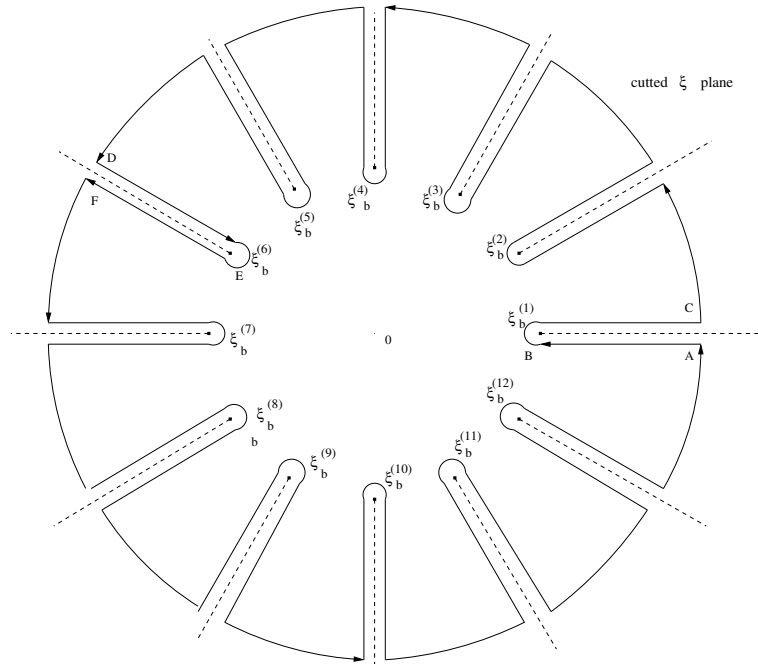


Figure 3.2: The cutted ξ -plane of the Riemann surface $q = 12$, $p = 5$ is the interior of the oriented contour γ .

1. *Symmetry under a $2\pi/q$ rotation.* The set of roots is left invariant by a $2\pi i/q$ rotation in the ξ plane.
2. *Symmetry along the cuts.* Consider the rays γ_j , $j = 1, \dots, q$ defined by

$$\gamma_j = \{\xi, \arg \xi = \arg \xi_b^{(j)}, |\xi| \geq |\xi_b^{(j)}|\}, \quad j = 1, \dots, q. \quad (3.8)$$

Then, if $\xi \in \gamma_j$, $j = 1, \dots, q$, two of the q roots lie on the segment $(0, 1)$. If, in addition, $|\xi| \gg 1$, then one of these two roots belongs to the small circle around the origin and the other one belongs to the small circle around 1 (see Figure 3.1). We call this configuration *the basic configuration*.

3.1.2 Defining a new congruence operation

For reasons that will be clearer soon, we will introduce the $\tilde{\text{MOD}}$ operation, which is operatively defined by:

$$a \tilde{\text{MOD}} b = \begin{cases} a \text{ MOD } b & \text{if } a \text{ MOD } b \neq 0 \\ b & \text{if } a \text{ MOD } b = 0 \end{cases}, \quad (3.9)$$

for all positive integers a and b . Note that $\tilde{\text{MOD}}$ consists in a little deformation of the usual definition of the MOD operation on integers. We will use the elements of the ring obtained as the quotient set of \mathbb{Z} with respect to the congruence $\tilde{\text{MOD}} q$ for any further labelling or enumerative operation. This will avoid, for example, to use a 0 to identify the q -th root of the algebraic equation.

3.1.3 Roots dynamics and topological properties

To understand the topological properties of the Riemann surface Γ , we first cut the ξ -complex plane along the rays γ_j , $j = 1, \dots, q$, from the SRBPs $\xi_b^{(j)}$ to the branch point at ∞ , and we introduce the closed contour γ whose interior is such a cutted ξ -plane (see Figure 3.2). It is worth noting that in Subsection 3.1.4 we will slightly modify the labelling of the SRBPs, introducing a double index system. Our goal is to construct the q images \mathcal{I}_j , $j = 1, \dots, q$ of the cutted ξ -plane, through the q roots $w_j(\xi)$, $j = 1, \dots, q$ and to study their connections.

Our strategy will be to start from the basic configuration, applicable for $|\xi| \gg 1$, and to map out the structure of the Riemann surface as ξ is moved in along rays and it is moved around along circles.

Starting with $\xi \in \gamma_j$, it is natural to call w_j the root lying on the segment $(0, 1)$ and belonging to the small circle around 1. Then $w_{j+1}, \dots, w_{j+q-p-1}$ are the other roots of this circle ($\tilde{\text{MOD}} q$), enumerated in sequential and counterclockwise order. Analogously, we denote by w_{j+q-p} the root lying on the segment $(0, 1)$ and belonging to the small circle around 0; and by $w_{j+q-p+1}, \dots, w_{j+q-1}$ the other roots of this circle ($\tilde{\text{MOD}} q$), enumerated in sequential and counterclockwise order (see Figure 3.1).

Using the large ξ asymptotics (3.3) and the above basic symmetries of Γ , we infer the following basic motions.

- 1) As ξ moves along the cut γ_j , from ∞ to $\xi_b^{(j)}$, the two roots w_j and $w_{j+q-p} \tilde{\text{MOD}} q$, lying on the segment $(0, 1)$, move along it, from the small circles around 0 and 1 to the collision point μ . In addition, being $\xi_b^{(j)}$ a branch point of square root type, a 2π rotation of ξ around it corresponds to a π rotation of these two roots around μ . All this implies that, if ξ travels along the contour surrounding the cut γ_j as in Figure 3.3, then the two roots w_j and $w_{j+q-p} \tilde{\text{MOD}} q$ involved in the collision *exchange their position* (see Figure 3.4). The remaining roots are essentially not affected by this motion, moving back and forth on lines and going back to their starting positions. We have established the first basic motion:

$$\boxed{\begin{array}{l} \xi\text{-motion around} \\ \text{the branch cut } \gamma_j \end{array}} \iff \boxed{\begin{array}{l} \text{cyclic permutation of the two} \\ \text{roots } \{w_j, w_{q-p+j}\} \tilde{\text{MOD}} q. \end{array}}$$

- 2) If, starting from the cut γ_j , ξ has a $2\pi/q$ counterclockwise rotation on a big circle, from the cut γ_j to the cut γ_{j+1} , then the $(q-p)$ roots surrounding 1 have a clockwise rotation around 1, while the p roots surrounding 0 have a clockwise rotation around 0. When ξ reaches γ_{j+1} , two new roots belonging to the two small circles get aligned on the segment $(0, 1)$; they are just w_{j+1} and $w_{j+1+q-p} \tilde{\text{MOD}} q$ (see Figure 3.5). Therefore the two sets of roots undergo *cyclic permutations*, which is the second basic motion:

$$\boxed{\begin{array}{l} \xi - \text{rotation} \\ \text{from } \gamma_j \text{ to } \gamma_{j+1} \end{array}} \iff \boxed{\begin{array}{l} \text{cyclic permutation of the two sets} \\ \{w_1, \dots, w_{q-p}\}, \{w_{q-p+1}, \dots, w_q\} \tilde{\text{MOD}} q. \end{array}}$$

Repeating q times the above two motions with respect to the other cuts, in sequential order, the point ξ draws the whole closed contour γ . Correspondingly, due to the above

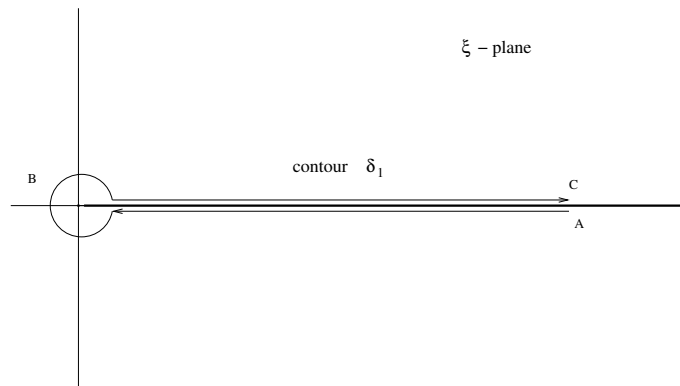


Figure 3.3: The contour surrounding the cut γ_1 .

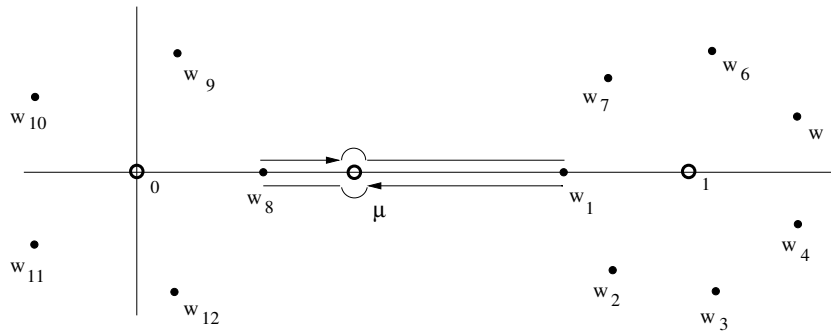


Figure 3.4: Exchange of a pair of roots. As ξ travels on the contour surrounding the cut γ_j , as in Figure 3.3, w_j and w_{j+q-p} interchange their positions, while the other $(q-p)$ roots are essentially not affected by this motion.

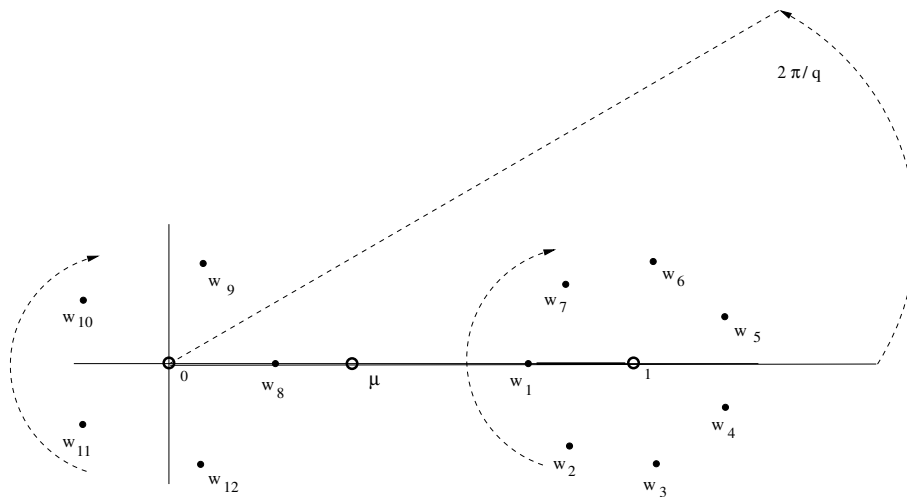


Figure 3.5: Cyclic permutation of the two groups of roots. If $\xi \in \gamma_j$, the roots w_j and w_{j+q-p} are aligned on the segment $(0, 1)$; after a $2\pi/q$ counterclockwise rotation of ξ on a big circle, the two groups of roots $\{w_j, \dots, w_{j+q-p-1}\}$ and $\{w_{j+q-p-1}, \dots, w_{j+q-1}\}$ undergo a clockwise rotation. When ξ reaches γ_{j+1} , then the roots w_{j+1} and $w_{j+1+q-p}$ get aligned on the segment $(0, 1)$.

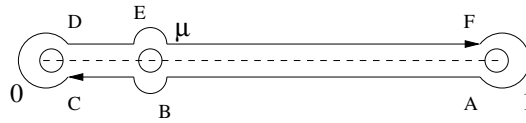
cutted w - plane

Figure 3.6: As ξ draws the closed contour γ in Figure 3.2, each root draws a closed contour around the cut $(0, 1)$ in the w -plane. Therefore the image of the cutted ξ plane is the w plane cutted along the segment $[0, 1]$.

basic motions and symmetries, each root w_j draws the closed contour in Figure 3.6 around the cut $[0, 1]$ of the w -plane, with the following details, which can be easily understood comparing Figure 3.2 and Figure 3.6.

- i) As ξ moves on γ through the points A, B and C , around the cut γ_j , w_j moves along the cut $[0, 1]$ through the homologous points, exchanging its position with the root $w_{j+q-p} \text{ MÖD } q$.
- ii) As ξ moves on γ from C to D , the relevant part of the motion of w_j consists in a clockwise rotation around 0, from C to D .
- iii) As ξ moves on γ through the points D, E and F , around the cut γ_{j-q+p} , w_j moves along the cut $[0, 1]$ through the homologous points, exchanging its position with the root $w_{j-q+p} \text{ MÖD } q$.
- iv) As ξ completes the contour γ , moving from F to the starting point A , also w_j completes its closed contour around $[0, 1]$, and the relevant part of this motion consists in a clockwise rotation around 0, from F to A .

From the above considerations we finally infer the following

Topological properties of Γ . *The Riemann surface Γ is a q - sheeted covering of the ξ - plane of genus 0. In the finite part of Γ there are q square root branch points: $(\xi_b^{(j)}, \mu) \in \Gamma$, $j = 1, \dots, q$; the j -th branch point connects the sheets \mathcal{F}_j and \mathcal{F}_{j+q-p} , and each sheet \mathcal{F}_j contains just the two square root branch points $(\xi_b^{(j)}, \mu)$ and $(\xi_b^{(j-q+p)}, \mu)$ (see Figure 3.7). The compactification of Γ is achieved at $\xi = \infty$, where the branch point $(\infty, 1)$, of order $(q - p - 1)$, connects the first $(q - p)$ sheets, and where the branch point $(\infty, 0)$, of order $p - 1$, connects the remaining p sheets. As ξ turns in a counterclockwise way around $(\infty, 1)$, the connected sheets are visited in the order: $\mathcal{F}_j, \mathcal{F}_{j+p}, \mathcal{F}_{j+2p}, \dots$; as ξ turns in a counterclockwise way around $(\infty, 0)$ instead, the connected sheets are visited in the order: $\mathcal{F}_j, \mathcal{F}_{j+q-p}, \mathcal{F}_{j+2(q-p)}, \dots$. All the above indices are defined $\text{MÖD } q$.*

As an illustrative example, the Riemann surface $q = 12, p = 5$ is drawn in Figure 3.8.

3.1.4 Branch points enumeration

Starting from the results obtained in the previous paragraphs, in what follows we will describe an algebro-combinatoric method to predict the period of a single root of the algebraic equation (3.2) as ξ moves periodically along a closed path on the branched ξ -plane. For this purpose, we need to introduce a change in the labelling of the branch points with respect to what we described previously.

$\xi_b^{(1)}$	$\mathcal{F}_1 \longleftrightarrow \mathcal{F}_{q-p+1}$
$\xi_b^{(2)}$	$\mathcal{F}_2 \longleftrightarrow \mathcal{F}_{q-p+2}$
\cdot	\cdot
\cdot	\cdot
\cdot	\cdot
$\xi_b^{(q-p)}$	$\mathcal{F}_p \longleftrightarrow \mathcal{F}_q$
$\xi_b^{(q-p+1)}$	$\mathcal{F}_{p+1} \longleftrightarrow \mathcal{F}_1$
\cdot	\cdot
\cdot	\cdot
\cdot	\cdot
$\xi_b^{(q-1)}$	$\mathcal{F}_{q-1} \longleftrightarrow \mathcal{F}_{q-p-1}$
$\xi_b^{(q)}$	$\mathcal{F}_q \longleftrightarrow \mathcal{F}_{q-p}$

Figure 3.7: The table summarizing the connection rules of the Riemann surface. The sheets \mathcal{F}_j is connected with the sheet $\mathcal{F}_{j+q-p} \text{ MÖD } q$ at the SRBP $\xi_b^{(j)}$. The sheets \mathcal{F}_j is connected with the sheet $\mathcal{F}_{j-q+p} \text{ MÖD } q$ at the SRBP $\xi_b^{(j-q+p)}$.

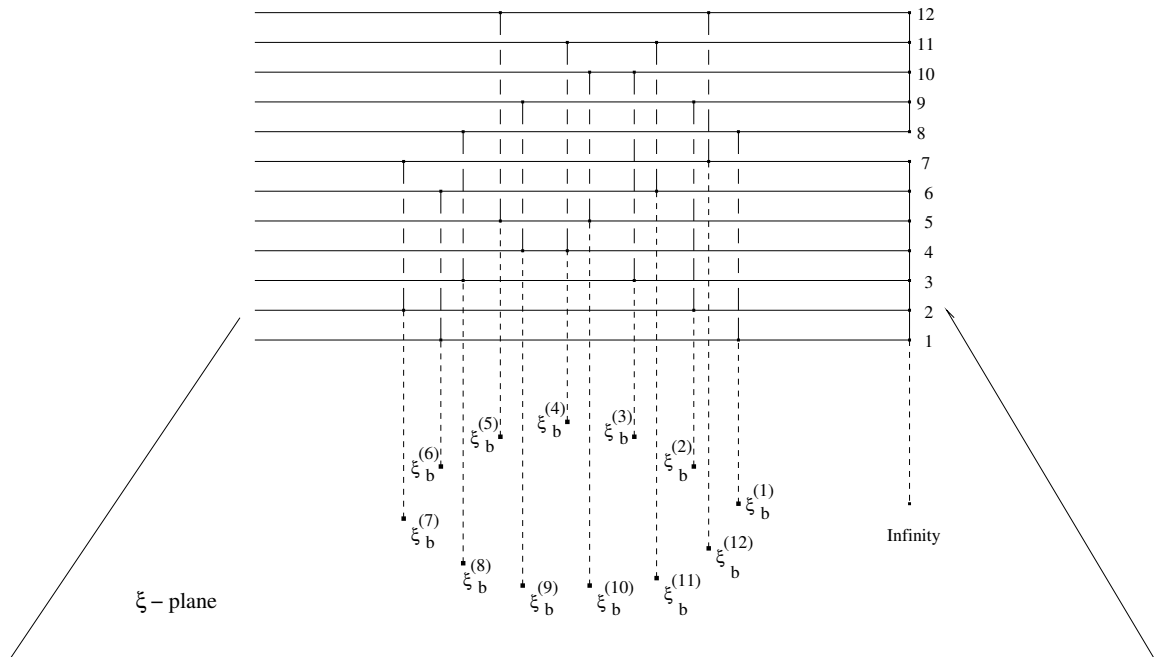


Figure 3.8: The topological properties of Γ for $q = 12$ and $p = 5$.

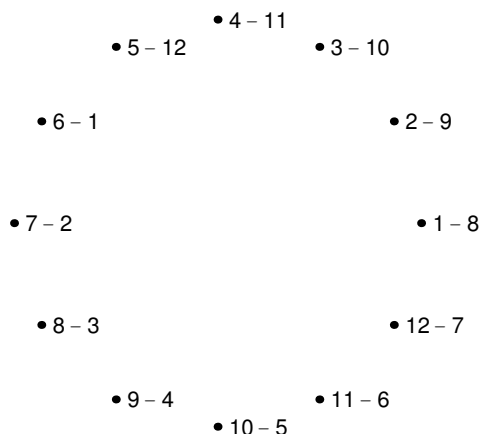


Figure 3.9: Branch points double indexes ($p = 5$, $q = 12$)

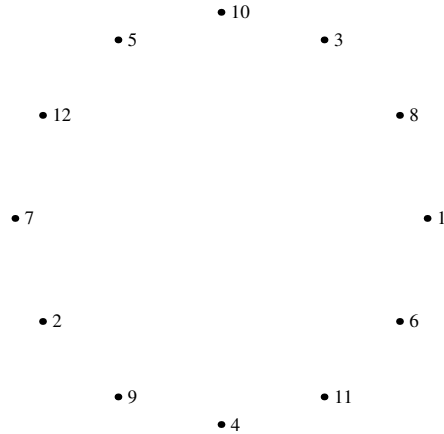
In what follows, to label the branch points, we will use a double index. To start the enumeration, pick arbitrarily one of the q square root branch points. Then, beginning from the chosen one, apply a double index to each branch point, so that the first indexes are the consecutive natural numbers (anti-clockwise), while the second ones are the consecutive natural numbers $\text{M}\ddot{\text{O}}\text{D } q$, starting from $q-p+1$ (anti-clockwise). In this way, we reconstruct the connections between the sheets of the Riemann surface as described in Subsection 3.1.3: each label gives the two sheets which are connected by the corresponding branch point (for instance, look at the situation in Figure 3.9, where $p = 5$ and $q = 12$).

3.1.5 Graph Theory and Monodromy Group

Now that we have a labelling system for the SRBPs and the connection rules for the sheets of the Riemann surface, we can use some graph theory to describe the monodromy group associated to the w -roots system. Summarizing, the monodromy group is the group of transformations which acts on a certain systems of roots of an algebraic equation when the independent variable (ξ in our case) moves, for an integer number of times, along a closed path on the corresponding Riemann Surface (in such a way that it includes a certain - finite or infinite - number of branch points). If the system of roots is composed by q roots, the monodromy group is a subgroup of the permutation group \mathcal{S}_q .

Since in our physical problem ξ can move only on a circular path (the circle Ξ), you can easily convince yourselves that such path can make inclusion only of consecutive (adjacent) branch points on B (the circle where the SRBPs lie). So, for our purposes, it is convenient to study only the cases in which the ξ -path (i.e. the path along which ξ moves) includes consecutive branch points.

To each (mutual) disposition of the ξ -path and B , the circle of the SRBPs, we can associate a planar graph. To construct it, just trace q nodes corresponding to the q sheets of the Riemann Surface on a regular polygon. Now, label these nodes, starting from an arbitrarily chosen one (anti-clockwise). The first node will receive the number 1: $l_1 = 1$, where l_j is the label of the j -th node of the graph. The labels of the following nodes (anti-clockwise) will be given by the following rule: $l_{j+1} = (l_j + q - p) \text{M}\ddot{\text{O}}\text{D } q$, $j = 1, \dots, q - 1$, where $\text{M}\ddot{\text{O}}\text{D}$ is the operation introduced in Subsection 3.1.2 (see Figure 3.10). The reason for such a weird labelling of the nodes is justified by the fact that in this way the edges of the graph will be traced more easily.

Figure 3.10: Nodes labelling ($p = 5, q = 12$).

If the ξ -path will include, among the others, the branch point labelled $\{h, (h + q - p) \text{ M}\ddot{\text{O}}\text{D } q\}$, with $h = 1, \dots, q$, we will connect with an edge the nodes labelled respectively h and $(h + q - p) \text{ M}\ddot{\text{O}}\text{D } q$ in the graph. For example, in Figure 3.11, you can see all the possible graph that one can obtain including an increasing number of consecutive branch points inside the ξ -path (up to $q - 1$ branch points), starting from the branch point $\{1, (q - p + 1)\}$, when $p = 5$ and $q = 12$.

Note that the highest degree of connection is obtained when exactly $q - 1$ branch points are included inside the ξ -path. In fact, from the general theory described in the previous sections, we already know that, an inclusion of exactly q SRBPs inside the ξ -path is equivalent to the inclusion of the branch point at infinity, so the period of the zeros will be $q - p$ or p (see (3.3)). Furthermore, in this case, the first $q - p$ roots have period $q - p$ and the last p roots have period p .

From now on, we will concentrate only on the case of the inclusion of consecutive square root branch points inside the ξ -path, starting from the branch point $\{1, (q - p + 1)\}$, with a maximum of $q - 1$ branch points included.

How to interpret the graphs? We will call *line* a path on the graph made of connected edges. If, for a certain situation of branch points inclusion, on the corresponding graph the j -th node is contained in a line which connects exactly b nodes, the period of the corresponding j -th w -root of the algebraic equation (3.2), $w_j(\xi)$, while ξ moves along the closed path, will be exactly b . We define *degree of connection* of the j -th node as the number of nodes connected by the line passing through the j -th node. If the j -th node is unconnected (i.e. it is touched by no edge), the period of $w_j(\xi)$ will be 1.

So, for a certain situation of branch points inclusion, we are interested in measuring the lengths of the lines in the corresponding graph. For such a graph with q nodes (considered at the moment without labels), the set of all the lengths of these lines corresponds to an element of \mathcal{S}_q / \sim , where the equivalence relation \sim is introduced identifying two elements of \mathcal{S}_q if they have the same lengths of the corresponding decompositions in cycles.

For instance, look at the first image on the right column of Figure 3.11. In this situation, it is clear that w_7 has period 1; $w_2, w_3, w_4, w_5, w_9, w_{10}, w_{11}$ and w_{12} have period 2; w_1, w_6 and w_8 have period 3. Precisely, this situation corresponds to the permutation $(1, 6, 8)(2, 9)(3, 10)(4, 11)(5, 12)(7)$, namely a permutation with 1 cycle of length 3, 4 cycles of length 2 and 1 cycle of length 1 (it is sometimes useful to describe this in terms of integer partitions of q : $12 = 3 + 2 + 2 + 2 + 2 + 1$). So, our graph is in correspondence with all the permutations in \mathcal{S}_q that can be written as 1 cycle of length 3, 4 cycles of length 2 and 1 cycle of length 1. The permutation $(1, 6, 8)(2, 9)(3, 10)(4, 11)(5, 12)(7)$ is an element of the

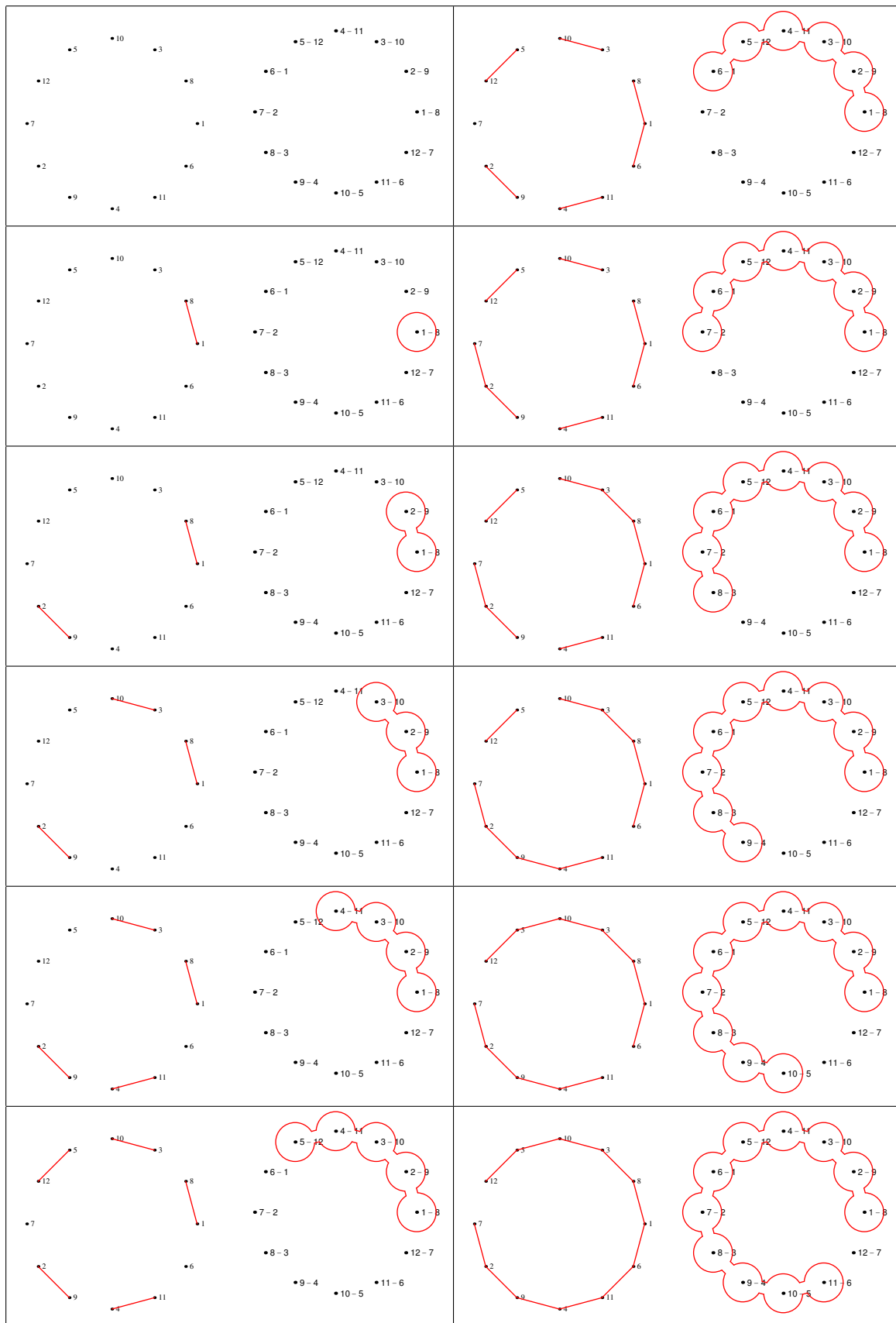


Figure 3.11: Consecutive branch points inclusions ($p = 5, q = 12$).

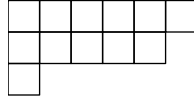


Figure 3.12: Ferrer diagram corresponding to the inclusion of 6 consecutive branch points ($p = 5, q = 12$).

monodromy group. If we do not limit ourselves to consider consecutive inclusions of branch points inside the ξ -path, with this technique we can build the complete monodromy group.

Through this link with the permutation group, we can give a more synthetic description of a graph using Ferrer diagrams, namely Young tableaux without numbers. In our case, a Ferrer diagram is a disposition of q blank boxes in rows and columns, such that the number of boxes in each column is equal to the length of the single cycle of the corresponding permutation and the number of columns is the number of cycles in which the permutation is decomposed (for instance, to the situation illustrated by the first image on the right column of Figure 3.11, there corresponds the Ferrer diagram contained in Figure 3.12).

Since the lines in the graph represent the various cycles of the corresponding permutation and the heights of the boxes in the columns of a Ferrer diagram represent the lengths of the lines in the corresponding graph, we thereby reduced the problem of knowing the period of a root of the equation (3.2), while ξ moves along a closed path, to the measure of one of the columns of an appropriate Ferrer diagram.

3.1.6 The bumping rule

In the previous Section we showed that, for fixed p and q , a particular Ferrer diagram corresponds to each situation of inclusion of branch points inside a ξ -path. We reduced the problem of knowing the period of the w -roots to finding the degree of connection of the single nodes of a certain graph; from this we reduced once more the problem to knowing the length of the columns of the corresponding Ferrer diagram.

The next step will be to understand how to recursively build such Ferrer diagrams. To do this we introduce a *bumping rule* for the boxes which compose the diagram itself. Once p and q are fixed, such a rule will describe how a Ferrer diagram associated to the inclusion of b branch points inside the ξ -path will change after the introduction of one more branch point, namely, when the ξ -path includes $b + 1$ branch points.

First of all, we need two sequences:

$$q_k = p_{k-1} , q_0 = q \tag{3.10}$$

$$p_k = q_{k-1} \text{ MOD } p_{k-1} , p_0 = q - p , \tag{3.11}$$

with $0 \leq k \leq \bar{k}$, for a certain fixed number \bar{k} such that

$$q_{\bar{k}} = 1 ; \tag{3.12}$$

notice that \bar{k} always exists due to the decreasing nature of the sequence $\{q_k\}$. We need also an auxiliary recursive sequence, written as a combination of the previous two,

$$b_k = b_{k-1} + q_{k-1} - p_{k-1} , b_0 = 0 . \tag{3.13}$$

Notice that the use of two different sequences in (3.10) is completely redundant, and one can easily reduce these formulas to expressions which involve the use of only one of them. We will come back on this point later, but at the moment we will keep this formulation for the sake of simplicity. Let us just notice two facts:

- 1) the b -sequence (3.13) divides the discrete segment $[1, q - 1]$ into \bar{k} parts of length $q_k - p_k$;

- 2) inserting the first of the (3.10) in the recursion (3.13) and using this last relation recursively, one gets

$$\begin{aligned}
 b_0 = 0, \quad b_k &= b_{k-1} + q_{k-1} - q_k = b_{k-2} + q_{k-2} - q_{k-1} + q_{k-1} - q_k \\
 &= b_{k-2} + q_{k-2} - q_k = \dots = b_{k-h} + q_{k-h} - q_k \\
 &= b_0 + q_0 - q_k = q - q_k.
 \end{aligned} \tag{3.14}$$

Now, let us fix a ξ -path which includes b branch points starting from the one labelled $\{1, (q-p+1)\}$. If we modify the ξ -path in such a way that it includes the next adjacent branch point, $\{b+1, (b+1+q-p) \text{ MÖD } q\}$, we must modify also the graph corresponding to the previous situation, adding a new edge between the two nodes $(b+1)$ and $(b+1+q-p) \text{ MÖD } q$. If $0 \leq b < b_1 - 1 = q - p - 1$, then each new edge added to the graph will evidently connect a single unconnected node to a line composed by a certain number of edges (at least, to another single unconnected node). When $b = b_1 - 1$, it is impossible to trace a new edge connecting two unconnected nodes or a single node to a line: the insertion of a new edge in a graph at this point will cause the connection of two lines, producing a new longer line in the graph. To understand how to go on with this picture, imagine to build a new auxiliary graph in the following way: associate to our graph a new one, for any line of the first graph you have a weighted node in the second one, with weights equal to the lengths of the lines. We can now proceed increasing the value of b , namely with $b_1 \leq b < b_2 - 1$, using the new described graph analogously to what we have done in the case $0 \leq b < b_1 - 1$, with the only difference that the length of a line in this new graph is not just the number of nodes touched by the line, but the sum of all the weights of the nodes touched by the line. If $b_1 \leq b < b_2 - 1$, then each new edge added to the new auxiliary graph will evidently connect a single unconnected weighted node to a weighted line composed by a certain number of edges (at least, to another single unconnected weighted node). If $b = b_2 - 1$, it is impossible to trace a new edge connecting two unconnected weighted nodes or a single weighted node to a weighted line: the insertion of a new edge in the new graph at this point will cause the connection of two weighted lines, producing a new longer line in the auxiliary graph. To proceed, we must build a new auxiliary graph, in the same way described before. And so on, building a new auxiliary graph every time we arrive to include exactly b_k branch points inside the ξ -path, until we reach $b = q - 1$. The number of consecutive branch points we must move to pass from a situation of b_k branch points included in the ξ -path to a situation of b_{k+1} branch points included in the ξ -path is $q_k - p_k$. In this language q_k is the number of weighted nodes of the graph on which we work when $b_k \leq b < b_{k+1}$, while p_k is the number of weighted nodes of the new auxiliary graph we will build when exactly b_{k+1} branch points will be included.

The use of Ferrer diagrams strongly simplifies this picture. First of all we need two technical definitions (actually, the second one will not be used immediately).

- 1) The *height* of a column in a Ferrer diagram is the number of boxes which lies in the column.
- 2) For each k between 0 and \bar{k} we have a Ferrer diagram with only two possible heights for the columns: these Ferrer diagrams will have totally q_k columns, p_k tallest columns, all composed by the same number of boxes, and $q_k - p_k$ equal columns with height less or equal the height of the previous ones. Each of these diagrams corresponds to the inclusion of exactly b_k branch points. A *k-level Ferrer diagram* is a Ferrer diagram with exactly q_k columns.

When $b = b_k$, the heights of the columns of the corresponding Ferrer diagram represent the values of the weights of the nodes of the corresponding weighted graph (a graph with

weighted nodes). When $b_k < b < b_{k+1}$, the heights of the columns of the corresponding Ferrer diagrams represent the lengths of the weighted lines in the corresponding weighted graphs. When $b = b_k$, we will observe only two kinds of weights, since in the $(k - 1)$ -th auxiliary graph we connected in pairs all the nodes, with the exception of the last one of them, which remained unconnected. The latter will be the first one appearing in a connection at the moment of the inclusion of one more branch point inside the ξ -path. In terms of Ferrer diagrams, this means that, sorting the columns of the diagram in decreasing order of height from left to right, we must move each time the shortest column on the right under the tallest available column on the left. Accordingly to what we said at the end of the previous paragraph, q_k is the number of columns in a Ferrer diagram when $b = b_k$, while p_k is the number of columns that the Ferrer diagram will have when $b = b_{k+1}$. So, for each value of k , we can move the short columns on the right *only* under the first p_k tallest column on the left; for each k , we must move globally $q_k - p_k$ columns.

All the above considerations lead to the following proposition.

The bumping rule. *The Ferrer diagram, corresponding to the inclusion of b consecutive branch points inside the ξ -path, can be obtained from the Ferrer diagram, corresponding to the inclusion of $b - 1$ consecutive branch points inside the ξ -path, moving its whole last right column to a lower position, in order to increase the height of one of the first columns (while the total amount of boxes still remains the same): such column is the first available one from the left before the p_j -th column, where j refers to the element of the sequence (3.13) which satisfies the relation $b_j \leq b < b_{j+1}$. If all the first p_j columns are occupied, the process starts again moving the last column on the right under the first column on the left.*

It is worth stressing here again that we are focalizing only on the case in which we are including consecutive branch points, and the first branch point included in the ξ -path is the branch point $\{1, (q - p + 1)\}$, with a maximum of $q - 1$ branch points included.

Let us see some graphical examples to understand how the bumping rule works. We pass from a k -level Ferrer diagram to a $(k + 1)$ -level Ferrer diagram once we have moved all the shortest columns under the tallest ones. The bumping rule says how to pass, including consecutively branch point after branch point, from one configuration to another.

See for instance the next table and Figure 3.14a where are displayed the values for the quantities b , number of consecutive branch points included in the ξ -path, b_k , q_k , p_k and the corresponding Ferrer diagrams.

b	k	$b - b_k$	q_k	p_k	b	k	$b - b_k$	q_k	p_k
0	0	0	12	7	6	1	1		
1	0	1			7	2	0	5	2
2	0	2			8	2	1		
3	0	3			9	2	2		
4	0	4			10	3	0	2	1
5	1	0	7	5	11	4	0	1	0

In Figure 3.13, you can see two usual bumping situations, comparing a wrong bumping (on the left) and the correct one (on the right) for two choices of p and q .

We can describe by a recursive rule also the height of the two kinds of columns of the k -level Ferrer-diagram. Denote by $T_k^{(1)}$ and $T_k^{(2)}$ respectively the height of the first p_k columns and the height of the last $q_k - p_k$ columns. We have that:

$$\begin{cases} T_k^{(1)} p_k + T_k^{(2)} (q_k - p_k) = q_0 & , \quad T_0^{(1)} = 1 \\ T_{k+1}^{(1)} = T_k^{(1)} + T_k^{(2)} \left(\left\lfloor \frac{q_k}{p_k} \right\rfloor + 1 \right) & , \quad T_0^{(2)} = 1 , \end{cases} \quad (3.15)$$

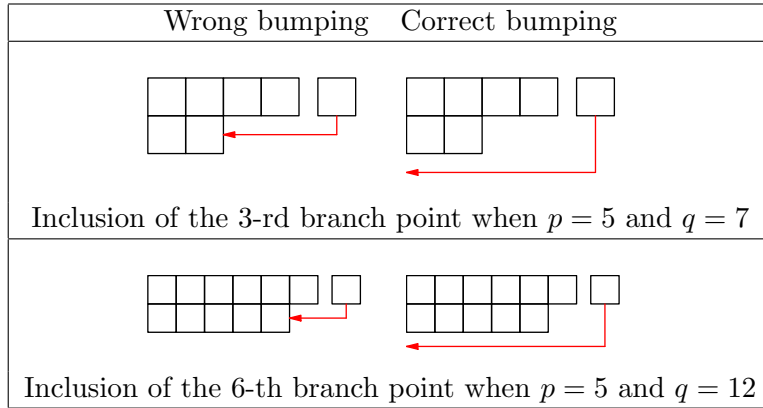


Figure 3.13: Wrong bumpings *vs* Correct bumpings

where $\lfloor x \rfloor$ is the floor of the number x . Indeed, the first of the (3.15) is a sort of conservation rule for the number of boxes in a Ferrer-diagram at each level k . The second of the (3.15) comes directly from the bumping rule: at each level, the height of the first column is the sum of the height it had at the previous level plus the height of the last column multiplied a certain number of times, proportional to the number of operations needed to move between the two considered levels.

Although the relations (3.15) are enough to determine the two quantities $T^{(1)}$ and $T^{(2)}$, it will be better to put them in a different form:

$$\begin{cases} T_{k+1}^{(1)} = T_k^{(1)} + T_k^{(2)} \left(\left\lfloor \frac{q_k}{p_k} \right\rfloor + 1 \right) & , \quad T_0^{(1)} = 1 , \\ T_{k+1}^{(2)} = T_k^{(1)} + T_k^{(2)} \left(\left\lfloor \frac{q_k}{p_k} \right\rfloor \right) & , \quad T_0^{(2)} = 1 ; \end{cases} \quad (3.16)$$

as you can see, these relations are almost identical to the (3.15) (indeed, it is possible to obtain the ones from the others), except for the fact that the (3.16) are two-steps-recursive relations. Via these last formulas, the link between the Ferrer-diagrams and the continued-fraction expansion of the number $\frac{1}{1-\mu}$ that we are going to present in the next section will be more clear .

3.1.7 Link with the Continued Fractions Theory

Let us remind some basic notions about simple continued fractions. Be x a non-negative real number. We associate to the real number x an integer sequence $\{a_k\}$ such that:

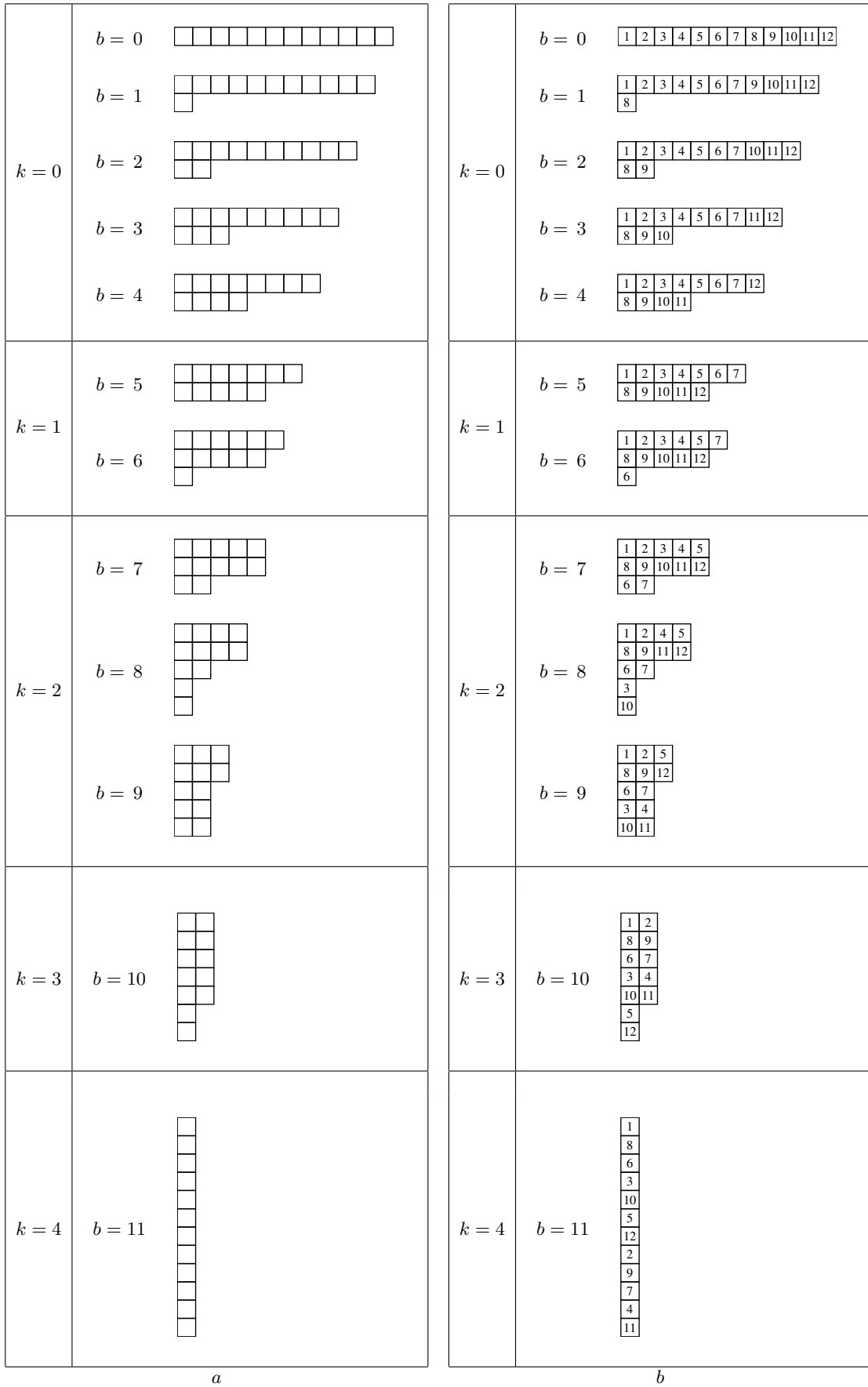
$$x = a_0 + \frac{1}{a_1 + \frac{1}{a_2 + \frac{1}{a_3 + \dots}}} . \quad (3.17)$$

We say that $\langle a_0, a_1, a_2, \dots \rangle$ is the *simple continued fraction* of x with a_k positive integers $\forall k > 0$ (as usual, for the sake of simplicity, we will often avoid repeating the adjective *simple* when we will refer to *simple* continued fractions). The elements a_k of the continued fraction expansion are called *partial quotients*.

The integer sequence $\{a_k\}$ is *finite* if and only if the corresponding number x is a rational number. The number of elements in the sequence is called the *length* of the continued fraction.

If a number h exists such that starting from the element a_h , the sequence $\{a_k\}$ becomes periodic, we say that the sequence of the partial quotients is *periodic* and we mark the periodic terms with a bar when we write explicitly the continued fraction:

$$\begin{aligned} \langle a_0, a_1, \dots, a_{h-1}, \overline{a_h, a_{h+1}, \dots, a_{N-1}, a_N} \rangle = \\ \langle a_0, a_1, \dots, a_{h-1}, a_h, a_{h+1}, \dots, a_{N-1}, a_N, \overline{a_h, a_{h+1}, \dots, a_{N-1}, a_N, a_h, \dots} \rangle . \end{aligned} \quad (3.18)$$



a

b

Figure 3.14: Ferrer diagrams for consecutive branch points inclusions ($p = 5, q = 12$): *a*) non-numbered Ferrer diagrams; *b*) numbered Ferrer diagrams.

The integer sequence $\{a_k\}$ is periodic if and only if the corresponding number x is an irrational quadratic number (namely the sum of a rational number plus the square root of a rational number).

The partial quotients can be recursively calculated introducing the auxiliary sequence of the *remainders* r_k :

$$\begin{cases} r_k = \frac{1}{r_{k-1} - [r_{k-1}]} & , \quad r_0 = x & ; \\ a_k = [r_k] & . \end{cases} \quad (3.19)$$

The rational number $c_n \equiv c_n(x)$ obtained truncating the continued fraction of x at the n -th term is called the n -th *convergent* of the continued fraction:

$$c_n = \frac{P_n}{Q_n} = \langle a_0, a_1, \dots, a_n \rangle = a_0 + \frac{1}{a_1 + \frac{1}{\dots + \frac{1}{a_n}}} . \quad (3.20)$$

The numerator P_n and the denominator Q_n of the n -th convergent c_n incur in the following second-order recurrence relations:

$$\begin{aligned} P_n &= a_n P_{n-1} + P_{n-2}, & P_{-2} &= 0, & P_{-1} &= 1; \\ Q_n &= a_n Q_{n-1} + Q_{n-2}, & Q_{-2} &= 1, & Q_{-1} &= 0. \end{aligned} \quad (3.21)$$

Now we have enough results to rephrase the quantities introduced in the previous sections in the language of the continued fractions. First of all, let us eliminate from the q -sequence the dependence on the p -sequence in formula (3.10):

$$q_n = q_{n-2} \text{ MOD } q_{n-1}, \quad q_0 = q, \quad q_1 = q - p ; \quad (3.22)$$

since, if x and y are positive natural numbers,

$$\frac{x - (x \text{ MOD } y)}{y} = \left\lfloor \frac{x}{y} \right\rfloor ,$$

by definition of floor function, we can reshuffle formula (3.22) in the following way:

$$\frac{q_n}{q_{n-1}} = \frac{q_{n-2}}{q_{n-1}} - \left\lfloor \frac{q_{n-2}}{q_{n-1}} \right\rfloor, \quad q_0 = q, \quad q_1 = q - p . \quad (3.23)$$

Now, let us set

$$r_k = \frac{q_k}{q_{k+1}} \quad \text{with } 0 \leq k \leq \bar{k} . \quad (3.24)$$

Using relation (3.23), we recover formula (3.19) for the quantity r_k ,

$$r_k = \frac{1}{r_{k-1} - [r_{k-1}]} \quad \text{with } r_0 = \frac{q_0}{q_1} = \frac{q}{q-p} = \frac{1}{1-\mu} . \quad (3.25)$$

Finally, we discover that the q -sequence, which gives the number of column in the Ferrer diagrams, can be calculated inverting formula (3.24),

$$q_k = \frac{q_{k-1}}{r_{k-1}} = q \left(\prod_{j=0}^{k-1} \frac{1}{r_j} \right), \quad q_0 = q, \quad r_0 = \frac{1}{1-\mu}, \quad 0 \leq k \leq \bar{k} , \quad (3.26)$$

where the r_k are the terms of the sequence of the remainders (see(3.25)) of the continued fraction expansion of the number $\frac{1}{1-\mu}$, with partial quotients

$$a_k = [r_k] = \left\lfloor \frac{q_k}{p_k} \right\rfloor \quad (3.27)$$

and length \bar{k} . The p -sequence can be calculated using the relation:

$$p_k = q_{k+1}, \quad 0 \leq k \leq \bar{k} . \quad (3.28)$$

Furthermore, we can give a more convenient rephrase of the heights of the columns in the Ferrer diagrams (3.16), $T_k^{(1)}$ and $T_k^{(2)}$, using the language of the continued fractions. In fact, subtracting the two recursions (3.16) one gets

$$T_{k+1}^{(1)} = T_{k+1}^{(2)} + T_k^{(2)} ; \quad (3.29)$$

the insertion of this last formula in the second of the (3.16) yields, via (3.27), a 3-terms linear recursion for $T_k^{(2)}$:

$$T_{k+1}^{(2)} = a_k T_k^{(2)} + T_{k-1}^{(2)} . \quad (3.30)$$

A comparison of this last recursion relation with the (3.21) and an analogous comparison of the starting conditions entail:

$$T_k^{(2)} = P_{k-1} , \quad (3.31)$$

where P_k is the numerator of the k -th convergent of the continued fraction expansion of $\frac{1}{1-\mu}$. Then (3.29) and (3.31) imply

$$T_k^{(1)} = P_{k-1} + P_{k-2} . \quad (3.32)$$

Now we have a nice rephrasing of all the quantities implied in the description of the Ferrer diagrams (number of them corresponding to the inclusions of consecutive branch points, number of columns and number of boxes in the columns) in terms of the continued fraction expansion of the (rational) number $\frac{1}{1-\mu}$.

We conclude this section showing a more convenient way of writing the fundamental b -sequence (3.13). Combining (3.24), (3.25) and (3.27), one gets:

$$q_k = q_{k-2} - a_{k-2} q_{k-1} , \quad q_0 = q , \quad q_1 = q - p ; \quad (3.33)$$

comparing this last relation with the recursions (3.21) via the following ansatz:

$$q_k = (-1)^k (\alpha P_{k-2} + \beta Q_{k-2}) , \quad k \geq 0 , \quad (3.34)$$

one gets for the two integer constants α and β

$$\alpha = (p - q) , \quad \beta = q ; \quad (3.35)$$

the insertion of (3.34) and (3.35) in (3.14) entails

$$b_k = q - q_k = q - (-1)^k [(p - q) P_{k-2} + q Q_{k-2}] , \quad k \geq 0 . \quad (3.36)$$

3.1.8 Following a single zero

Now that we have a simple description of the Ferrer diagrams in terms of the continued fraction expansion of $\frac{1}{1-\mu}$ and the two main ingredients for a period formula, the heights $T^{(1)}$ and $T^{(2)}$, we still miss an important step. Our final goal is to fix one of the q w -roots of the algebraic equation (3.2) using the enumeration depicted in Subsection 3.1.3 and to predict the period of such root when the variable ξ moves along a closed path which includes b consecutive branch points on the ξ -plane starting from the branch point labelled $\{1, q - p + 1\}$. To achieve this result we must put numbers inside the Ferrer diagrams boxes, in such a way that, if we fix a single column, all the roots labelled with the numbers

appearing in the chosen column have the same period, equal to the height of the column itself.

For instance, look at Figure 3.14b when $b = 8$. We can read this image, inferring that the $1 - st$, $3 - rd$, $6 - th$, $8 - th$ and $10 - th$ roots have period 5; the $2 - nd$, $7 - th$ and $9 - th$ roots have period 3; the $4 - th$, $5 - th$, $11 - th$ and $12 - th$ roots have period 2.

The consideration presented in the previous sections yields that, if we apply the bumping rule starting from the first numbered Ferrer diagram (which has all the boxes on a line and numerated from left to right in the natural order, $1, 2, \dots, q$), then for any $b \geq 0$ we get the right enumeration inside the Ferrer diagrams boxes.

Generally, we must identify, for a k -level Ferrer diagram, in which column a certain numbered box lies (starting the counting of the columns from the left); namely, to identify which column a certain root corresponds to in a k -level Ferrer diagram. It is worth stressing that, at the moment, we are not trying to make such an identification for a generic Ferrer diagram. What we will show is that, once we made this operation for a k -level Ferrer diagram, we will be able to perform the same operation, with some little adjustment, for a generic Ferrer diagram.

Let us introduce the following symbol:

$$l_h(s) = l_{h-1}(s) \text{ m\~{O}D } p_{h-1} \quad , \quad l_0(s) = s \quad , \quad \forall s \in \{1, 2, \dots, q\} \quad , \quad (3.37)$$

where $\text{m\~{O}D}$ is the modulus operation we introduced in (3.9). At the k -th step, this symbol gives exactly the column in which the box with the number s lies in the k -level Ferrer diagram. Indeed, at the k -th step we have a Ferrer diagram with q_k columns: at the following step, the last $q_k - p_k$ columns from the left orderly move over the first p_k columns. As usually, the $\text{m\~{O}D}$ operation avoid the presence of 0-labelled boxes. In this way, we can use this symbol to solve the problem of identifying the height of the column corresponding to a certain root in a k -level Ferrer diagram, i.e. after the inclusion of b_k branch points in the ξ -circle (see (3.13)).

3.1.9 The period formula for $0 < \mu < 1$ and $\mu \in \mathbb{Q}$

It is left to understand the behavior of the column heights for all the Ferrer diagrams, and not only for the diagrams corresponding to the k -levels. Let us fix a k -level Ferrer diagram and suppose that there are b branch points included in the ξ -circle with $b_h \leq b < b_{h+1}$. Suppose to be interested in the period of the s -th root. At each inclusion of a consecutive branch point, some of the columns are moved.

Case 1: If $l_h(s) > b - b_h + p_h$ then we have that the column we are interested in has height $T_h^{(2)}$ and it has not been moved with respect to the position it occupied when exactly b_h branch points were included in the ξ -circle.

Case 2: If $l_h(s) \leq b - b_h + p_h$ then we must consider two subcases:

- If $l_h(s) \leq p_h$ then the height of the column we are interested in was $T_h^{(1)}$ when the number of branch points included in the ξ -circle was exactly b_h ; if in the ξ -circle there are $b > b_h$ branch points (but $b < b_{h+1}$), some of the last $(q_h - p_h)$ columns, with height $T_h^{(2)}$, have been moved. The number of such columns moved under the $T_h^{(1)}$ tall column $l_h(s)$ depends whether $l_h(s) \text{ m\~{O}D } p_h$ is smaller than $(b - b_h) \text{ m\~{O}D } p_h$ or not. If $l_h(s) \text{ m\~{O}D } p_h < (b - b_h) \text{ m\~{O}D } p_h$ then the number of $T_h^{(2)}$ tall columns moved under the column $l_h(s)$ is $(\lfloor \frac{b-b_h-1}{p_h} \rfloor)$. If $l_h(s) \text{ m\~{O}D } p_h \geq (b - b_h) \text{ m\~{O}D } p_h$ then one more $T_h^{(2)}$ tall column moved under the column $l_h(s)$, so their total number is $(\lfloor \frac{b-b_h-1}{p_h} \rfloor + 1)$.

- If $l_h(s) > p_h$ then the height of the column we are interested in was $T_h^{(2)}$ when the number of branch points included in the ξ -circle was exactly b_h . If in the ξ -circle there are $b > b_h$ branch points (but $b < b_{h+1}$), some of the last $q_h - p_h$ columns, with height $T_h^{(2)}$, have been moved; the column $l_h(s)$ has been moved under the $T_h^{(1)}$ tall column $l_h(s) \text{ MÖD } p_h$ and, like in the previous subcase, the total number of $T_h^{(2)}$ tall columns moved under the column $l_h(s) \text{ MÖD } p_h$ depends whether $l_h(s) \text{ MÖD } p_h$ is smaller than $(b - b_h) \text{ MÖD } p_h$ or not. If $l_h(s) \text{ MÖD } p_h < (b - b_h) \text{ MÖD } p_h$ then the number of $T_h^{(2)}$ tall columns moved under the column $l_h(s) \text{ MÖD } p_h$ is $(\lfloor \frac{b-b_h-1}{p_h} \rfloor)$. If $l_h(s) \text{ MÖD } p_h \geq (b - b_h) \text{ MÖD } p_h$ then one more $T_h^{(2)}$ tall column moved under the column $l_h(s) \text{ MÖD } p_h$, so their total number is $(\lfloor \frac{b-b_h-1}{p_h} \rfloor + 1)$.

From the above considerations, we finally infer the following

Theorem 1. *Be $0 < \mu < 1$ and $\mu \in \mathbb{Q}$. Be the roots of the algebraic equation (3.2) labelled following the description of Subsection 3.1.3. Let $T(s, b)$ be the period of the s -th root of the algebraic equation (3.2) when ξ moves along a closed path on the ξ -plane, including b consecutive adjacent branch points starting from the branch point with label $\{1, q - p + 1\}$. Let h be the integer for which we have $0 \leq b_h \leq b < b_{h+1} \leq q - 1$ and $l_h(s)$ the symbol (3.37). Be $T_h^{(1)}$ and $T_h^{(2)}$ the quantities described by the recursions (3.16). Then we have the following period formula:*

$$T(s, b) = \begin{cases} T_h^{(1)} + \left(\left\lfloor \frac{b-b_h-1}{p_h} \right\rfloor \right) T_h^{(2)} & \text{if } l_h(s) \leq b - b_h + p_h \text{ and} \\ & (b - b_h) \text{ MÖD } p_h < l_h(s) \text{ MÖD } p_h \\ T_h^{(1)} + \left(\left\lfloor \frac{b-b_h-1}{p_h} \right\rfloor + 1 \right) T_h^{(2)} & \text{if } l_h(s) \leq b - b_h + p_h \text{ and} \\ & (b - b_h) \text{ MÖD } p_h \geq l_h(s) \text{ MÖD } p_h \\ T_h^{(2)} & \text{if } l_h(s) > b - b_h + p_h . \end{cases} \quad (3.38)$$

Making use of what we have see about simple continued fractions in Subsection 3.1.7, we can rephrase the previous formula in the following way

$$T(s, b) = \begin{cases} P_{h-2} + \left(\left\lfloor \frac{b-b_h-1}{q-b_{h+1}} \right\rfloor + 1 \right) P_{h-1} & \text{if } l_h(s) \leq b + q - (b_h + b_{h+1}) \text{ and} \\ & (b - b_h) \text{ MÖD } (q - b_{h+1}) < l_h(s) \text{ MÖD } (q - b_{h+1}) \\ P_{h-2} + \left(\left\lfloor \frac{b-b_h-1}{q-b_{h+1}} \right\rfloor + 2 \right) P_{h-1} & \text{if } l_h(s) \leq b + q - (b_h + b_{h+1}) \text{ and} \\ & (b - b_h) \text{ MÖD } (q - b_{h+1}) \geq l_h(s) \text{ MÖD } (q - b_{h+1}) \\ P_{h-1} & \text{if } l_h(s) > b + q - (b_h + b_{h+1}) . \end{cases} \quad (3.39)$$

This formula tells that, for any situation of consecutive branch points inclusion, generically we have only three possible periods for the roots of the algebraic equation (3.2). The sum of the first and the third of the (3.39) gives always the second. There are some cases in which the roots have only two possible periods, whenever b takes the following special values:

$$b = b_h + n(q - b_{h+1}) , \quad 0 \leq n \leq a_h - 1 , \quad n \in \mathbb{N} ; \quad (3.40)$$

indeed, in these cases, the condition on the first of the (3.39) fails since, for the (3.9), $(b - b_h) \text{ MÖD } (q - b_{h+1}) = q - b_{h+1}$ and $1 \leq l_h(s) \text{ MÖD } (q - b_{h+1}) \leq q - b_{h+1}$, so it cannot be that $(b - b_h) \text{ MÖD } (q - b_{h+1}) < l_h(s) \text{ MÖD } (q - b_{h+1})$ for any value of s .

For instance, in the following table you can compare the values of $T(s, b)$ when $p = 5$ and $q = 12$ for $1 \leq s \leq q$ and $0 \leq b \leq q$.

$T(s, b)$	1	2	3	4	5	6	7	8	9	10	11	12
$b = 0$	1	1	1	1	1	1	1	1	1	1	1	1
$b = 1$	2	1	1	1	1	1	1	2	1	1	1	1
$b = 2$	2	2	1	1	1	1	1	2	2	1	1	1
$b = 3$	2	2	2	1	1	1	1	2	2	2	1	1
$b = 4$	2	2	2	2	1	1	1	2	2	2	2	1
$b = 5$	2	2	2	2	2	1	1	2	2	2	2	2
$b = 6$	3	2	2	2	2	3	1	3	2	2	2	2
$b = 7$	3	3	2	2	2	3	3	3	3	2	2	2
$b = 8$	5	3	5	2	2	5	3	5	3	5	2	2
$b = 9$	5	5	5	5	2	5	5	5	5	5	5	2
$b = 10$	7	5	7	5	7	7	5	7	5	7	5	7
$b = 11$	12	12	12	12	12	12	12	12	12	12	12	12
$b = 12$	7	7	7	7	7	7	7	5	5	5	5	5

Values of $T(s, b)$ when $p = 5$ and $q = 12$.

3.1.10 The irrational case: $\mu \notin \mathbb{Q}$

We can treat the case in which μ is an *irrational* number as a limit of the case in which μ is a rational number. When μ is irrational, the number of roots of the equation (3.1) diverges, as q , number of branch points on the ξ -plane, approaches infinity. So we must analyze the previous formulas in the limit:

$$p, q \rightarrow \infty \text{ with } 0 < \mu = \frac{p}{q} < 1 . \quad (3.41)$$

namely in the limit in which the integers p and q diverge with their ratio μ fixed.

If μ is an irrational number, it follows that the Riemann surface Γ (3.1) becomes an ∞ -sheeted covering of the complex ξ plane. Like in Subsection (3.1.1), we can analyze its behavior for large $|\xi|$ and its branch points:

1) $\xi \sim \infty$. If $|\xi| \gg 1$, there are two different asymptotics:

$$\begin{aligned} w(\xi) &\sim -(-\xi)^{-\frac{1}{\mu}}, \quad \xi \sim \infty, \\ w(\xi) &\sim 1 + \xi^{-\frac{1}{1-\mu}}, \quad \xi \sim \infty. \end{aligned} \quad (3.42)$$

2) In the finite part, we have an infinite number of SRBPs densely distributed on the circle centered at the origin of the ξ -plane and of radius

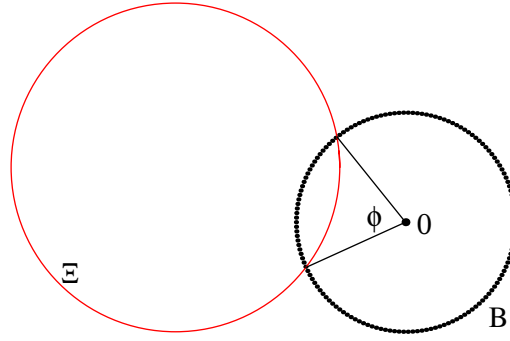
$$r_b = \frac{1}{1-\mu} \left(\frac{1-\mu}{\mu} \right)^\mu > 0 . \quad (3.43)$$

Again, each of the infinite SRBPs corresponds to the collision of a pair of roots.

In the limit (3.41), the continued fraction of $\frac{1}{1-\mu}$ has length \bar{k} that tends to infinity: $\bar{k} \rightarrow \infty$. The first step is to *normalize* the q -sequence (3.22), introducing the new sequence $\{\rho_k\} \sim \left\{ \frac{q_k}{q} \right\}$:

$$\rho_k = \frac{\rho_{k-1}}{r_{k-1}}, \quad \rho_0 = 1, \quad \rho_1 = 1 - \mu, \quad (3.44)$$

where r_k is the sequence of the (irrational) remainders of the continued fraction of $\frac{1}{1-\mu}$ (see (3.25)). In the limit (3.41), the ρ -sequence becomes a strictly decreasing sequence of irrational numbers such that $\rho_k \rightarrow 0$ for $k \rightarrow \infty$.

Figure 3.15: The definition of the angle ϕ

Finally, to obtain the proper continuous variable which replaces the discrete index b , we focalize our attention to the physical situation in which the ξ -path is a circle. Let be B the circle on which the SRBPs lie and Ξ the circle along which the ξ variable periodically moves. We define the variable ν , which is 0 if Ξ does not contain any arc of B and 1 if Ξ does contain the whole circle B . If B and Ξ intersect, select the arc of the B circle which is contained inside the evolutionary circle Ξ and denote by ν the corresponding angle ϕ , normalized by 2π (see Figure 3.15). Since

$$\nu = \frac{\phi}{2\pi} = \frac{b}{q} , \quad (3.45)$$

this is the proper continuous variable that replace b in the case μ is an irrational number.

The next step will be to normalize the fundamental b -sequence (3.36), introducing the new sequence $\{\nu_k\} \sim \left\{ \frac{b_k}{q} \right\}$:

$$\nu_k = 1 - \rho_k , \quad \nu_0 = 0 , \quad k \in \mathbb{N} ; \quad (3.46)$$

in the limit (3.41), we have that $\nu_k \rightarrow 1$ for $k \rightarrow \infty$. We can rephrase ν_k with the language of continued fraction. From (3.36), in the limit (3.41) we have:

$$\nu_k = 1 - (-1)^k [(\mu - 1) P_{k-2} + Q_{k-2}] , \quad k \in \mathbb{N} . \quad (3.47)$$

We are finally ready to enunciate the period formula in the case in which μ is an irrational number.

Theorem 2. *Be $0 < \mu < 1$ and $\mu \notin \mathbb{Q}$. Let $T(\nu)$ be the period of one of the roots of the algebraic equation (3.1) when ξ moves along a circular path Ξ on the ξ -plane, intersecting the SRBPs circle B in such a way that $0 \leq \nu < 1$ (see (3.45)). Let h be the integer such that $0 \leq \nu_h \leq \nu < \nu_{h+1} < 1$. Be P_k the numerator of the k -th convergent of the continued fraction expansion of $\frac{1}{1-\mu}$ (see (3.21)). If $\nu = 0$, then $T(\nu) = 1$. Otherwise, we have that $T(\nu)$ must have one of the following three values:*

$$T(\nu) = \begin{cases} P_{h-2} + \left(\left\lfloor \frac{\nu - \nu_h}{1 - \nu_{h+1}} \right\rfloor + 1 \right) P_{h-1} \\ P_{h-2} + \left(\left\lfloor \frac{\nu - \nu_h}{1 - \nu_{h+1}} \right\rfloor + 2 \right) P_{h-1} \\ P_{h-1} . \end{cases} \quad (3.48)$$

If $\nu = 1$, namely if the evolutionary circle Ξ contains entirely the SRBP circle B , then the dynamics goes back simple, because the evolutionary curve effectively surrounds only the

irrational branch point at infinity. The time evolution of the generic root of (3.1) in this case is quasiperiodic, involving a (nonlinear) superposition of two periodic evolutions with noncongruent periods, 1 and $\frac{1}{\mu}$ or 1 and $\frac{1}{1-\mu}$, as can be easily understood observing the exponents of the asymptotics (3.42).

Notice that, like before, the sum of the first and the third in the previous formula (3.48) always gives the second. We must stress that in this case there are no labels for the roots, so we cannot assign the three periods to the roots in terms of their labels as we did in the rational case. For the moment, we will limit our discussion affirming that the period of a single root must be one of those three displayed in the previous theorem.

For $\nu = 0$ we know that the period $T(\nu)$ is equal to 1. Since 1 is the accumulation point of the sequence $\{\nu_k\}$, if ν is close to 1 (i.e. if the evolutionary circle Ξ contains almost completely the SRBP circle B), a small change in the time trajectory results in a drastic change of period. In fact, $T(\nu)$ approaches infinity as $\nu \rightarrow 1$ and the values of $T(\nu)$ depends on the partial quotients a_k of the continued fraction expansion of $\frac{1}{1-\mu}$; such partial quotients are well-known to be almost chaotic and unpredictable in their sequence for a generic irrational number (for almost all the irrational number, except for the quadratic irrationals).

It is difficult to describe the behavior of $T(\nu)$ as $\nu \rightarrow 1$ for a generic μ , since, as we said before, $T(\nu)$ depends on the partial quotients a_k of the continued fraction expansion of $\frac{1}{1-\mu}$, whose behavior is known to be chaotic for a generic irrational number. In the next subsection we will see how to produce a convenient (and amazing) example in which it will be possible to show explicitly the asymptotic behavior of $T(\nu)$ for $\nu \sim 1$.

3.1.11 A remarkable example

In this final section, we will display the special example with the following (conveniently chosen) *quadratic irrational* value of μ in the interval $0 < \mu < 1$:

$$\mu = \frac{2}{3 + \sqrt{5}} = \frac{1}{1 + \varphi} \quad , \quad (3.49)$$

such that

$$\frac{1}{1 - \mu} = \varphi = \frac{1 + \sqrt{5}}{2} \quad , \quad (3.50)$$

where of course φ is the *golden ratio*, namely the positive solution of the second degree equation

$$\varphi^2 - \varphi - 1 = 0 \quad . \quad (3.51)$$

From the theory summarized in Subsection 3.1.7, since φ is a quadratic irrational number, we know that its continued fraction expansion is periodic. Furthermore, it has the nice property that all its infinite partial quotients (3.27) are equal to 1:

$$\varphi = 1 + \frac{1}{1 + \frac{1}{1 + \frac{1}{\dots}}} \quad , \quad a_k = 1 \quad \forall k \geq 0 \quad . \quad (3.52)$$

So, in this particular case, relation (3.25) becomes:

$$r_k = \frac{1}{r_{k-1} - 1} \quad \text{with} \quad r_0 = \varphi \quad , \quad k \geq 1 \quad . \quad (3.53)$$

Combining this last relation with (3.44) one gets:

$$\rho_{k+1} = \rho_{k-1} - \rho_k \quad \text{with} \quad \rho_0 = 1 \quad , \quad \rho_1 = \frac{1}{\varphi} = \varphi - 1 \quad , \quad k \geq 1 \quad (3.54)$$

and from this, using (3.46),

$$\nu_{k+1} = \nu_{k-1} - \nu_k + 1 \quad \text{with } \nu_0 = 0, \nu_1 = 1 - \frac{1}{\varphi}, k \geq 1. \quad (3.55)$$

Solving this last relation with respect to k , one gets

$$\nu_k = 1 - \varphi^{-k}, \quad k \geq 0. \quad (3.56)$$

More surprisingly, (3.52) implies, via (3.21), the following relation for the numerators of the convergents:

$$P_k = P_{k-1} + P_{k-2}, \quad P_{-2} = 0, \quad P_{-1} = 1, \quad k \geq 0, \quad (3.57)$$

which is exactly the recurrence relation for the Fibonacci's numbers. Using Binet formula, we have:

$$P_k = \frac{1}{\sqrt{5}} \left[\varphi^{k+2} - (-\varphi)^{-(k+2)} \right], \quad k \geq -2. \quad (3.58)$$

Making use of formula (3.56), we can explicitly invert the inequality $\nu_k \leq \nu < \nu_{k+1}$, finding, for a fixed value of ν in the interval $0 < \nu < 1$, the integer number k such that $\nu_k \leq \nu < \nu_{k+1}$:

$$k \equiv k(\nu) = \begin{cases} - \left\lfloor \frac{\log(1-\nu)}{\log(\varphi)} \right\rfloor - 1, & \text{if } 0 < \nu < 1; \\ 0, & \text{if } \nu = 0. \end{cases} \quad (3.59)$$

Since, by definition of floor function,

$$x - 1 < \lfloor x \rfloor \leq x, \quad \forall x \in \mathbb{R} \quad \text{and} \quad x \geq 0$$

for the argument of the floor function in formula (3.48), via (3.59), we get:

$$0 < \frac{\nu - \nu_{k(\nu)}}{1 - \nu_{k(\nu)+1}} < \varphi - 1 < 1; \quad (3.60)$$

so the floor function in formula (3.48) is always 0 and the root period $T(\nu)$ has one of the following values:

$$T(\nu) = \{P_{k+1}, P_k, P_{k-1}\} \quad \text{with } 0 \leq \nu_k \leq \nu < \nu_{k+1} < 1, \quad (3.61)$$

namely three consecutive Fibonacci's numbers. From relation (3.57), via (3.59), we have, for $0 < \nu < 1$,

$$\frac{1}{\sqrt{5}} \left[\frac{\varphi}{1-\nu} - \frac{1-\nu}{\varphi} \right] < P_{k(\nu)} < \frac{1}{\sqrt{5}} \left[\frac{\varphi}{1-\nu} + \frac{1-\nu}{\varphi} \right] \quad (3.62)$$

From the above relations (3.62) and (3.60), and from the period formula (3.48), we obtain the following lower and upper bounds for the period values in terms of ν in the interval $0 < \nu < 1$:

$$\frac{\nu(2-\nu)}{\sqrt{5}(1-\nu)} \leq T(\nu) < \frac{7 + \sqrt{5} + (\sqrt{5} - 3)\nu(2-\nu)}{2\sqrt{5}(1-\nu)}. \quad (3.63)$$

These inequalities entail that the integer $T(\nu)$ diverges proportionally to $(1-\nu)^{-1}$ as $\nu \rightarrow 1$. Imposing the upper bound in (3.63) equal to 8 and solving with respect to ν , one can determine that for $0 < \nu < 0.761987\dots$, namely for an inclusion of almost three fourths of the B circle inside the Ξ circle, the period will be surely lower than 8.

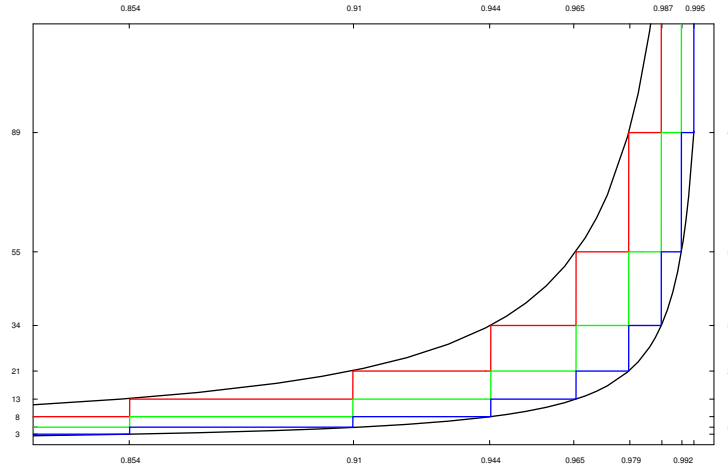


Figure 3.16: $T(\nu)$ vs ν . In red, green and blue respectively the three different values of $T(\nu)$, while the black continuous lines are the lower and upper bounds in (3.63).

In the following table, one can compare the first values of the quantities showed in this section: for each value of k , the values of $\nu(k)$, the lower and the upper bounds (3.63) and the three possible values of the period $T(\nu)$ are given.

k	$\nu(k)$	<i>lowerbound</i>	$T(\nu(k))$	<i>upperbound</i>
0	0	0.000	1	2.06525
1	0.381966	0.447214	2, 1	3.17082
2	0.618034	1.000	3, 2, 1	5.02492
3	0.763932	1.78885	5, 3, 2	8.06525
4	0.854102	3.000	8, 5, 3	13.0095
5	0.909830	4.91935	13, 8, 5	21.0249
6	0.944272	8.000	21, 13, 8	34.0036
7	0.965558	12.9692	34, 21, 13	55.0095
8	0.978714	21.000	55, 34, 21	89.0014
9	0.986844	33.9882	89, 55, 34	144.004
10	0.991869	55.000	144, 89, 55	233.001
11	0.994975	88.9955	233, 144, 89	377.001
12	0.996894	144.000	377, 233, 144	610.001
13	0.998081	232.998	610, 377, 233	987.001
14	0.998814	377.000	987, 610, 377	1597.001
15	0.999267	609.999	1597, 987, 610	2584.001

3.2 The case $\mu > 1$

Here we study the Riemann surface Γ consisting of points $(\xi, w) \in \Gamma$ such that:

$$w^{-\mu}(w-1)^{\mu-1} = \xi, \quad (3.64)$$

where

$$\mu = \frac{p}{q} > 1,$$

and $p \in \mathbb{N}$ and $q \in \mathbb{N}^+$ are coprime natural numbers. Therefore Γ is an *algebraic* Riemann surface characterized by the polynomial (of degree p) equation

$$(w-1)^{q-p} = w^p \xi^q, \quad 0 < q < p \quad (3.65)$$

which now defines the p -valued function $w = w(\xi)$. Since, $\forall \xi \in \mathbb{C}$, the polynomial (3.65) admits p complex roots and each root corresponds to a sheet of the Riemann surface Γ , it follows that Γ is a p -sheeted covering of the complex ξ plane.

3.2.1 The Riemann surface and its singularities

The Riemann surface Γ possesses the following distinguished points.

1) $\xi = \infty$. If $|\xi| \gg 1$, we have the asymptotics:

$$w(\xi) \sim -(-\xi)^{-\frac{q}{p}}, \quad \xi \sim \infty. \quad (3.66)$$

Therefore the ∞ -*configuration* consists of all the p roots lying on a small circle of radius $O(|\xi|^{-\frac{q}{p}})$ centered at the origin (see Figure 3.17), and a counterclockwise 2π - rotation of ξ on a big circle implies a clockwise rotation of each root around the origin of the angle $(2\pi q/p)$. From the point of view of the Riemann surface Γ , the branch point $(\infty, 0)$, of order $(p - 1)$, attaches all the p sheets.

2) $\xi = 0$. If $|\xi| \ll 1$, we have two different asymptotics:

$$\begin{aligned} w(\xi) &\sim 1 + (1)^{\frac{1}{p-q}} \xi^{\frac{q}{p-q}}, \quad \xi \sim 0, \\ w(\xi) &= \frac{1}{\xi^{\frac{1}{q}}} + O(\xi^{-2}), \quad \xi \sim 0. \end{aligned} \quad (3.67)$$

Therefore the 0-*configuration* consists of $(p - q)$ roots lying on a small circle of radius $O(|\xi|^{\frac{q}{p-q}})$ around 1, and of q roots lying on a big circle of radius $O(|\xi|^{-1})$ around the origin. A counterclockwise 2π -rotation of ξ on a small circle around the origin implies that the $(p - q)$ roots surrounding 1 undergo a cyclic permutation ruled by the first of the (3.67), while the remaining q roots at ∞ undergo a 2π -clockwise rotation, going back to their initial positions. From the point of view of Γ , we see that the branch point $(0, 1)$ attaches $(p - q)$ sheets, while $w(\xi)$ has a simple pole in each of the remaining q sheets.

3) The remaining singularities in the finite part of the complex ξ plane are q square root branch points (SRBPs):

$$(\xi_b^{(j)}, \mu) \in \Gamma, \quad j = 1, \dots, q, \quad (3.68)$$

defined by the equation:

$$\xi^q = \frac{q^q (p - q)^{p-q}}{p^p}. \quad (3.69)$$

Therefore the *SRBP-configuration* consists of q SRBPs lying on the circle centered at the origin and of radius

$$r_b = \frac{q}{p - q} \left(\frac{p - q}{p} \right)^{\frac{p}{q}} > 0; \quad (3.70)$$

here we use the positive principal determination. We remark that at least one of the branch points is positive. Also here we find it convenient to order them in a sequential and counterclockwise way (see Figure 3.18); a convenient choice of the first SRBP $\xi_b^{(1)}$, clearly arbitrary at this stage, is suggested by the direct problem and will be discussed later. Each SRBPs corresponds to the collision of a pair of roots.

The genus of Γ is 0; this is an immediate consequence of the Hurwitz formula (see [61]): $V = 2(J + G - 1)$, where V is the ramification index of the surface, J is the number of sheets and G is its genus. In our case $J = p$ and $V = q + (p - 1) + (p - q - 1)$, implying $G = 0$.

Equation (3.65) exhibits several symmetries. The ones used here are:

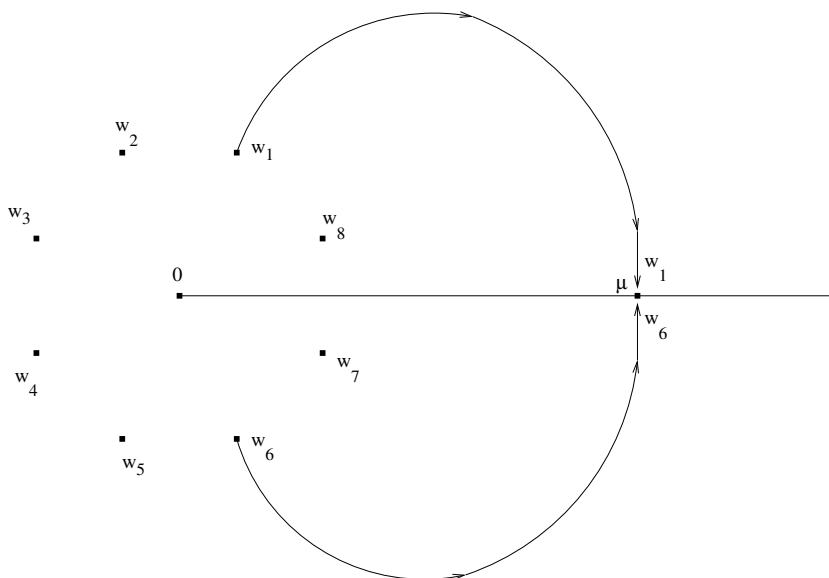


Figure 3.17: The ∞ -configuration of the Riemann surface for $p = 8$ and $q = 5$: for $\xi \gg 1$, the p roots w_j , $j = 1, \dots, p$ lie on a small circle centered at the origin and of radius $O(\xi^{-(q/p)})$. As ξ travels along the cut γ_1 (see Figure 3.18), from ∞ to $\xi_b^{(1)}$, the complex conjugate roots w_1 and w_6 abandon the ∞ -configuration and collide at μ . After fixing w_1 , the enumeration of the other roots (sheets) is sequential and counterclockwise.

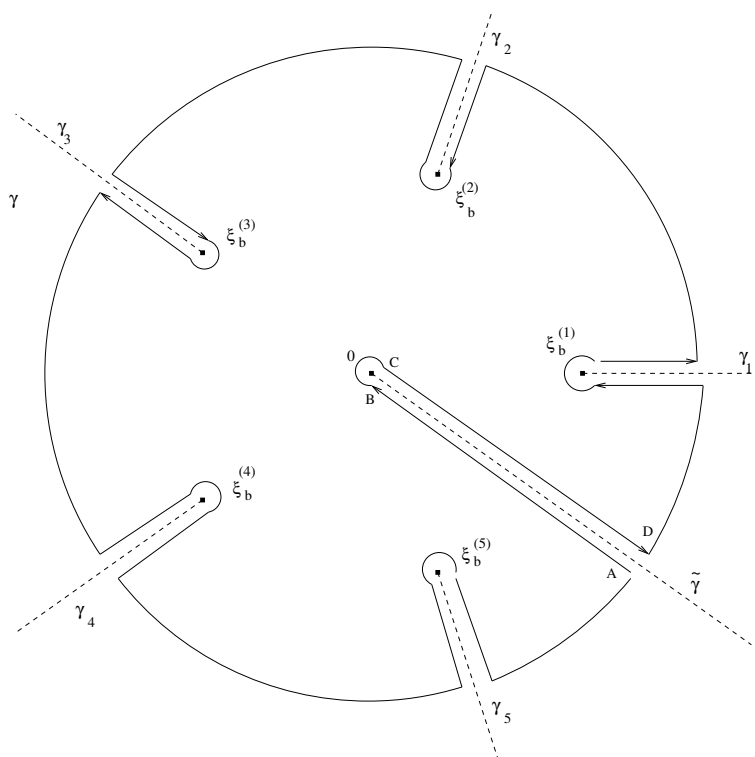


Figure 3.18: The cutted ξ -plane for the Riemann surface $q = 5$, $p = 8$.

1. *Symmetry with respect to a $2\pi/q$ rotation.* The set of roots is left invariant by a $2\pi i/q$ rotation in the ξ plane.
2. *Reality symmetry.* If $\xi \in \mathbb{R}$, the roots are either real or in complex conjugate pairs.

3.2.2 Roots dynamics and topological properties

To trivialize the monodromy of the roots we cut the complex ξ -plane as follows. We consider, as in the case $0 < \mu < 1$, the cuts γ_j , $j = 1, \dots, q$, defined by

$$\gamma_j = \{\xi, \arg(\xi) = \arg(\xi_b^{(j)}), |\xi| \geq |\xi_b^{(j)}|\}, \quad j = 1, \dots, q, \quad (3.71)$$

corresponding to the square root branch points $\xi_b^{(j)}$, $j = 1, \dots, q$, together with the cut $\tilde{\gamma}$ connecting the branch points 0 and ∞ (see Figure 3.18).

A convenient enumeration of the roots is a consequence of the following fact. As ξ travels along the cut γ_j , from ∞ to $\xi_b^{(j)}$, two complex conjugate roots abandon the small circle around the origin (the ∞ -configuration) and collide at the point μ , orthogonally to the real axis (see Fig.2). Let us denote by w_j the root of this pair characterized by a positive imaginary part and let us enumerate all the other roots of the ∞ -configuration sequentially, in a counterclockwise way, $\text{M}\ddot{\text{O}}\text{D } p$ (see Figure 3.17). As we shall see below, with respects to our cutted plane, the first q roots (sheets) of this sequence: $\{w_1, \dots, w_q\}$ ($\{\mathcal{F}_1, \dots, \mathcal{F}_q\}$) and the remaining $(p - q)$ roots (sheets): $\{w_{q+1}, \dots, w_p\}$ ($\{\mathcal{F}_{q+1}, \dots, \mathcal{F}_p\}$) turn out to have quite different dynamical (topological) properties. We will call them, respectively, *roots (sheets) of type q* and *roots (sheets) of type $(p - q)$* .

Using the large ξ asymptotics (3.66) and the above basic symmetries of Γ , we infer the following basic motions.

- 1) Since $\xi_b^{(j)}$ is a branch point of square root type, from the above considerations it follows that, as ξ moves around the cut γ_j as in Figure 3.19, the two roots w_j and $w_{\varphi(j)}$, $j = 1, \dots, q$, exchange their positions (see Figure 3.20), where

$$\varphi(j) = j + q - (p - q) \left\lfloor \frac{j - 1}{p - q} \right\rfloor, \quad j = 1, \dots, q, \quad (3.72)$$

while the remaining roots have a trivial monodromy. We have established the first basic motion:

$$\boxed{\xi - \text{motion around the branch cut } \gamma_j} \Leftrightarrow \boxed{\text{cyclic permutation of the two roots } \{w_j, w_{\varphi(j)}\}.$$

We remark that w_j belongs to the first set of q roots, while $w_{\varphi(j)}$ belongs to the complementary set of $(p - q)$ roots.

- 2) If ξ moves from γ_j to γ_{j+1} on a big circle, from the asymptotics (3.66) it follows that the ∞ -configuration of p roots exhibits a clockwise rotation of the angle $2\pi/p$ (see Figure 3.21). Therefore all the roots undergo a *cyclic permutation*, which is the second basic motion:

$$\boxed{\xi - \text{rotation from } \gamma_j \text{ to } \gamma_{j+1}} \Leftrightarrow \boxed{\text{cyclic permutation of all the roots } \{w_1, \dots, w_p\}.$$

Repeating these two motions with respect to the other SRBP cuts, in sequential and counterclockwise order, the point ξ draws a closed contour but now, unlike the case $0 < \mu < 1$, the associated monodromy of $(p - q)$ roots will be nontrivial, since this closed ξ -contour includes the branch point $\xi = 0$. More precisely, it is possible to show, using the symmetries 1 and 2, that the roots w_j , $j = 1, \dots, q$ of the first group go back to their original

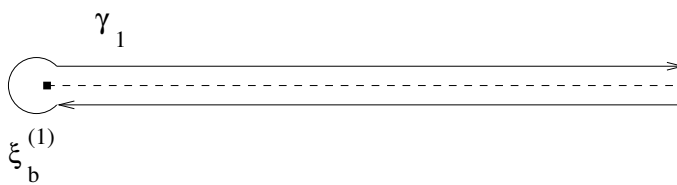


Figure 3.19: The motion of ξ around the cut γ_1 .

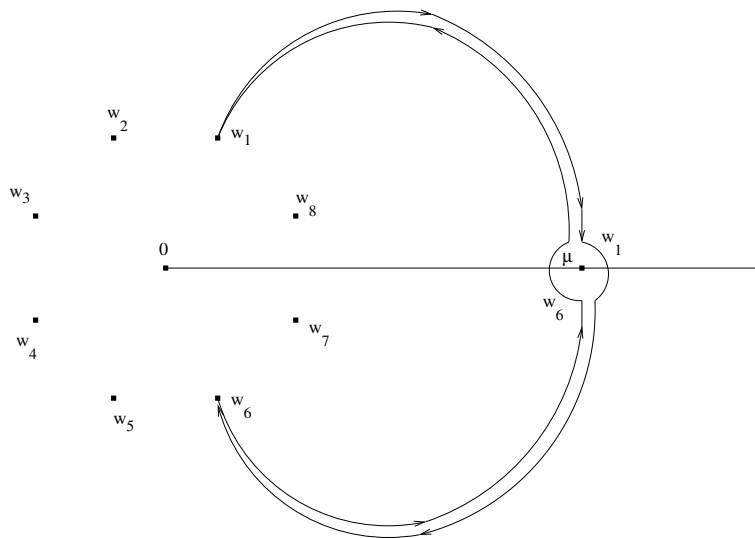


Figure 3.20: As ξ travels around the branch cut γ_1 , the the complex conjugate roots w_1 and w_6 exchange their positions colliding in μ . The remaining roots have a trivial monodromy. Riemann surface $q = 5$, $p = 8$.

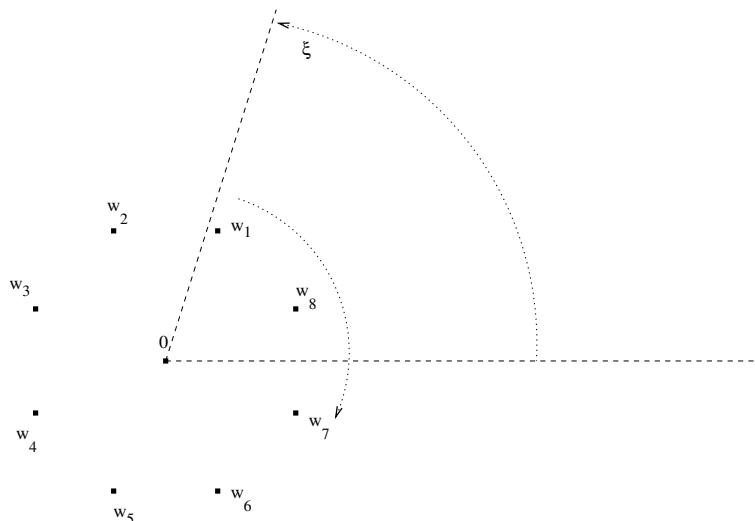


Figure 3.21: As ξ travels from the branch cut γ_1 to the branch cut γ_2 on a big circle, the ∞ -configuration has a $2\pi/p$ clockwise rotation, corresponding to a backward cyclic permutation of the p roots: $\{w_1, w_2, \dots, w_p\} \rightarrow \{w_2, \dots, w_p, w_1\}$. Riemann surface $q = 5$, $p = 8$.

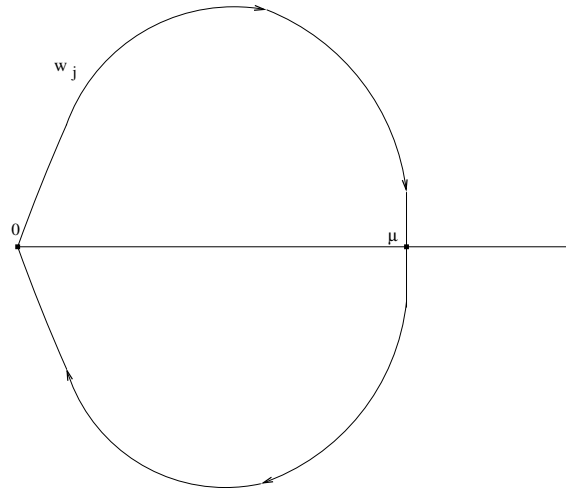


Figure 3.22: As ξ travels on the closed contour surrounding all cuts, the roots of type q : $w_j, j = 1, \dots, q$ draw the closed contour represented in this figure. The exterior of such a contour is the image of the cutted ξ -plane via the roots $w_j, j = 1, \dots, q$.

positions, drawing the closed contour in Figure 3.22, while the remaining $(p - q)$ roots of the complementary subset exchange their positions through a sequence of \tilde{q} backward cyclic permutations:

$$\{w_{q+1}, \dots, w_p\} \rightarrow \{w_{q+1+\tilde{q}}, \dots, w_p, w_{q+1}, \dots, w_{q+\tilde{q}}\}, \quad (3.73)$$

where

$$\tilde{q} = q \text{ MÖD } (p - q). \quad (3.74)$$

To trivialize this monodromy, the closed ξ -contour should also go around the cut $\tilde{\gamma}$ as in Figure 3.18. Indeed,

- 3) when ξ travels around the cut $\tilde{\gamma}$, through the points A, B, C, D (see Figure 3.18), the roots $w_j, j = 1, \dots, q$ of the first subset have a trivial monodromy, while the nontrivial motion of the remaining $(p - q)$ roots of the complementary subset can be decomposed as follows. As ξ moves from A to B , the $(p - q)$ roots of the second subset go from the ∞ -configuration to the 0-configuration (see Figure), in which they lie, equispaced, on a small circle around 1. When ξ has a clockwise 2π rotation around the origin, from B to C , they have a $(2\pi q / (p - q))$ clockwise rotation around 1, resulting in \tilde{q} forward cyclic permutations, which is the inverse of the transformation (3.73). This is the third basic motion:

clockwise 2π -rotation of ξ around 0	\Leftrightarrow	\tilde{q} cyclic permutations of the roots of type $(p - q)$.
---	-------------------	---

Since this transformation is the inverse of (3.73), when ξ moves from C to D , completing the motion around the cut $\tilde{\gamma}$, the roots of type $(p - q)$ go back to the ∞ -configuration trivializing their monodromy.

From the above considerations, we finally infer the following

Topological properties of Γ . *The Riemann surface Γ is a p -sheeted covering of the ξ -plane of genus 0. In the finite part of Γ there are q square root branch points: $(\xi_b^{(j)}, \mu) \in \Gamma, j = 1, \dots, q$; the j -th square root branch point connects the sheets \mathcal{F}_j and $\mathcal{F}_{\varphi(j)}$; the branch point $(0, 1)$, of order $(p - q - 1)$, connects the $(p - q)$ sheets $\mathcal{F}_j, j = q + 1, \dots, p$. The compactification of Γ is achieved at $\xi = \infty$, where the branch point $(\infty, 0)$, of order $(p - 1)$, connects all the the p sheets. As ξ turns in a counterclockwise way around the branch point*

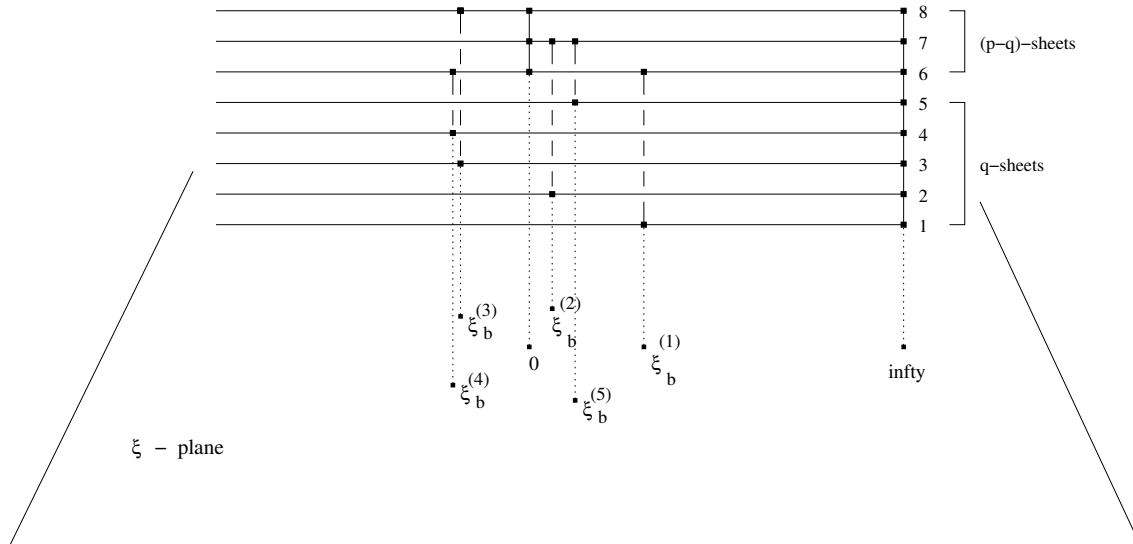


Figure 3.23: The topological properties of Γ for $q = 5$ and $p = 8$.

$(0, 1)$, the sheets of type $(p - q)$ are visited in the order: $\mathcal{F}_j, \mathcal{F}_{j+\bar{q}}, \mathcal{F}_{j+2\bar{q}}, \dots \text{M}\ddot{\text{O}}\text{D } (p - q)$. As ξ turns in a counterclockwise way around the branch point $(\infty, 0)$, all the sheets are visited in the order: $\mathcal{F}_j, \mathcal{F}_{j-\bar{q}}, \mathcal{F}_{j-2\bar{q}}, \dots \text{M}\ddot{\text{O}}\text{D } p$.

The Riemann surfaces $q = 5, p = 8$ is drawn in Figure 3.23.

Another convenient way to illustrate the topological properties of Γ is via a connection table in which it is shown how the two subsets of sheets (roots) are connected at the square root branch points (see Figures 3.24 and 3.25). With respect to that, we distinguish two different situations.

- i) If $p > 2q$, any sheet of type $(p - q)$ is connected at most to one sheet of type q (see Fig. 3.24). Consequently, the sheets of type q are connected among themselves only through the branch point $(0, 1)$. Any increase of period, can occur only when the evolutionary circle includes the origin $\xi = 0$.
- ii) If $p < 2q$, some sheet of type $(p - q)$ is connected to more than one sheet of type q (see Figure 3.25). Consequently, there are sheets of type q which are connected among them-selves via that $(p - q)$ -sheet, also when the origin $\xi = 0$ is not included in the evolutionary circle. For instance, if $q = 5$ and $p = 8$, since the sheets $\mathcal{F}_1, \mathcal{F}_4$, of type q , are connected via the sheet \mathcal{F}_6 , of type $(p - q)$ (see Figures 3.23 and 3.25), it will occur an increase of the period when the evolutionary circle, containing initially the adjacent branch points $\xi_b^{(1)}, \xi_b^{(5)}$, varies with continuity including also $\xi_b^{(4)}$.

3.2.3 Branch points enumeration

Analogously to what we did for the case $0 < \mu < 1$, starting from the results obtained in the previous paragraphs, we will describe an algebro-combinatoric method to predict the period of a single root of the algebraic equation (3.65) as ξ moves periodically along a closed path on the branched ξ -plane. For this purpose, we need to introduce a change in the labelling of the branch points with respect to what we described previously.

In what follows, to label the branch points, we will use a double index. To start the enumeration, pick arbitrarily one of the q square root branch points. Then, beginning from the chosen one, apply a double index to each branch point, so that the first indexes are the consecutive natural numbers (anti-clockwise), starting from $p - q + 1$, while the second ones

ξ_b	q sheets		$(p - q)$ sheets
1	\mathcal{F}_1	\longleftrightarrow	\mathcal{F}_{q+1}
2	\mathcal{F}_2	\longleftrightarrow	\mathcal{F}_{q+2}
.	.		.
.	.		.
.	.		.
$q - 1$	\mathcal{F}_{q-1}	\longleftrightarrow	\mathcal{F}_{2q-1}
q	\mathcal{F}_q	\longleftrightarrow	\mathcal{F}_{2q}
			\mathcal{F}_{2q+1}
			.
			.
			.
			\mathcal{F}_p

Figure 3.24: The connection table in the case $2q < p$. On each horizontal line we indicate, for each square root branch point, the sheets of type q and $(p - q)$ which are connect by it. In this case any sheet of type $(p - q)$ is connected to at most one sheet of type q . Consequently, the sheets of type q are connected among themselves only through the branch point $(0, 1)$ and an increase of the period can occur only when the evolutionary circle includes the origin $\xi = 0$.

ξ_b	q sheets		$(p - q)$ sheets	ξ_b	q sheets		$(p - q)$ sheets
1	\mathcal{F}_1	\longleftrightarrow	\mathcal{F}_{q+1}	$2(p - q) + 1$	$\mathcal{F}_{2(p-q)+1}$	\longleftrightarrow	\mathcal{F}_{q+1}
2	\mathcal{F}_2	\longleftrightarrow	\mathcal{F}_{q+2}	$2(p - q) + 2$	$\mathcal{F}_{2(p-q)+2}$	\longleftrightarrow	\mathcal{F}_{q+2}
.
.
.
$p - q$	\mathcal{F}_{p-q}	\longleftrightarrow	\mathcal{F}_p	$\tilde{q}(p - q)$	$\mathcal{F}_{\tilde{q}(p-q)}$	\longleftrightarrow	\mathcal{F}_p
$p - q + 1$	\mathcal{F}_{p-q+1}	\longleftrightarrow	\mathcal{F}_{q+1}	$\tilde{q}(p - q) + 1$	$\mathcal{F}_{\tilde{q}(p-q)+1}$	\longleftrightarrow	\mathcal{F}_{q+1}
$p - q + 2$	\mathcal{F}_{p-q+2}	\longleftrightarrow	\mathcal{F}_{q+2}	$\tilde{q}(p - q) + 2$	$\mathcal{F}_{\tilde{q}(p-q)+2}$	\longleftrightarrow	\mathcal{F}_{q+2}
.
.
.
$2(p - q)$	$\mathcal{F}_{2(p-q)}$	\longleftrightarrow	\mathcal{F}_p	q	\mathcal{F}_q	\longleftrightarrow	$\mathcal{F}_{2q-\tilde{q}(p-q)}$

Figure 3.25: The connection table in the case $p < 2q$. On each horizontal line we indicate, for each square root branch point, the sheets of type q and $(p - q)$ which are connect by it. In this case, some sheet of type $(p - q)$ is connected to more than one sheet of type q . Consequently, there are sheets of type q which are connected among them-selves via that $(p - q)$ -sheet, also when the origin $\xi = 0$ is not included in the evolutionary circle.

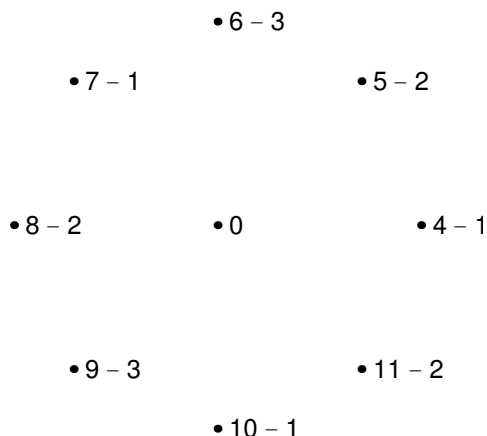


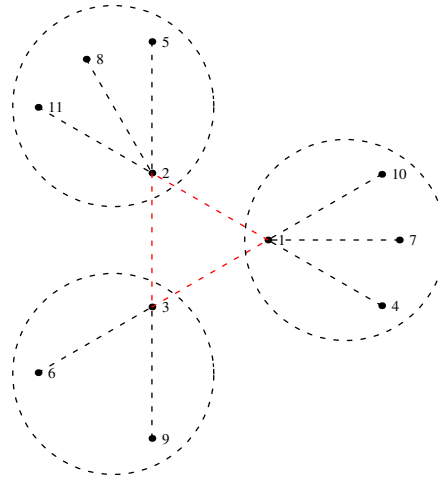
Figure 3.26: Branch points double indexes ($p = 11$, $q = 8$)

are the consecutive natural numbers $\text{MÖD}(p - q)$. In this way, we somewhat reconstruct the connections between the sheets of the Riemann surface as described in Subsection 3.2.2 with the following difference: the SRBPs, that were labelled in the previous section with the first q natural numbers starting from 1, now have the first indexes corresponding to the first q natural numbers starting from $p - q + 1$; similarly, the q -sheets, that were labelled in the previous section with the first q natural numbers starting from 1, now have indexes corresponding to the first q natural numbers starting from $p - q + 1$; while the $(p - q)$ -sheets, that were labelled in the previous section with the $(p - q)$ natural numbers between $q + 1$ and p , now have indexes corresponding to the first $(p - q)$ natural numbers starting from 1. The reason of this shuffling is that now we can rephrase the whole system of labelling without consequences on the root dynamics and so that the branch point with double index $\{k, k \text{ MÖD}(p - q)\}$ (with $k = p - q + 1, p - q, \dots, p$) corresponds to the connection of the k -th q -sheet with the $(p - q)$ -sheet labelled $k \text{ MÖD}(p - q)$ (for instance, look at the situation in Figure 3.26, where $p = 11$ and $q = 8$, namely in a case in which $2q > p$; notice that we leave marked the origin, since it corresponds to a branch point that attaches $(p - q)$ sheets.).

3.2.4 Graph Theory and Monodromy Group

Repeating step by step the procedure illustrated in the case $0 < \mu < 1$, now that we have a labelling system for the SRBPs and the connection rules for the sheets of the Riemann surface, we can use some graph theory to describe the monodromy group associated to the w -roots system. Actually, it is possible to infer the same results on the root-periods without this apparatus of combinatoric techniques. Nevertheless, it will be useful to use it also in this case, since this will prove the generality of the method and will aid to have a global and more systematic view of the monodromy group associated with the Riemann surface (3.64).

We remember that, since in our physical problem ξ can move only on a circular path (the circle Ξ), you can easily convince yourselves that such path can make inclusion only of consecutive (adjacent) branch points on B (the circle where the SRBPs lie) and of the branch point in the origin. So, for our purposes, it is convenient to study only the cases in which the ξ -path (i.e. the path along which ξ moves) includes consecutive branch points, distinguishing two fundamental subcases: the case in which the origin is inside such path

Figure 3.27: Graph construction and nodes labelling ($p = 11$, $q = 8$).

and the case in which the origin is outside such path.

To construct the planar graph corresponding to a certain (mutual) disposition of the ξ -path and B , start with tracing $(p - q)$ nodes, corresponding to the $(p - q)$ -sheets of the Riemann surface, on a regular polygon. Now, label with the first consecutive $(p - q)$ natural numbers these $(p - q)$ nodes, starting from an arbitrarily chosen one (anti-clockwise). Then, trace near to the k -th node a number of new nodes equal to the number of integers congruous to $k \pmod{p - q}$ and contained in the closed interval $\{p - q + 1, p\}$: these nodes will correspond to the q -sheets of the Riemann surface. For example, look at Figure 3.27 where it is shown the graph construction and the nodes labelling system for the case $p = 11$ and $q = 8$. Near the node number 2, you can see the nodes number 5, 8 and 11, the three numbers in the interval $\{4, 11\}$ which satisfy the congruence: $5 \equiv 8 \equiv 11 \equiv 2 \pmod{3}$. The reason for such a weird labelling of the nodes is justified by the fact that in this way the edges of the graph will be traced more easily.

If the ξ -path will include, among the others, the branch point labelled $\{h, h \pmod{p - q}\}$, with $h = p - q + 1, \dots, p$, we will connect with an edge the nodes labelled respectively h and $h \pmod{p - q}$ in the graph. Particularly, if the ξ -path will include, among the others, the branch point in the origin, we will connect simultaneously with $(p - q)$ edges the $(p - q)$ nodes disposed on the inner regular polygon vertexes, namely the nodes labelled with the integers from 1 to $(p - q)$, corresponding to the $(p - q)$ -sheets. For example, in Figures 3.28 and 3.29, you can see all the possible graph that one can obtain, for $p = 11$ and $q = 8$, including an increasing number of consecutive branch points inside the ξ -path, starting from the branch point $\{(p - q + 1), 1\}$, when the origin is respectively not-included and included inside the ξ -path.

Like in the case $0 < \mu < 1$, higher is the number of SRBPs included in the ξ -path, higher is the degree of connection of the graph. Thou, there is a big difference between the two subcases *origin outside* and *origin inside* the ξ -path. Let us define again a *line* on a graph as a path on the graph made of connected edges. For example, in the third picture of the right column of Figure 3.28, you can observe one unconnected node and three *unconnected* lines, one touching four edges and two lines touching three edges each. In the same, in the fifth picture on the left column of Figure 3.29, you can observe four unconnected nodes and one complicated line touching seven nodes. What happens when the origin is included inside the ξ -path, from the point of view of the graphs, is that there are no unconnected lines (i.e., on the graph, it is possible to observe only one line, of variable length).

We remember that, for a certain situation of branch points inclusion, if on the corre-

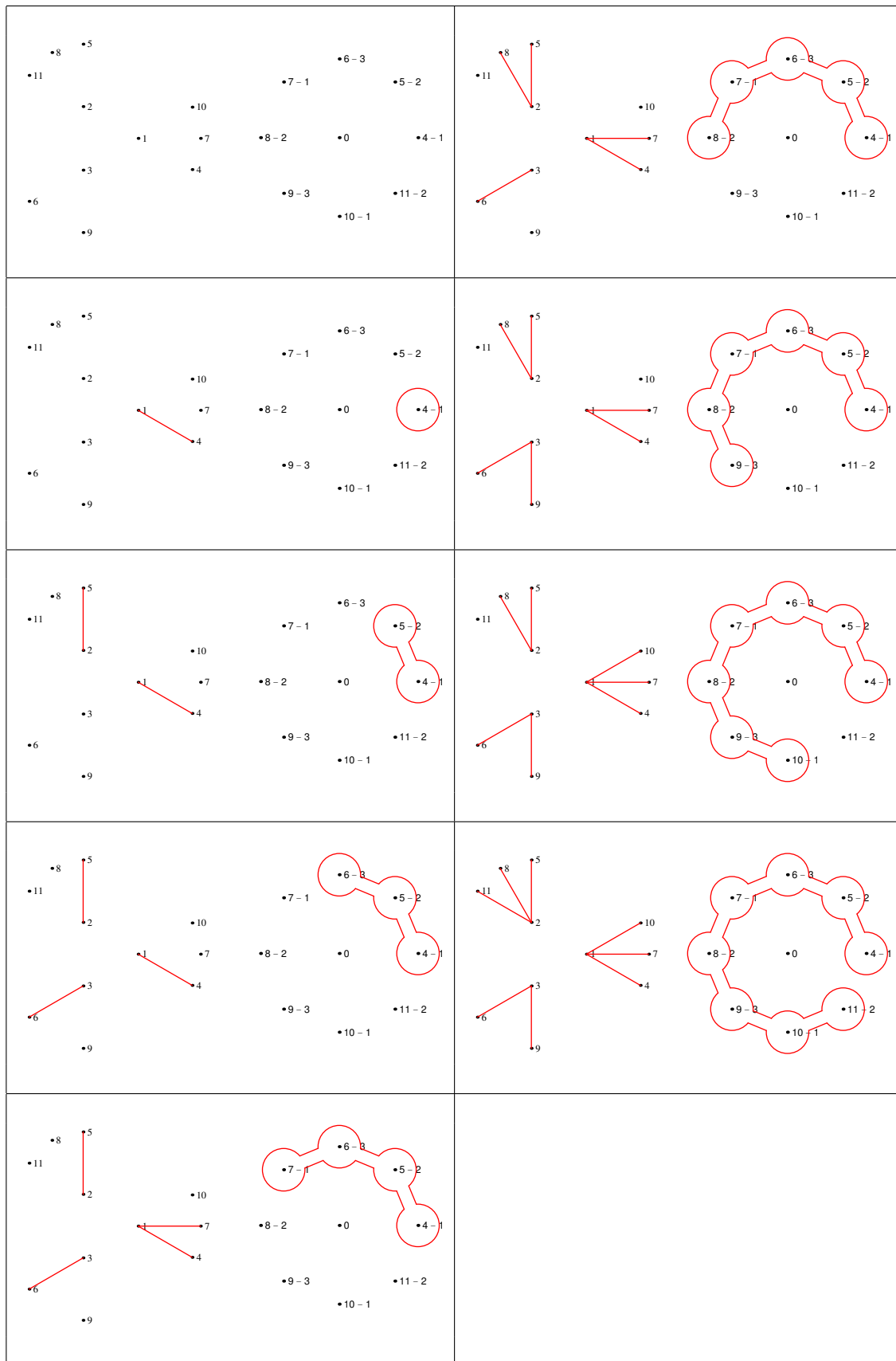


Figure 3.28: Consecutive branch points inclusions ($p = 11, q = 8$, origin outside).

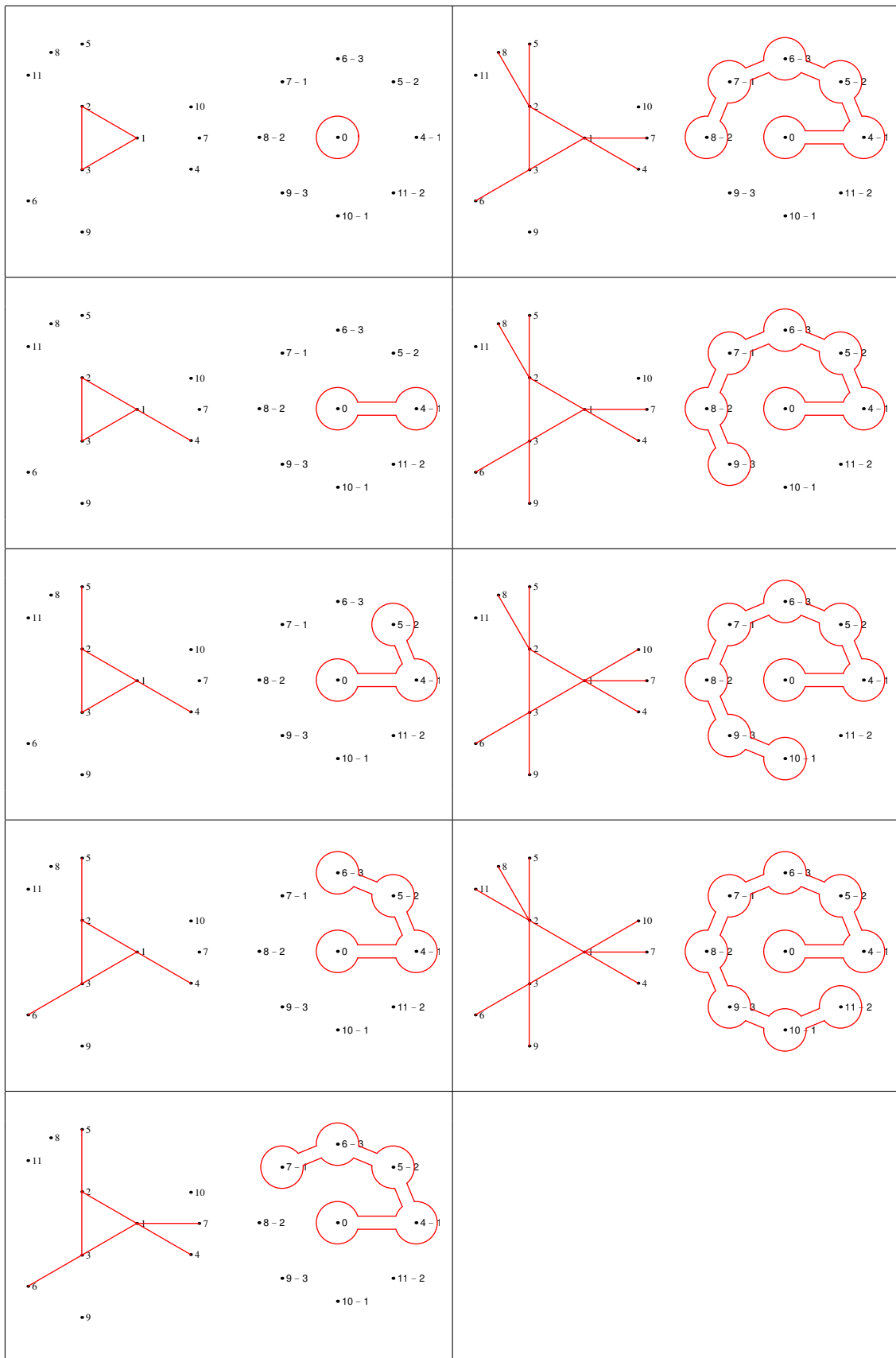


Figure 3.29: Consecutive branch points inclusions ($p = 11, q = 8$, origin inside).

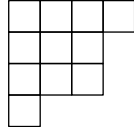


Figure 3.30: Ferrer diagram corresponding to the inclusion of 7 consecutive SRBPs but not of the origin ($p = 11$, $q = 8$).

sponding graph the j -th node is contained in a line which connects exactly b nodes, the period of the corresponding j -th w -root of the algebraic equation (3.65), $w_j(\xi)$, while ξ moves along the closed path, will be exactly b . If the j -th node is unconnected (i.e. it is touched by no edge), the period of $w_j(\xi)$ will be 1.

So, for a certain situation of branch points inclusion, we are interested in measuring the lengths of the lines in the corresponding graph. For such a graph with p nodes (considered at the moment without labels), the set of all the lengths of these lines corresponds to an element of \mathcal{S}_p / \sim , where the equivalence relation \sim is introduced identifying two elements of \mathcal{S}_p if they have the same lengths of the corresponding decompositions in cycles.

For instance, look at the third image on the right column of Figure 3.28. In this situation, it is clear that w_{11} has period 1; w_2, w_3, w_5, w_6, w_8 and w_9 have period 3; w_1, w_4, w_7 and w_{10} have period 4. Precisely, this situation corresponds to the permutation $(1, 4, 7, 10)(2, 5, 8)(3, 6, 9)(11)$, namely a permutation with 1 cycle of length 1, 2 cycles of length 3 and 1 cycle of length 4 (it is sometimes useful to describe this in terms of integer partitions of p : $11 = 4 + 3 + 3 + 1$). So, our graph is in correspondence with all the permutations in \mathcal{S}_p that can be written as 1 cycle of length 1, 2 cycles of length 3 and 1 cycle of length 4. The permutation $(1, 4, 7, 10)(2, 5, 8)(3, 6, 9)(11)$ is an element of the monodromy group. If we do not limit ourselves to consider consecutive inclusions of branch points inside the ξ -path, with this technique we can build the complete monodromy group.

As we did in the case $0 < \mu < 1$, to simplify the description of such graphs we introduce Ferrer diagrams, i.e. dispositions of p blank boxes in rows and columns, such that the number of boxes in each column is equal to the length of the single cycle of the corresponding permutation and the number of columns is the number of cycles in which the permutation is decomposed (for instance, to the situation illustrated by the third image on the right column of Figure 3.28, there corresponds the Ferrer diagram contained in Figure 3.30).

Again, in this way we thereby reduced the problem of knowing the period of a root of the equation (3.65), while ξ moves along a closed path, to the measure of one of the columns of an appropriate Ferrer diagram.

3.2.5 The bumping rules

In the previous Section we showed that, for fixed p and q , a particular Ferrer diagram corresponds to each situation of inclusion of branch points inside a ξ -path. We reduced the problem of knowing the period of the w -roots to finding the degree of connection of the single nodes of a certain graph; from this we reduced once more the problem to knowing the length of the columns of the corresponding Ferrer diagram.

Analogously to what we have done in the case $0 < \mu < 1$, we will show how to recursively build such Ferrer diagrams. To do this we introduce a *bumping rule* for the boxes which compose the diagram itself. Once p and q are fixed, such a rule will describe how a Ferrer diagram associated to the inclusion of b SRBPs inside the ξ -path will change after the introduction of one more branch point, namely, when the ξ -path includes $b + 1$ branch points. In this case it will be not necessary to introduce any recurrence relation nor any description in terms of k -level Ferrer diagrams, but it will be important to distinguish between two subcases, whether the origin is *outside* or *inside* the ξ -path.

Case 1. *Origin outside the ξ -path.* Suppose that the origin is not included inside a ξ -path which includes b square root branch points starting from the one labelled $\{(p - q + 1), 1\}$. If we modify this ξ -path in such a way that it includes the next adjacent square root branch point, $\{p - q + b + 1, (p - q + b + 1) \text{ MÖD } (p - q)\}$, and the origin remains outside, then we must modify also the graph corresponding to the previous situation, adding a new edge between the two nodes $(p - q + b + 1)$ and $(p - q + b + 1) \text{ MÖD } (p - q)$. Since $0 \leq b \leq q$, then each new edge added to the graph will evidently connect a single unconnected node to a line composed by a certain number of edges (at least, to another single unconnected node). Namely, it will never happen that the addition of one more edge will produce the connection between two lines. In terms of Ferrer diagrams, this means that the addition of one more SRBP inside the ξ -path, in case of exclusion of the origin, entails the movement of a single box of the diagram (it never happens that one must move a whole column). The final number of lines in the graph is $(q - p)$, so, in the bumping, we must move orderly single boxes under the first $(p - q)$ columns. See, for instance, Figure 3.31a.

Case 2. *Origin inside the ξ -path.* Suppose that the origin is included inside a ξ -path which includes b square root branch points starting from the one labelled $\{(p - q + 1), 1\}$. Notice that, since the branch point in the origin attaches the $(p - q)$ -sheets, in this case the nodes of the corresponding graph in the inner regular polygon, labelled $1, 2, \dots, (p - q)$, are all connected on a line which contains exactly $(p - q)$ edges. Moreover, notice that the Ferrer diagram corresponding to the inclusion of only the origin has the first column of height $(p - q)$, while all the other q columns of unitary height. Like in case 1, if we modify this ξ -path in such a way that it includes the next adjacent square root branch point, $\{p - q + b + 1, (p - q + b + 1) \text{ MÖD } (p - q)\}$, and the origin remains inside, then we must modify also the graph corresponding to the previous situation, adding a new edge between the two nodes $(p - q + b + 1)$ and $(p - q + b + 1) \text{ MÖD } (p - q)$. Each new edge added to the graph will evidently be connected to the single line that contains all the edges of the graph. In terms of Ferrer diagrams, this means that the addition of one more SRBP inside the ξ -path, in case of inclusion of the origin, entails always the movement of a single box of the diagram under the first column. See, for instance, Figure 3.32a.

All the above considerations lead to the following proposition.

The bumping rule. *In the case in which the ξ -path does not include the origin, the Ferrer diagram, corresponding to the inclusion of b consecutive square root branch points inside the ξ -path, can be obtained from the Ferrer diagram, corresponding to the inclusion of $b - 1$ consecutive square root branch points inside the ξ -path, moving its last box to a lower position, in order to increase the height of one of the first $(p - q)$ columns (while the total amount of boxes still remains the same): such column is the first available one from the left before the $(p - q)$ -th column (included). If all the first $(p - q)$ columns are occupied, the process starts again moving the last box on the right under the first column on the left.*

In the case in which the ξ -path does include the origin, the Ferrer diagram, corresponding to the inclusion of b consecutive square root branch points inside the ξ -path, can be obtained from the Ferrer diagram, corresponding to the inclusion of $b - 1$ consecutive square root branch points inside the ξ -path, moving its last box under the first column, in order to increase its height (while the total amount of boxes still remains the same). The height of the first column is equal to $(p - q)$ when the ξ -path includes only the branch point in the origin.

It is worth stressing here again that we are focalizing only on the case in which we are including consecutive square root branch points, and the first branch point included in the ξ -path is the branch point $\{(p - q + 1), 1\}$.

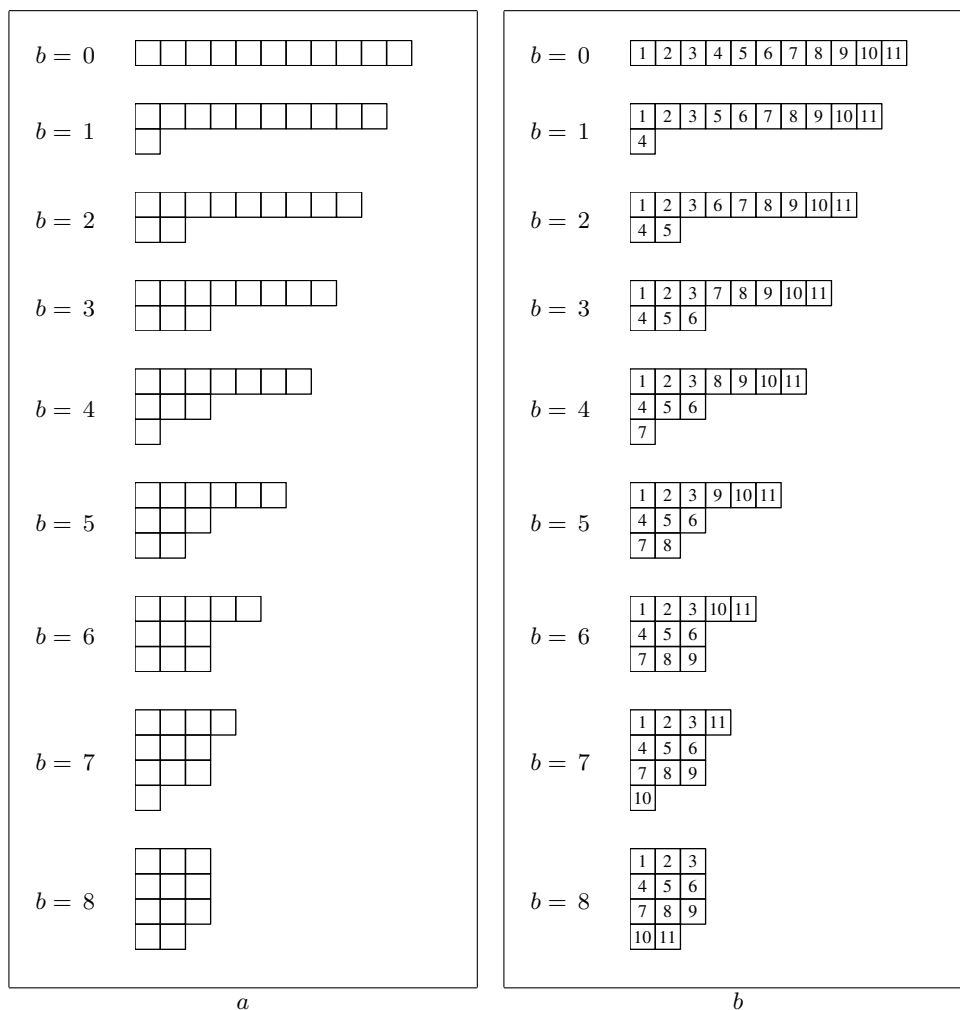


Figure 3.31: Ferrer diagrams for consecutive branch points inclusions ($p = 11$, $q = 8$, origin outside): a) non-numbered Ferrer diagrams; b) numbered Ferrer diagrams.

3.2.6 The period formula for $\mu > 1$ and $\mu \in \mathbb{Q}$

Our final goal is to fix one of the p w -roots of the algebraic equation (3.65) using the enumeration depicted in Subsection 3.2.2 and to predict the period of such root when the variable ξ moves along a closed path which includes b consecutive branch points on the ξ -plane starting from the branch point labelled $\{1, q - p + 1\}$. To achieve this result we must put numbers inside the Ferrer diagrams boxes, in such a way that, if we fix a single column, all the roots labelled with the numbers appearing in the chosen column have the same period, equal to the height of the column itself.

For instance, look at Figure 3.31b when $b = 7$. We can read this image, inferring that the $1 - st$, $4 - th$, $7 - th$ and $10 - th$ roots have period 4; the $2 - nd$, $3 - rd$, $5 - th$, $6 - th$, $8 - th$ and $9 - th$ roots have period 3; the $11 - th$ root has period 1.

Now, let us fix a Ferrer diagram and suppose that there are b square root branch points included in the ξ -circle with $0 \leq b \leq q$. Suppose to be interested in the period of the s -th root. At each inclusion of a consecutive square root branch point, some of the boxes are moved. We are interested in understanding the height of the column contains the box labelled s . Again, we must distinguish between the two cases that depends whether the origin is or is not inside the ξ -path.

Origin outside the ξ -path.

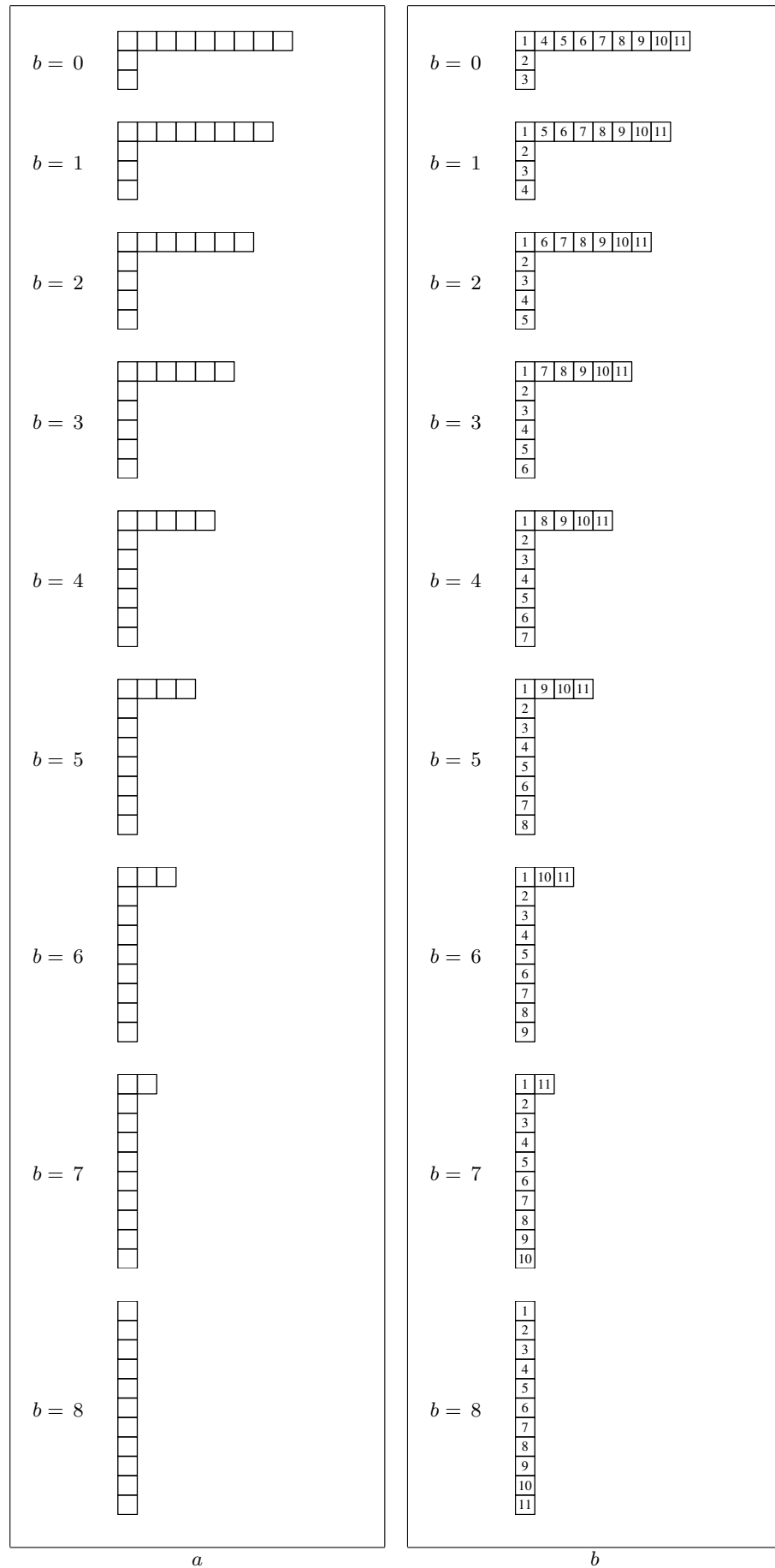


Figure 3.32: Ferrer diagrams for consecutive branch points inclusions ($p = 11, q = 8$, origin inside): a) non-numbered Ferrer diagrams; b) numbered Ferrer diagrams.

Case 1: If $s > b + p - q$ then we have that the column we are interested in has height 1 and it has not been moved with respect to the position it occupied when no square root branch points were included in the ξ -circle.

Case 2: If $s \leq b + p - q$ then we must consider two subcases:

- If $s \leq p - q$ then s is the label of the first box of one of the s -th column. The number of single boxes moved under the column s depends whether s is smaller than $b \text{ MÖD } (p - q)$ or not. If $s < b \text{ MÖD } (p - q)$ then the number of boxes moved under the s -th column is $(\lfloor \frac{b-1}{p-q} \rfloor)$. If $s \geq b \text{ MÖD } (p - q)$ then one more single box moved under the s -th column, so the final number of moved boxes is $(\lfloor \frac{b-1}{p-q} \rfloor + 1)$.
- If $s > p - q$ then the column s has been moved under the column $s \text{ MÖD } (p - q)$. The total number of boxes moved under the column $s \text{ MÖD } (p - q)$ depends whether $s \text{ MÖD } (p - q)$ is smaller than $b \text{ MÖD } (p - q)$ or not. If $s \text{ MÖD } (p - q) < b \text{ MÖD } (p - q)$ then the number of boxes moved under the column $s \text{ MÖD } (p - q)$ is $(\lfloor \frac{b-1}{p-q} \rfloor)$. If $s \text{ MÖD } (p - q) \geq b \text{ MÖD } (p - q)$ then one more single box moved under the column $s \text{ MÖD } (p - q)$, so the final number of moved boxes is $(\lfloor \frac{b-1}{p-q} \rfloor + 1)$.

Origin inside the ξ -path.

Case 1: If $s > b + p - q$ then we have that the column we are interested in has height 1 and it has not been moved with respect to the position it occupied when no square root branch points were included in the ξ -circle.

Case 2: If $s \leq b + p - q$ then s is the label of the s -th box in the first column. The height of the first column is $b + p - q$.

From the above considerations, we finally infer the following

Theorem 3. *Be $\mu > 1$ and $\mu \in \mathbb{Q}$. Be the roots of the algebraic equation (3.65) labelled following the description of Subsection 3.2.2. Let $T(s, b)$ be the period of the s -th root of the algebraic equation (3.65) when ξ moves along a closed path on the ξ -plane, including b consecutive adjacent square root branch points starting from the branch point with label $\{p - q + 1, 1\}$. If the origin is not included inside the closed path along which ξ moves, we have the following period formula:*

$$T(s, b) = \begin{cases} \left\lfloor \frac{b-1}{p-q} \right\rfloor + 1 & \text{if } s \leq b + p - q \\ & \text{and } b \text{ MÖD } (p - q) < s \text{ MÖD } (p - q) \\ \left\lfloor \frac{b-1}{p-q} \right\rfloor + 2 & \text{if } s \leq b + p - q \\ & \text{and } b \text{ MÖD } (p - q) \geq s \text{ MÖD } (p - q) \\ 1 & \text{if } s > b + p - q ; \end{cases} \quad (3.75)$$

while, if the origin is included inside the closed path along which ξ moves, we have the following period formula:

$$T(s, b) = \begin{cases} b + p - q & \text{if } s \leq b + p - q \\ 1 & \text{if } s > b + p - q . \end{cases} \quad (3.76)$$

Formula (3.75) tells that, for any situation of consecutive SRBPs inclusion with the origin outside the ξ -path, generically we have only three possible periods for the roots of the algebraic equation (3.65). The sum of the first and the third of the (3.75) gives always the second. Formula (3.76) tells that, for any situation of consecutive SRBPs inclusion with the origin inside the ξ -path, generically we have only two possible periods for the roots of the algebraic equation (3.65).

For instance, in the following tables you can compare the values of $T(s, b)$ when $p = 11$ and $q = 8$ for $1 \leq s \leq p$ and $0 \leq b \leq q$.

$T(s, b)$	1	2	3	4	5	6	7	8	9	10	11
$b = 0$	1	1	1	1	1	1	1	1	1	1	1
$b = 1$	2	1	1	2	1	1	1	1	1	1	1
$b = 2$	2	2	1	2	2	1	1	1	1	1	1
$b = 3$	2	2	2	2	2	2	1	1	1	1	1
$b = 4$	3	2	2	3	2	2	3	1	1	1	1
$b = 5$	3	3	2	3	3	2	3	3	1	1	1
$b = 6$	3	3	3	3	3	3	3	3	3	1	1
$b = 7$	4	3	3	4	3	3	4	3	3	4	1
$b = 8$	4	4	3	4	4	3	4	4	3	4	4

Origin outside the ξ -path

$T(s, b)$	1	2	3	4	5	6	7	8	9	10	11
$b = 0$	3	3	3	1	1	1	1	1	1	1	1
$b = 1$	4	4	4	4	1	1	1	1	1	1	1
$b = 2$	5	5	5	5	5	1	1	1	1	1	1
$b = 3$	6	6	6	6	6	6	1	1	1	1	1
$b = 4$	7	7	7	7	7	7	7	1	1	1	1
$b = 5$	8	8	8	8	8	8	8	8	1	1	1
$b = 6$	9	9	9	9	9	9	9	9	9	1	1
$b = 7$	10	10	10	10	10	10	10	10	10	10	1
$b = 8$	11	11	11	11	11	11	11	11	11	11	11

Origin inside the ξ -path

3.2.7 The irrational case: $\mu \notin \mathbb{Q}$

Like in Section 3.1, we can treat the case in which μ is an *irrational* number as a limit of the case in which μ is a rational number. When μ is irrational, the number of roots of the equation (3.64) diverges, as q , number of branch points on the ξ -plane, approaches infinity. So we must analyze the previous formulas in the limit:

$$p, q \rightarrow \infty \text{ with } \mu = \frac{p}{q} > 1 . \tag{3.77}$$

namely in the limit in which the integers p and q diverge with their ratio μ fixed.

If μ is an irrational number, it follows that the Riemann surface Γ (3.64) becomes an ∞ -sheeted covering of the complex ξ plane. Like in Subsection (3.2.1), we can analyze its behavior for $|\xi| \gg 1$, $|\xi| \ll 1$ and its branch points:

1) $\xi = \infty$. If $|\xi| \gg 1$, we have the asymptotics:

$$w(\xi) \sim -(-\xi)^{-\frac{1}{\mu}}, \xi \sim \infty. \tag{3.78}$$

Therefore, for $|\xi| \gg 1$, all the (infinite) roots lie on a small circle of radius $O(|\xi|^{-\frac{1}{\mu}})$ centered at the origin, and a counterclockwise 2π -rotation of ξ on a big circle implies a clockwise rotation of each root around the origin of the angle $(2\pi/\mu)$.

2) $\xi = 0$. If $|\xi| \ll 1$, we have the asymptotics:

$$w(\xi) \sim 1 + \xi^{\frac{1}{\mu-1}}, \quad \xi \sim 0. \quad (3.79)$$

Therefore we have an infinite number of roots lying on a small circle of radius $O(|\xi|^{\frac{1}{\mu-1}})$ around 1. There still remains an infinite number of roots lying on a big circle of radius $O(|\xi|^{-1})$ around the origin in the w -plane.

3) In the finite part, we have an infinite number of SRBPs densely distributed on the circle centered at the origin of the ξ -plane and of radius

$$r_b = \frac{1}{\mu-1} \left(\frac{\mu-1}{\mu} \right)^\mu > 0; \quad (3.80)$$

Again, each of the infinite SRBPs corresponds to the collision of a pair of roots.

Finally, to obtain the proper continuous variable which replaces the discrete index b , we will make use of the same variable ν introduced in Section 3.1. We focalize our attention to the physical situation in which the ξ -path is a circle. Let be B the circle on which the SRBPs lie and Ξ the circle along which the ξ variable periodically moves. We define the variable ν , which is 0 if Ξ does not contain any arc of B and 1 if Ξ does contain the whole circle B . If B and Ξ intersect, select the arc of the B circle which is contained inside the evolutionary circle Ξ and denote by ν the corresponding angle ϕ , normalized by 2π (see Figure 3.15 and formula (3.45)).

We can restate the theorem in Subsection 3.2.6 as following.

Theorem 4. *Be $\mu > 1$ and $\mu \notin \mathbb{Q}$. Let $T(\nu)$ be the period of one of the roots of the algebraic equation (3.64) when ξ moves along a circular path Ξ on the ξ -plane, intersecting the SRBPs circle B in such a way that $0 \leq \nu < 1$ (see (3.45)). If the origin is not included inside the closed path along which ξ moves and $\nu = 0$, then $T(\nu) = 1$. If the origin is not included and $\nu > 0$, then $T(\nu)$ must have one of the following three values:*

$$T(\nu) = \begin{cases} \left\lfloor \frac{\nu}{\mu-1} \right\rfloor + 1 \\ \left\lfloor \frac{\nu}{\mu-1} \right\rfloor + 2 \\ 1 \end{cases}. \quad (3.81)$$

If the origin is included inside the closed path along which ξ moves and $\nu = 0$, then $T(\nu) = 1$ or the time evolution of the generic root of the equation (3.64) is quasiperiodic, involving a (nonlinear) superposition of two noncongruent periods, 1 and $\frac{1}{\mu-1}$. If the origin is included inside the closed path along which ξ moves $\nu > 0$, then $T(\nu) = 1$ or time evolution of the generic root of the equation (3.64) is aperiodic.

Notice that, like before, the sum of the first and the third in the previous formula (3.81) always gives the second. It is worth noticing that, in the case of validity of formula (3.81), if $\mu > 2$ it happens that the floor function in (3.81) vanishes, and the only possible values for $T(\nu)$ are 1 or 2. We must stress that in this case there are no labels for the roots, so we cannot assign the three periods to the roots in terms of their labels as we did in the rational case.

3.3 The case $\mu < 0$

Here we study the Riemann surface Γ consisting of points $(\xi, w) \in \Gamma$ such that:

$$w^{-\mu}(w-1)^{\mu-1} = \xi, \quad (3.82)$$

where

$$\mu = \frac{p}{q} < 0, \text{ with } p < 0 < q,$$

and $|p| \in \mathbb{N}$ and $q \in \mathbb{N}^+$ are coprime natural numbers. Therefore Γ is an *algebraic* Riemann surface characterized by the polynomial (of degree $q + |p|$) equation

$$\xi^q (w-1)^{q+|p|} = w^{|p|}, \quad p < 0 < q, \quad (3.83)$$

which now defines the $(q + |p|)$ -valued function $w = w(\xi)$. Since, $\forall \xi \in \mathbb{C}$, the polynomial (3.83) admits $q + |p|$ complex roots and each root corresponds to a sheet of the Riemann surface Γ , it follows that Γ is a p -sheeted covering of the complex ξ plane.

3.3.1 The period formula for $\mu < 0$

Clearly, the case $\mu < 0$ becomes identical to the case illustrated in the previous section ($\mu > 1$) via the following replacement

$$w \mapsto 1 - w, \quad \xi \mapsto -\xi, \quad -p \mapsto p - q, \quad q - p \mapsto p \quad (3.84)$$

without modifying q . So, via this prescription (3.84), we automatically get all the results for the case $\mu < 0$ directly from the findings presented in the final subsections of Section 3.2.

Theorem 5. *Be $\mu < 0$ and $\mu \in \mathbb{Q}$. Be the roots of the algebraic equation (3.83) labelled following the description of Subsection 3.2.2 (making use of the replacement (3.84)). Let $T(s, b)$ be the period of the s -th root of the algebraic equation (3.83) when ξ moves along a closed path on the ξ -plane, including b consecutive adjacent square root branch points starting from the branch point with label $\{|p| + 1, 1\}$. If the origin is not included inside the closed path along which ξ moves, we have the following period formula:*

$$T(s, b) = \begin{cases} \left\lfloor \frac{b-1}{|p|} \right\rfloor + 1 & \text{if } s \leq b + |p| \\ & \text{and } b \text{ M\O{D} } |p| < s \text{ M\O{D} } |p| \\ \left\lfloor \frac{b-1}{|p|} \right\rfloor + 2 & \text{if } s \leq b + |p| \\ & \text{and } b \text{ M\O{D} } |p| \geq s \text{ M\O{D} } |p| \\ 1 & \text{if } s > b + |p| ; \end{cases} \quad (3.85)$$

while, if the origin is included inside the closed path along which ξ moves, we have the following period formula:

$$T(s, b) = \begin{cases} b + |p| & \text{if } s \leq b + |p| \\ 1 & \text{if } s > b + |p|. \end{cases} \quad (3.86)$$

Formula (3.85) tells that, for any situation of consecutive SRBPs inclusion with the origin outside the ξ -path, generically we have only three possible periods for the roots of the algebraic equation (3.83). The sum of the first and the third of the (3.85) gives always the

second. Formula (3.86) tells that, for any situation of consecutive SRBPs inclusion with the origin inside the ξ -path, generically we have only two possible periods for the roots of the algebraic equation (3.83).

Like in Section 3.1, we can treat the case in which μ is an *irrational* number as a limit of the case in which μ is a rational number. When μ is irrational, the number of roots of the equation (3.82) diverges, as q , number of branch points on the ξ -plane, approaches infinity. So we must analyze the previous formulas in the limit:

$$p, q \rightarrow \infty \quad \text{with} \quad \mu = \frac{p}{q} < 0 \quad . \quad (3.87)$$

namely in the limit in which the integers p and q diverge with their ratio μ fixed.

If μ is an irrational number, it follows that the Riemann surface Γ (3.82) becomes an ∞ -sheeted covering of the complex ξ -plane.

To enunciate the period formula, we need a proper continuous variable. Again, we will make use of the same variable ν introduced in Section 3.1 (see Figure 3.15 and formula (3.45)).

Theorem 6. *Be $\mu < 0$ and $\mu \notin \mathbb{Q}$. Let $T(\nu)$ be the period of one of the roots of the algebraic equation (3.82) when ξ moves along a circular path Ξ on the ξ -plane, intersecting the SRBPs circle B in such a way that $0 \leq \nu < 1$ (see (3.45)). If the origin is not included inside the closed path along which ξ moves and $\nu = 0$, then $T(\nu) = 1$. If the origin is not included and $\nu > 0$, then $T(\nu)$ must have one of the following three values:*

$$T(\nu) = \begin{cases} \left\lfloor \frac{\nu}{|\mu|} \right\rfloor + 1 \\ \left\lfloor \frac{\nu}{|\mu|} \right\rfloor + 2 \\ 1 \quad . \end{cases} \quad (3.88)$$

If the origin is included inside the closed path along which ξ moves and $\nu = 0$, then $T(\nu) = 1$ or the time evolution of the generic root of the equation (3.82) is quasiperiodic, involving a (nonlinear) superposition of two noncongruent periods, 1 and $\frac{1}{|\mu|}$. If the origin is included inside the closed path along which ξ moves $\nu > 0$, then $T(\nu) = 1$ or time evolution of the generic root of the equation (3.82) is aperiodic.

Notice that, like before, the sum of the first and the third in the previous formula (3.88) always gives the second. It is worth noticing that, in the case of validity of formula (3.88), if $\mu < -1$ it happens that the floor function in (3.81) vanishes, and the only possible values for $T(\nu)$ are 1 or 2. We must stress that in this case there are no labels for the roots, so we cannot assign the three periods to the roots in terms of their labels as we did in the rational case.

CHAPTER 4

Complex Dynamics

In Chapter 2 we introduced the new three-body Aristotelian model (2.10) and we showed that the problem of understanding its physical behavior (at least in the “semisymmetrical” case, see (2.2)) – characterized by a huge variety of *regular* and *irregular* motions – was strictly connected to the problem of understanding the (*branching*) structure of the Riemann surface Γ associated to the non-differential equation (2.98) in which appears the fundamental parameter μ . In Chapter 3 we illustrated how the analysis of Γ is possible and we reported several results about the periods of the roots of equation (2.98), in both cases of *rational* and *irrational* μ .

In this chapter we come back to our physical problem (2.10) and we discuss the implications of the findings reported in Chapter 3. We explain the transition from regular to irregular motions (as travels on the Riemann surface Γ) and in which sense the model treated herein displays a *sensitive dependance* on the initial conditions and on the parameters. In the final section we will discuss the generality of our findings and some remaining open questions.

The results reported herein mainly refers to [1] and [3], both papers co-written by the author of this thesis in collaboration with F. Calogero, D. Gomez-Ullate and P. M. Santini.

4.1 Root behavior in terms of the initial conditions

In Section 2.6 we proved that the solution of our model (2.10) in the “semisymmetrical” case, (2.2), can be written in terms of the function $\check{w}(t)$, (2.112), which is defined via the relation

$$\check{w}(t) = w[\xi(t)], \quad (4.1)$$

with

$$\xi(t) = R[\eta + \exp(2i\omega t)] = \bar{\xi} + R \exp(2i\omega t), \quad (4.2)$$

and $w(\xi)$ implicitly defined by the *nondifferential* equation

$$(w - 1)^{\mu-1} w^{-\mu} = \xi. \quad (4.3)$$

The parameter μ is defined in terms of the coupling constants g and f , see (2.2), while R and $\bar{\xi}$ are defined in terms of the three initial data $z_1(0)$, $z_2(0)$ and $z_3(0)$, see (2.114) and

(2.115),

$$\begin{aligned}
Z &= \frac{z_1(0) + z_2(0) + z_3(0)}{3} , \\
R &= \frac{3(f + 8g)}{2i\omega [2z_3(0) - z_1(0) - z_2(0)]^2} \left[1 - \frac{1}{\tilde{w}(0)} \right]^{\mu-1} , \\
\bar{\xi} &= R\eta , \\
\eta &= \frac{i\omega \left\{ [z_1(0) - z_2(0)]^2 + [z_2(0) - z_3(0)]^2 + [z_3(0) - z_1(0)]^2 \right\}}{3(f + 2g)} - 1 , \\
\tilde{w}(0) &= \frac{2\mu [2z_3(0) - z_1(0) - z_2(0)]^2}{[z_1(0) - z_2(0)]^2 + [z_2(0) - z_3(0)]^2 + [z_3(0) - z_1(0)]^2} .
\end{aligned}$$

In Chapter 3 we studied the *curve* (4.3) with ξ moving on a *generic circular* closed path on the corresponding Riemann surface. As we have seen, it results that, if μ is *rational*, namely $\mu = p/q$, the nondifferential equation (4.3) becomes *polynomial* (in the dependent variable w), of finite degree J , with $J = p$ if $\mu > 1$, $J = q$ if $0 < \mu < 1$ or $J = q + |p|$ if $\mu < 0$. From the topological point of view, the nondifferential equation (4.3) defines a J -sheeted covering of the *complex* ξ -plane of genus *zero* (of course $J = \infty$ if μ is irrational). The function $w(\xi)$ defined implicitly by this equation features *square-root* branch points ξ_b located on a circle B centered at the origin of the *complex* ξ -plane (see 2.103):

$$\begin{aligned}
\xi_b &= \xi_b^{(k)} = r_b \exp(2\pi i \mu k) , \quad k = 1, 2, 3, \dots , \\
\xi_b &= \xi_b^{(k)} = r_b \exp \left[i \frac{2\pi p k}{q} \right] , \quad k = 1, 2, \dots, q , \\
r_b &= (\mu - 1)^{-1} \left(\frac{\mu - 1}{\mu} \right)^\mu .
\end{aligned}$$

We find out that, for ξ moving on a *circular* path (which includes consecutive branch points on the Riemann surface Γ), *all* the J roots have at most three different periods (one of which might be *infinite*).

It is worth recalling now that the question of identifying, among *all* the roots $\tilde{w}_j(t)$ of this *nondifferential* equation (4.3), the “physical” one $\tilde{w}(t)$, i. e. the one that evolves from the initial datum (2.115) and in particular of specifying the character of its time evolution among the (at most 3) alternatives, is a problem whose solution was still not found at the time this thesis is written and that is object of further researches (see [2]). Let us re-emphasize that the time evolution of $\tilde{w}(t) \equiv w[\xi(t)]$ coincides with the evolution of a *generic* root $w(\xi)$ of (4.3) as the independent variable ξ travels (making a complete counterclockwise tour in the *complex* ξ -plane in every time interval $T = \pi/\omega$, see (2.8)) on the circle Ξ with center $\bar{\xi}$ and radius $|R|$, see (4.2), and correspondingly the dependent variable $w(\xi)$ travels on its Riemann surface Γ .

In Chapter 3 we proved that eventually after a time $\tilde{T} = \tilde{j}T$ which is a *finite integer* multiple \tilde{j} of the basic period T , with $1 \leq \tilde{j} \leq J$, the *generic* root $\tilde{w}(t)$ shall necessarily return to its initial position, $\tilde{w}(\tilde{T}) = \tilde{w}(0)$, entailing that its evolution as a function of the time t is *periodic* with this period \tilde{T} ,

$$\tilde{w}(t + \tilde{T}) \equiv \tilde{w}(t + \tilde{j}T) = \tilde{w}(t) . \quad (4.4)$$

It is clear from 2.112 that the time evolution of the solution $z_n(t)$ of our model (2.10) is *mainly* determined by the time evolution of the function $\tilde{w}(t)$.

Clearly, $\xi = [\bar{\xi} + R \exp(2i\omega t)]^q$ carries all the time dependence in equation 4.3. But the factor $[\eta \exp(-2i\omega t) - 1]^{1/2}$ displays a quite simple time evolution, *periodic* with period T if $|\eta| < 1$ and *antiperiodic* with period T hence *periodic* with period $2T$ if $|\eta| > 1$. If $\check{w}(t)$ is *periodic* with period \check{T} , its square root $[\check{w}(t)]^{1/2}$, appearing in the right-hand side of the solution formulas (13), is clearly as well *periodic* with period \check{T} or *antiperiodic* with period \check{T} hence *periodic* with period $2\check{T}$ depending whether the closed trajectory of $\check{w}(t)$ in the complex \check{w} -plane does not or does enclose the (branch) point $\check{w} = 0$. Likewise the square root $[12\mu - 3\check{w}(t)]^{1/2}$ (see (2.112)) is also *periodic* with period \check{T} or *antiperiodic* with period \check{T} hence *periodic* with period $2\check{T}$ depending whether the closed trajectory of $\check{w}(t)$ in the complex \check{w} -plane does not or does enclose the (branch) point $\check{w} = 4\mu$ (but note that a change of sign of this square root only entails an exchange between the two equal particles 1 and 2). In conclusion one sees that – provided one considers particles 1 and 2 as *indistinguishable* – then, if the time evolution of $\check{w}(t)$ is *periodic* with period \check{T} , $\check{w}(t + \check{T}) = \check{w}(t)$, the physical motion of the 3 particles $z_n(t)$ is also *completely periodic* either with the same period \check{T} or with period $2\check{T}$, provided \check{T} is an *integer multiple* of T ; finally, if the motion of $\check{w}(t)$ is not periodic then clearly the functions $z_n(t)$ are also not periodic.

In the case of a *rational* value of the parameter μ , *all* solutions of our physical problem (2.10) with (2.2) are *completely periodic* with a period which is either

$$\check{T} = \check{j}T \quad \text{with } 1 \leq \check{j} \leq J \quad (4.5)$$

or it is $2\check{T}$.

In this section we will try to understand, starting from the findings reported in Chapter 3 how the value of the integer \check{j} (which might be *quite large* if J is *quite large*) depends on the initial data of our problem.

4.1.1 The two circles B and Ξ

In this subsection we list all our findings concerning the time evolution of a generic root $\check{w}(t)$, when ξ moves not along a *generic* circular path Ξ , but along the circular path Ξ fixed by the initial conditions, see (4.2). We refer at first mainly to the *rational* case but including immediately results for the *irrational* case whenever it is convenient to do so in order to shorten our presentation. The remaining information on the *irrational* case is provided below (see Proposition 9).

Before starting, we recall that we define *active* branch points those branch points that cause a reshuffling of roots that involves the “physical” root $\check{w}(t)$, while the *inactive* ones are those that do *not* cause a reshuffling of roots that involves the “physical” root $\check{w}(t)$, either because they cause no reshuffling at all being located *outside* the relevant circle (Ξ in the *complex* ξ -plane in the context of the present analysis, C in the *complex* τ -plane in the context of the discussion made above when the distinction among *active* and *inactive* branch points was first introduced, see Chapter 2), or because they cause a reshuffling which however does not involve the physical root $\check{w}(t)$.

First of all it is useful to visualize the two circles B and Ξ in the *complex* ξ -plane (draw them!): recall that the circle B on which the branch points sit is centered at the origin and its radius $|r_b|$ only depends on the parameter μ see (2.103), while both the center $\bar{\xi}$ and the radius $|R|$ of the circle Ξ traveled upon by $\xi(t)$ see (4.2), *do depend* on the initial data, see (2.114) and (2.115).

Proposition 1. *If the circle Ξ is inside the circle B (i. e. $|\bar{\xi}| + |R| < |r_b|$, see (2.114), (2.115) and (2.103)), and (a) μ is inside the interval $0 < \mu < 1$ or (b) μ is outside this interval ($\mu > 1$ or $\mu < 0$) and moreover the circle Ξ does not include the origin $\xi = 0$ (i. e. $|R| < |\bar{\xi}|$)*

or equivalently $|\eta| > 1$), then $\tilde{j} = 1$, i. e. the generic solution $\tilde{w}(t)$ is periodic with period T , $\tilde{w}(t+T) = \tilde{w}(t)$. This outcome applies equally if μ is rational or irrational.

Remark 2. In all the cases identified in this Proposition 1 there are no branch points at all inside the circle Ξ : indeed the outcome detailed by this Proposition 1 applies in all the cases in which this happens (see our discussion above), even (in the case with rational μ) if the circles B and Ξ do cross each other marginally; and of course in all these cases all the roots $\tilde{w}_j(t)$ are periodic with period T , and in the context of the physical problem (2.10) the solution is characterized by the simple periodicity rule (2.12). The restriction (1.29) on the initial data is sufficient (but of course not necessary) to guarantee that we are in this regime.

Proposition 3. If the circle Ξ is inside the circle B (i. e. $|\bar{\xi}| + |R| < |r_b|$), the circle Ξ does include the origin $\xi = 0$ (i. e. $|R| > |\bar{\xi}|$ or equivalently $|\eta| < 1$), and μ is outside the interval $0 < \mu < 1$ then in the rational case, see (2.26),

$$(a) \tilde{j} = 1 \text{ or } \tilde{j} = p - q \text{ if } \mu > 1$$

$$(b) \tilde{j} = 1 \text{ or } \tilde{j} = |p| \text{ if } \mu < 0.$$

In the irrational case the time evolution of the generic root $\tilde{w}(t)$ is either periodic with the basic period T , or quasiperiodic, involving in particular a (nonlinear) superposition of two periodic evolutions with two noncongruent periods, specifically (a) with period T and $\frac{T}{\mu-1}$ if $\mu > 1$, (b) with period T and $\frac{T}{|\mu|}$ if $\mu < 0$.

Remark 4. In the case identified in this Proposition 3 the only branch point inside Ξ is that at $\xi = 0$, which is indeed only present if $\mu > 1$ or $\mu < 0$. Hence in the rational case with $p > q$ (i. e. $\mu > 1$), $p - q$ roots $\tilde{w}_j(t)$ get cyclically exchanged among themselves, entailing that the time evolution of each of them has period $(p - q) T$, while the remaining q roots have period T ; with an analogous phenomenology in the $\mu < 0$. Likewise, when μ is irrational, the periodicity of the time evolution of the generic root $\tilde{w}(t)$ has period T if the branch point at $\xi = 0$ is inactive (i. e., it does not appear on the sheet on which $\tilde{w}(0)$ lives), otherwise its time evolution can be inferred by replacing ξ with $\xi(t)$, see (4.2), in the formula characterizing the branch point at $\xi = 0$, see Chapter 3. Note however that for the special initial data such that the two circles B and Ξ are concentric (i. e., $\eta = 0$) the quasiperiodic time evolution of $\tilde{w}(t)$ is instead periodic (a) with period $\frac{T}{\mu-1}$ if $\mu > 1$, (b) with period $\frac{T}{|\mu|}$ if $\mu < 0$.

Proposition 5. If the circle Ξ is outside the circle B (i. e. $|R| > |\bar{\xi}| + |r_b|$) then in the rational case, see (2.26),

$$(a) \tilde{j} = p \text{ if } \mu > 1,$$

$$(b) \tilde{j} = q - p = q + |p| \text{ if } \mu < 0$$

$$(c) \tilde{j} = p \text{ or } \tilde{j} = q - p \text{ if } 0 < \mu < 1.$$

In the irrational case the time evolution of the generic root $\tilde{w}(t)$ is quasiperiodic, involving a (nonlinear) superposition of two periodic evolutions with two noncongruent periods, specifically

$$(a) \text{ with periods } T \text{ and } \frac{T}{\mu} \text{ if } \mu > 1,$$

$$(b) \text{ with periods } T \text{ and } \frac{T}{1-\mu} \text{ if } \mu < 0,$$

$$(c) \text{ with periods } T \text{ and } \frac{T}{\mu} \text{ or } T \text{ and } \frac{T}{1-\mu} \text{ if } 0 < \mu < 1.$$

Remark 6. In all the cases encompassed in this Proposition 5 the branch points of $w(\xi)$ in the *finite* part of the *complex* ξ -plane are *all inside* the circle Ξ , hence the dynamics of the roots $\tilde{w}_j(t)$ can be understood in terms of the branch point of $w(\xi)$ at $\xi = \infty$. Therefore in the *rational* case with $p > q$ (i. e. $\mu > 1$) *all* the p roots get cyclically exchanged, so that each of them gets back to its original value after a period pT ; likewise if $p < 0$ (i. e. $\mu < 0$) *all* the $q + |p|$ roots get cyclically exchanged, so that each of them gets back to its original value after a period $(q + |p|)T$. In the other *rational* case, $0 < p < q$ (i. e. $0 < \mu < 1$), p roots get cyclically exchanged among themselves, and the remaining $q - p$ roots get cyclically exchanged among themselves, so that the *generic* root $\tilde{w}(t)$ has period pT if it belongs to the first set, and $(q - p)T$ if it belongs to the second. And the outcome in the *irrational* case can as well be understood in terms of the exponent of the branch point at $\xi = \infty$, see Subsections 3.1.1 and 3.2.1.

The situation is less straightforward (hence more interesting) if the two circles B and Ξ *do intersect* each other (i. e. $|\bar{\xi}| - |R| < |r_b| < |\bar{\xi}| + |R|$). Then the parameter that plays a crucial role is the number b of *square-root* branch points, sitting on the circle B , that fall *inside* the circle Ξ . This number b is *finite*, $1 \leq b \leq q$ (note that the case $b = 0$ is taken care of by Proposition 1) only in the *rational* case, to which we restrict consideration in the following Proposition 7 (and we exclude from consideration the *nongeneric* case in which the circle Ξ hits one of the branch points sitting on the circle B). Then *two* or *three* (but no more!) different alternatives are possible for the value of the *positive integer* \tilde{j} , as detailed below.

Hereafter the notation $\lfloor x \rfloor$ denotes the *floor* of the *real* number x , namely the *largest integer number not larger than* x (hence for instance $\lfloor -0.3 \rfloor = -1$, $\lfloor 0 \rfloor = 0$).

Proposition 7. (i). If $p > q$ (i. e. $\mu > 1$, see (2.26)) and the origin $\xi = 0$ is outside the circle Ξ (i. e. $|\eta| > 1$), then \tilde{j} can take one of the following 3 values:

$$\tilde{j} = 1 \quad \text{or} \quad \tilde{j} = \left\lfloor \frac{b-1}{p-q} \right\rfloor + 1 \quad \text{or} \quad \tilde{j} = \left\lfloor \frac{b-1}{p-q} \right\rfloor + 2. \quad (4.6)$$

(ii). If $p > q$ (i. e. $\mu > 1$, see (2.26)) and the origin $\xi = 0$ is inside the circle Ξ (i. e. $|\eta| < 1$), then \tilde{j} can take one of the following 2 values:

$$\tilde{j} = 1 \quad \text{or} \quad \tilde{j} = b + p - q. \quad (4.7)$$

(i'). If $p < 0$ (i. e. $\mu < 0$, see (2.26)) and the origin $\xi = 0$ is outside the circle Ξ (i. e. $|\eta| > 1$), then \tilde{j} can take one of the following 3 values:

$$\tilde{j} = 1 \quad \text{or} \quad \tilde{j} = \left\lfloor \frac{b-1}{|p|} \right\rfloor + 1 \quad \text{or} \quad \tilde{j} = \left\lfloor \frac{b-1}{|p|} \right\rfloor + 2. \quad (4.8)$$

(ii'). If $p < 0$ (i. e. $\mu < 0$, see (2.26)) and the origin $\xi = 0$ is inside the circle Ξ (i. e. $|\eta| < 1$), then \tilde{j} can take one of the following 2 values:

$$\tilde{j} = 1 \quad \text{or} \quad \tilde{j} = b + |p|. \quad (4.9)$$

(iii). The situation is more intriguing if $0 < p < q$ (i. e., $0 < \mu < 1$, see (2.26)). Then one must introduce the simple continued fraction expansion of the number

$$\frac{q}{q-p} = \frac{1}{1-\mu} = a_0 + \frac{1}{a_1 + \frac{1}{a_2 + \dots}}. \quad (4.10)$$

The k th convergent C_k of this continued fraction expansion (4.10), and in particular its numerator P_k and denominator Q_k ,

$$C_k = \frac{P_k}{Q_k}, \quad (4.11)$$

are then defined by the recursions

$$P_k = a_k P_{k-1} + P_{k-2}, \quad P_{-2} = 0, \quad P_{-1} = 1, \quad k = 0, 1, 2, \dots \quad (4.12)$$

$$Q_k = a_k Q_{k-1} + Q_{k-2}, \quad Q_{-2} = 1, \quad Q_{-1} = 0, \quad k = 0, 1, 2, \dots \quad (4.13)$$

Note that these formulas apply equally if μ is rational or irrational; of course depending whether μ is rational or irrational the continued fraction expansion does or does not terminate. In the rational case under present discussion we also introduce another sequence of nonnegative integers:

$$b_k = q - (-)^k [(p - q) P_{k-2} + q Q_{k-2}], \quad k = 0, 1, 2, \dots \quad (4.14)$$

Given b , let the integer h and the period $T(b)$ be defined by the following formulas:

$$b_h \leq b < b_{h+1}, \quad (4.15)$$

$$T(b) = P_{h-2} + \left(\left\lfloor \frac{b - b_{h-1}}{q - b_{h+1}} \right\rfloor + 2 \right) P_{h-1}. \quad (4.16)$$

Then the roots of the polynomial can have only one of the following three periods \tilde{j} :

$$\tilde{j} = T(b) \quad \text{or} \quad \tilde{j} = T(b) - P_{h-1} \quad \text{or} \quad \tilde{j} = P_{h-1}. \quad (4.17)$$

This is the generic case; there are however some cases in which the roots have only the two periods $T(b)$ and P_{h-1} . This happens of course when $T(b) = 2P_{h-1}$ and whenever b takes the following special values:

$$b = b_h + n(q - b_{h+1}), \quad 0 \leq n \leq a_h - 1, \quad n \text{ integer}. \quad (4.18)$$

Remark 8. In case (i) of Proposition 7 the mechanism that yields periods longer than unity is the coming into play of the b square-root branch points enclosed *inside* the circle Ξ , which cause a certain number of roots $\tilde{w}_j(t)$ to exchange pairwise their roles through the time evolution. But this phenomenology only affects some roots; others remain unaffected, hence their periods remain unity, and this explains the first entry in (4.6). The precise form of the other entries in this formula, (4.6), requires of course a more detailed treatment, see [2]; the outcome there depends on how many pair exchanges actually do take place, or, equivalently, how many sheets of the Riemann surface get actually visited, and this depends in a fairly detailed manner on the specific structure of this surface. But note that only *two* different periods may emerge, differing by only *one* unit.

In case (ii) of Proposition 7 the second mechanism, associated with the presence of the branch point at $\xi = 0$, comes additionally into play, causing the connection of *all* the b sheets containing the b square-root branch points, both among themselves and with the $(p - q)$ sheets containing the branch point at $\xi = 0$. The corresponding $(b + p - q)$ roots get permuted among themselves through the time evolution, with the period indicated by the second entry in (4.7) (note that whenever p is *quite large* and b is *close* to its *maximal* value $q - 1$, the resulting period is *quite large*). The remaining $(q - b)$ sheets, corresponding to the $(q - b)$ branch points lying on the circle B *outside* the circle Ξ , are isolated, hence the corresponding roots do *not* take part in the quadrille, so that their period remains unity, as indicated by the first entry in (4.7).

The cases (i') and (ii') of Proposition 7 require no additional discussion.

In case (iii) of Proposition 7 (with $0 < p < q$, i. e. $0 < \mu < 1$) there is no branch point at $\xi = 0$; hence the mechanism is now *absent* that previously caused the connection of all the sheets associated with the b *square-root* branch points sitting on the circle B *inside* the circle Ξ . This implies, see [2], that each sheet of the Riemann surface contains *only two* branch points, whose projections on the circle B are separated by $(p - q)$ other branch points. Note that this entails that two branch points which are *adjacent* on the circle B in the *complex* ξ -plane are instead topologically far apart on the Riemann surface of the function $w(\xi)$, living on sheets which are not directly connected. As a consequence the period of the time evolution of the root $\tilde{w}(t)$ does not change, as the initial data change causing the circle Ξ to change its position and dimension so that the number b of *square-root* branch points enclosed in it increases, until some crucial *square-root* branch point gets thereby included inside the circle Ξ , causing the connection of two separate groups of connected sheets; and this mechanism occurs more and more frequently as b increases more and more. This explained *qualitatively* the piecewise constant behavior of the period as b increases, characterized by shorter and shorter steps and by bigger and bigger jumps, see (4.16)-(4.17). The exact treatment of this mechanism, yielding (4.16)-(4.17), is rather complicated, as indicated by the role played by the *continued fraction* expansion of the number $\frac{q}{q-p}$. The details are given in [2]. Here we limit ourselves to emphasizing that, for given initial data, the *generic* root $\tilde{w}(t)$ can have only 3 possible periods, the third of which is just the sum of the first two, see (4.17).

Let us now discuss the case in which μ is an *irrational* number, recalling that we are now considering initial data ($|\bar{\xi}| - |R| < |r_b| < |\bar{\xi}| + |R|$) such that the two circles B and Ξ *do intersect* each other (the results for the other cases have been given in Propositions 1 - 5). One must then introduce the ratio ν of the length of the arc of the circle B that is *inside* the circle Ξ , to the length of the *entire* circle B , see formula (3.45). Here we rephrase (3.45) and ν in terms of $\bar{\xi}$, R and r_b , obtaining

$$\nu = \frac{1}{\pi} \arccos \left(\frac{|r_b|^2 + |\bar{\xi}|^2 - |R|^2}{2 |r_b \bar{\xi}|} \right), \quad (4.19)$$

where the determination of the arccos function must be chosen so that $0 < \nu < 1$. The results for the periods are then given by the following

Proposition 9. (i) If $\mu > 1$ and the origin $\xi = 0$ is *outside* the circle Ξ (i. e. $|\eta| > 1$), the time evolution of the generic root $\tilde{w}(t)$ is still *periodic* with period $\tilde{T} = \tilde{j}T$ and \tilde{j} can take one of the following 3 values:

$$\tilde{j} = 1 \quad \text{or} \quad \tilde{j} = \left\lfloor \frac{\nu}{\mu - 1} \right\rfloor + 1 \quad \text{or} \quad \tilde{j} = \left\lfloor \frac{\nu}{\mu - 1} \right\rfloor + 2. \quad (4.20)$$

Note that the second and third entry only differ by one unit and moreover that, if $\mu > 2$, the floor functions vanish, hence for all values of μ larger than 2 (and $|\eta| > 1$) the only possible values for \tilde{j} are 1 or 2.

(ii) If $\mu > 1$ and the origin $\xi = 0$ is *inside* the circle Ξ (i. e. $|\eta| < 1$), the time evolution of the generic root $\tilde{w}(t)$ is either *periodic* with period T or *aperiodic*.

(i'). If $\mu < 0$ and the origin $\xi = 0$ is *outside* the circle Ξ (i. e. $|\eta| > 1$), the time evolution of the generic root $\tilde{w}(t)$ is still *periodic* with period $\tilde{T} = \tilde{j}T$ and \tilde{j} can take one of the following 3 values:

$$\tilde{j} = 1 \quad \text{or} \quad \tilde{j} = \left\lfloor \frac{\nu}{|\mu|} \right\rfloor + 1 \quad \text{or} \quad \tilde{j} = \left\lfloor \frac{\nu}{|\mu|} \right\rfloor + 2. \quad (4.21)$$

Again the second and third entry only differ by one unit and moreover if $|\mu| > 1$ the floor functions vanish, hence we conclude that for all values of μ smaller than -1 the only possible values for \tilde{j} are 1 or 2.

(ii') If $\mu < 0$ and the origin $\xi = 0$ is inside the circle Ξ (i. e. $|\eta| < 1$), the time evolution of the generic root $\tilde{w}(t)$ is either periodic with period T or aperiodic.

(iii). The case $0 < \mu < 1$ is again more intriguing, and it requires again the use of the continued fraction expansion of $\frac{1}{1-\mu}$, which however now does not terminate. We define now in addition the (endless) sequence of real numbers

$$\nu_k = 1 - (-)^k [(\mu - 1) P_{k-2} + Q_{k-2}], \quad k = 0, 1, 2, \dots \quad (4.22)$$

(entailing $\nu_0 = 0$), and we then identify the nonnegative integer h via the inequalities

$$0 \leq \nu_h \leq \nu < \nu_{h+1} < 1. \quad (4.23)$$

Let $T(\nu)$ be defined by the following expression:

$$T(\nu) = P_{h-2} + \left(\left\lfloor \frac{\nu - \nu_h}{1 - \nu_{h+1}} \right\rfloor + 2 \right) P_{h-1}. \quad (4.24)$$

Then the motion of the generic root $\tilde{w}(t)$ is again periodic with period $\tilde{T} = \tilde{j}T$ where \tilde{j} can take one of the following 3 values:

$$\tilde{j} = T(\nu) \quad \text{or} \quad \tilde{j} = T(\nu) - P_{h-1} \quad \text{or} \quad \tilde{j} = P_{h-1}. \quad (4.25)$$

Remark 10. The results for this case with *irrational* μ can be obtained from those for *rational* μ (see Proposition 7) by taking appropriately the limit in which

- (a) the integers p and q diverge with their ratio μ fixed (see (2.26)), and
- (b) the number b of *square-root* branch points *inside* the circle Ξ , as well as the *total* number q of *square-root* branch points, also diverge with their ratio fixed (recall that *all* these *square-root* branch points sit, densely equispaced, on the circle B in the complex ξ -plane although on *different* sheets of the Riemann surface of the function $w(\xi)$ – hence this ratio coincides with the quantity ν defined, and evaluated in terms of the initial data, above, see (4.19)).

This also suggests obvious extensions to the present case with *irrational* μ of comments contained in the Remark 8, which will not be repeated here. We therefore limit below our remarks to aspects of the results reported in Proposition 9 having no immediate counterpart in the comments contained in Remark 8.

In the cases (i) respectively (i') of Proposition 9 the rules giving the period of the time evolution of the *generic* root $\tilde{w}(t)$, see (4.20) respectively (4.21), are fairly straightforward and generally yield rather small periods, unless $\mu = 1 + \varepsilon$ respectively $\mu = -\varepsilon$ with ε an *irrational* number *positive* but *extremely small*.

In cases (ii) and (ii') of Proposition 9 the situation is quite interesting because the time evolution of the generic root $\tilde{w}(t)$ can be either *periodic* with the basic period T or *aperiodic*. Note that in these cases the circle Ξ intersects the circle B that is *densely* filled with *square-root* branch points, and moreover the branch point at $\xi = 0$ (which is now of *irrational* exponent, see (1.46)) is *inside* the circle Ξ . This entails that, of the *infinity* of *square-root* branch points located on the piece of the circle B that is *inside* Ξ , either *none*, or *all*, are *active*. The first case obtains if the root $\tilde{w}(t)$ under consideration is *initially* on a sheet containing a branch point that does *not* fall inside Ξ , hence the time evolution of this root $\tilde{w}(t) \equiv w[\xi(t)]$ as the point $\xi(t)$ travels round and round on the circle Ξ brings

it back to its point of departure after a single round; equivalently, in this case the root $\tilde{w}(t) \equiv w[\xi(t)]$ belongs to a set of roots that does *not* get permuted as the point $\xi(t)$ travels round and round on the circle Ξ . In the second case the root $\tilde{w}(t)$ under consideration starts from a sheet of the Riemann surface that contains a branch point inside B , so that, when $\xi(t)$ travels round and round on the circle Ξ , an *endless* sequence of *different* sheets get accessed by $\tilde{w}(t) \equiv w[\xi(t)]$; equivalently, such a root $\tilde{w}(t) \equiv w[\xi(t)]$ belongs to a set (including an *infinity* of roots) that does get permuted as the point $\xi(t)$ travels round and round on the circle Ξ , with both mechanisms – the pairwise exchange of some roots, and the cyclic permutation of an *infinite* number of roots – playing a role at each round. The identification of which sheets get thereby accessed, and in which order – namely the specific shape of the trajectory when looked at, as it were stroboscopically, at the discrete sequence of instants $T_k = kT$, $k = 1, 2, 3, \dots$ – is discussed in [2]. The extent to which this regime yields *irregular* motions is discussed further below, also to illuminate the distinction in these regimes between the time evolution entailed by our model with a given *irrational* value of μ , and that of the analogous models with *rational* values of μ providing more and more accurate approximations of the given *irrational* value of μ .

In case (iii) the time evolution is still *isochronous*, inasmuch as the results reported above entail that, for *any* given initial data (excluding, of course, the *special* ones leading to a collision; which are *special* in the same sense as a *rational* number is *special* in the context of *real* numbers), the motion of every root $\tilde{w}_j(t)$ is *periodic* with one of the 3 periods entailed by (4.25) (and note that the value of the integer \tilde{j} provided by the *third* of these 3 formulas is just the sum of the 2 values for \tilde{j} provided by the first 2 of these 3 formulas). It is indeed clear that the initial data yielding such an outcome are included in an *open set* of such data, having of course *full dimensionality* in the space of initial data, *all* yielding the *same* outcome: since the periods do *not* change, see (4.25), if the change of the initial data, hence the change in the ratio ν , is sufficiently tiny. However the measures of these sets of data yielding the *same* outcome gets progressively *smaller* as the predicted periods get *larger*, and moreover the corresponding predictions involve more and more terms in the (never ending) *continued fraction* expansion of the irrational number $\frac{1}{1-\mu}$, see (4.10), displaying thereby, as ν increases towards unity, a *progressively more sensitive* dependence of the periodicity of our system on the initial data and moreover on the parameters (the coupling constants, that determine the value of μ , see (2.25)) of our physical model (2.10).

In Figure 4.1, 4.2 and 4.3 we shortly and visually summarize our findings concerning the the periodicity (if any) of the time evolution of a *generic* root $\tilde{w}(t)$ of (4.3) with (4.2). The identification of analogous, but of course more definite, results for the *physical* root $\tilde{w}(t)$, and the consequential information on the periodicity (if any) of the solution of the physical problem (2.10) – as well as some additional information on the corresponding trajectories of the coordinates $z_n(t)$ – are still open problems at the time this thesis is written and they will be provided in [2].

4.2 Dependence of the solution on initial conditions

In this section we analyze the dependence of the period of the solutions $z_n(t)$ of (2.10) on the initial data $z_n(0)$. We know from the previous section that this period depends on the number and labels of the active branch points that fall inside the circle Ξ described by $\xi(t)$ in (4.2). The position of the branch points is fixed but the center $\bar{\xi}$ and radius $|R|$ of the circle Ξ changes with the initial conditions as described by (4.2), (2.114) and (2.115). For the time being we concentrate our analysis in the case where μ is rational, stating the following

Proposition 11. *If μ is a rational number, the system (2.10) is isochronous, i.e. for*

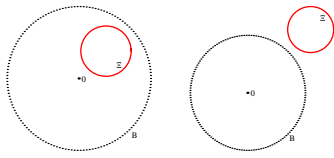
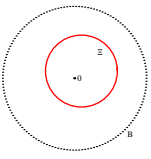
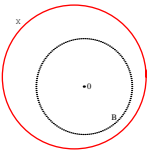
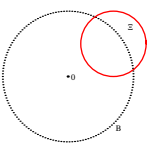
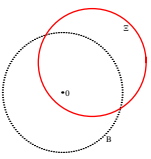
Ξ -circle vs B -circle	$\mu < 0$ and $\mu \in \mathbb{Q}$, $\mu = \frac{p}{q}$	$\mu < 0$ and $\mu \notin \mathbb{Q}$
 <p data-bbox="231 515 566 571"> $\bar{\xi} + R < r_b$ $R > \bar{\xi} + r_b$ $R < \bar{\xi}$ </p>	<p data-bbox="662 369 901 403">The generic root \tilde{w} is:</p> <p data-bbox="662 425 901 459">periodic with period \mathbf{T}</p> <p data-bbox="726 481 837 515">see Prop.1</p>	<p data-bbox="1029 369 1268 403">The generic root \tilde{w} is:</p> <p data-bbox="1029 425 1268 459">periodic with period \mathbf{T}</p> <p data-bbox="1093 481 1204 515">see Prop.1</p>
 <p data-bbox="327 840 478 896"> $\bar{\xi} + R < r_b$ $R > \bar{\xi}$ </p>	<p data-bbox="662 616 901 649">The generic root \tilde{w} is:</p> <p data-bbox="630 672 933 705">periodic with period $\tilde{\mathbf{T}} = \tilde{\mathbf{j}} \mathbf{T}$</p> <p data-bbox="662 705 901 750">and $\tilde{\mathbf{j}}$ can take one of the following values:</p> <p data-bbox="750 772 813 806">$\tilde{\mathbf{j}} = 1$</p> <p data-bbox="734 828 829 862">or $\tilde{\mathbf{j}} = \mathbf{p}$</p> <p data-bbox="726 884 837 918">see Prop.3</p>	<p data-bbox="1029 627 1268 660">The generic root \tilde{w} is:</p> <p data-bbox="1029 683 1268 716">periodic with period \mathbf{T}</p> <p data-bbox="1029 739 1284 772">or quasi-periodic:</p> <p data-bbox="1029 772 1284 851">(nonlinear) superposition of two periodic evolutions with periods \mathbf{T} and $\frac{\mathbf{T}}{ \mu }$</p> <p data-bbox="1093 873 1204 907">see Prop.3</p>
 <p data-bbox="327 1164 478 1198"> $R < \bar{\xi} - r_b$ </p>	<p data-bbox="662 996 901 1030">The generic root \tilde{w} is:</p> <p data-bbox="630 1052 933 1086">periodic with period $\tilde{\mathbf{T}} = \tilde{\mathbf{j}} \mathbf{T}$</p> <p data-bbox="702 1086 861 1120">and $\tilde{\mathbf{j}} = \mathbf{q} + \mathbf{p}$</p> <p data-bbox="726 1131 837 1164">see Prop.5</p>	<p data-bbox="1029 974 1268 1008">The generic root \tilde{w} is:</p> <p data-bbox="1029 1030 1284 1064">quasi-periodic:</p> <p data-bbox="1029 1064 1284 1142">(nonlinear) superposition of two periodic evolutions with periods \mathbf{T} and $\frac{\mathbf{T}}{1-\mu}$</p> <p data-bbox="1093 1153 1204 1187">see Prop.5</p>
 <p data-bbox="263 1489 534 1545"> $\bar{\xi} - R < r_b < \bar{\xi} + R$ $R < \bar{\xi}$ </p>	<p data-bbox="662 1243 901 1276">The generic root \tilde{w} is:</p> <p data-bbox="630 1299 933 1332">periodic with period $\tilde{\mathbf{T}} = \tilde{\mathbf{j}} \mathbf{T}$</p> <p data-bbox="662 1332 901 1377">and $\tilde{\mathbf{j}}$ can take one of the following values:</p> <p data-bbox="750 1400 813 1433">$\tilde{\mathbf{j}} = 1$</p> <p data-bbox="686 1456 877 1489">or $\tilde{\mathbf{j}} = \left\lfloor \frac{\mathbf{b}-1}{ \mathbf{p} } \right\rfloor + 1$</p> <p data-bbox="686 1512 877 1545">or $\tilde{\mathbf{j}} = \left\lfloor \frac{\mathbf{b}-1}{ \mathbf{p} } \right\rfloor + 2$</p> <p data-bbox="726 1579 837 1612">see Prop.7</p>	<p data-bbox="1029 1243 1268 1276">The generic root \tilde{w} is:</p> <p data-bbox="997 1299 1300 1332">periodic with period $\tilde{\mathbf{T}} = \tilde{\mathbf{j}} \mathbf{T}$</p> <p data-bbox="1029 1332 1268 1377">and $\tilde{\mathbf{j}}$ can take one of the following values:</p> <p data-bbox="1109 1400 1189 1433">$\tilde{\mathbf{j}} = 1$</p> <p data-bbox="1061 1456 1236 1489">or $\tilde{\mathbf{j}} = \left\lfloor \frac{\nu}{ \mu } \right\rfloor + 1$</p> <p data-bbox="1061 1512 1236 1545">or $\tilde{\mathbf{j}} = \left\lfloor \frac{\nu}{ \mu } \right\rfloor + 2$</p> <p data-bbox="1093 1579 1204 1612">see Prop.9</p>
 <p data-bbox="263 1870 534 1926"> $\bar{\xi} - R < r_b < \bar{\xi} + R$ $R > \bar{\xi}$ </p>	<p data-bbox="662 1646 901 1680">The generic root \tilde{w} is:</p> <p data-bbox="630 1702 933 1736">periodic with period $\tilde{\mathbf{T}} = \tilde{\mathbf{j}} \mathbf{T}$</p> <p data-bbox="662 1736 901 1780">and $\tilde{\mathbf{j}}$ can take one of the following values:</p> <p data-bbox="750 1803 813 1836">$\tilde{\mathbf{j}} = 1$</p> <p data-bbox="710 1859 853 1892">or $\tilde{\mathbf{j}} = \mathbf{b} + \mathbf{p}$</p> <p data-bbox="726 1915 837 1948">see Prop.7</p>	<p data-bbox="1029 1702 1268 1736">The generic root \tilde{w} is:</p> <p data-bbox="1029 1758 1268 1792">periodic with period \mathbf{T}</p> <p data-bbox="1077 1814 1220 1848">or aperiodic</p> <p data-bbox="1093 1859 1204 1892">see Prop.9</p>

Figure 4.1: Periods, with respect to the mutual position of the Ξ -circle and the B -circle, for rational and irrational values of $\mu < 0$ (b is the number of consecutive SRBPs included in Ξ ; the variable ν is defined as in (3.45)).

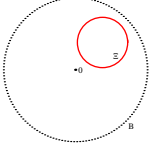
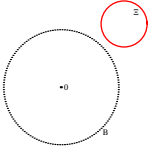
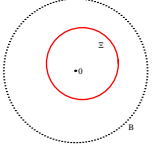
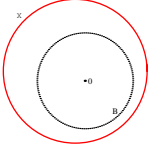
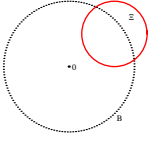
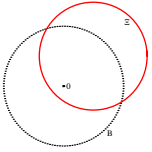
Ξ -circle vs B -circle	$0 < \mu < 1$ and $\mu \in \mathbb{Q}, \mu = \frac{p}{q}$	$0 < \mu < 1$ and $\mu \notin \mathbb{Q}$
 $ \tilde{\xi} + R < r_b $ $ R < \tilde{\xi} $  $ R > \tilde{\xi} + r_b $	<p>The generic root \tilde{w} is:</p> <p>periodic with period \mathbf{T}</p> <p><i>see Prop.1</i></p>	<p>The generic root \tilde{w} is:</p> <p>periodic with period \mathbf{T}</p> <p><i>see Prop.1</i></p>
 $ \tilde{\xi} + R < r_b $ $ R > \tilde{\xi} $	<p>The generic root \tilde{w} is:</p> <p>periodic with period \mathbf{T}</p> <p><i>see Prop.1</i></p>	<p>The generic root \tilde{w} is:</p> <p>periodic with period \mathbf{T}</p> <p><i>see Prop.1</i></p>
 $ R < \tilde{\xi} - r_b $	<p>The generic root \tilde{w} is:</p> <p>periodic with period $\tilde{\mathbf{T}} = \tilde{\mathbf{j}} \mathbf{T}$</p> <p>and $\tilde{\mathbf{j}}$ can take one of the following values:</p> $\tilde{\mathbf{j}} = \mathbf{q} - \mathbf{p} \text{ or } \tilde{\mathbf{j}} = \mathbf{p}$ <p><i>see Prop.5</i></p>	<p>The generic root \tilde{w} is:</p> <p>quasi-periodic: (nonlinear) superposition of two periodic evolutions with periods \mathbf{T} and $\frac{\mathbf{T}}{\mu}$</p> <p>or with periods \mathbf{T} and $\frac{\mathbf{T}}{1-\mu}$</p> <p><i>see Prop.5</i></p>
  $ \tilde{\xi} - R < r_b < \tilde{\xi} + R $	$\frac{q}{q-p} = a_0 + \frac{1}{a_1 + \frac{1}{a_2 + \dots}}$ $P_k = a_k P_{k-1} + P_{k-2}$ $Q_k = a_k Q_{k-1} + Q_{k-2}$ $P_{-2} = 0, P_{-1} = 1, Q_{-2} = 1, Q_{-1} = 0$ $b_k = q - (-)^k [(p-q) P_{k-2} + q Q_{k-2}]$ $b_h \leq b < b_{h+1}$ $T(b) = P_{h-2} + \frac{b-b_h-1}{q-b_{h+1}} + 2 P_{h-1}$ <p>The generic root \tilde{w} is:</p> <p>periodic with period $\tilde{\mathbf{T}} = \tilde{\mathbf{j}} \mathbf{T}$</p> <p>and $\tilde{\mathbf{j}}$ can take one of the following values:</p> $\tilde{\mathbf{j}} = \mathbf{T}(b)$ <p>or $\tilde{\mathbf{j}} = \mathbf{T}(b) - \mathbf{P}_{h-1}$</p> <p>or $\tilde{\mathbf{j}} = \mathbf{P}_{h-1}$</p> <p><i>see Prop.7</i></p>	$\frac{1}{1-\mu} = a_0 + \frac{1}{a_1 + \frac{1}{a_2 + \dots}}$ $P_k = a_k P_{k-1} + P_{k-2}$ $Q_k = a_k Q_{k-1} + Q_{k-2}$ $P_{-2} = 0, P_{-1} = 1, Q_{-2} = 1, Q_{-1} = 0$ $\nu_k = q - (-)^k [(\mu-1) P_{k-2} + Q_{k-2}]$ $0 \leq \nu_h \leq \nu < \nu_{h+1} < 1$ $T(\nu) = P_{h-2} + \frac{\nu-\nu_h}{1-\nu_{h+1}} + 2 P_{h-1}$ <p>The generic root \tilde{w} is:</p> <p>periodic with period $\tilde{\mathbf{T}} = \tilde{\mathbf{j}} \mathbf{T}$</p> <p>and $\tilde{\mathbf{j}}$ can take one of the following values:</p> $\tilde{\mathbf{j}} = \mathbf{T}(\nu)$ <p>or $\tilde{\mathbf{j}} = \mathbf{T}(\nu) - \mathbf{P}_{h-1}$</p> <p>or $\tilde{\mathbf{j}} = \mathbf{P}_{h-1}$</p> <p><i>see Prop.9</i></p>

Figure 4.2: Periods, with respect to the mutual position of the Ξ -circle and the B -circle, for rational and irrational values of $0 < \mu < 1$ (b is the number of consecutive SRBPs included in Ξ ; the variable ν is defined as in (3.45)).

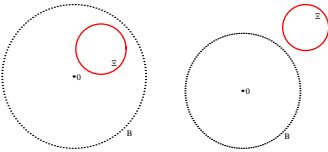
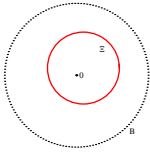
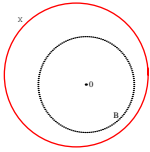
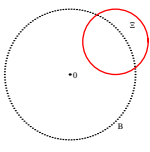
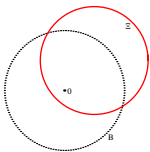
Ξ -circle vs B -circle	$\mu > 1$ and $\mu \in \mathbb{Q}$, $\mu = \frac{p}{q}$	$\mu > 1$ and $\mu \notin \mathbb{Q}$
 <p data-bbox="236 517 564 573"> $\bar{\xi} + R < r_b$ $R > \bar{\xi} + r_b$ $R < \bar{\xi}$ </p>	<p data-bbox="655 376 903 506"> The generic root \tilde{w} is: periodic with period \mathbf{T} <i>see Prop.1</i> </p>	<p data-bbox="1023 376 1270 506"> The generic root \tilde{w} is: periodic with period \mathbf{T} <i>see Prop.1</i> </p>
 <p data-bbox="325 842 475 898"> $\bar{\xi} + R < r_b$ $R > \bar{\xi}$ </p>	<p data-bbox="632 622 935 909"> The generic root \tilde{w} is: periodic with period $\tilde{\mathbf{T}} = \tilde{\mathbf{j}} \mathbf{T}$ and $\tilde{\mathbf{j}}$ can take one of the following values: $\tilde{\mathbf{j}} = 1$ or $\tilde{\mathbf{j}} = \mathbf{p} - \mathbf{q}$ <i>see Prop.3</i> </p>	<p data-bbox="1023 633 1278 898"> The generic root \tilde{w} is: periodic with period \mathbf{T} or quasi-periodic: (nonlinear) superposition of two periodic evolutions with periods \mathbf{T} and $\frac{\mathbf{T}}{\mu-1}$ <i>see Prop.3</i> </p>
 <p data-bbox="325 1167 475 1200"> $R < \bar{\xi} - r_b$ </p>	<p data-bbox="632 999 935 1155"> The generic root \tilde{w} is: periodic with period $\tilde{\mathbf{T}} = \tilde{\mathbf{j}} \mathbf{T}$ and $\tilde{\mathbf{j}} = \mathbf{p}$ <i>see Prop.5</i> </p>	<p data-bbox="1023 976 1278 1178"> The generic root \tilde{w} is: quasi-periodic: (nonlinear) superposition of two periodic evolutions with periods \mathbf{T} and $\frac{\mathbf{T}}{\mu}$ <i>see Prop.5</i> </p>
 <p data-bbox="268 1491 531 1547"> $\bar{\xi} - R < r_b < \bar{\xi} + R$ $R < \bar{\xi}$ </p>	<p data-bbox="632 1245 935 1603"> The generic root \tilde{w} is: periodic with period $\tilde{\mathbf{T}} = \tilde{\mathbf{j}} \mathbf{T}$ and $\tilde{\mathbf{j}}$ can take one of the following values: $\tilde{\mathbf{j}} = 1$ or $\tilde{\mathbf{j}} = \left\lfloor \frac{\mathbf{b}-1}{\mathbf{p}-\mathbf{q}} \right\rfloor + 1$ or $\tilde{\mathbf{j}} = \left\lfloor \frac{\mathbf{b}-1}{\mathbf{p}-\mathbf{q}} \right\rfloor + 2$ <i>see Prop.7</i> </p>	<p data-bbox="999 1245 1302 1603"> The generic root \tilde{w} is: periodic with period $\tilde{\mathbf{T}} = \tilde{\mathbf{j}} \mathbf{T}$ and $\tilde{\mathbf{j}}$ can take one of the following values: $\tilde{\mathbf{j}} = 1$ or $\tilde{\mathbf{j}} = \left\lfloor \frac{\nu}{\mu-1} \right\rfloor + 1$ or $\tilde{\mathbf{j}} = \left\lfloor \frac{\nu}{\mu-1} \right\rfloor + 2$ <i>see Prop.9</i> </p>
 <p data-bbox="268 1872 531 1928"> $\bar{\xi} - R < r_b < \bar{\xi} + R$ $R > \bar{\xi}$ </p>	<p data-bbox="632 1653 935 1939"> The generic root \tilde{w} is: periodic with period $\tilde{\mathbf{T}} = \tilde{\mathbf{j}} \mathbf{T}$ and $\tilde{\mathbf{j}}$ can take one of the following values: $\tilde{\mathbf{j}} = 1$ or $\tilde{\mathbf{j}} = \mathbf{b} + \mathbf{p} - \mathbf{q}$ <i>see Prop.7</i> </p>	<p data-bbox="1023 1709 1270 1883"> The generic root \tilde{w} is: periodic with period \mathbf{T} or aperiodic <i>see Prop.9</i> </p>

Figure 4.3: Periods, with respect to the mutual position of the Ξ -circle and the B -circle, for rational and irrational values of $\mu > 1$ (b is the number of consecutive SRBPs included in Ξ ; the variable ν is defined as in (3.45)).

every initial data $\{z_1(0), z_2(0), z_3(0)\}$ there is an open set S in phase space that contains the initial data, such that all trajectories of (2.10) with initial data in S have the same period.

Proof. It suffices to realize that the only way the period of the orbit can change is if the circle Ξ encircles a different number of *active* branch points. We recall that an active branch point is a branch point whose projection on the complex plane lies inside the circle Ξ and it sits on a sheet that is accessed by $\check{w}(t)$ as $\xi(t)$ turns on the circle Ξ . Obviously the active or inactive character of a branch point depends on the other branch points enclosed by Ξ and their characterization requires a detailed knowledge of the geometry of the Riemann surface. For $\mu \in \mathbb{Q}$ the active branch points are isolated in the complex plane and since the center and radius of the circle Ξ have a continuous dependence on the initial data $\{z_1(0), z_2(0), z_3(0)\}$, given one point in phase space there is an open set S that contains it such that the branch point configuration inside Ξ for every point in S is the same. \square

We see thus that the periodic orbits of (2.10) in the μ -rational case are stable with respect to small changes in the initial position. The phase space is divided into a finite number of *regions of isochronicity*, each of them having positive measure. The boundaries of these regions have null measure and correspond to the the initial data for which the circle Ξ contains an active branch point. In the three-body problem (2.10) these are the initial data for which a collision occurs at some finite time t and therefore we will refer to these boundaries as *collision manifolds*.

Proposition 12. *If μ is a rational number, the collision manifolds are algebraic.*

Proof. The condition that defines a collision manifold is

$$|\xi_b - \bar{\xi}| = |R|, \quad (4.26)$$

where ξ_b denotes an active branch point.

From (2.114) it is clear that both the center $\bar{\xi}$ and the radius $|R|$ of Ξ are algebraic functions of $\{z_1(0), z_2(0), z_3(0)\}$ and since ξ_b does not depend on the initial data, then the relation (4.26) defines an algebraic manifold. \square

4.2.1 Sections of phase space

A convenient way of visualizing the collision manifolds and the regions of isochronicity is to look at sections of phase space. This will be done by keeping fixed the initial positions of two particles and letting the initial position of the third particle vary. In particular, we have chosen the following values

$$z_1(0) = (0, 0), \quad (4.27a)$$

$$z_2(0) = (x, y), \quad (4.27b)$$

$$z_3(0) = (1, 0), \quad (4.27c)$$

and we are interested in analyzing $T(x, y)$, the period of the orbit as a function of $z_2(0) = (x, y)$. The calculation of the period can be explicitly performed by purely algebraic considerations: as x and y change we know how the center and radius of the circle Ξ change (see expression (4.2) with (2.114) and (2.115)). Since the position of the branch points ξ_b of $w(\xi)$ is fixed (2.103), the number and the labels of the branch points enclosed by Ξ can be easily calculated. The final and the more complicated step is to use our knowledge of the geometry of the Riemann surface obtained in Chapter 3 to predict the period of $\check{w}(t)$ (we stress once again that the identification, among the J roots of (4.3), of the root which describes the physical model is still an open problem).

From this point on it will be convenient to separate the analysis for the two cases $\mu > 1$ and $0 < \mu < 1$ for which the Riemann surfaces have different properties (see Chapter 3).

4.2.1.1 Case $\mu > 1$

We set the coupling constants of the three-body problem to the following values:

$$f = -12, \quad g = 0.5, \quad (4.28)$$

which imply that $\mu = 11/8$. We also set the frequency parameter

$$\omega = 2\pi,$$

so that the fundamental period is unity. The results of the calculation have been displayed in Figure 4.4. A 2-dimensional section showing the regions of isochronicity can be seen in Figures 4.4a and 4.4b (which corresponds to a zoom of the dotted square of Figure 4.4a). These regions are defined by the intersection of a set of algebraic curves that correspond to the collision manifolds. In the two figures below we have plotted a 1-dimensional section of the above plots, corresponding to the x coordinate of $z_2(0)$, while the y coordinate has been fixed to the value $y = 1$ in Figure 4.4c and $y = 0.8$ in Figure 4.4d (corresponding to the dotted lines on the above figures). Note that period is a piecewise constant function of x with finite jumps at the collision curves.

The following four Figures 4.4e–h show the relative position of the evolution circle Ξ with respect to the circle of B of branch points for the different values of the initial conditions depicted in Figure 4.4b. In Figure 4.4e note that although the circle Ξ encloses (the projection of) one square-root branch point, this branch point is inactive, i.e. it is lying on a higher sheet of the Riemann surface which is not accessed by the evolution, and therefore the period of $\check{w}(t)$ is one. In Figure 4.4f the circle Ξ now encircles the branch point on the principal sheet and two other inactive ones, and therefore the period of $\check{w}(t)$ corresponding to these initial conditions is two. In Figure 4.4g we see that the inclusion of the origin has quite a drastic effect, since the branch point at $\xi = 0$ attaches $p - q$ sheets together. The inclusion of the origin means that all the four square-root branch points enclosed by Ξ become active and the period jumps from 2 to 7. When the origin is included, every successive square-root branch point included by Ξ causes the period to rise by one (this can be seen explicitly in Figure 4.4d), and for instance in Figure 4.4h the period is 10. We shall prove below that this drastic effect of the inclusion of the origin will give rise to a sensitive dependence of the system on the initial data when the parameter μ is an irrational number.

4.2.1.2 Case $0 < \mu < 1$

In this case we have chosen an example where the coupling constants of the three-body problem assume the following values:

$$f = 16, \quad g = 7, \quad (4.29)$$

entailing that $\mu = 5/12$. As in the previous case we also set $\omega = 2\pi$. The dependence of the period of $\check{w}(t)$ on the initial conditions (4.27) has been displayed in Figure 4.5. In the first line, figures 4.5a and 4.5b show the 2D plots of $T(x, y)$, the second being a zoom of the first corresponding to the area marked by a dotted square. Below these figures we show again the 1-dimensional sections that correspond to fixing the value of y to $y = -1$ and $y = -1.3$ respectively (dotted lines in Figures a and b). We see that the isochronous character of the model is manifest in the piecewise constant behavior of the period as a function of the initial conditions, with jumps at the values of (x, y) that correspond to a *collision curve*. As stated in Proposition 12 these collision curves are algebraic and their defining equations can be easily derived from (4.26) and (2.114). However, the expressions are rather involved and we have chosen just to show the plots rather than performing a full

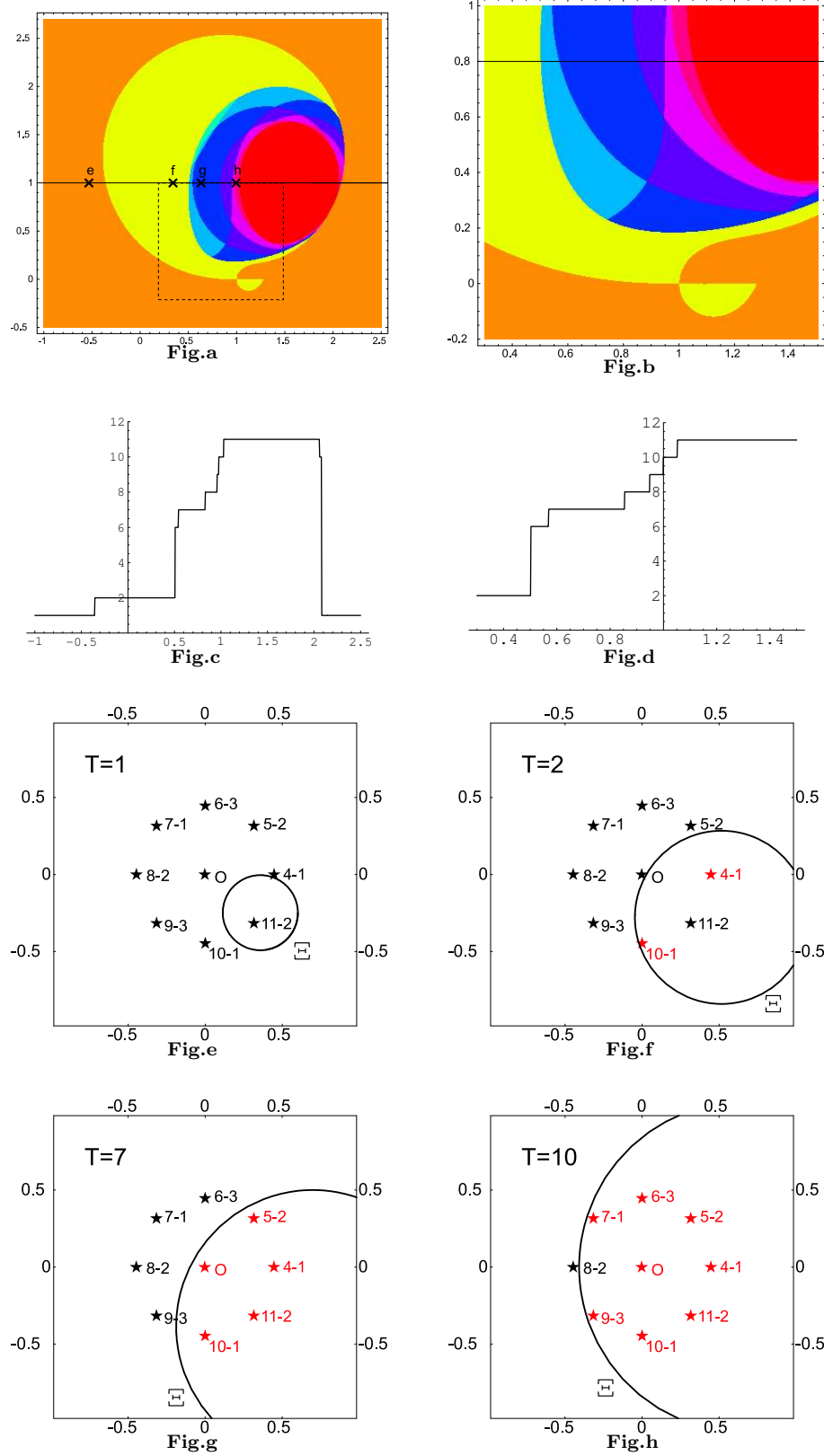


Figure 4.4: Period of the solution as a function of the initial data for the case $\mu = 11/8$

analytical description. The four Figures 4.5e–h show the relative position of the evolution circle Ξ with respect to the circle of B of branch points for the different values of the initial conditions depicted in Figure 4.5b. In the first of them, Figure 4.5e we see that Ξ encloses six branch points, but all of them are inactive and therefore the period of $\check{w}(t)$ is one (note that the origin is not a branch point in the case $0 < \mu < 1$). In Figure 4.5f only one active branch point is enclosed giving rise to a period of $T = 2$. Similarly, in the other two figures the periods are $T = 3$ and $T = 5$. Note that in this case the only singularities of the Riemann surface in the finite complex plane are square root branch points (a finite number of them if μ is rational). This means that each sheet is only attached to another sheet and it is more difficult for the period to have big jumps as new branch points are included. This is in contrast to the case $\mu > 1$ where the origin is a branch point of order $p - q$. As a matter of fact, in the case $0 < \mu < 1$ there is no sensitive dependence of the initial data even if μ is irrational.

4.2.2 Sensitive dependence on initial conditions

We concentrate in this section on the case $\mu > 1$ to prove the following

Proposition 13. *If the coupling constants f and g of the dynamical system (2.10) are such that μ is an irrational number greater than one, then the collision manifolds are dense on an open set S in phase space.*

Proof. The proof is constructive since the open set S can be explicitly computed:

$$S = \{(z_1(0), z_2(0), z_3(0)) \quad \text{s.t.} \quad r_b - |R| < |\bar{\xi}| < |R|\} \quad (4.30)$$

where r_b depends only on μ and is given by (2.103), and R and $\bar{\xi}$ are given by (2.114) and (2.115). This set S corresponds to the initial data of (2.10) such that the circle Ξ encloses the origin $\xi = 0$ and has a non-trivial intersection with the circle B of square-root branch points. When $\mu > 1$ and the origin is included in Ξ , all the square root branch points enclosed by Ξ are active since the branch point at the origin connects all the sheets. But these active branch points fill densely the circle B when μ is irrational, therefore the collision manifolds are dense in S . \square

Corollary 14. *Under the assumptions of the previous Proposition 13, the solutions of the dynamical system (2.10) with initial data in the open set S feature sensitive dependence on their initial conditions.*

It is fundamental to stress that the mechanism that leads to a sensitive dependence in the model treated herein is different from the sensitive dependence with positive Lyapunov exponents that usually appears in chaotic dynamical systems. As opposed to the characteristic exponential divergence, in our system two trajectories that start very close to each other do remain close to each other for quite some time until eventually they depart from each other in a drastic manner. This paradigm can be understood both from the physical and the mathematical points of view. From a physical point of view, the origin of the departure is due to a near collision between the two different particles: in one trajectory the particles slide past each other in one way, while in the other they scatter in the opposite way, as depicted in Figure 4.5. The future of the two trajectories from that point on is completely different and they become uncorrelated.

From a mathematical point of view the origin of the sensitive dependence is due to the fact that the circle Ξ passes very close to an active square root branch point ξ_b . Both trajectories $\check{w}(t)$ travel on very close paths on the Riemann surface for possibly many periods until eventually they reach the sheet on which the branch point ξ_b sits. Then one

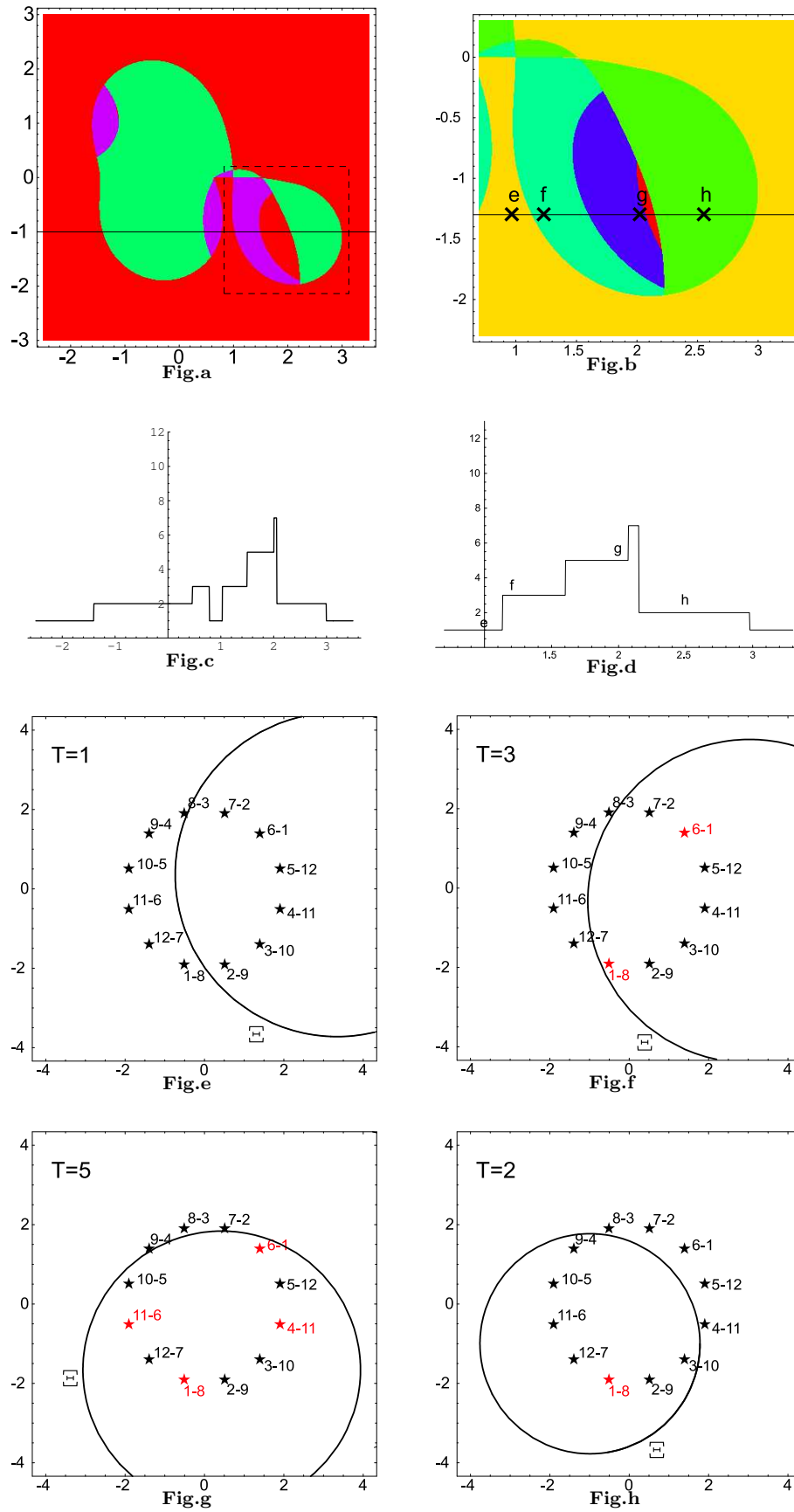


Figure 4.5: Period of the solution as a function of the initial data for the case $\mu = 5/12$

trajectory continues on the same branch while the other one crosses the cut and jumps to a different branch of the Riemann surface, following different paths from that point on.

Numerical techniques of integration will have problems when integrating the equations (2.10) with initial conditions in S under the assumptions of Proposition 13. The result of the integration will be very close to the true trajectory for some time until the error accumulated causes the numerical take some branch on the “wrong” side. Predicting at which time this happens however requires to be able to identify on which sheet each branch point lies, or otherwise speaking, which of all the branch points is the one that lies on the principal sheet. Identifying which is the branch point that lies on the principal sheet is still an open problem, but this determination would require infinite precision of calculus if μ is an irrational. It seems that the near misses described above happen at a time which is almost impossible to predict in real applications.

We have tried to illustrate this sensitive dependence in Figure 4.7. In the first column we have plotted the map $T(x, y)$ representing the dependence of the period of $\tilde{w}(t)$ on the initial positions (4.27) for a range of values of x and y that includes part of the region S defined by (4.30). In the second column of Figure 4.7 we have plotted the period for a fixed value of y , specifically for $y = 0.7$, corresponding to the dotted line in the 2D plots of the first column. In this column we clearly appreciate that the period has a jump at the point where the circle Ξ passes by the origin. In the third column of figure 4.7 we have plotted the relative positions of the circles B and Ξ corresponding to a point that belongs to S . We have chosen the point $(x = 0.7, y = 0.7)$ which is represented by a cross in the plots of the first column. Each of the lines corresponds to a different value of the coupling constants, such that the parameter μ has more or less the same magnitude but its rational expression has a larger denominator. The specific values chosen can be read from the following table:

f	g	μ	$T(0.7, 0.7)$
-12	0.5	11/8	7
-12.1	0.5	37/27	23
-12.2	0.5	56/41	35
-12.35	0.5	227/167	147

Figure 4.6: Sequence of values of μ in Figure 4.7.

4.2.3 Rational approximations to irrational values of μ

Last but not least let us elaborate on the character of the *aperiodic* time evolution indicated under item (ii) of Proposition 9, including the extent it is *irregular* and it depends *sensitively* on its initial data. It is illuminating to relate this question with the finding reported under item (ii) of Proposition 7, also in order to provide a better understanding of the relationship among the *aperiodic* time evolution that can emerge when μ is *irrational* (see item (ii) of Proposition 9) and the corresponding behavior – say, with the same initial data – for a sequence of models with *rational* values of μ (see (2.26)) that provide better and better approximations to that *irrational* value of μ ; keeping in mind the *qualitative* difference among the *aperiodic* time evolution emerging when μ is *irrational*, and the *periodic* – indeed, even *isochronous* – time evolutions prevailing whenever μ is *rational*, albeit with the qualifications indicated under item (ii) of Remark 8. Note that we are now discussing the case $\mu > 1$ (an analogous discussion in the $\mu < 0$ case can be forsaken), with initial data such that the two circles B and Ξ in the *complex* ξ -plane *do intersect* and moreover the origin $\xi = 0$ falls *inside* the circle Ξ (i. e. $|r_b| < |\bar{\xi}| + |R|$ and $|\eta| < 1$).

Let us then consider a given *irrational* value of $\mu > 1$ and let the *rational* number $\frac{p}{q}$

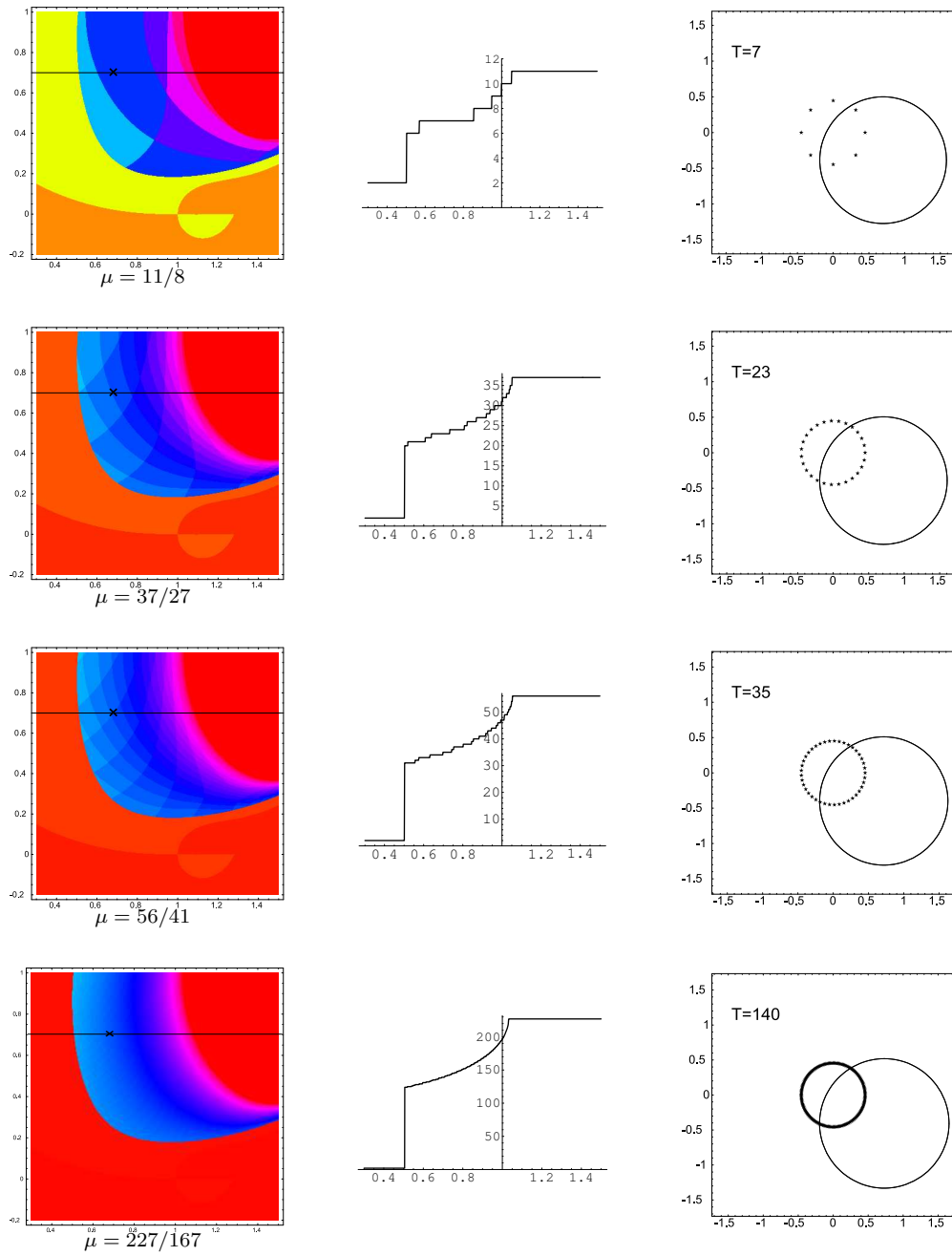


Figure 4.7: Sensitive dependence of the period on initial data.

(with $p > q$) provide a *very good* approximation to μ , which of course entails that the *positive integers* p and q are both *very large*. Consider then the *difference*

$$\Delta \tilde{j} = \Delta b \quad (4.31)$$

(see the second entry in (4.7)) between the *two* positive integers that characterize the *two* periods of the *two* time evolutions of $\tilde{w}(t)$ corresponding to *two* sets of initial data that differ *very little*. Here clearly the quantity Δb is the *difference* between the number of branch points that are enclosed inside the circle Ξ for these *two* different sets of initial data. Since the number q of branch points on B is *very large*, it stands to reason that

$$\Delta b = \lfloor O(q\delta) \rfloor, \quad (4.32)$$

where the *quite small* (*positive*) number δ provides a (dimensionless) measure of the difference between the *two* sets of initial data (see for instance (4.19), which clearly becomes approximately applicable when q is *very large*). The *floor* symbol $\lfloor \rfloor$ has been introduced in the right-hand side of this formula to account for the integer character of the numbers b hence of their difference Δb , while the *order of magnitude* symbol $O(\)$ indicates that the difference Δb is proportional (in fact equal, given the latitude left by our definition of the quantity δ) to the quantity $q\delta$ up to *corrections* which become *negligibly small* when δ is *very small* and q is *very large*, but irrespective of the value of the quantity $q\delta$ itself which, as the product of the *large* number q by the *small* number δ , is required to be neither *small* nor *large*.

The relation

$$\Delta \tilde{j} = \lfloor O(q\delta) \rfloor \quad (4.33)$$

implied by this argument indicates that, for any given q , one can always choose (finitely different) initial data which differ by such a tiny amount that the corresponding periods are identical, confirming our previous statement about the *isochronous* character of our model whenever the parameter μ is *rational*. But conversely this finding also implies that, for any set of initial data in the sector under present consideration (i. e. that characterized by the inequalities $|\eta| < 1$ and $|\bar{\xi}| + |R| > |r_b|$, and by the additional specification to identify the physical root $\tilde{w}(t)$), if our physical model (2.10) is characterized by an *irrational* value of μ , see (2.25), and one replaces this value by a more and more accurate *rational* approximation of it, see (2.26) – as it would for instance be inevitable in any numerical simulation – corresponding to larger and larger values of p and q , then one shall have to choose the two different assignments of initial data closer and closer to avoid a drastic change of period – and for these very close sets of data the motion is indeed *periodic* with a period which becomes larger and larger the better one approximates the actual, *irrational*, value of μ . We repeat again that in any numerical simulation the accuracy of the computation, in order to get the correct period, shall also have to increase more and more (with no limit), because of the occurrence of closer and closer *near misses* through the time evolution (associated with the coming into play of *active* branch points sitting on the circle B closer and closer to the points of intersection with the circle Ξ). And finally, if one insists in treating the problem with a truly *irrational* μ , then, no matter how close the initial data are, the change in the periods becomes *infinite* because the difference Δb in the number of *active square-roots* branch points on the circle B included *inside* the circle Ξ is *infinite* (see (4.31)), signifying that the motion is *aperiodic*, and that its evolution is indeed characterized by an *infinite* number of *near misses*, making it truly *irregular*.

This phenomenology, together with that of the *near misses* as described above, illustrates rather clearly the *irregular* character of the motions of our physical model when the coupling constants have appropriate values (such as to produce an irrational value of μ outside the interval $0 < \mu < 1$) and the initial data are in the sector identified above. Note

that the Lyapunov coefficients associated with the corresponding trajectories vanish, because these coefficients – as usually defined – compare the difference (after an *infinitely long* time) of two trajectories that, to begin with, differ *infinitesimally*; whereas our mechanism causing the *irregular* character of the motion requires, to come into play, an *arbitrarily small but finite* difference among the initial data. The difference between these two notions corresponds to the fact that inside the interval between two *different* real numbers – however close they may be – there always is an *infinity* of *rational* numbers; while this is *not* the case between two real numbers that differ only *infinitesimally*! This observation suggests that, in an *applicative* context, the mechanism causing a *sensitive dependence* on the initial data manifested by our model may be *phenomenologically* relevant even when no Lyapunov coefficient, defined in the usual manner, is *positive*. As already observed previously, see Chapter 1 and, for instance, [6, 7], this mechanism is in some sense analogous to that yielding *aperiodic* trajectories in a triangular billiard with *irrational* angles; although in that case – in contrast to ours – this outcome is mainly attributable to the essentially singular character of the corners.

4.3 Outlook

In this thesis we have introduced and discussed a 3-body problem in the plane suitable to illustrate a mechanism of transition from *regular* to *irregular* motions. This model is the simplest one we managed to manufacture for this purpose. Its simplicity permitted us to discuss in considerable detail the mathematical structure underlining this phenomenology: this machinery cannot however be too simple since it must capture (at least some of) the subtleties associated with the *onset* of an *irregular* behavior.

Our main motivation to undertake this research project is the hunch that this mechanism of transition have a fairly general validity and be relevant in interesting applicative contexts. Hence we plan to pursue this study by focussing on other cases where this mechanism is known to play a key role, including examples (see, for instance, [6, 7] and [62]) featuring a pattern of branch points covering densely an *area* of the *complex* plane of the independent variable rather than being confined just to reside densely on a *line* as is the case in the model treated herein; and eventually to extend the application of this approach to problems of direct applicative interest.

In this connection the following final observation is perhaps relevant. In the present work as well as in others (see [6, 7, 62] and in the references cited at the beginning of Section 1.2) the main focus has been on models featuring a transition from an *isochronous* to an *irregular* regime, and in this context much emphasis was put on the “trick” (see Subsection 1.1.2) and in particular on the relationship it entails between the *periodicity* of the (“physical”) dependent variables $z_n(t)$ as functions of the *real* independent variable t (“time”) and the *analyticity* of other, related (“auxiliary”) dependent variables $\zeta_n(\tau)$ as functions of a *complex* independent variable τ . But our findings can also be interpreted *directly* in terms of the *analytic properties* of the physical dependent variables $z_n(t)$ as functions of the independent variable t considered itself as a *complex* variable. Then the time evolution, which corresponded to a uniform travel round and round on the circle C in the *complex* τ -plane or equivalently on the circle Ξ in the *complex* ξ -plane, is represented as a uniform travel to the right along the *real* axis in the *complex* t -plane, while, via the relations (see (2.7) and (4.2))

$$t = (2i\omega)^{-1} \log(1 + 2i\omega\tau) = (2i\omega)^{-1} \log\left(\frac{\xi - \bar{\xi}}{R}\right), \quad (4.34)$$

the pattern of branch points in the *complex* τ -plane or equivalently in the *complex* ξ -plane gets mapped into a somewhat analogous pattern in the *complex* t -plane, *repeated*

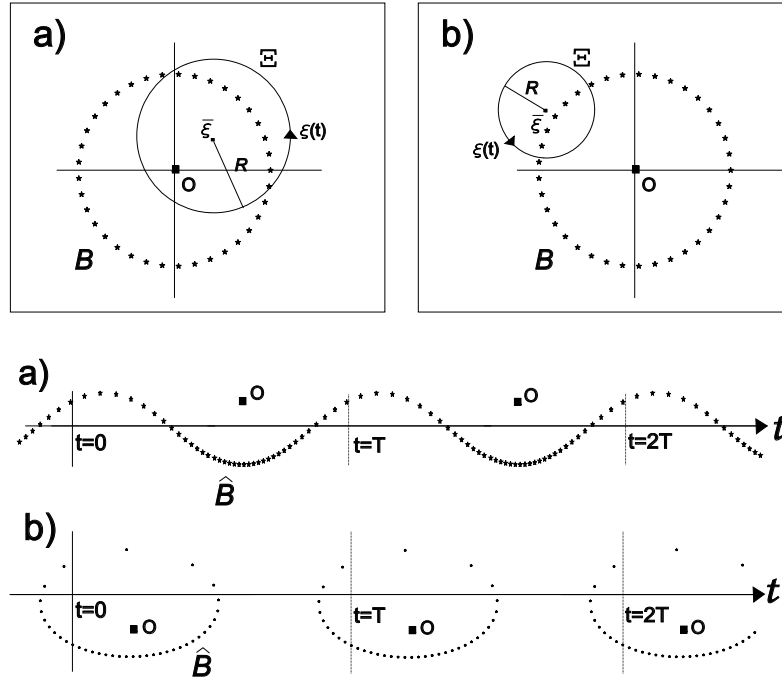


Figure 4.8: Evolutionary paths and branch points of the solutions in the complex ξ -plane and t -plane for $\mu = 15/37$.

periodically in the *real* direction with period T , see (2.8). In particular – to mention the main features relevant to our treatment, see above – the circle B on which the *square-root* branch points in the *complex* ξ -plane sit, gets mapped in the *complex* t -plane into a curve \hat{B} on which sit the *square-root* branch points in the *complex* t -plane; note that this curve \hat{B} (in contrast to the circle B) *does* now *depend* on the initial data. This curve is of course repeated periodically; it is *closed* and contained in each vertical slab of width T (see Figure 4.8b) if the point $\bar{\xi}$ is *outside* B , otherwise it is *open*, starting in one slab and ending in the adjoining slab at a point shifted by the amount T ; and it does not or does cross (of course twice in each period) the *real* axis in the *complex* t -plane depending whether, in the *complex* ξ -plane, the two circles B and Ξ do not or do intersect each other (see Figure 4.8a).

Likewise, depending whether it is *inside* or *outside* the circle Ξ , the point $\xi = 0$ – which, as entailed by our analysis, is a highly relevant branch point in the *complex* ξ -plane (unless $0 < \mu < 1$) – gets mapped into an analogous branch point located in each vertical slab *above* or *below* the *real* axis in the *complex* t -plane; while the other branch point, at $\xi = \infty$ in the *complex* ξ -plane, gets mapped into an analogous branch point located at infinity in the *lower half* of the *complex* t -plane. Clearly the physical mechanism of *near misses*, which is the main cause of the eventual *irregularity* of the motion, becomes relevant only for initial data such that the curve \hat{B} crosses the *real* axis, thereby causing (if μ is *irrational*) an infinity of *square-root* branch points of the functions $z_n(t)$ to occur *arbitrarily close* to the *real* axis in the *complex* t -plane – branch points which are however *active* (namely, they actually cause a *near miss* in the physical evolution) in only some (yet still an infinity) of the infinite number of vertical slabs in which the *complex* t -plane gets now naturally partitioned. The *near miss* implies that the two particles involved in it slide past each other from one side or the other depending whether the corresponding branch point is just above or just below the *real* axis in the *complex* t -plane. The *sensitive* dependence on the initial data is due to the fact that any tiny change of them causes some *active* branch

point in the *complex t*-plane which is very close to real axis to cross over from one side of it to the other, thereby drastically changing the outcome of the corresponding *near miss*.

This terse discussion shows clearly that the explanation of the *irregular* behavior of a dynamical system in terms of travel on a Riemann surface is by no means restricted to *isochronous* systems. We found it convenient to illustrate in detail this paradigm by focussing in this thesis on a simple *isochronous* model and by using firstly τ and then ξ as independent *complex* variables – but, as outlined just above, our analysis can also be done – albeit less neatly – by using directly the independent *complex* variable t ; and the occurrence of a kind of periodic partition of the *complex t*-plane into an infinite sequence of vertical slabs – characteristic of our *isochronous* model – does not play an essential role to explain the *irregular* character of the motion when such a phenomenology does indeed emerge. The essential point is the possibility to reinterpret the time evolution as travel on a Riemann surface, the structure of which is sufficiently complicated to cause an *irregular* motion featuring a *sensitive dependence* on its initial data. The essential feature causing such an outcome is the presence of an *infinity* of branch points *arbitrarily close* to the *real* axis in the *complex t*-plane, the positions of which, as well as the identification of which of them are *active*, depends on the *initial data* nontrivially. The model treated in this work shows that such a structure can be complicated enough to cause an *irregular* motion, yet amenable to a simple mathematical description yielding a rather detailed understanding of this motion; this suggests the efficacy also in more general contexts of this paradigm to understand (certain) *irregular* motions featuring a *sensitive dependence* on their initial data and possibly even to *predict* their behavior to the extent such a paradoxical achievement (predicting the unpredictable!) can at all be feasible.

APPENDIX A

The Algebraic Equations (2.39)

In this appendix we solve, in the semisymmetrical case, see (2.2), the nonlinear algebraic equations (2.39) that characterize the equilibrium configurations and we thereby compute the “eigenvalue” $\gamma^{(3)}$, namely we obtain its two expressions (2.51a) and (2.51b).

The equations to be solved read (see (2.39))

$$\alpha_1 = \frac{2g}{\alpha_1 - \alpha_3} + \frac{2f}{\alpha_1 - \alpha_2} , \quad (\text{A.1a})$$

$$\alpha_2 = \frac{2g}{\alpha_2 - \alpha_3} - \frac{2f}{\alpha_1 - \alpha_2} , \quad (\text{A.1b})$$

$$\alpha_3 = \frac{2g}{\alpha_3 - \alpha_1} + \frac{2g}{\alpha_3 - \alpha_2} , \quad (\text{A.1c})$$

and they of course imply the relation

$$\alpha_1 + \alpha_2 + \alpha_3 = 0 . \quad (\text{A.2})$$

It is now convenient to set

$$S = \alpha_1 + \alpha_2 , \quad D = \alpha_1 - \alpha_2 , \quad (\text{A.3a})$$

entailing

$$\alpha_1 = \frac{S + D}{2} , \quad \alpha_2 = \frac{S - D}{2} , \quad \alpha_3 = -S . \quad (\text{A.3b})$$

From (the sum of) (A.1a) and (A.1b) we easily get

$$S (9 S^2 - D^2) = 24 g S , \quad (\text{A.4})$$

and from this we get two types of solutions. The *first* solution is characterized by $S = 0$, implying (see (A.3b) and (A.1a))

$$\alpha_3 = 0 , \quad \alpha_1 = -\alpha_2 = \alpha , \quad \alpha^2 = f + 2g , \quad (\text{A.5})$$

entailing (via (2.38)) the solution (2.49) for the equilibrium configuration, as well as (via (2.40b) with (2.2)) the expressions

$$\beta_3 = \frac{f}{2(f + 2g)} = \frac{\varphi}{2(\varphi + 2)} , \quad (\text{A.6a})$$

$$\beta_1 = \beta_2 = \frac{2g}{f + 2g} = \frac{2}{\varphi + 2} , \quad (\text{A.6b})$$

hence, via (2.47), the first expression, (2.51a), for $\gamma^{(3)}$.

The *second* solution is characterized by

$$9 S^2 - D^2 = 24 g . \quad (\text{A.7})$$

We now subtract (A.1b) from (A.1a) and we thereby easily get

$$D^2 = \frac{-8 g D^2}{9 S^2 - D^2} + 4 f , \quad (\text{A.8})$$

hence, via the preceding relation,

$$D^2 = 3 f , \quad S^2 = \frac{f + 8 g}{3} . \quad (\text{A.9})$$

And via (2.40b) with (2.2) and (A.3b) this is easily seen to yield

$$\beta_1 + \beta_2 + \beta_3 = \frac{f + 8 g}{6 g} = \frac{\varphi + 8}{6} , \quad (\text{A.10})$$

namely, via (2.47), the second expression, (2.51b), of $\gamma^{(3)}$.

Note moreover that, *in both cases*, one gets the relation

$$(\alpha_1 - \alpha_2)^2 + (\alpha_2 - \alpha_3)^2 + (\alpha_3 - \alpha_1)^2 = 6 (f + 2g) , \quad (\text{A.11})$$

as can be easily verified from (A.5) as well as from (A.3) with (A.9).

APPENDIX B

Solution of the ODE (2.87)

In this Appendix we explain how to integrate the ODE (2.87) in the general case when the three coupling constants g_n are *all* different, namely when the restriction (2.2) identifying the semisymmetrical case does *not* apply, and we also provide the solution of the ODE (2.87) in the two special cases (belonging to the semisymmetrical class characterized by the restriction (2.2)) the treatment of which had been omitted in Section 2.5, and as well in another special case not belonging to the semisymmetrical class.

The general case

In this subsection of Appendix B we indicate how the ODE (2.87) can be integrated in the general case when the three coupling constants g_n are *all* different. It is then convenient to set

$$V(\tau) = \tan[\theta(\tau)] , \quad (\text{B.1})$$

so that this ODE read

$$\frac{V' V (V^2 - 3)}{(V^2 + 1) (A V^3 + C V^2 + A V + C - 2)} = \frac{1}{(\tau - \tau_1)} \quad (\text{B.2})$$

with

$$A = \frac{\sqrt{3} (g_1 - g_2)}{2 (g_1 + g_2 + g_3)} , \quad C = \frac{4 g_1 + 4 g_2 + g_3}{2 (g_1 + g_2 + g_3)} . \quad (\text{B.3})$$

To integrate this ODE we set

$$A V^3 + C V^2 + A V + C - 2 = A (V - V_1) (V - V_2) (V - V_3) , \quad (\text{B.4})$$

so that the *three* quantities V_n are the *three* roots of this polynomial of *third* degree in V . We then decompose this rational function of V in simple fractions,

$$\frac{V (V^2 - 3)}{(V^2 + 1) (A V^3 + C V^2 + A V + C - 2)} = \sum_{j=1}^5 \frac{\mu_j}{V - V_j} , \quad (\text{B.5})$$

where of course

$$V_4 = i , \quad V_5 = -i , \quad (\text{B.6})$$

and the *five* quantities μ_j are easily evaluated in terms of A , C and the 3 roots V_n .

The integration of the ODE (B.2) is now trivial (using (B.5)), and it yields (using (B.6)) the final formula

$$[V(\tau) - i]^{\lambda_4} [V(\tau) + i]^{\lambda_5} \prod_{n=1}^3 [V(\tau) - V_n]^{\lambda_n} = K (\tau - \tau_1) , \quad (\text{B.7})$$

where K is the integration constant.

Two special subcases of the semisymmetrical case

In this subsection of Appendix B we provide the solution of the ODE (2.87) in the two special subcases (of the semisymmetrical case) the treatment of which had been omitted in Section 2.5, and as well in another special case *not* belonging to the semisymmetrical class.

If

$$g_1 + g_2 + g_3 = 0 , \quad (\text{B.8})$$

ρ is constant (namely τ -independent, $\rho(\tau) = \rho(0)$, see (2.84c)). Moreover, via the restriction (2.2) characterizing the semisymmetrical class, we get (see also (2.25))

$$f = -2g, \quad \varphi = -2, \quad \mu = 0 . \quad (\text{B.9a})$$

Then (2.89) is replaced by

$$u(\tau) \exp[-2u^2(\tau)] = \exp\left[\frac{3f(\tau - \tau_0)}{\rho^2(0)}\right] . \quad (\text{B.9b})$$

Let us also note that, if (2.2) were replaced by

$$g_1 = -g_2 = g, \quad g_3 = 0 , \quad (\text{B.10a})$$

which is also consistent with (B.8), then (2.89) with (2.86) would be replaced by

$$\theta(\tau) + \sin[2\theta(\tau)] = \frac{2\sqrt{3}g(\tau_0 - \tau)}{\rho^2(0)} . \quad (\text{B.10b})$$

Returning to the semisymmetrical case characterized by validity of the restriction (2.2) we now consider the second case the treatment of which had been omitted in Section 2.5, namely

$$f = -8g, \quad \varphi = -8 . \quad (\text{B.11a})$$

Note that in this case μ diverges, see (2.25). Then (2.89) is replaced by

$$u(\tau) \exp[u^2(\tau)] = [K(\tau - \tau_1)]^{-1/2} . \quad (\text{B.11b})$$

Note that the two values $\varphi = -2$ and $\varphi = -8$ were already identified as special boundary cases in the treatments of Section 2.4, see for instance (2.73a), and of Section 2.6.

APPENDIX C

Explicitly Solvable Cases

In this section we identify several cases which are *nontrivial* (namely, with at least *two nonvanishing* coupling constants, hence not reducible to the disjointed union of a two-body, and a free one-body, problem), for which the solution $z_n(t)$ of our model (2.10) can be exhibited in *completely explicit* form. All these cases belong to the semisymmetrical case with coupling constants f and g that are *congruent* so that φ , see (2.2), is *real* and *rational*, as well as μ , see (2.25) and (2.26). They correspond to special assignments of the coupling constants that cause the (relevant) algebraic equation (2.117) to be *polynomial* of degree at most *four*, hence *explicitly* solvable for $\tilde{w}(t)$. Hence *all* their solutions $z_n(t)$ are *completely periodic*, except for a lower dimensional set of solutions that become *singular* due to the collision of *two* particles, or even more exceptionally, of all *three* particles (note that, at the singularity, the values of the particle coordinates are finite, but their velocities diverge). These solutions, besides their intrinsic interest as motions in the plane determined by the equations of motion (2.10), allow to verify the findings discussed in Section 2.6, including the structure of the Riemann surface associated with the solution $w(\xi)$ of (2.98), which in all these cases is a polynomial equation in w of degree at most *four*.

In the following table, in the first column are reported the cases in which equation (2.98) becomes a second degree polynomial equation; in the second column are reported the cases in which equation (2.98) becomes a third degree polynomial equation; in the third column are reported the cases in which equation (2.98) becomes a fourth degree polynomial equation.

2 – nd degree	3 – rd degree	4 – th degree
$\varphi = -14, \mu = 2$	$\varphi = -20, \mu = \frac{3}{2}$	$\varphi = -26, \mu = \frac{4}{3}$
$\varphi = 4, \mu = \frac{1}{2}$	$\varphi = -11, \mu = 3$	$\varphi = -10, \mu = 4$
$\varphi = -5, \mu = -1$	$\varphi = 10, \mu = \frac{2}{3}$	$\varphi = 16, \mu = \frac{3}{4}$
	$\varphi = -6, \mu = -2$	$\varphi = 4, \mu = \frac{1}{2}$
	$\varphi = -4, \mu = -\frac{1}{2}$	$\varphi = 0, \mu = \frac{1}{4}$
	$\varphi = 1, \mu = \frac{1}{3}$ (the integrable case)	$\varphi = -\frac{13}{2}, \mu = -3$
		$\varphi = -\frac{7}{2}, \mu = -\frac{1}{3}$

APPENDIX D

Relation with More Standard (Newtonian) Three-Body Problems

In this Appendix we indicate the relation among the three-body problems treated in this thesis, characterized by equations of motion of *Aristotelian* type (“the particle *velocities* are proportional to assigned external and interparticle forces”), with analogous many-body problems characterized by equations of motion of *Newtonian* type (“the particle *accelerations* are proportional to assigned external and interparticle forces”). The results reviewed in this section are of interest inasmuch as they relate the model treated in this thesis to other, somewhat more physical and certainly more classical, many-body problems, including a prototypical three-body model introduced, and shown to be solvable by quadratures, by Carl Jacobi one and a half centuries ago [63], and the one-dimensional Newtonian many-body problem with two-body forces proportional to the inverse cube of the interparticle distance introduced and solved over four decades ago (firstly in the quantal context [64] and then in the classical context [65], see Section 1.2.1), which contributed to the bloom in the investigation of integrable dynamical systems of the last few decades (see for instance [5]).

By differentiating the equations of motion (2.1) and using them again to eliminate the first derivatives in the right-hand sides one gets the following *second-order* equations of motion of Newtonian type:

$$\zeta_n'' = -\frac{2g_{n+1}^2}{(\zeta_n - \zeta_{n+2})^3} - \frac{2g_{n+2}^2}{(\zeta_n - \zeta_{n+1})^3} + \frac{g_{n+1}(g_n - g_{n+2})}{(\zeta_n - \zeta_{n+2})^2(\zeta_{n+2} - \zeta_{n+1})} + \frac{g_{n+2}(g_n - g_{n+1})}{(\zeta_n - \zeta_{n+1})^2(\zeta_{n+1} - \zeta_{n+2})}. \quad (\text{D.1})$$

Likewise from the equations of motion (2.10) one gets

$$\ddot{z}_n + \omega^2 z_n = -\frac{2g_{n+1}^2}{(z_n - z_{n+2})^3} - \frac{2g_{n+2}^2}{(z_n - z_{n+1})^3} + \frac{g_{n+1}(g_n - g_{n+2})}{(z_n - z_{n+2})^2(z_{n+2} - z_{n+1})} + \frac{g_{n+2}(g_n - g_{n+1})}{(z_n - z_{n+1})^2(z_{n+1} - z_{n+2})}. \quad (\text{D.2})$$

Of course the solutions of the *first-order* equations of motion, (2.1) respectively (2.10), satisfy as well the corresponding *second-order* equations of motion, (D.1) respectively (D.2)

), but they provide only a subset of the solutions of the latter. On the other hand it is again true that the solutions of the second-order equations of motion (D.1) and (D.2) are related via the trick (2.7).

In the integrable “equal-particle” case, see (2.3), these equations of motion simplify and correspond respectively to the Newtonian equations of motion yielded by the two standard N -body Hamiltonians

$$H(\underline{\zeta}, \underline{\pi}) = \sum_{n=1}^N \frac{\pi_n^2}{2} - \sum_{m,n=1; m \neq n}^N \frac{g^2}{2(\zeta_n - \zeta_m)^2}, \quad (\text{D.3})$$

respectively

$$H(\underline{z}, \underline{p}) = \sum_{n=1}^N \frac{p_n^2 + \omega^2 z_n^2}{2} - \sum_{m,n=1; m \neq n}^N \frac{g^2}{2(\zeta_n - \zeta_m)^2}, \quad (\text{D.4})$$

with $N = 3$, the complete integrability of which is by now a classical result (even in the N -body case with $N > 3$: see for instance [5]).

In fact the more general *three-body* Hamiltonian models

$$H(\underline{\zeta}, \underline{\pi}) = \sum_{n=1}^3 \left[\frac{\pi_n^2}{2} - \frac{g_n^2}{(\zeta_{n+1} - \zeta_{n+2})^2} \right], \quad (\text{D.5})$$

respectively

$$H(\underline{z}, \underline{p}) = \sum_{n=1}^3 \left[\frac{p_n^2 + \omega^2 z_n^2}{2} - \frac{g_n^2}{(z_{n+1} - z_{n+2})^2} \right], \quad (\text{D.6})$$

featuring three *different* coupling constants g_n , that yield the equations of motion

$$\zeta_n'' = -\frac{2g_{n+1}^2}{(\zeta_n - \zeta_{n+2})^3} - \frac{2g_{n+2}^2}{(\zeta_n - \zeta_{n+1})^3}, \quad (\text{D.7})$$

respectively

$$\ddot{z}_n + \omega^2 z_n = -\frac{2g_{n+1}^2}{(z_n - z_{n+2})^3} - \frac{2g_{n+2}^2}{(z_n - z_{n+1})^3}, \quad (\text{D.8})$$

are also solvable by quadratures. For the equations of motion (D.7) this discovery is due to Carl Jacobi [63]; while the solutions of the equations of motion (D.8) can be easily obtained from those of the equations of motion (D.7) via the trick (2.7). For a detailed discussion of these solutions, and additional indications on key contributions to the study of this problem, the interested reader is referred to [6] and [5]. But we also plan to revisit this problem, because we believe that additional study of these models, (D.7) and (D.8), shall shed additional light on the mechanism responsible for the *onset* of a certain kind of *deterministic chaos*, as discussed above.

Non senza fatica si giunge al fine.
Girolamo Frescobaldi, "Toccata Nona", 1627

LIST OF FIGURES

1.1	Different values of the period in terms of λ	25
1.2	A numerical example of the dynamics of the Calogero-Moser model.	26
1.3	Orders of a permutation of 7 elements	32
1.4	Possible periods for the first few N	32
1.5	A few different periodic motions for $N = 7$	33
1.6	First few values of $G(N)$	34
1.7	The functions $\log G(N)$ and $\sqrt{N \log N}$ for N up to 301	35
1.8	Different values of the period in terms of λ	43
1.9	Observed period jumps	43
1.10	A numerical example of the dynamics of the Goldfish model.	45
1.11	Scattering of two bodies in the three-body problem 1.18 corresponding to a <i>near miss</i> . The two outcomes originate from two sets of initial data close to each other such that a square-root branch point τ_b falls on different sides of the circle \mathbb{C}	51
3.1	The basic configuration of roots, for $\xi \in \gamma_1$, $ \xi \gg 1$, for the Riemann surface $q = 12$, $p = 5$	97
3.2	The cutted ξ -plane of the Riemann surface $q = 12$, $p = 5$ is the interior of the oriented contour γ	97
3.3	The contour surrounding the cut γ_1	99
3.4	Exchange of a pair of roots. As ξ travels on the contour surrounding the cut γ_j , as in Figure 3.3, w_j and w_{j+q-p} interchange their positions, while the other $(q-p)$ roots are essentially not affected by this motion.	99
3.5	Cyclic permutation of the two groups of roots. If $\xi \in \gamma_j$, the roots w_j and w_{j+q-p} are aligned on the segment $(0, 1)$; after a $2\pi/q$ counterclockwise rotation of ξ on a big circle, the two groups of roots $\{w_j, \dots, w_{j+q-p-1}\}$ and $\{w_{j+q-p-1}, \dots, w_{j+q-1}\}$ undergo a clockwise rotation. When ξ reaches γ_{j+1} , then the roots w_{j+1} and $w_{j+1+q-p}$ get aligned on the segment $(0, 1)$	99
3.6	As ξ draws the closed contour γ in Figure 3.2, each root draws a closed contour around the cut $(0, 1)$ in the w -plane. Therefore the image of the cutted ξ plane is the w plane cutted along the segment $[0, 1]$	100
3.7	The table summarizing the connection rules of the Riemann surface. The sheets \mathcal{F}_j is connected with the sheet $\mathcal{F}_{j+q-p} \text{ MÖD } q$ at the SRBP $\xi_b^{(j)}$. The sheets \mathcal{F}_j is connected with the sheet $\mathcal{F}_{j-q+p} \text{ MÖD } q$ at the SRBP $\xi_b^{(j-q+p)}$	101
3.8	The topological properties of Γ for $q = 12$ and $p = 5$	101

3.9	Branch points double indexes ($p = 5, q = 12$)	102
3.10	Nodes labelling ($p = 5, q = 12$).	103
3.11	Consecutive branch points inclusions ($p = 5, q = 12$).	104
3.12	Ferrer diagram corresponding to the inclusion of 6 consecutive branch points ($p = 5, q = 12$).	105
3.13	Wrong bumpings <i>vs</i> Correct bumpings	108
3.14	Ferrer diagrams for consecutive branch points inclusions ($p = 5, q = 12$): <i>a</i>) non-numbered Ferrer diagrams; <i>b</i>) numbered Ferrer diagrams.	109
3.15	The definition of the angle ϕ	115
3.16	$T(\nu)$ <i>vs</i> ν . In red, green and blue respectively the three different values of $T(\nu)$, while the black continuous lines are the lower and upper bounds in (3.63).	118
3.17	The ∞ -configuration of the Riemann surface for $p = 8$ and $q = 5$: for $\xi \gg 1$, the p roots $w_j, j = 1, \dots, p$ lie on a small circle centered at the origin and of radius $O(\xi^{-(q/p)})$. As ξ travels along the cut γ_1 (see Figure 3.18), from ∞ to $\xi_b^{(1)}$, the complex conjugate roots w_1 and w_6 abandon the ∞ -configuration and collide at μ . After fixing w_1 , the enumeration of the other roots (sheets) is sequential and counterclockwise.	120
3.18	The cutted ξ -plane for the Riemann surface $q = 5, p = 8$	120
3.19	The motion of ξ around the cut γ_1	122
3.20	As ξ travels around the branch cut γ_1 , the the complex conjugate roots w_1 and w_6 exchange their positions colliding in μ . The remaining roots have a trivial monodromy. Riemann surface $q = 5, p = 8$	122
3.21	As ξ travels from the branch cut γ_1 to the branch cut γ_2 on a big circle, the ∞ -configuration has a $2\pi/p$ clockwise rotation, corresponding to a back- ward cyclic permutation of the p roots: $\{w_1, w_2, \dots, w_p\} \rightarrow \{w_2, \dots, w_p, w_1\}$. Riemann surface $q = 5, p = 8$	122
3.22	As ξ travels on the closed contour surrounding all cuts, the roots of type q : $w_j, j = 1, \dots, q$ draw the closed contour represented in this figure. The exterior of such a contour is the image of the cutted ξ -plane via the roots $w_j, j = 1, \dots, q$	123
3.23	The topological properties of Γ for $q = 5$ and $p = 8$	124
3.24	The connection table in the case $2q < p$. On each horizontal line we indicate, for each square root branch point, the sheets of type q and $(p - q)$ which are connect by it. In this case any sheet of type $(p - q)$ is connected to at most one sheet of type q . Consequently, the sheets of type q are connected among themselves only through the branch point $(0, 1)$ and an increase of the period can occur only when the evolutionary circle includes the origin $\xi = 0$	125
3.25	The connection table in the case $p < 2q$. On each horizontal line we indicate, for each square root branch point, the sheets of type q and $(p - q)$ which are connect by it. In this case, some sheet of type $(p - q)$ is connected to more than one sheet of type q . Consequently, there are sheets of type q which are connected among them-selves via that $(p - q)$ -sheet, also when the origin $\xi = 0$ is not included in the evolutionary circle.	125
3.26	Branch points double indexes ($p = 11, q = 8$)	126
3.27	Graph construction and nodes labelling ($p = 11, q = 8$).	127
3.28	Consecutive branch points inclusions ($p = 11, q = 8$, origin outside).	128
3.29	Consecutive branch points inclusions ($p = 11, q = 8$, origin inside).	129
3.30	Ferrer diagram corresponding to the inclusion of 7 consecutive SRBPs but not of the origin ($p = 11, q = 8$).	130

3.31	Ferrer diagrams for consecutive branch points inclusions ($p = 11$, $q = 8$, origin outside): <i>a</i>) non-numbered Ferrer diagrams; <i>b</i>) numbered Ferrer diagrams.	132
3.32	Ferrer diagrams for consecutive branch points inclusions ($p = 11$, $q = 8$, origin inside): <i>a</i>) non-numbered Ferrer diagrams; <i>b</i>) numbered Ferrer diagrams.	133
4.1	Periods, with respect to the mutual position of the Ξ -circle and the B -circle, for rational and irrational values of $\mu < 0$ (b is the number of consecutive SRBPs included in Ξ ; the variable ν is defined as in (3.45)).	148
4.2	Periods, with respect to the mutual position of the Ξ -circle and the B -circle, for rational and irrational values of $0 < \mu < 1$ (b is the number of consecutive SRBPs included in Ξ ; the variable ν is defined as in (3.45)).	149
4.3	Periods, with respect to the mutual position of the Ξ -circle and the B -circle, for rational and irrational values of $\mu > 1$ (b is the number of consecutive SRBPs included in Ξ ; the variable ν is defined as in (3.45)).	150
4.4	Period of the solution as a function of the initial data for the case $\mu = 11/8$	153
4.5	Period of the solution as a function of the initial data for the case $\mu = 5/12$	155
4.6	Sequence of values of μ in Figure 4.7.	156
4.7	Sensitive dependence of the period on initial data.	157
4.8	Evolutionary paths and branch points of the solutions in the complex ξ -plane and t -plane for $\mu = 15/37$	160

BIBLIOGRAPHY

- [1] F. Calogero, D. Gomez-Ullate, P. M. Santini and M. Sommacal, “The transition from regular to irregular motions, explained as travel on Riemann surfaces”, *J. Phys.* **A38**, 1-24 (2005).
- [2] F. Calogero, D. Gomez-Ullate, P. M. Santini and M. Sommacal, “Towards a theory of chaos as travel on Riemann surfaces”, (in preparation).
- [3] F. Calogero, D. Gomez-Ullate, P. M. Santini and M. Sommacal, “An integrable dynamical system with sensitive dependence on initial conditions”, (in preparation).
- [4] F. Calogero, “A class of integrable Hamiltonian systems whose solutions are (perhaps) all completely periodic”, *J. Math. Phys.* **38**, 5711-5719 (1997).
- [5] F. Calogero, *Classical many-body problems amenable to exact treatments*, Lecture Notes in Physics Monograph **m 66**, Springer, Berlin (2001).
- [6] F. Calogero and M. Sommacal, “Periodic solutions of a system of complex ODEs. II. Higher periods”, *J. Nonlinear Math. Phys.* **9**, 1-33 (2002).
- [7] F. Calogero, J.-P. Francoise and M. Sommacal, “Periodic solutions of a many-rotator problem in the plane. II. Analysis of various motions”, *J. Nonlinear Math. Phys.* **10**, 157-214 (2003).
- [8] H. M. Farkas and I. Kra, *Riemann Surfaces*, Springer-Verlag, 1992.
- [9] R. Miranda, *Algebraic Curves and Riemann Surfaces*, American Mathematical Society, Graduate Studies in Mathematics, Vol. 5, 1995.
- [10] M. Bruschi and F. Calogero, “Novel variants of the goldfish many-body model”, (in preparation).
- [11] F. Calogero, “Differential equations featuring many periodic solutions”, in: L. Mason and Y. Nutku (eds), *Geometry and integrability*, London Mathematical Society Lecture Notes, vol. **295**, Cambridge University Press, Cambridge, 2003, pp. 9-21.
- [12] F. Calogero, “Periodic solutions of a system of complex ODEs”, *Phys. Lett.* **A293**, 146-150 (2002).
- [13] F. Calogero, “On a modified version of a solvable ODE due to Painlevé”, *J. Phys. A: Math. Gen.* **35**, 985-992 (2002).

- [14] F. Calogero, “On modified versions of some solvable ODEs due to Chazy”, *J. Phys. A: Math. Gen.* **35**, 4249-4256 (2002).
- [15] F. Calogero, “Solvable three-body problem and Painlevé conjectures”, *Theor. Math. Phys.* **133**, 1443-1452 (2002); Erratum **134**, 139 (2003).
- [16] F. Calogero, “A complex deformation of the classical gravitational many-body problem that features a lot of completely periodic motions”, *J. Phys. A: Math. Gen.* **35**, 3619-3627 (2002).
- [17] F. Calogero, “Partially superintegrable (indeed isochronous) systems are not rare”, in: *New Trends in Integrability and Partial Solvability*, edited by A. B. Shabat, A. Gonzalez-Lopez, M. Manas, L. Martinez Alonso and M. A. Rodriguez, NATO Science Series, II. Mathematics, Physics and Chemistry, vol. **132**, Proceedings of the NATO Advanced Research Workshop held in Cadiz, Spain, 2-16 June 2002, Kluwer, 2004, pp. 49-77.
- [18] F. Calogero, “General solution of a three-body problem in the plane”, *J. Phys. A: Math. Gen.* **36**, 7291-7299 (2003).
- [19] F. Calogero, “Solution of the goldfish N-body problem in the plane with (only) nearest-neighbor coupling constants all equal to minus one half”, *J. Nonlinear Math. Phys.* **11**, 1-11 (2004).
- [20] F. Calogero, “Two new classes of isochronous Hamiltonian systems”, *J. Nonlinear Math. Phys.* **11**, 208-222 (2004).
- [21] F. Calogero, “Isochronous dynamical systems”, *Applicable Anal* (in press).
- [22] F. Calogero, “A technique to identify solvable dynamical systems, and a solvable generalization of the goldfish many-body problem”, *J. Math. Phys.* **45**, 2266-2279 (2004).
- [23] F. Calogero, “A technique to identify solvable dynamical systems, and another solvable extension of the goldfish many-body problem”, *J. Math. Phys.* **45**, 4661-4678 (2004).
- [24] F. Calogero, “Isochronous systems”, *Proceedings of the Conference on Geometry, Integrability and Physics*, Varna, June 2004 (in press).
- [25] F. Calogero, “Isochronous systems”, in: *Encyclopedia of Mathematical Physics*, edited by J.-P. Francoise, G. Naber and Tsou Sheung Tsun (in press).
- [26] F. Calogero and A. Degasperis, “Novel solution of the integrable system describing the resonant interaction of three waves”, *Physica D* **200**, 242-256 (2005).
- [27] F. Calogero, L. Di Cerbo and R. Droghei, “On isochronous Bruschi-Ragnisco-Ruijsenaars-Toda lattices: equilibrium configurations, behavior in their neighborhood, diophantine relations and conjectures”, (in preparation).
- [28] F. Calogero, L. Di Cerbo and R. Droghei, “On isochronous Shabat-Yamilov lattices: equilibrium configurations, behavior in their neighborhood, diophantine relations and conjectures”, (in preparation).
- [29] F. Calogero and J.-P. Francoise, “Periodic solutions of a many-rotator problem in the plane”, *Inverse Problems* **17**, 1-8 (2001).
- [30] F. Calogero and J.-P. Francoise, “Periodic motions galore: how to modify nonlinear evolution equations so that they feature a lot of periodic solutions”, *J. Nonlinear Math. Phys.* **9**, 99-125 (2002).

- [31] F. Calogero and J.-P. Francoise, “Nonlinear evolution ODEs featuring many periodic solutions”, *Theor. Math. Phys.* **137**, 1663-1675 (2003).
- [32] F. Calogero and J.-P. Francoise, “Isochronous motions galore: nonlinearly coupled oscillators with lots of isochronous solutions”, in: *Superintegrability in Classical and Quantum Systems*, Proceedings of the Workshop on Superintegrability in Classical and Quantum Systems, Centre de Recherches Mathématiques (CRM), Université de Montréal, September 16-21 (2003), CRM Proceedings & Lecture Notes, vol. **37**, American Mathematical Society, 2004, pp. 15-27.
- [33] F. Calogero and J.-P. Francoise, “New solvable many-body problems in the plane”, *Annales Henri Poincaré* (submitted to).
- [34] F. Calogero, J.-P. Francoise and A. Guillot, “A further solvable three-body problem in the plane”, *J. Math. Phys.* **10**, 157-214 (2003).
- [35] F. Calogero and V. I. Inozemtsev, “Nonlinear harmonic oscillators”, *J. Phys. A: Math. Gen.* **35**, 10365-10375 (2002).
- [36] F. Calogero and S. Iona, “Novel solvable extension of the goldfish many-body model”, *J. Math. Phys.* (submitted to).
- [37] M. Mariani and F. Calogero, “A modified Schwarzian Korteweg de Vries equation in 2+1 dimensions with lots of periodic solutions”, *Yadernaya Fizika* (in press).
- [38] D. Gómez-Ullate, A. N. W. Hone and M. Sommacal, “New many-body problems in the plane with periodic solutions”, *New J. Phys.* **6**, 1–23 (2004).
- [39] S. Iona and F. Calogero, “Integrable systems of quartic oscillators in ordinary (three-dimensional) space”, *J. Phys. A: Math. Gen.* **35**, 3091-3098 (2002).
- [40] M. Mariani, “Identificazione e studio di sistemi dinamici ed equazioni di evoluzione nonlineari che posseggono molte soluzioni completamente periodiche (isocrone)”, Tesi di Laurea in Fisica, Università di Roma “La Sapienza”, 2003.
- [41] M. Mariani and F. Calogero, “Isochronous PDEs”, *Yadernaya Fizika* (in press).
- [42] M. Sommacal, “Studio di problemi a molti corpi nel piano con tecniche numeriche ed analitiche”, Tesi di Laurea in Fisica, Università di Roma “La Sapienza”, 2002.
- [43] F. Calogero, “The Neatest Many-Body Problem Amenable to Exact Treatments (a Goldfish?)”, *Physica* **D152-153**, 78-84 (2001).
- [44] F. Calogero, “Tricks of the Trade: Relating and Deriving Solvable and Integrable Dynamical Systems”, in *Calogero-Moser-Sutherland Models*, Editors: van Diejen J F and Vinet L, Proceedings of the Workshop on Calogero-Moser-Sutherland Models held in Montreal, 10-15 March 1997, CRM Series in Mathematical Physics, Springer, 93-116 (2000).
- [45] E. L. Ince, *Ordinary differential equations*, Dover, New York, 1956.
- [46] F. Calogero, “Motion of Poles and Zeros of Special Solutions of Nonlinear and Linear Partial Differential Equations, and Related ‘Solvable’ Many-Body Problems”, *Nuovo Cimento* **B43**, 177-241 (1978).
- [47] D. Gomez-Ullate and M. Sommacal, “Periods of the Goldfish many-body problem”, *J. Nonlin. Math. Phys.*, Vol. 12, Supplement 1, 351-362 (2005).

- [48] T. Prosen, “Parametric statistics of zeros of Husimi representations of quantum chaotic eigenstates and random polynomials”, *J. Phys.* **A29**, 5429-5440 (1996).
- [49] S. N. M. Ruijsenaars and H. Schneider, “A New Class of Integrable Systems and its relation to solitons”, *Ann. Phys. (NY)* **170**, 370-405 (1986).
- [50] E. Landau, “Über die Maximalordnung der Permutationen gegebenen Grades”, *Archiv der Math. und Phys.* (1903), 92-103. Handbuch der Lehre von der Verteilung der primzahlen, 2nd Ed. Chelsea, New York, 1953.
- [51] J. Grantham, “The Largest Prime Dividing the Maximal Order of an Element of \mathcal{S}_n ”, *Math. Comput.* **64**, 407-410 (1995).
- [52] Shah S M, “An inequality for the arithmetical function $g(x)$ ”, *J. Ind. Math. Soc.* **3**, 316-318 (1938).
- [53] J. Massias, “Majoration explicite de l’ordre maximum d’un element du group symétrique”, *Ann. Fac. Sci. Toulouse Math.* **6**(5), no. 3-4, 269-281 (1984) · J. Massias, J. Nicolas and G. Robin, “Effective Bounds for the Maximal Order of an Element in the Symmetric Group”, *Math. Comput.* **53**, 665-678 (1989) · W. Miller, “The Maximum Order of an Element of a Finite Symmetric Group”, *The American Mathematical Monthly*, **94**, 497-506 (1987) · M. B. Nathanson, “On the Greatest Order of an Element of the Symmetric Group”, *The American Mathematical Monthly*, **79**, 500-501 (1972) · J. L. Nicolas, “Sur l’ordre maximum d’un élément dans le group \mathcal{S}_n des permutations”, *Acta Arithmetica XIV* (1968) 315-325 · J. L. Nicolas, “Calcul de l’ordre maximum d’un élément du groupe symétrique”, “Rev. Francaise Informat. Recherche Operationelle”, **3**, 43-50 (1969).
- [54] Erdélyi A (Editor), *Higher Transcendental Functions*, McGraw-Hill, 1953.
- [55] M. D. Kruskal and P. A. Clarkson, “The Painlevé-Kowalewski and poly-Painlevé tests for integrability”, *Studies Appl. Math.* **86**, 87-165 (1992) · R. D. Costin and M. D. Kruskal, “Nonintegrability criteria for a class of differential equations with two regular singular points”, *Nonlinearity* **16**, 1295-1317 (2003) · R. D. Costin, “Integrability properties of a generalized Lamé equation: applications to the Hénon-Heiles system”, *Methods Appl. Anal.* **4**, 113-123 (1997).
- [56] T. Bountis, L. Drossos and I. C. Percival, “Non-integrable systems with algebraic singularities in complex time”, *J. Phys. A: Math. Gen.* **23**, 3217-3236 (1991) · T. Bountis, “Investigating non-integrability and chaos in complex time”, in: *NATO ASI Conf. Proc.*, Como, September 1993 & *Phys. D* **86**, 256-267 (1995) · A. S. Fokas and T. Bountis, “Order and the ubiquitous occurrence of chaos”, *Physica* **A228**, 236-244 (1996) · S. Abenda, V. Marinakis and T. Bountis, “On the connection between hyperelliptic separability and Painlevé integrability”, *J. Phys. A: Math. Gen.* **34**, 3521-3539 (2001).
- [57] S. L. Ziglin, *Funktsional. Anal. i Prilozhen* **16**(3), 30-41 (1982); S. L. Ziglin, *Func. Anal. Appl.* **16**, 181 (1983).
- [58] H. Ito, *J. Appl. Math. Phys.* **38**, 459-476 (1987); H. Ito, *Kodai Math. J.* **8**, 130 (1985); H. Ito, *Kodai Math. J.* **1**, 120-138 (1985); J.-P. Francoise and M. Irigoyen, *C. R. Acad. Sci. Paris Ser. I Math.* **311**(3), 165-167 (1990); J.-P. Francoise and M. Irigoyen, *J. Geom. Phys.* **10**, 231-243 (1993); A. Braider and R. C. Churchill, *J. Differential Equations* **2**(4), 451-481 (1990); R. C. Churchill and D. L. Rod, *SIAM J. Math. Anal.* **22**(6), 1790-1802 (1991); D. L. Rod, *Canadian Math. Soc., Conf. Proc.* **8**, 599-608 (1987); D. L. Rod, *Contemporary Mathematics* **81**, 259-270 (1988).

- [59] H. Yoshida, *Cel. Mech.* **31**, 363-381 (1983); H. Yoshida, *Physica* **D21**(1), 163-170 (1986); H. Yoshida, *Physica* **D29**(12), 128-142 (1987); H. Yoshida, *Celestial Mech.* **44**(4), 313-316 (1988); H. Yoshida, *Phys. Lett.* **A141**(34), 108-112 (1989).
- [60] J. J. Morales-Ruiz, "Differential Galois Theory and Non-Integrability of Hamiltonian Systems", *Progress in Mathematics* **179**, 97 (1999) · J. J. Morales-Ruiz, "Kovalevskaya, Liapounov, Painleve, Ziglin and the differential Galois theory", *Regul. Chaotic Dyn.* **5**(3), 251-272 (2000) · J. J. Morales-Ruiz and J. P. Ramis, "Galoisian obstructions to integrability of Hamiltonian systems", *Methods and Applications of Analysis* **8**, 33-112 (2001) · J. J. Morales-Ruiz and J. P. Ramis, "A note on the non-integrability of some Hamiltonian systems with a homogeneous potential", *Methods and Applications of Analysis* **8**, 113-120 (2001).
- [61] G. Springer, *Introduction to Riemann surfaces*, New York Chelsea, 1957.
- [62] E. Induti, "Studio del moto nel piano complesso di N particelle attratte verso l'origine da una forza lineare ed interagenti a coppie con una forza proporzionale ad una potenza inversa dispari della loro mutua distanza", Dissertation for the "Laurea in Fisica", Università di Roma "La Sapienza", 2005.
- [63] C. Jacobi, "Problema trium corporum mutuis attractionibus cubis distantiarum inverse proportionalibus recta linea se moventium", in *Gesammelte Werke*, vol. **4**, Berlin, 1866, pp. 533-539.
- [64] F. Calogero, "Solution of a three-body problem in one dimension", *J. Math. Phys.* **10**, 2191-2196 (1969).
- [65] J. Moser, "Three integrable Hamiltonian systems connected with isospectral deformations", *Adv. Math.* **16**, 197-220 (1975).